1-1-1996

Polyelectrolyte adsorption on metals : effects of an applied surface potential.

Marianne Yarmey
University of Massachusetts Amherst

POLYELECTROLYTE ADSORPTION ON METALS: EFFECTS OF AN APPLIED SURFACE POTENTIAL

A Dissertation Presented

by

MARIANNE YARMEY

Submitted to the Graduate School of the
University of Massachusetts Amherst in partial fulfillment
of the requirements for the degree of

DOCTOR OF PHILOSOPHY

May 1996

Department of Polymer Science and Engineering

POLYELECTROLYTE ADSORPTION ON METALS: EFFECTS OF AN APPLIED SURFACE POTENTIAL

A Dissertation Presented

by

MARIANNE YARMEY

Approved as to style and content by:

David A. Hoagland, Chair

Scott W. Barton, Member

Thomas J. McCarthy, Member

Richard J. Farris, Department Head
Polymer Science and Engineering

To my parents

ACKNOWLEDGMENTS

I would like to express my sincere gratitude towards my advisor, David Hoagland, for this guidance and continuous support during my graduate studies. His keen interest in fundamental science has instilled in me an appreciation for answering basic scientific questions. Likewise, I am indebted to my committee members, Scott Barton and Tom McCarthy. Their probing questions and useful suggestions made this thesis a better piece of work. Support of this research by the Center for the University of Massachusetts Industry Research on Polymers (CUMIRP) is gratefully acknowledged.

Several people were instrumental in the completion of this work and I am thankful for their contributions. Brian Price aided in the automation of my ellipsometric measurements saving me endless amounts of time. John Domian assisted with the instrumentation necessary to apply a potential to the adsorbing metal surface. Susan Dawson chemically grafted poly-(glutamic acid) onto a gold surface in an attempt to provide me with viable candidate for this study.

I am grateful for the many friends who have been there to support me through these challenging years of graduate school. They include Chris, Susan, Meredith, Brian, Geni, Malika, Lia, Wanda, Dan, and Ann. Their abilities to listen, to put things in perspective, to celebrate in my triumphs, and to comfort me in my defeats are truly appreciated.

Most importantly I would like to thank my family: Teddi who was a constant pillar of support and love; Susan who understood exactly what I was going through as she was concurrently pursing a Ph.D. in polymer science at UCONN; and finally, my parents who always believed in me and encouraged me to follow my dreams. Because of their love for their daughters, they sacrificed much in their own lives so that we could have the very best. For this, I will be forever grateful.

ABSTRACT

POLYELECTROLYTE ADSORPTION ON METALS: EFFECTS OF AN APPLIED SURFACE POTENTIAL

MAY 1996

MARIANNE YARMEY, B.S., UNIVERSITY OF MONTANA

Ph.D., UNIVERSITY OF MASSACHUSETTS AMHERST

Directed by: Professor David A. Hoagland

Electrostatic interactions may direct the behavior of polyelectrolytes at solution/solid interfaces, with these comparatively long-ranged interactions influencing both the adsorbed chain conformation and the amount of polymer adsorbed. The microscopic structure of adsorbed polyelectrolyte layers is difficult to measure, however, and present knowledge on the subject derives from a relatively small number of experiments. To provide further insight into the role of electrostatic interactions, this thesis examines, using *in situ* ellipsometry, the effect of a variable applied surface potential on the structure of an adsorbed polyelectrolyte layer at the solution/metal interface.

Previous investigators reported that significant changes in layer thickness accompanied variations in surface potential, a phenomenon presumably traced to the attraction or repulsion of segments from the surface. However, oxidation/reduction of the surface also accompanies variations in this potential, and these chemical rearrangements were ignored when the ellipsometric data were analyzed, resulting in an inaccurate determination of thicknesses and adsorbances. Our study is thus the first to establish a method by which ellipsometry can be combined with voltammetry to correctly determine the effects of an applied surface potential on the structure of an

adsorbed polyelectrolyte layer. As part of this method, we have established a protocol by which ellipsometric results can be corrected for surface oxidation/reduction.

Two amphoteric polyelectrolyte systems are examined: γ-globulin, which possesses a rigid globular structure, and gelatin, which exhibits a flexible coil conformation in solution. Both are adsorbed onto platinum from phosphate buffers at pH values above their isoelectric points, creating a net negative polymer charge. Locally, however, both positive and negative charges exist simultaneously on the polymer chains. Due to the extremely rigid conformation of γ-globulin, provided by 16 disulfide bond linkages, no potential-induced changes in adsorbed layer thickness or plateau adsorbance are observed after ellipsometric data is corrected for surface oxidation/reduction. In contrast, gelatin's flexible nature would appear more conducive to adsorbed layer alterations with surface potential. Again, however, upon investigation, no changes in adsorbed layer thickness or amount adsorbed are detected, irrespective of ionic strength. The results suggest that lateral segment-segment interactions within a flexible polyelectrolyte layer are more important to layer structure than long-range segment-surface interactions.

TABLE OF CONTENTS

LIST OF TABLES

LIST OF FIGURES

CHAPTER 1

INTRODUCTION TO POLYELECTROLYTE ADSORPTION

The adsorption of polymers at interfaces plays an essential role in numerous technologies ranging from enhanced oil recovery, drag reduction, and colloidal stabilization to drug delivery, biocompatibility of artificial implants, and biosensors. Over the past forty years, many experimental and theoretical studies have examined the adsorption of neutral polymers onto solid surfaces from nonpolar, nonionizing solvents. This body of work, which has been the subject of many review articles [1-10], has greatly increased our knowledge of uncharged polymers at interfaces. However, a comparable depth of understanding is lacking for polyelectrolytes. Because of environmental concerns, many industrial processes are being modified to use water as a solvent. It is in this realm that an understanding of polyelectrolyte adsorption becomes crucial. In addition, the many biomedical applications involving the adsorption of biopolymers at interfaces also require a knowledge of charged polymer adsorption. Some of these biopolymers are amphoteric polyelectrolytes (polyampholytes), simultaneously containing both basic and acidic groups, a feature that further complicates their adsorption behavior at interfaces.

Studies have shown that neutral polymer adsorption is dominated by short-range, attractive forces that allow multiple segments of the chain to anchor to the substrate through strong physical bonds (~ 1-4 kT) [11-13]. Only nearest-neighbor interactions play a major role. Unattached segments of the chain protrude into the solution above the adsorbing surface and experience no direct interaction with the surface. Parameters such as the molecular weight of the polymer, the concentration of

the polymer in solution, the solvency of the polymer, and the affinity of the polymer for the substrate can be used to control the adsorption.

Unlike neutral polymers, polyelectrolyte chains exhibit long-range segment-segment electrostatic interactions in aqueous solution due to the charges along their backbones. The length scale for these interactions depends strongly on ionic strength [14]. These same types of interactions arise between polymer and surface when both are charged. Therefore, such parameters as surface charge density, polymer charge, and ionic strength can be used to control the adsorption of charged polymers at interfaces. Unfortunately, these variables are typically not independent of one another and obtaining a complete understanding of polyelectrolyte adsorption is difficult.

The majority of experimental polyelectrolyte adsorption studies, summarized in several reviews [5,6,9,10,15,16], have relied on techniques that measure only the total adsorbed amount. More detailed information about the microscopic structure of the adsorbed layer is difficult to obtain. Although many theoretical models [17-20] can predict the conformation of adsorbed polyelectrolyte chains, experimental confirmation is lacking. Ellipsometry, a technique applicable to highly reflective substrates, is probably the simplest technique that returns some conformational information. This information can be interpreted as the average extension and refractive index of the layer. From this information, a minimal description of the structure of the adsorbed layer can be inferred.

1.1 Introduction to Thesis

The objective of this thesis is to provide insight into the structure of adsorbed polyelectrolyte layers at solution/solid interfaces and to determine the role that electrostatic interactions play in this structure. An applied surface potential is used to control the charge on the adsorbing surface. Ionic strength and pH are adjusted in order to vary the charge on the polymer. *In situ* adsorbed layer thicknesses, refractive

indexes, and adsorbances are monitored using ellipsometry so that the conformation of the adsorbed polyelectrolyte chains might be inferred. Figure 1.1 depicts differences in adsorbed layer thickness which might be expected depending on whether the electrostatic interaction between the surface and the polymer is attractive or repulsive.

Literature results [21-25] for the effect of an applied surface potential on the adsorption of polyelectrolytes at solid interfaces appear to be flawed, as the oxidation/reduction of the adsorbing surface with variation in applied surface potential has been ignored when analyzing ellipsometric data. Therefore, we hope not only to examine the role of electrostatic interactions on the adsorption of polyelectrolytes at interfaces, but also to establish how ellipsometry can be combined with voltammetry to correctly determine *in situ* adsorbed layer thicknesses, refractive indexes, and adsorbances. Experimental errors and uncertainties must be properly documented and analyzed, steps neglected by previous workers.

The following pages of this chapter highlight theoretical and experimental works from the literature that demonstrate the current state of knowledge about charged polymer adsorption. Chapter 2 reviews the fundamental principles of ellipsometry, along with a description of the ellipsometer solution cell which was constructed to allow for *in situ* adsorption measurements. Instrumentation necessary to apply a potential to an adsorbing surface is also detailed in Chapter 2. Chapter 3 describes the effect of an applied surface potential on the structure of adsorbed γ-globulin. In addition, experimental evidence is presented that demonstrates oxidation/reduction of an inert metal surface during variation in applied potential, even after polymer chains have been adsorbed. A method to correct ellipsometric results for this oxidation/reduction is also described. Because γ-globulin is a globular protein with a rigid tertiary structure, the polymer is not an ideal candidate for studying changes in chain conformation arising from variations in applied surface potential. Therefore, attention turned to a

polyelectrolyte that exhibits a random coil conformation in solution and adsorbs in this state onto an inert metal surface. Gelatin, a flexible polyampholyte, meets both requirements. Chapter 4 describes in detail the effects of an applied surface potential, as well as ionic strength, on the structure of an adsorbed gelatin layer. Chapter 5 concludes the thesis with a summary of the knowledge gained by this study and a discussion of suggested work. In Appendix A, polyelectrolyte systems are described for which little or no adsorption could be detected on an inert metal surface using ellipsometry. These failed attempts are presented so that other scientists exploring this field might benefit . Appendixes B and C contain data which supplement Chapters 3 and 4, respectively.

1.2 Theoretical Background

1.2.1 Physical Adsorption of Polyelectrolytes

Most theories for polyelectrolyte adsorption incorporate the electrostatic contributions to the adsorption free energy by adapting existing models for neutral polymer adsorption. One of the first theories to model the adsorption of flexible polyelectrolyte chains on charged interfaces was developed by Hesselink [26-28]. He extended an earlier theory by Hoeve [29,30] for the adsorption of uncharged, flexible polymers. Although Hesselink's theory can predict many of the experimental trends observed during polyelectrolyte adsorption onto charged surfaces, the theory has a serious limitation. A step function is assumed for the volume fraction of polymer segments as a function of distance from the surface. The invariant shape of this function causes unrealistically high adsorbed layer thicknesses to be predicted.

With the development of such lattice-based models for neutral polymer adsorption as Roe's model [13] and the self-consistent-field theory of Scheutjens and Fleer [11,12], the concentration profile near a surface no longer had to be predetermined

but was found by minimization of the free energy of adsorption. Van der Schee and Lyklema [17] and Papenhuijzen *et al.* [18] were able to extend lattice theories to include the adsorption of strongly charged polymers. Segmental charges on the polymer were assumed to be smeared out in planes parallel to the surface. Counterions and coions were considered point charges and distributed between these planes of charge according to Poisson-Boltzmann statistics. A very thin polymer layer is predicted to adsorb onto an oppositely charged surface due to strong replusions between polyelectrolyte chain segments at low ionic strength. Also, adsorbance is found to be independent of molecular weight at low salt concentrations. At high ionic strength, nonelectrostatic interactions become dominant as repulsions are screened, causing polyelectrolyte adsorption to resemble that of uncharged polymers.

Evers *et al.* [19] extended the Scheutjens and Fleer theory [11,12] to the adsorption of weak polyelectrolytes from aqueous solution. The degree of dissociation of the polyelectrolyte was allowed to vary with the distance from the surface. A maximum adsorbance for a weak polyelectrolyte on an oppositely charge surface was found at a pH where slightly less than half of the polyelectrolyte segments are charged. At this pH, the electrostatic attraction between the charged polymer segments and the oppositely charged surface is stronger than the mutual repulsion between the charged segments, allowing more chains to adsorb onto the surface.

Unlike the previous models, which treated ions as point charges, Böhmer *et al.*[20] were able to modify the Scheutjens and Fleer model [11,12] so that each ion, polyelectrolyte segment, and solvent molecule had a volume equal to that of a lattice site. The charges associated with ions and segments were assumed to be located on planes in the middle of each lattice layer, with the space between these planes devoid of charge. The electrical potential at each plane was then obtained by solving a discrete version of the Poisson-Boltzmann equation. The potential difference between these equidistant

planes depended on the charge in each plane, the separation between planes, and the dielectric constant. For a charged surface in contact with a solution containing only small ions, the results of this multi-layer Stern model are identical to that of the Gouy-Chapman theory if the surface potential and the salt concentration are not too high. Deviation from the Gouy-Chapman theory occurs when excluded volume effects become important at higher surface potentials and salt concentrations. Böhmer *et al.* modeled the configuration of a polyelectrolyte chain as a step-weighted walk on a lattice. The weighting factors for each step contained the nearest-neighbor contact energy (Flory-Huggins), the electrical potential , and the mixing entropy. The mixing entropy allowed the probability of a step toward a given lattice layer to decrease as the segment concentration in the layer increased. From these step-weighted walks, the volume fraction profile and the amount adsorbed was calculated. Predictions of this model agree well with many experimental results.

Van de Steeg *et al.* [31] used Böhmer's model [20] to numerically calculate the effects of salt concentration, segment charge, and surface charge density on the adsorption of polyelectrolytes to oppositely charged surfaces. Two regimes for polyelectrolyte adsorption were proposed: the *screening-reduced adsorption* regime and the *screening-enhanced adsorption* regime. If the attraction of a polyelectrolyte to a charged surface is purely electrostatic in nature, adsorption always decreases with increasing salt concentration due to screening by salt ions. This is called the *screening-reduced adsorption* regime. If the attraction between the polyelectrolyte and the charged surface is dominated by nonelectrostatic interactions, adsorption will increase with increasing ionic strength due to the screening of the repulsion between segments of the polymer chain. This is called the *screening-enhanced adsorption* regime. The subtle balance of electrostatic and nonelectrostatic forces between the polyelectrolyte and the surface determine which regime is favored.

In all of the models discussed thus far, adsorption is assumed to be an equilibrium phenomenon, an approximation reasonably well obeyed for many neutral polymers. However, the mechanism for polyelectrolyte adsorption is not necessarily the same as that for neutral polymers, and equilibrium models may fail badly. The binding energy per segment for neutral polymer adsorption is on the order of kT. Polyelectrolytes, on the other hand, have an electrostatic attraction to the surface causing the binding energy per segment to be many times kT. Barford *et al.* [32] proposed a sequential, non-equilibrium adsorption theory based on the continuum, self-consistent field theory of Edwards [33]. Barford's model proposes that when a polyelectrolyte arrives at an electrostatically attractive surface, it absorbs less strongly than previously adsorbed chains. This effect is due both to increased screening of the surface attraction and to the repulsive potential which is set up by charged segments of previously adsorbed chains. The predicted polymer concentration at which no more adsorption can take place is lower for sequential adsorption than for equilibrium adsorption.

Using mean field arguments, Muthukumar [34] derived explicit formulas for the adsorption of a single polyelectrolyte chain as a function of surface charge density, charge on the polymer, Debye screening length κ^{-1}, chain length L, and temperature T. This model is a generalization of Wiegel's continuum theory [35,36] which described the adsorption of a Gaussian polyelectrolyte onto a planar charged surface. Muthukumar's model allows the configuration of the polyelectrolyte chain to vary between a flexible coil and a rigid rod depending on the ionic strength of the solution. Adsorption is predicted to occur at a temperature below the critical temperature T_C, where T_C is proportional to $\kappa^{-3} L^{-1}$ in the weak screening limit and to $\kappa^{-11/5} L^{-1/5}$ in the strong screening limit. This theory does not apply when chains interact with each other or in the presence of nonelectrostatic interactions.

1.2.2 Grafted Polyelectrolyte Brushes

The models discussed thus far describe the physical adsorption of polymer chains onto a surface from solution. In contrast, these chains can also be chemically grafted onto a substrate. The distance between grafted points will determine the conformation of the attached polymer chains. At high grafting densities, excluded volume interactions force terminally-anchored chains to stretch out into the solution, causing polymer brushes to form. Several models for these neutral polymer brushes have been proposed [37-40] and subsequently modified for polyelectrolyte brushes.

Two groups, Miklavic *et al.* [41] and Misra *et al.* [42], extended the analytical self-consistent mean-field theory of grafted polymer brushes proposed by Milner, Witten, and Cates [37,38] to polyelectrolyte chains attached to a charged planar surface in an electrolyte solution. The segment density distribution and the brush height are predicted to be strongly affected by brush charge. In contrast, the surface charge has little effect on the conformation of highly stretched polyelectrolyte brushes. However, when brush height becomes comparable to the Debye screening length, i.e. shorter brushes or highly compressed brushes, surface charge is expected to play a more significant role.

Miklavic *et al.* [43] compared Monte Carlo simulation results with mean-field Poisson-Boltzmann approximations for polyelectrolyte brushes grafted onto two charged surfaces. They examined the dependence of osmotic pressure and configurational properties of the polyelectrolyte chains on system parameters. Better agreement is found between the osmotic pressure predicted by the mean-field theory and that determined by Monte Carlo simulations if contributions due to nearest-neighbor Coulombic repulsions are neglected. These nearest-neighbor interactions are important, however, for predicting the internal chain statistics such as the root-mean squared end-to-end distance of the polyelectrolyte. Results from Monte Carlo simulations for chain statistics are in good agreement with mean-field predictions except when the

polyelectrolyte has a high charge density. The mean-field theory underestimates the root-mean squared end-to-end distance of a highly charged polymer chain when specific monomer-monomer correlations are not taken into account. Intrachain, electrostatic repulsions, which extend beyond nearest-neighbor interactions and tend to favor stretched configurations, are reduced to a mean potential which responds only to variations in the average monomer-monomer correlations.

Granfeldt *et al.* [44] studied by Monte Carlo and mean-field methods the interaction of two planar surfaces bearing end-attached polyelectrolytes. The polyelectrolytes are modeled as flexible, linear chains adopting self-avoiding walk configurations. A mean-field potential, which satisfied an extended Poisson-Boltzmann equation, is used to describe the electrostatic interactions. Monomer distribution, electrostatic potential, and interaction potential are determined as a function of the polyelectrolyte charge, surface charge, and salt concentration. The interaction potential is found similar to that predicted by Miklavic *et al.* [41].

Pincus [45] proposed simple analytic scaling laws to describe polyelectrolytes end-grafted to planar surfaces. The approach, albeit approximate, provides physical insights to the previous numerical results presented by Miklavic *et al.* [41] and Misra *et al.* [42]. The most important conclusion of Pincus' work is that, in contrast to charged interfaces where there is exponential Debye screening in the presence of salt, the disjoining pressure associated with two polyelectrolyte grafted surfaces weakens only as a power law in the electrolyte concentration due to polymer elasticity.

Ross and Pincus [46] studied the effects of solvent quality on the properties of polyelectrolyte brushes. The Poisson-Boltzmann theory was used to describe the electrostatic interactions while the excluded volume and van der Waals-like monomer interactions were taken into account using the Flory-Huggins mean-field theory. A

first-order conformational phase transition to a collapsed state for a moderately to highly charged polyelectrolyte brush in the poor solvent regime was detected.

Schurr and Smith [47] proposed a simple theory for the extension (R_Z) of a single, uniformly charged linear polyelectrolyte attached at one end in a constant electric field E. For a polyelectrolyte made of a large number (N) of Kuhn lengths (b), the R_Z in the direction of E, is given by the following equation: $R_Z = (b / A) \ln (\sinh (NA) / NA)$, where $A = EQb / k T$ and Q is the effective charge of each Kuhn length. For any electric field strength, no matter how small, a polyion of sufficient length ($NA >> 1.0$) extends fully. When $A << 1.0$, as in weak electric fields, the head of the polymer chain is only weakly oriented, even though the stem and tail are completely aligned. In the linear regime, $NA < 1.0$, R_Z is proportional to E, Q, and N^2.

1.2.3 Adsorption of Charged-Neutral Diblock Copolymers

Another area of theoretical interest is the adsorption of diblock copolymers from a selective solvent onto a solid surface. In an adsorbed diblock copolymer layer, one block of the copolymer is preferentially adsorbed (anchor block) and the other block is largely excluded from the surface forming a brush (buoy block). Argillier and Tirrell [48] investigated the adsorption of a hydrophobic/ionic diblock copolymer from aqueous solution onto a flat hydrophobic surface by extending the scaling theory developed by Marques *et al.* [49], which describes the adsorption of a neutral diblock copolymer. The configurational free energy of a grafted polyelectrolyte chain, calculated by Pincus [45], was incorporated into the Marques theory. Through the minimization of the grand canonical free energy of the system, the equilibrium structure of the hydrophobic/ionic diblock copolymer layer was obtained. The surface density, thickness of the collapsed hydrophobic layer, and thickness of the extended polyelectrolyte brush were determined

as a function of such parameters as the molecular weight of the hydrophobic block, the molecular weight of the ionic block, the charge of the polymer, and the ionic strength.

Dan and Tirrell [50] adapted a scaling model for dense polymer brushes [51,52] to describe the aggregation of charged-neutral diblock copolymer chains in aqueous salt solutions. Both micelles and adsorbed layers, as well as, the equilibrium between the two were examined. The surface density of an adsorbed polymer layer and the aggregation number of micelles is found to increase with salt concentration as the thickness of the charged block decreased due to screening of charges. Layers adsorbed from dilute copolymer solutions, below the critical micelle concentration, obtain a higher surface density than layers at equilibrium with micellar solutions.

Wittmer and Joanny [53] also modeled the adsorption of charged-neutral diblock copolymers onto a planar surface. Upon adsorption, a dense polyelectrolyte brush is found only if the fraction of charged monomers in the polyelectrolyte block is smaller than a critical value. If the charge fraction is larger than this value, the copolymer did not adsorb due to the large osmotic pressure in the layer. The model assumes that the bulk solution and the surface are at thermodynamic equilibrium. Excluded volume interactions are ignored.

1.2.4 Protein Adsorption

The theories discussed thus far have dealt with polyelectrolytes that carry only one type of charged group. Proteins, on the other hand, constitute another group of charged polymers that exhibit at least two new complicating factors. First, these biopolymers are polyampholytes, carrying both positive and negative charges, and second, strong intramolecular interactions cause these molecules to possess a heightened degree of rigidity. Due to their relative complexity, a general theory describing protein adsorption onto interfaces still seems far beyond reach.

1.3 Experimental Background

1.3.1 Polyelectrolyte Adsorption

Over the past decade, many experimental groups have attempted to elucidate the effects of such parameters as surface charge density, polymer charge, and ionic strength on polyelectrolyte adsorption. Because of the sheer number of experiments, selected results which demonstrate a particular aspect of polyelectrolyte adsorption will be highlighted in this overview.

It is appropriate to begin with one of the simplest scenarios: strong polyelectrolytes adsorbed on uncharged surfaces. Poly(styrene sulfonate) (PSS), a negatively charged polymer, was adsorbed onto neutral polyoxymethylene crystals [54] and uncharged silica particles [55] from aqueous NaCl solution. At low salt concentrations, electrostatic interactions are found to dominate and oppose adsorption because of the strong mutual repulsion between segments which prevents their accumulation at the surface. At high ionic strength, substantial polyelectrolyte adsorption occurs due to the screening of these electrostatic interactions. The later behavior resembles that of neutral polymers adsorbed from relatively poor solvents. A linear dependence of adsorption on the log of the molecular weight and the square root of ionic strength is found.

Few experimental studies have monitored polyelectrolyte adsorption to surfaces bearing the same charge sign. One example is the adsorption of poly-(L-lysine) onto AgI crystals at three nitric acid concentrations [56]. At low pH, the polymer is positively charged. By adjusting the pI (where pI = -log (I^-)), the charge on the surface can be varied. When both the polymer and the surface have the same charge sign, the repulsion between the segments and the surface is so strong that no adsorption takes place at low ionic strength. With increasing salt concentration, the polymer begins to

adsorb onto the surface. This increase in adsorbance is due to the screening of electrostatic repulsions and the high chemical affinity of poly-(L-lysine) for AgI.

Many examples of polyelectrolytes adsorbed onto oppositely charged surfaces are described in the literature. Pure electrosorption (i.e. adsorption due only to electrostatic interactions, with no contribution from nonelectrostatic forces) is exemplified by the adsorption of a cationically modified polyacrylamide onto anionic silica particles [57]. A maximum in adsorbance has been detected when the mole fraction of cationic groups on the polyacrylamide (α) is 0.01. This maximum, also predicted by theory [27], is attributed to the increased number of chains needed to compensate the surface charge when the polymer is only slightly charged, as opposed to when the polymer is highly charged.

Polyelectrolytes can adsorb onto surfaces which are both electrostatically and chemically attractive. Uncharged polyacrylamide was found to adsorb onto negatively charged clay from aqueous salt solution due to nonelectrostatic interactions [58]. Upon modification of this polymer to include cationic groups, adsorption was detected on the negatively charged clay with a maximum in adsorbance observed at $\alpha = 0.01$. This maximum is once again ascribed to the increased number of chains needed to compensate the surface charge when polyacrylamide is weakly charged.

Thus far, only strong polyelectrolyte adsorption behavior has been discussed. However, weak polyelectrolytes are unique in that their degree of charge is a function of the pH, which may locally vary with distance from the surface. Blaakmeer *et al.* [59] adsorbed poly(acrylic acid) (PAA) onto positively charged polystyrene latex particles from 0.1 M KNO_3 solution. The surface charge on these particles remains constant, independent of solution pH. The amount of PAA adsorbed depends strongly on pH, with a maximum in adsorbance at a pH one unit below the intrinsic dissociation constant pK_o of the carboxylic acid groups of PAA. This maximum is caused by two opposing

forces. As pH rises, the charge density on the polymer increases, causing the electrostatic attractive forces between polymer and surface to increase, a trend favoring adsorption. However, the repulsive forces between charged segments of the chain also increase, creating an opposing trend. Others who have studied PAA adsorption onto surfaces were unable to detect this maximum in adsorbance due to the variation of surface charge with pH [60,61]. Ionic strength was shown by Blaakmeer *et al.* to have only a negligible effect on the adsorption of weak polyelectrolytes due to the adjustment of the degree of dissociation to compensate the surface charge more effectively. Therefore, the polymer-substrate complex is nearly neutral and variations in salt concentration are relatively unimportant.

In all of the examples presented above, salt ions were assumed to present no specific interactions with the solvent or surface. However, it is well known that specific adsorption of certain ions does occur. Coions can compete with polyelectrolyte segments for surface sites due to both electrostatic and nonelectrostatic interactions. Positively charged poly-(L-lysine) was adsorbed onto negatively charged silica particles from aqueous NaCl solution at three different pH values [62]. The amount of polymer adsorbed decreased with increasing charge on the poly-(L-lysine) (i.e., for lower pH) due to charge compensation effects. However, a new maximum in adsorption as a function of salt concentration was observed, suggesting specific adsorption of sodium ions on the negatively charged silica particles.

1.3.2 Structure of Adsorbed Polyelectrolyte Layers

Direct experimental evidence for the thickness and structure of adsorbed polyelectrolyte layers remains scarce due to the lack of systematic studies. Such techniques as neutron scattering/reflectivity, surface forces, ellipsometry, scanning tunneling microscopy (STM), and surface-enhanced Raman scattering (SERS) have

been utilized in an effort to describe the conformation of adsorbed polyelectrolyte chains. Presented below are a few illustrative examples of these studies.

Cosgrove *et al.* [63] adsorbed PSS onto both positively and negatively charged polystyrene latex particles. Small angle neutron scattering revealed that the polymer was confined to a thin adsorbed layer, even at high ionic strength. The thickness of the adsorbed layer increased slightly with increasing molecular weight. Adsorption was found to be higher when the polymer and surface had opposite charge. However, when both carried the same sign charge, nonelectrostatic interactions caused a significant amount of the polymer to be adsorbed.

Marra and Hair [64] used the surface forces apparatus to measure the forces between two mica surfaces covered with poly(2-vinylpyridine) (P2VP). In acid solution, where P2VP is fully charged, the conformation of adsorbed P2VP was found to be essentially flat at low ionic strength (< 0.1 M). Segment-surface binding affinity appeared to be strong, with electrostatic segmental repulsions stretching the flattened chains across the surface. Adsorbance was independent of molecular weight of the polymer. At salt concentrations equal to or above 0.1 M, the P2VP chains adsorbed in a loose conformation with tails and loops. Intersegmental electrostatic repulsions and surface charge effects were screened, causing the polyelectrolyte chains to approach the behavior of neutral polymers [17]. In alkaline solutions, where P2VP was uncharged, a large extension of the adsorbed layer was found. This observation can be explained by the disappearance of electrostatic segmental repulsions and electrostatic segment-surface attractions. At a constant adsorbed amount, the conformation of the adsorbed P2VP chains at the surface was determined to be independent of chain length.

1.3.3 Effects of Surface Potential on Adsorbed Polyelectrolyte Layers

Morrissey *et al.* [25] investigated the effect of an applied surface potential on the structure of adsorbed blood protein layers using ellipsometry. Serum albumin, fibrinogen, and γ-globulin were found to adsorb on platinum from 0.15 N NaCl solutions adjusted to pH = 7.4 by HCl or NaOH. At this pH, all three proteins were negatively charged. The potential applied at the platinum surface was varied between -245 and 845 mV vs. a standard Ag/AgCl reference electrode. By continuously varying the potential, the surface charge density could be controlled. Adsorbance for each protein was found to remain constant over the potential range examined, except at high positive potentials, where an abrupt adsorbance increase was noted. In these same experiments, the thickness of the layer was reported to rise at negative potentials, presumably because of repulsive electrostatic interactions between the negatively charged protein and the negatively charged surface. Conversely, at increasingly positive potentials, the thickness of the adsorbed layer decreased, an effect attributed to the attractive electrostatic interaction. All results are questionable, however, as oxidation/reduction of the platinum surface was ignored even though the potential varied over a range where oxidation/reduction is known to occur.

Several years later, Kawaguchi *et al.* [23,24] also used ellipsometry to monitor the thickness of a polyelectrolyte, in this case, sodium poly(styrene sulfonate) (NaPSS) adsorbed from aqueous NaCl solution onto platinum. Changes in layer thickness with potential were reported and attributed to electrostatic attractive and repulsive forces between the polymer and the surface. Again, results must be questioned since oxidation/reduction of the platinum was neglected.

Lippert and Brandt [65] used surface-enhanced Raman scattering (SERS) to gain insight into the effect of an applied potential on the adsorption of partially protonated P2VP onto silver. At potentials positive to that at which the surface has zero charge

(PZC), the pyridinium ion species were found to adsorb through chloride ions onto the surface. Near the PZC, neutral pyridine groups predominantly adsorbed.

Garrell and Beer [66] used SERS to look at the effect of an applied surface potential on the adsorption of partially protonated poly(4-vinylpyridine) (P4VP) onto silver. At -5 mV vs. Ag/AgCl (PZC = -855 mV vs. Ag/AgCl in 0.1 M KCl solution at pH = 2.0), no polymer adsorbed onto the surface. As the potential became more negative, the P4VP began to adsorb to the surface via neutral segments. Adsorption through the protonated pyridyl rings was not observed until the potential was increased to -555 mV. The driving force for the adsorption of these positive moieties is not coulombic as the surface charge remained positive. A possible explanation invokes the pairing of chloride ions with the positive pyridyl groups.

1.3.4 Protein Adsorption

Proteins usually adsorb as a compact layer [67], with a maximum in adsorbance exhibited at the isoelectric point of the protein-sorbent complex [68-71]. This maximum is thought to be caused by the minimization of charge-charge repulsions between adsorbed molecules at the isoelectric pH. Norde, however, showed that the reduction in the amount adsorbed away from the isoelectric point for albumin on negatively charged polystyrene surfaces is due to structural rearrangements in the adsorbing molecule rather than increased lateral charge repulsions [72,73]. Most proteins adsorb on both hydrophobic and hydrophilic surfaces even if the protein and surface possess similar charge [73,74]. Albumin provides a good example of this behavior. Ribonuclease, on the other hand, adsorbs on hydrophobic surfaces at all charge conditions, but adsorbs on hydrophilic surfaces only when electrostatic interactions are favorable [75,76]. Proteins such as albumin that adsorb onto hydrophilic surfaces at electrostatically unfavorable conditions generally possess low structural stability, suggesting that the unfavorable

enthalpy change that occurs upon adsorption is overcompensated by the gain in entropy as the protein secondary structure is reduced. In contrast, ribonuclease has high structural stability, causing adsorption to be ruled by electrostatic interactions and partial dehydration of the surface and protein.

Ionic strength effects are found to be important in protein adsorption, the amount adsorbed generally increasing with ionic strength due to the screening of charge interactions by small ions. However, the role that these ions play in protein adsorption seems more complicated than indiscriminate screening of charge interactions. Koutsoukos *et al.*[68] found that the effect of ionic strength on the adsorption of albumin depended on the type of surface to which the protein adsorbed. In other studies, adsorption appeared to be sensitive to the type of ions present [77-79].

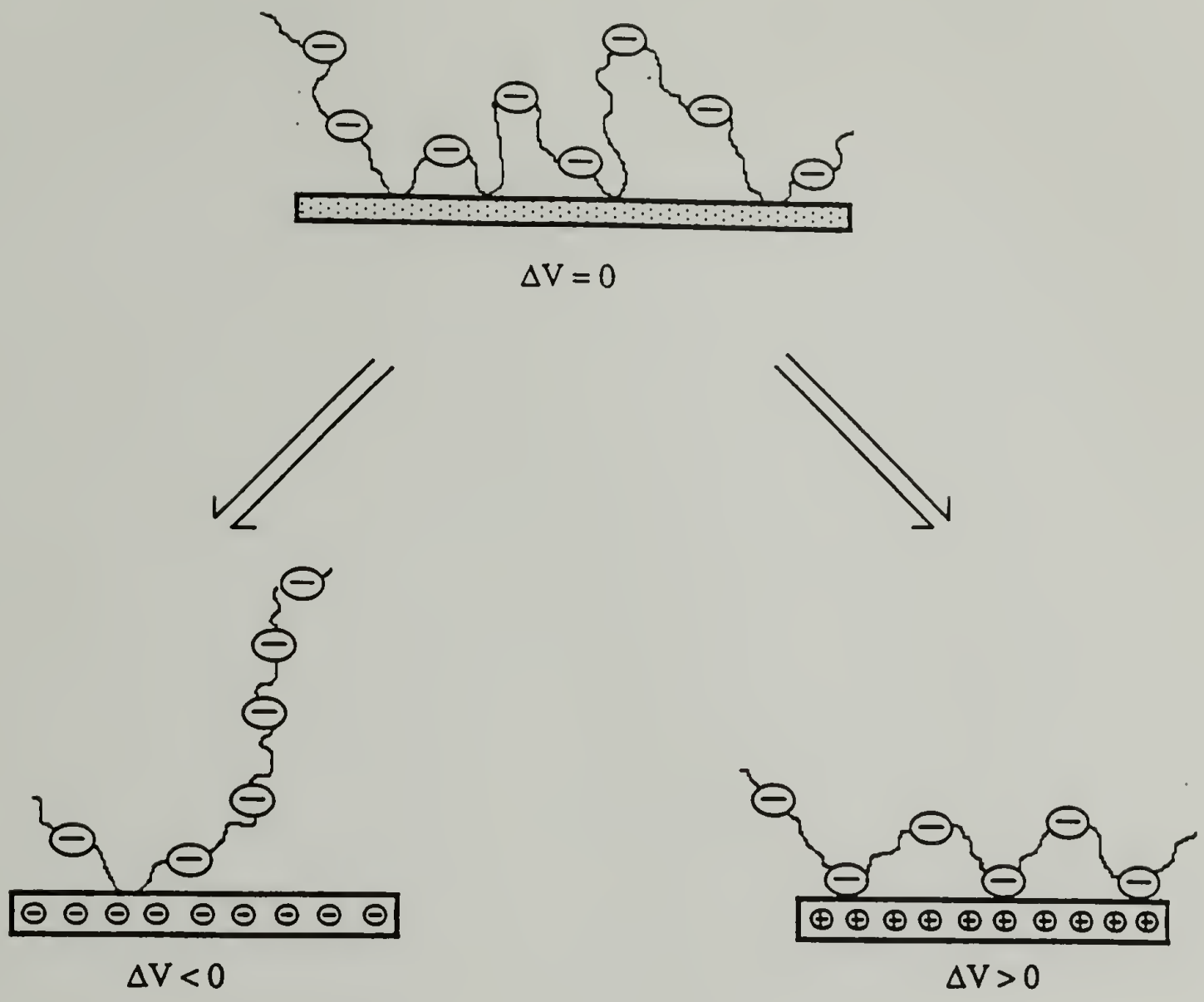

Figure 1.1. Cartoon of the effect of applied surface potential on polyelectrolyte adsorption.

1.4 References

(1) Lipatov, Y. S.; Sergeeva, L. M. *Adsorption of Polymers*; Wiley: New York, 1974.

(2) Dickinson, E.; Lal, M. *Advances in Molecular Relaxation and Interaction Processes* **1980**, *17*, 1.

(3) Takahashi, A.; Kawaguchi, M. *Advances in Polymer Science* **1982**, *46*, 1.

(4) Fleer, G. J.; Lyklema, J. In *Adsorption from Solution at the Solid/Liquid Interface*; G. D. Parfitt and C. H. Rochester, Ed.; Academic Press: London, 1983; 153.

(5) Cohen Stuart, M. A.; Cosgrove, T.; Vincent, B. *Advances in Colloid and Interface Science* **1986**, *24*, 143.

(6) Robb, I. D. *Comprehensive Polymer Science* **1989**, *2*, 733.

(7) Silberberg, A. In *Encyclopedia of Polymer Science and Engineering* Wiley: New York, 1985; Vol. 1; 577.

(8) Ploehn, H. J.; Russel, W. B. *Advances in Chemical Engineering* **1990**, *15*, 137.

(9) Kawaguchi, M.; Takahashi, A. *Advances in Colloid and Interface Science* **1992**, *37*, 219.

(10) Fleer, G. J.; Cohen Stuart, M. A.; Scheutjens, J. M. H. M.; Cosgrove, T.; Vincent, B. *Polymers at Interfaces*; Chapman & Hall: London, 1993.

(11) Scheutjens, J. M. H. M.; Fleer, G. J. *Journal of Physical Chemistry* **1979**, *83*, 1619.

(12) Scheutjens, J. M. H. M.; Fleer, G. J. *Journal of Physical Chemistry* **1980**, *84*, 178.

(13) Roe, R. J. *Journal of Chemical Physics* **1974**, *60*, 4192.

(14) Eisenberg, A.; King, M. *Ion Containing Polymers*; Adademic Press: New York, 1977.

(15) Cohen Stuart, M. A.; Fleer, G. J.; Lyklema, J.; Norde, W.; Scheutjens, J. M. H. M. *Advances in Colloid and Interface Science* **1991**, *34*, 477.

(16) Cohen Stuart, M. A. *Journal de Physique II* **1988**, *49*, 1001.

(17) van der Schee, H. A.; Lyklema, J. *Journal of Physical Chemistry* **1984**, *88*, 6661.

(18) Papenhuijzen, J.; van der Schee, H. A.; Fleer, G. J. *Journal of Colloid and Interface Science* **1985**, *104*, 540.

(19) Evers, O. A.; Fleer, G. J.; Scheutjens, J. M. H. M.; Lyklema, J. *Journal of Colloid and Interface Science* **1986**, *111*, 446.

(20) Böhmer, M. R.; Evers, O. A.; Scheutjens, J. M. H. M. *Macromolecules* **1990**, *23*, 2288.

(21) Besio, G. J. Ph.D. Thesis, Princeton University, 1986.

(22) Ivarsson, B. A.; Hegg, P.-O.; Lundström, K. I.; Jönsson, U. *Colloids and Surfaces* **1985**, *13*, 169.

(23) Kawaguchi, M.; Hayashi, K.; Takahashi, A. *Colloids and Surfaces* **1988**, *31*, 73.

(24) Kawaguchi, M.; Hayashi, K.; Takahashi, A. *Macromolecules* **1988**, *21*, 1016.

(25) Morrissey, B. W.; Smith, L. E.; Stromberg, R. R.; Fenstermaker, C. A. *Journal of Colloid and Interface Science* **1976**, *56*, 557.

(26) Hesselink, F. T. *Journal of Electroanalytical Chemistry and Interfacial Electrochemistry* **1972**, *37*, 317.

(27) Hesselink, F. T. *Journal of Colloid and Interface Science* **1977**, *60*, 448.

(28) Hesselink, F. T. In *Adsorption from Solution at Solid/Liquid Interface*; C. H. Rochester and G. D. Parfitt, Ed.; Academic Press: London, 1983; 377.

(29) Hoeve, C. A. J. *Journal of Chemical Physics* **1966**, *44*, 1505.

(30) Hoeve, C. A. J. *Journal of Polymer Science* **1970**, *C30*, 361.

(31) van de Steeg, H. G. M.; Cohen Stuart, M. A.; de Keizer, A.; Bijsterbosch, B. H. *Langmuir* **1992**, *8*, 2538.

(32) Barford, W.; Ball, R. C.; Nex, C. M. M. *Journal. Chemical Society (London). Faraday Transactions. I* **1986**, *82*, 3233.

(33) Edwards, S. F. *Proceedings Physics Society* **1965**, *85*, 613.

(34) Muthukumar, M. *Journal of Chemical Physics* **1987**, *86*, 7230.

(35) Wiegel, F. W. *Journal Physics A* **1977**, *10*, 299.

(36) Wiegel, F. W. In *Phase Transitions and Critical Phenomena*; C. Domb and J. L. Lebowitz, Ed.; Academic: New York, 1983; Vol. 7.

(37) Milner, S. T.; Witten, T. A.; Cates, M. E. *Macromolecules* **1988**, *21*, 2610.

(38) Milner, S. T.; Witten, T. A.; Cates, M. E. *Europhysics Letters* **1988**, *5*, 413.

(39) Zhulina, E. B.; Priamitsyn, V. A.; Borisov, O. V. *Polymer Science USSR* **1989**, *31*, 205.

(40) Zhulina, E. B.; Borisov, O. V.; Priamitsyn, V. A. *Journal of Colloid and Interface Science* **1990**, *137*, 495.

(41) Miklavic, S. J.; Marcelja, S. *Journal of Physical Chemistry* **1988**, *92*, 6718.

(42) Misra, S.; Varanasi, S. *Macromolecules* **1989**, *22*, 4173.

(43) Miklavic, S. J.; Woodward, C. E.; Jönsson, B.; Åkesson, T. *Macromolecules* **1990**, *23*, 4149.

(44) Granfeldt, M. K.; Miklavic, S. J.; Marcelja, S.; Woodward, C. E. *Macromolecules* **1990**, *23*, 4760.

(45) Pincus, P. *Macromolecules* **1991**, *24*, 2912.

(46) Ross, R. S.; Pincus, P. *Macromolecules* **1992**, *25*, 2177.

(47) Schurr, J. M.; Smith, S. B. *Biopolymers* **1990**, *29*, 1161.

(48) Argillier, J.-F.; Tirrell, M. *Theoretica Chimica Acta* **1992**, *82*, 343.

(49) Marques, C.; Joanny, J. F.; Leibler, L. *Macromolecules* **1988**, *21*, 1051.

(50) Dan, N.; Tirrell, M. *Macromolecules* **1993**, *26*, 4310.

(51) Alexander, S. *Journal de Physique II* **1977**, *38*, 977.

(52) de Gennes, P. G. *Macromolecules* **1980**, *13*, 1069.

(53) Wittmer, J.; Joanny, J. F. *Macromolecules* **1993**, *26*, 2691.

(54) Papenhuijzen, J.; Fleer, G. J.; Bijsterbosch, B. H. *Journal of Colloid and Interface Science* **1985**, *104*, 530.

(55) Marra, J.; van der Schee, H. A.; Fleer, G. J.; Lyklema, J. In *Adsorption from Solution*; R. H. Ottewill, C. H. Rochester and A. L. Smith, Ed.; Academic Press: 1983; 245.

(56) van der Schee, H. A. Ph.D. Thesis, Wageningen University, The Netherlands, 1984.

(57) Wang, T. K.; Audebert, R. *Journal of Colloid and Interface Science* **1988**, *121*, 32.

(58) Durand, G.; Lafuma, F.; Audebert, R. *Progress in Colloid and Polymer Science* **1988**, *266*, 278.

(59) Blaakmeer, J.; Böhmer, M. R.; Cohen Stuart, M. A.; Fleer, G. J. *Macromolecules* **1990**, *23*, 2301.

(60) Foissy, A.; Attar, A. E.; Lamarche, J. M. *Journal of Colloid and Interface Science* **1983**, *96*, 275.

(61) Gebhardt, J. E.; Fuerstenau, D. W. *Colloids and Surfaces* **1983**, *7*, 221.

(62) Bonekamp, B. C. Ph.D. Thesis, Wageningen University, The Netherlands, 1984.

(63) Cosgrove, T.; Obey, T. M.; Vincent, B. *Journal of Colloid and Interface Science* **1986**, *111*, 409.

(64) Marra, J.; Hair, M. L. *Journal of Physical Chemistry* **1988**, *92*, 6044.

(65) Lippert, J. L.; Brandt, E. S. *Langmuir* **1988**, *4*, 127.

(66) Garrell, R. L.; Beer, K. D. *Langmuir* **1989**, *5*, 452.

(67) Soderquist, M. E.; Walton, A. G. *Journal of Colloid and Interface Science* **1980**, *75*, 386.

(68) Koutsoukos, P. G.; Mumme-Young, C. A.; Norde, W.; Lyklema, J. *Colloids and Surfaces* **1982**, *5*, 93.

(69) Bagchi, P.; Birnbaum, S. M. *Journal of Colloid and Interface Science* **1981**, *83*, 460.

(70) Shirahama, H.; Takeda, K.; Suzawa, T. *Journal of Colloid and Interface Science* **1986**, *109*, 552.

(71) Morrissey, B. W.; Stromberg, R. R. *Journal of Colloid and Interface Science* **1974**, *46*, 152.

(72) Norde, W.; Lyklema, J. *Journal of Colloid and Interface Science* **1978**, *66*, 257, 266, 277, 285, 295.

(73) Norde, W. *Advances in Colloid and Interface Science* **1986**, *25*, 267.

(74) Norde, W.; Lyklema, J. *Colloids and Surfaces* **1989**, *38*, 1.

(75) Norde, W. In *Surfactants in Solution*; K. L. Mittal and P. Bothorel, Ed.; Plenum Press: New York, 1986; Vol. 5; 1027.

(76) Norde, W. *Colloids and Surfaces* **1984**, *10*, 21.

(77) McLaren, A. D. *Journal of Physical Chemistry* **1954**, *58*, 129.

(78) Mizutani, T. *Journal of Colloid and Interface Science* **1981**, *82*, 162.

(79) van Dulm, P.; Norde, W.; Lyklema, J. *Journal of Colloid and Interface Science* **1981**, *82*, 77.

CHAPTER 2

ELLIPSOMETRY: EXPERIMENT AND APPARATUS

2.1 Introduction

Ellipsometry is an optical technique that directly measures the thickness and refractive index of an adsorbed film on a solid substrate, and less directly, the amount of material adsorbed. Optical constants of a bare reflecting surface can also be measured. In this project, ellipsometry is used as the principal tool to probe the structure of adsorbed polyelectrolyte layers on inert metal surfaces. Ellipsometry has the advantage that it is non-invasive, sensitive to adsorbed layer thicknesses on the order of 10 Å, and adaptable to the study of adsorbed polymer layers with solvent present [1-3]. Few alternative surface characterization techniques have all of these capabilities. Determination of the thickness and refractive index of an adsorbed polyelectrolyte layer in the presence of solvent is of particular importance to the present project, because the thickness yields considerable insight into the conformation of adsorbed polymer chains. Although much is known about the molecular dimensions of a polyelectrolyte chain in solution, there remain many questions as to how these dimensions change when the chain is adsorbed onto a substrate with surface charge or how an applied surface potential affects the structure of an adsorbed layer. In attempt to answer these questions, an ellipsometer solution cell was constructed to study the structure of an adsorbed polyelectrolyte layer in the swollen state.

In this chapter, the fundamental principles of ellipsometry are reviewed. A description of the constructed ellipsometer solution cell is presented alongside experimental

results that verify its operation. The instrumentation necessary to apply a potential to an adsorbing metal surface is also detailed.

2.2 Ellipsometry

A Rudolph Research AutoEL II nulling ellipsometer is used to determine the thicknesses and refractive indexes of adsorbed polyelectrolyte layers. A simplified diagram of the components of this ellipsometer is shown in Figure 2.1. A low power helium-neon laser produces a collimated beam of monochromatic (632.8 nm) light which initially passes through a rotatable polarizer prism. The beam is then converted to elliptical polarization by a mica quarter-wave-plate compensator, which has a fast axis and an orthogonal slow axis. The component of light parallel to the slow axis is retarded by one quarter wavelength relative to that parallel to the fast axis. When the fast and slow components emerge, they recombine and strike the reflecting surface as elliptically polarized light. The angle of incidence, measured from the surface normal, is 70°. The optical properties of the surface cause the polarization state of the incident light to be altered. In the simplest case, this polarization change can be directly related to the thickness and refractive index of an adsorbed layer. The altered and reflected beam passes through a rotatable analyzer prism (linear polarizer), finally striking a light sensitive phototransistor. The detector's electrical output, which is proportional to the beam intensity, is sent to a microprocessor. The intensity of the beam is a function of the azimuthal angles of the polarizer and analyzer prisms, as well as the optical properties of the adsorbed layer.

In a nulling ellipsometer, the microprocessor is programmed to minimize the intensity of the beam by alternately actuating stepper motors that rotate the polarizer and analyzer prisms about their respective azimuthal axes until the detector senses a minimum in intensity. The azimuthal angle at which this intensity minimum occurs is

reported with respect to the plane of incidence. With the compensator's fast axis fixed at a 45° angle relative to this plane, the polarizer can be positioned so that the incident beam becomes linearly polarized upon reflection. Therefore, extinction of the reflected beam can be achieved by orienting the analyzer so that its transmission axis lies perpendicular to that of the reflected beam. At the point of minimum intensity, the polarizer azimuthal angle yields the ellipsometric parameter Δ and the analyzer azimuthal angle yields the ellipsometric parameter Ψ. These parameters are fed into an IBM computer with an A/D board and stored with a time stamp for further data analysis.

2.3 Analysis of Ellipsometric Parameters Δ and Ψ

When a polarized beam of light is reflected from a surface, the polarization of that light changes. This change in polarization can be represented by the ratio of reflection coefficient for light polarized with electric vector parallel to the plane of incidence (r^p) to that for light polarized with electric vector parallel to the plane of the surface (r^s). Both reflection coefficients are complex numbers, conveying the change in amplitude and the change in phase of the light. For a bare, reflecting surface, they are mathematically expressed by the well-known Fresnel equations:

$$r_{12}^p = \frac{n_2\cos\theta_1 - n_1\cos\theta_2}{n_1\cos\theta_1 + n_2\cos\theta_2}$$
$$r_{12}^s = \frac{n_1\cos\theta_1 - n_2\cos\theta_2}{n_1\cos\theta_1 + n_2\cos\theta_2} \qquad (2.1)$$

where n_1 is the refractive index of the medium above the surface, n_2 is the refractive index of the surface, θ_1 is the angle of incidence, and θ_2 is the angle of refraction. The ratio of these reflection coefficients ρ can be written:

$$\rho = r^p / r^s = \tan\Psi \exp (i \Delta) \qquad (2.2)$$

where the ellipsometric parameter Δ symbolizes the differential change in phase of the reflected light for the electric vector parallel (p) and perpendicular (s) to the plane of incidence and the tangent of Ψ expresses the amplitude attenuation upon reflection for the two components. Equations (2.1) and (2.2) allow the refractive index of a bare reflecting surface to be calculated. In general, a substrate which not only reflects but also adsorbs light will produce a complex refractive index N equal to n - ik, where n is the real part of the refractive index and k is the imaginary part, termed the extinction coefficient.

With an adsorbed film, reflection coefficients are changed appreciably. Assuming a homogeneous, single-layer, adsorbed film model (Figure 2.2), Drude extended the Fresnel equations so that the total reflection coefficients (R^p, R^s) of a film-covered surface could be determined using the following equations:

$$R^p = \frac{r_{12}^p + r_{23}^p \exp D}{1 + r_{12}^p r_{23}^p \exp D}$$

$$R^s = \frac{r_{12}^s + r_{23}^s \exp D}{1 + r_{12}^s r_{23}^s \exp D} \qquad (2.3)$$

where

$$D = - 4\pi i n_2 \cos\theta_2 t / \lambda \qquad (2.4).$$

The Fresnel reflection coefficients symbolized by r_{12} refer to the reflection between the medium and the film. Those coefficients noted by r_{23} refer to reflection between the film and the substrate. The refractive index of the film is represented by n_2, θ_2 is the

angle of refraction, t is the thickness of the adsorbed film layer, and λ is the wavelength. The equation for the ratio of total reflection coefficients ρ

$$\rho = R^p / R^s = \tan\Psi \exp(i\Delta) \tag{2.5}$$

is the same as Equation (2.2). By measuring Δ and Ψ, with an adsorbed layer present, the root-mean-square thickness t and refractive index of the layer n_2 can be determined using Equations (2.3), (2.4), and (2.5). Due to the iterative process required to solve these equations, McCrackin's NBS program [4] is used in this investigation to match measured Δ and Ψ values to the closest thickness and refractive index values.

Throughout this thesis, film thicknesses and refractive indexes were determined by assuming a homogeneous, single-layer model. However, an adsorbed polymer film is not homogeneous, but instead, the polymer segment density usually decreases at increasing distances from the surface. McCrackin *et al.* [5] determined that the thickness calculated via the simple, homogeneous, single-film model was 1.7 times the root-mean-square thickness of a linear, exponential, or Gaussian profile of polymer segment density. Details of the polymer segment density are unimportant to this study, so the simplistic single-layer model introduces no detrimental artifacts. As a statistical measure, layer thicknesses inferred by this model probably come close to the first moment of the segment density profile relative to the surface plane.

Once the thickness and refractive index have been determined, the amount of polymer adsorbed onto the substrate A (mass/area) can be calculated using the equation:

$$A = (n_2 - n_1)\, t / (dn/dc) \tag{2.6}$$

where n_2 is once again the refractive index of the adsorbed film, n_1 is the refractive index of the solvent above the film, t is the thickness of the film, and dn/dc is the refractive index increment of the polymer solution. This equation assumes that in the adsorbed layer n_2 is a linear superposition of the refractive indexes of polymer and solvent.

When a polyelectrolyte is adsorbed onto a surface, determining the amount of polymer adsorbed becomes more complicated. Not only does the adsorbed layer contain polyelectrolyte chains and solvent molecules, it also contains counterions associated with the polymer and possibly small ions with the same sign as the polymer (Figure 2.3). Therefore, to determine the adsorbed amount (mole/area) for polymer, positive ion, and negative ion (Γ_p, Γ_+, and Γ_-, respectively), three steps are taken. First, Donnan equilibrium [6,7] is assumed. Donnan equilibrium describes the partitioning of the counterions between the bulk solution and the adsorbed layer. For this equilibrium to exist, the chemical potential of the salt in the bulk solution must be equal to the chemical potential of the salt in the adsorbed layer, as expressed by the following equation:

$$C_+^o C_-^o = \left[\frac{\Gamma_+}{t} + C_+^o \right] \left[\frac{\Gamma_-}{t} + C_-^o \right] \tag{2.7}$$

where $C_+{}^o$, $C_-{}^o$, and $C_p{}^o$ are the concentrations (mole/volume) of negative ions, positive ions, and polyelectrolyte respectively in the bulk solution. Second, charge neutrality must be imposed in the bulk solution and in the adsorbed layer. This neutrality can be expressed by the pair of equations:

$$C_+^o = C_-^o + \nu C_p^o$$
$$\Gamma_+ = \Gamma_- + \nu \Gamma_p \qquad (2.8)$$

The symbol ν represents the charge on each monomer repeat unit, and t is the thickness of the adsorbed layer. Assuming the additivity rule for osmotic coefficients [8], Miller and Frommer [9] derived the following equation from Equations (2.7) and (2.8):

$$C_+^o (C_-^o + \nu\phi_p C_p^o) = \left[C_-^o + \frac{\Gamma_- + \nu\phi_o\Gamma_p}{t} \right]\left[C_+^o + \frac{\Gamma_+}{t} \right] \qquad (2.9)$$

where ϕ_p and ϕ_o are the osmotic coefficients for the salt-free bulk polymer solution and the adsorbed layer. Finally, the Lorenz-Lorentz equation [6] relates composition to refractive index, a necessary step to determine Γ_p. This equation is shown below:

$$n_f = \left[\frac{\bar{M} + 2d\bar{R}}{\bar{M} - d\bar{R}} \right]^{1/2} \qquad (2.10)$$

where n_f is the refractive index of the film, $\bar{M}$ is the mean molecular weight, $\bar{R}$ is the mean molar refractivity, and d is the density of the adsorbed layer. $\bar{M}$ and $\bar{R}$ are given by

$$\bar{M} = \sum (x_{.i} M_i)$$
$$\bar{R} = \sum (x_i R_i) \qquad (2.11)$$

where x_i is the mole fraction of component i, and M_i and R_i are the corresponding component molecular weight and molar refractivity. The layer density can be expressed:

$$d = d_o + (M_+ - d_o V_+^o)\left(C_+^o + \frac{\Gamma_+}{t}\right) + (M_- - d_o V_-^o)\left(C_-^o + \frac{\Gamma_-}{t}\right) + (M_p - d_o V_p^o)\left(C_p^o + \frac{\Gamma_p}{t}\right) \qquad (2.12)$$

where d_o is the density of water, M_+, M_-, and M_p are the molecular weights, and V_+^o, V_-^o, and V_p^o are the molar volumes of cation, anion, and polyelectrolyte, respectively.

Inputting t into Equation (2.9) and assuming Γ_p values, n_f, Γ_+ and Γ_- can be determined using Equations (2.9), (2.10), (2.11), and (2.12). That value of Γ_p, minimizing the error between the calculated refractive index and the ellipsometrically-measured refractive index, is the actual amount of polymer adsorbed. The adsorbance value determined by this method equals that determined using a simple, single-layer model (see Equation 2.6) if dn/dc corresponds to dialysis dilution, or in other words, dilution at constant chemical potential of the salt.

2.4 Ellipsometer Solution Cell

A diagram of the ellipsometer solution cell constructed for *in situ* measurements of polymer adsorption is shown in Figure 2.4. This trapezoidal-shaped cell consists of two principal components, a base plate and a upper shell, which are sealed together by a Teflon O-ring with six screws around the periphery. Centered on the base plate is a raised Teflon platform onto which the adsorbing substrate is mounted. A thin Teflon bar is positioned over one edge of the surface to secure it to the platform by the tightening of two screws at either end of the bar.

The upper shell houses two removable, fused silica windows (diameter = 25 mm, thickness = 6.0 mm, parallelism = 5 arc seconds) which are inclined at an angle of incidence of 70° with respect to the base of the cell. This arrangement allows the laser beam to enter and exit the cell at normal incidence to the windows, preventing a change in the polarization of light when the beam strikes the windows. Six equally spaced screws and a window retainer ring hold each window to the cell body over a Teflon O-ring. The main purpose of this window attachment scheme is to reduce stress-induced birefringence. Another fused silica window at the top of the cell allows for correct alignment of the reflecting surface once the cell has been placed in the ellipsometer. This alignment employs an autocollimating telescope fastened to the ellipsometer midway between the polarizer and analyzer modules. Also positioned at the top of the cell are two filling ports. Rubber septa can seal these ports against the outside environment, preventing evaporation of solvent and allowing the cell to be purged with N_2.

Temperature control is very important for *in situ* ellipsometric measurements, as solvent refractive index varies greatly with temperature. The cell was therefore machined from aluminum to facilitate heat transfer, and the metal surfaces subsequently coated with Teflon to prevent corrosion (Berghof/America). The nonconductive Teflon coating isolates potentiostat functions by blocking current flow from solution to container. A Peltier element or thermoelectric heater/cooler (Melcor, CP1.4-127-06L) is positioned beneath the cell. A Teflon encapsulated thermistor (YSI, 10° K at 25° C), inserted through one of the cell's filling ports, provides data to a thermoelectric cooler controller (Alpha Omega, series 1 TC2) able to regulate temperature within +/- 0.2° C. To maintain temperature at 25° C, a steel plate was placed beneath the Peltier element to act as a heat sink. During operation above 25° C, a Watlow silicone rubber rectangular heater was placed in this position. A second temperature controller (Cole Palmer Digi

Sense, Model 2168-70) maintained the temperature of the heater near that desired for the cell itself.

If this ellipsometer solution cell were to be reconstructed, the following design improvements are suggested. First, the sample volume of the cell should be decreased to lessen the time for temperature equilibration. This feature would facilitate the study of adsorption kinetics. Second, the alignment window at the top of the cell could be lowered so that this window is not the highest point of the cell cavity, eliminating the problem of trapped air bubbles obscuring the alignment window. Finally, a viewing window mounted on the side of the cell and facing the operator is recommended, an alteration that would permit visual observations of the substrate during ellipsometric runs.

2.5 Verification of Ellipsometer Solution Cell Operation

The adsorption of polystyrene (PS) onto chromium from cyclohexane near the theta temperature was chosen as a test of the ellipsometer solution cell operation. This system was previously studied by Lee and Fuller [10,11] and Takahashi *et al.*[12], and our results are therefore to be compared to the ellipsometric thicknesses and adsorbances reported by these groups.

A 1 in. by 1 in. chrome ferrotype plate (Doran Enterprises) was first cleaned by immersing the plate in warm toluene for 15 minutes, dipping in chromic acid for one minute, rinsing thoroughly with distilled water, and finally passing through a flame. Immediately after this procedure, the mirror smooth surface was mounted on the base plate of the solution cell. The cell was then assembled and aligned in the ellipsometer.

Parameters Δ and Ψ of the freshly cleaned chrome ferrotype surface were measured under HPLC grade cyclohexane (Aldrich) ($n_{solvent} = 1.415$) once an equilibrium temperature of 35° C had been attained. From these values, the complex

refractive index of the surface N was determined to be 3.5791 - i 4.3905. A solvent volume of 30 milliliters was then siphoned out of the cell using a syringe and replaced with the same volume of a concentrated polymer solution, resulting in a final polymer concentration of 600 parts per million (ppm). This solution had been previously prepared by dissolving a narrow molecular weight distribution PS standard (Polymer Laboratories, molecular weight of 8.5×10^6) in cyclohexane at 45° C and then equilibrating the mixture at 40° C for 3 days to allow for complete dissolution. A concentration of 600 ppm was chosen because this value lies in the plateau region of the adsorption isotherm for this system [12].

Parameters Δ and Ψ are plotted as a function of time in Figures 2.5 and 2.6. McCrackin's FORTRAN computer program [4] was used to match each measured Δ and Ψ value to the corresponding adsorbed layer thickness and refractive index (Figure 2.7). A mean layer thickness of approximately 1200 Å was found with solvent present (Figure 2.8). This level is thought reasonable as the radius of gyration for PS in cyclohexane at 35° C has been reported at 870 Å [13,14] and the result compares well with previous studies [10-12]. In Figure 2.9, the refractive index of the adsorbed PS layer in the presence of cyclohexane is plotted as a function of time.

The amount of PS adsorbed was calculated using Equation (2.6). The refractive index increment dn/dc for polystyrene in cyclohexane at 35° C is 0.168 cm^3/g. As shown in Figure 2.10, a plateau adsorbance of 3.2 mg/m^2 was reached after a period of approximately 2 hours. The amount of polymer adsorbed compares favorably with the adsorbance value of 5.0 mg/m^2 reported by Takahashi *et al.* [12], the slight difference between results probably caused by variability in surface roughness or surface cleaning procedures.

2.6 Application of an Electric Surface Potential

A home-built potentiostat was used to control the potential applied to the adsorbing surface in our studies. Figure 2.11 illustrates the simple electronic circuit upon which this instrument was based. Three electrodes, which included a working electrode, reference electrode, and counter electrode, were connected to the potentiostat and then inserted into the ellipsometer solution cell (Figure 2.12). The working electrode, which is the adsorbing substrate, must be composed of an inert metal such as gold, platinum, or mercury to minimize electrochemical oxidation of the surface upon application of a voltage. In our experiments, a platinum foil (25 X 25 X 0.5 mm, 99.9985 % purity, Johnson Matthey), connected to the potentiostat ground with a flattened platinum wire, was used as the working electrode. Good physical contact between the flattened wire and the platinum surface was assured by pressing the pieces together beneath a Teflon bar screwed onto the raised platform of the cell base plate.

A miniature Ag/AgCl electrode (Cypress Systems, Inc.) was inserted through the top of the cell, with its tip positioned near the surface to reduce the voltage drop across the solution. Ideally, the counter electrode would be similar in size to the working electrode and centered directly above the working electrode to provide a uniform electric field. To avoid obstruction of the optical path of the laser beam, the counter electrode used in our experiments was a coiled 6 inch platinum wire (0.51 mm diameter, 99.95% purity, Fisher). The wire was inserted through the top of the ellipsometer cell and positioned just above the adsorbing surface, but not in the plane of reflection. The counter electrode was made of an inert metal to prevent the formation of extraneous substances by electrolysis; their desorption and readsorption at the working electrode would be deleterious.

A potentiostat operates with a feedback loop in which the potential between the reference and working electrodes is compared to an externally set value. If the

measured surface potential and the set value are different, current is passed through the counter electrode to the working electrode with the correct magnitude and sign to make this difference approach zero.

2.7 Summary

This chapter describes how a commercially available nulling ellipsometer was used to measure the thickness and refractive index of a neutral polymer layer on a metal surface with solvent present. The fundamental equations of ellipsometry were presented to demonstrate how the ellipsometric parameters Δ and Ψ could be converted into adsorbed layer thicknesses, refractive indexes, and adsorbances. The specifications of a custom ellipsometer solution cell, constructed to allow for the measurement of *in situ* polymer adsorption, were detailed. Experimental results for the adsorption of PS on chrome from cyclohexane at 35° C compared favorably with literature thickness and adsorbance values, suggesting that the newly built cell worked properly. Finally, equipment to apply a surface potential to the adsorbing metal substrate was outlined.

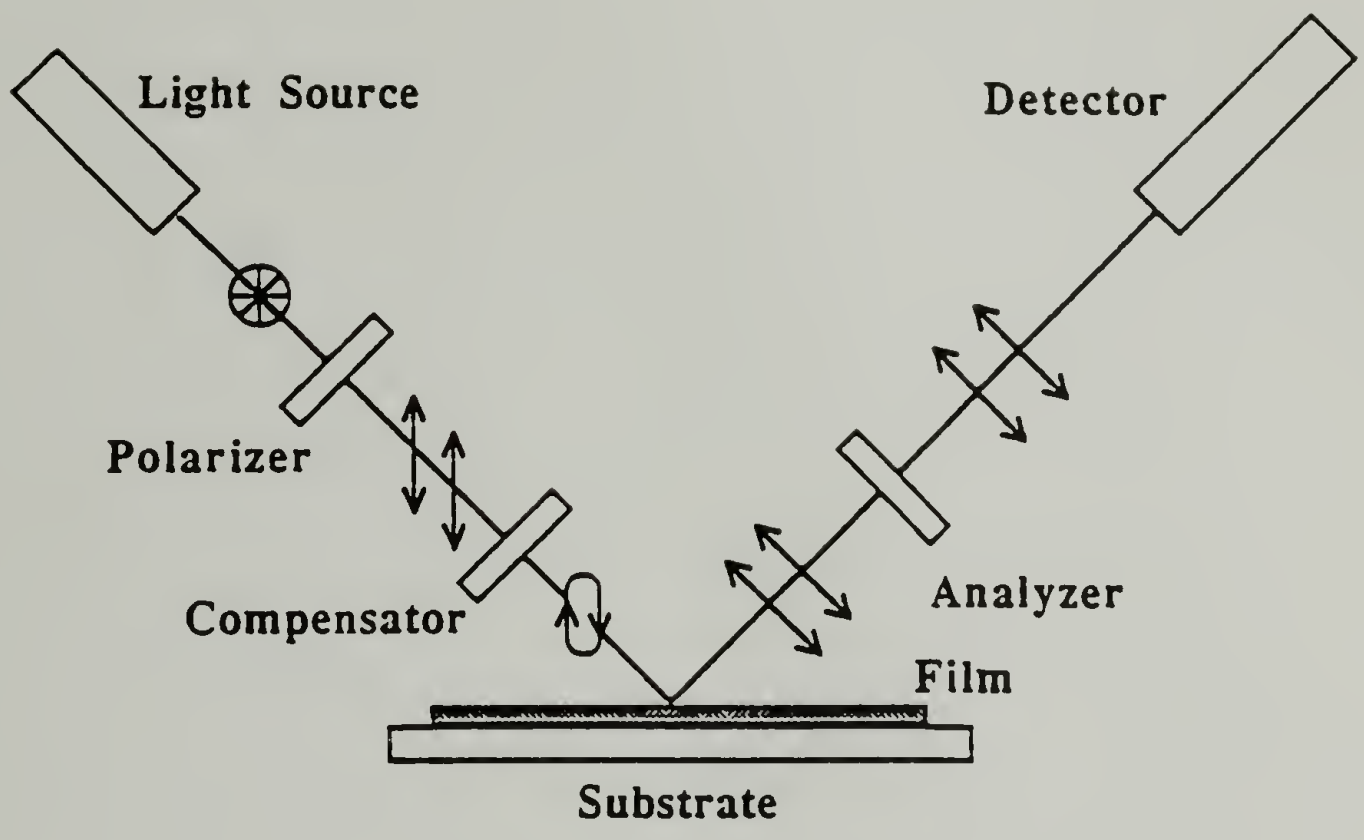

Figure 2.1. Components of an ellipsometer.

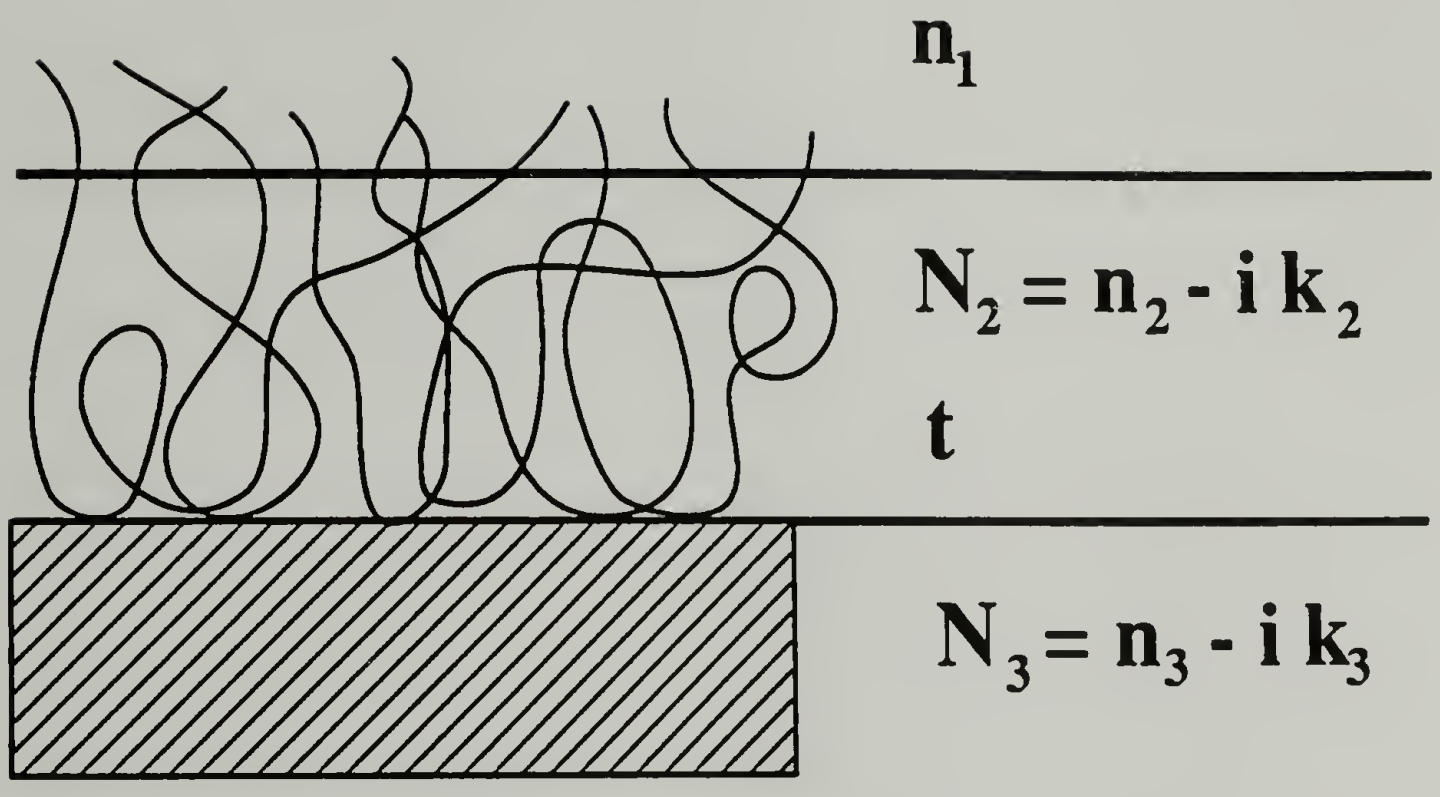

Figure 2.2. Homogeneous, single-layer, adsorbed film model.

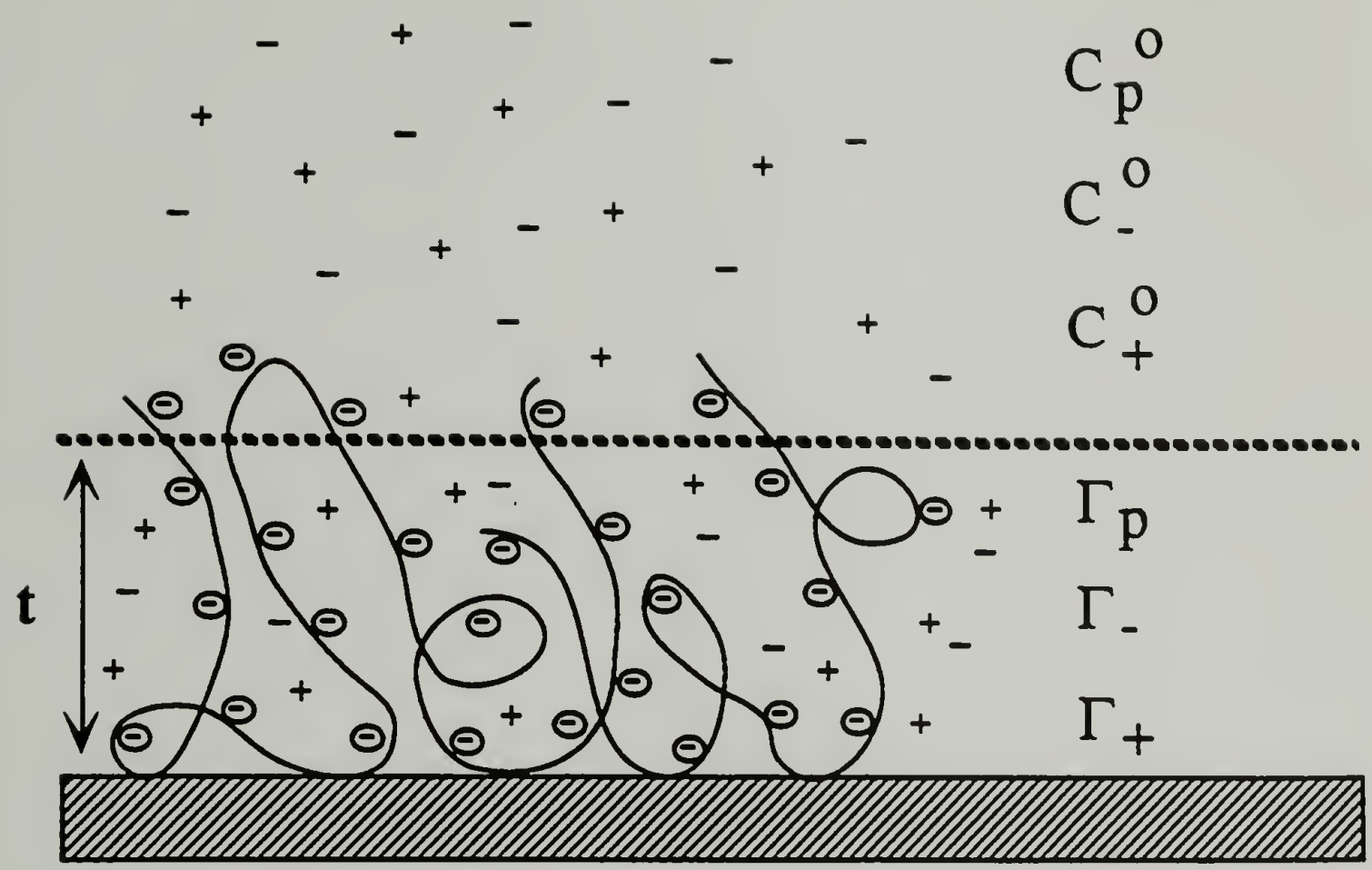

Figure 2.3. Polyelectrolyte Layer Model.

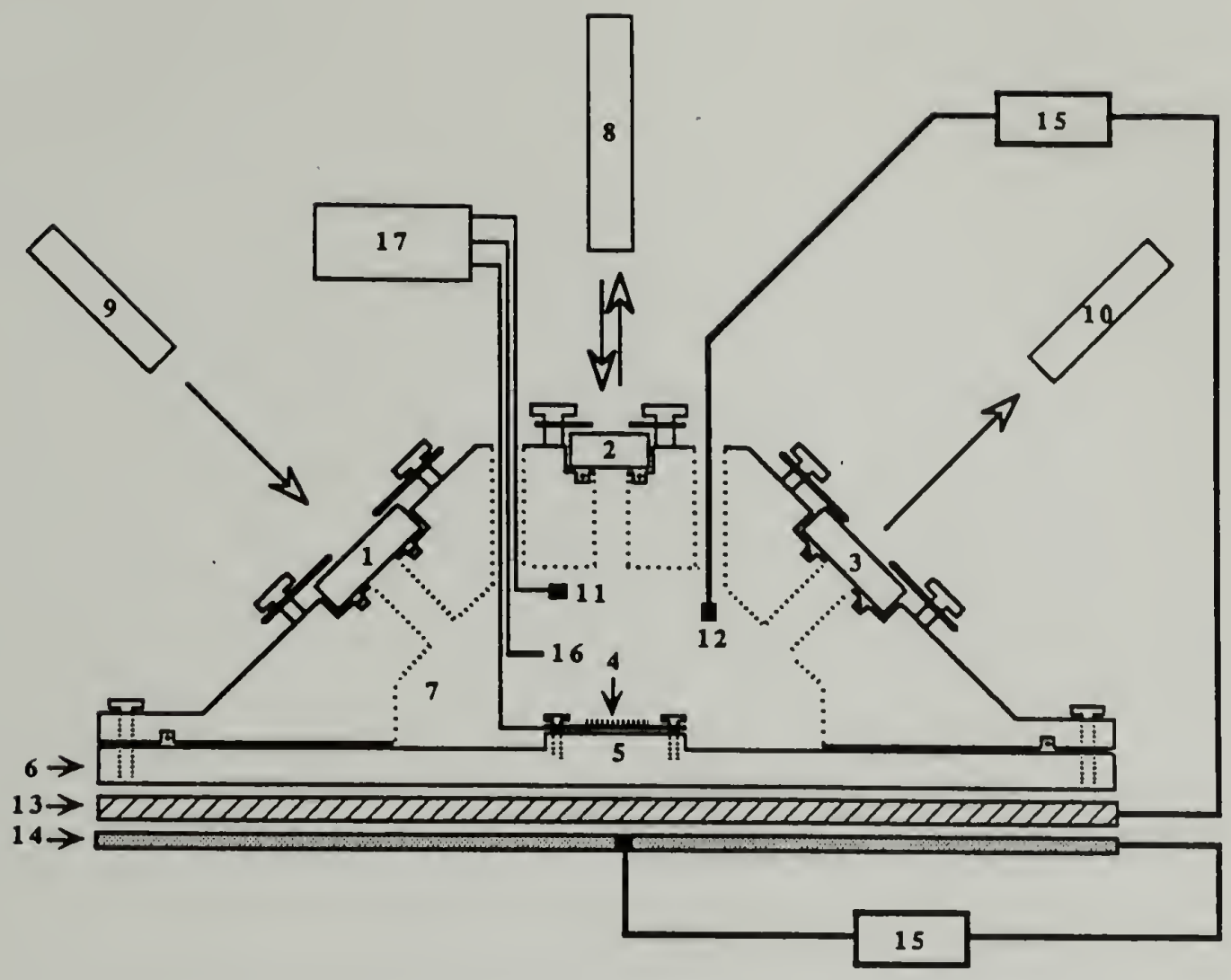

1. Entry window (optical flat)
2. Alignment window (optical flat)
3. Exit window (optical flat)
4. Sample (working electrode)
5. Tilt stage
6. Base plate
7. Solution chamber
8. Alignment beam and telescope
9. Incident beam and polarization optics
10. Reflected beam and polarization detection optics
11. Auxillary electrode
12. Thermistors
13. Peltier element
14. Woven wire resistive heater
15. Temperature controllers
16. Reference electrode
17. Potentiostat

Figure 2.4. Ellipsometer Solution Cell.

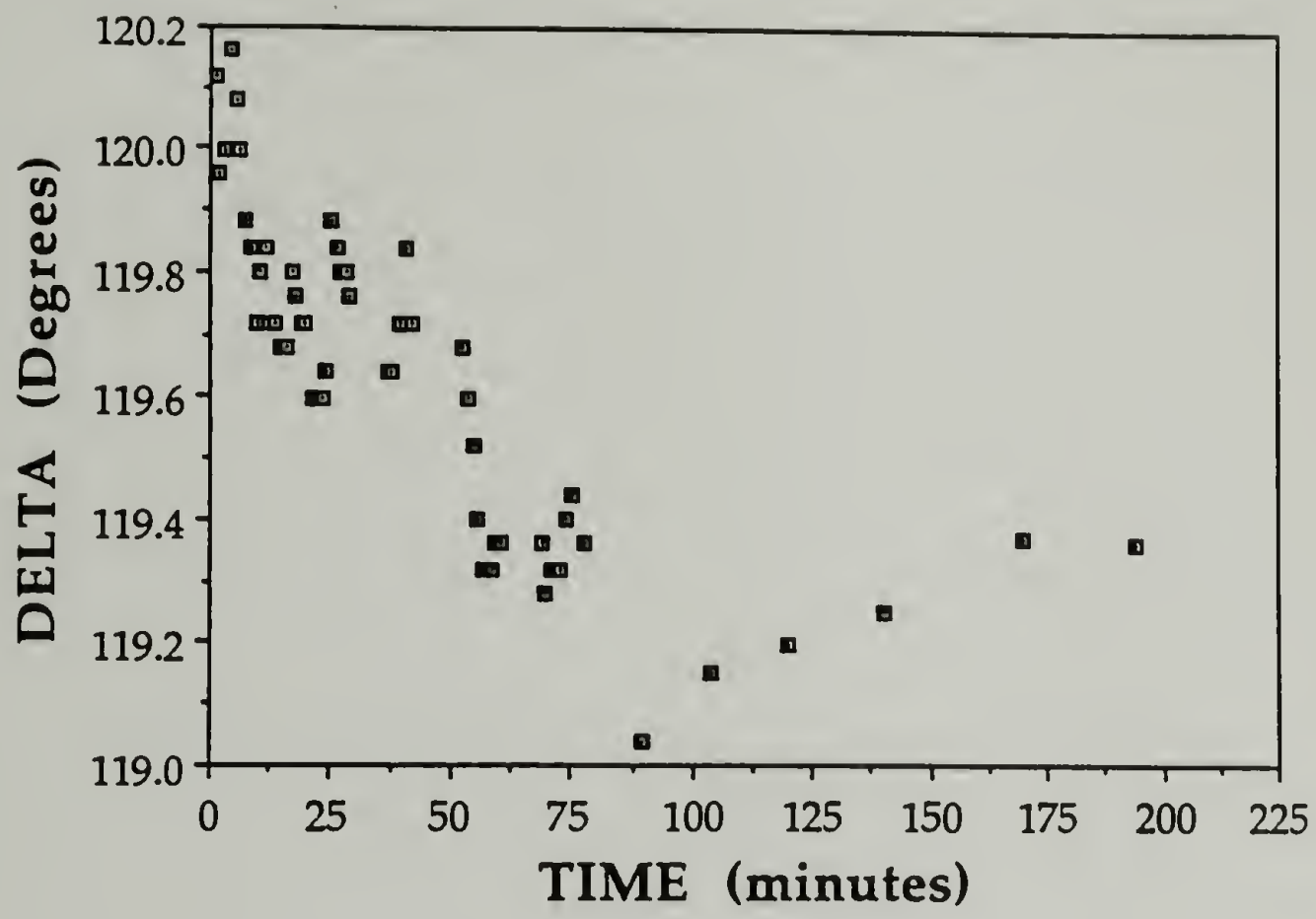

Figure 2.5. Delta as a function of time for PS (Mw = $8.5x10^6$) adsorbed onto chrome from cyclohexane at 35° C. The concentration of the polymer solution was 600 ppm.

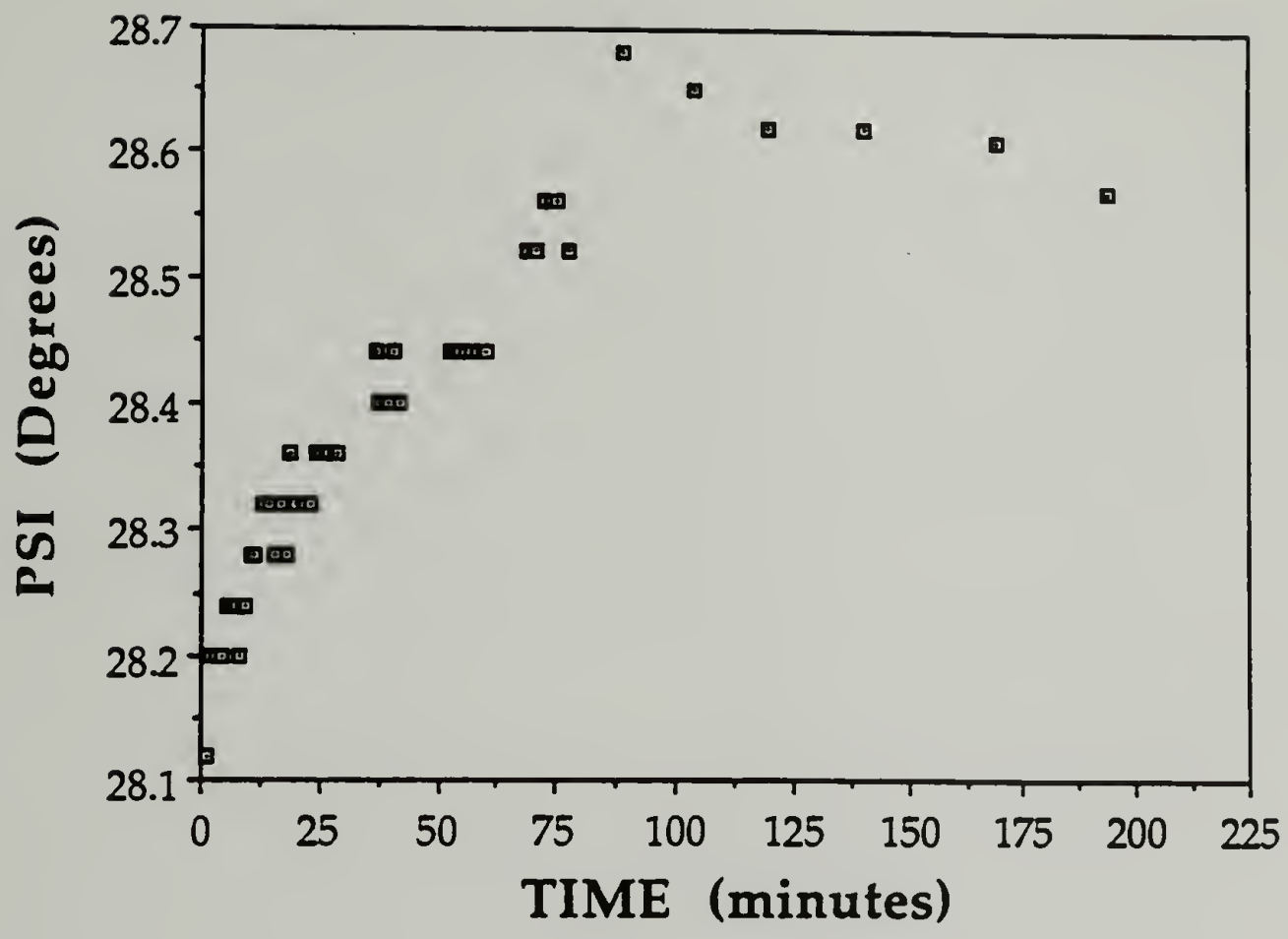

Figure 2.6. Psi as a function of time for PS (Mw = $8.5x10^6$) adsorbed onto chrome from cyclohexane at 35° C. The concentration of the polymer solution was 600 ppm.

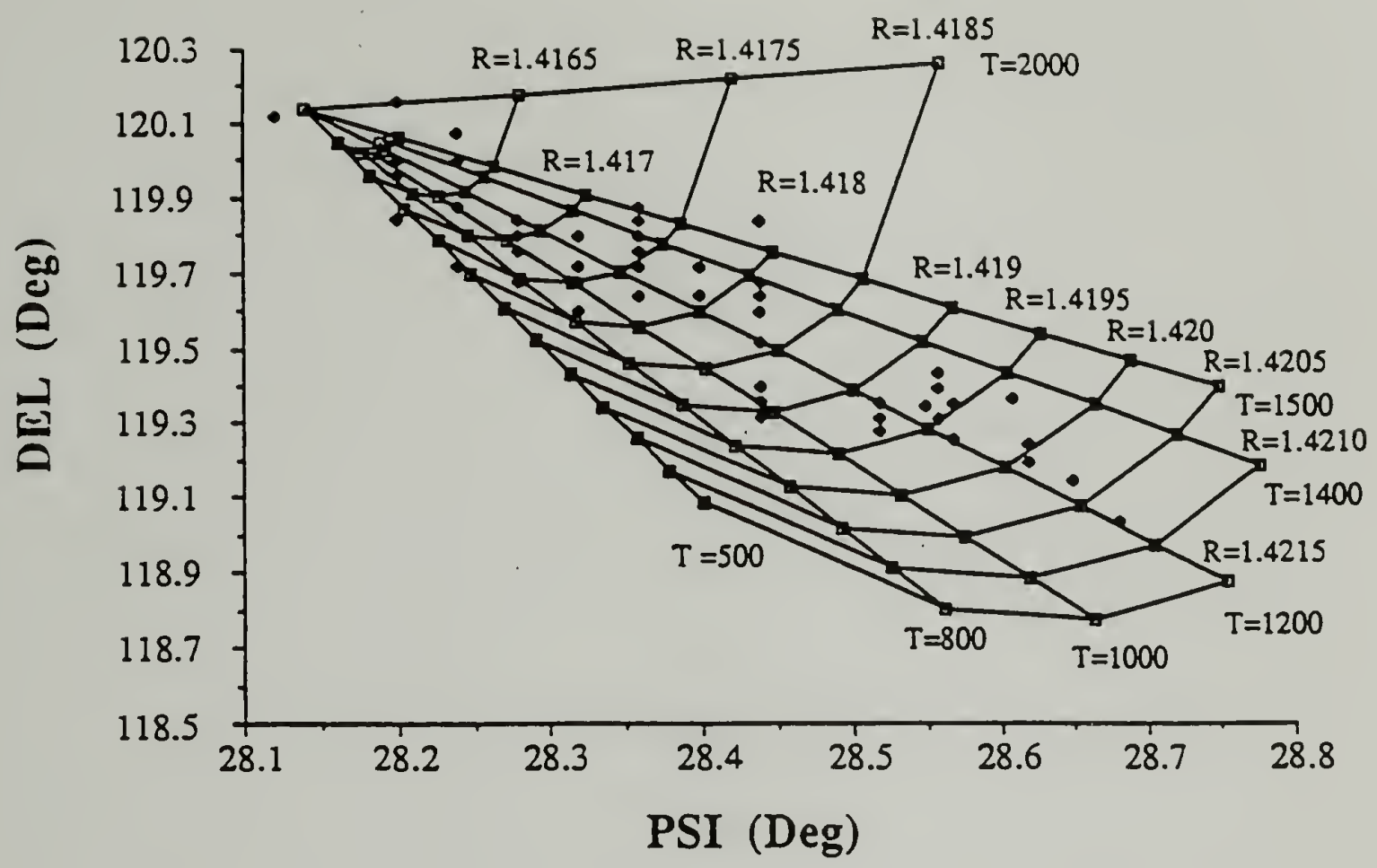

Figure 2.7. An illustration of how McCrackin's computer program matches each measured Delta and Psi value to the corresponding adsorbed layer thickness and refractive index.

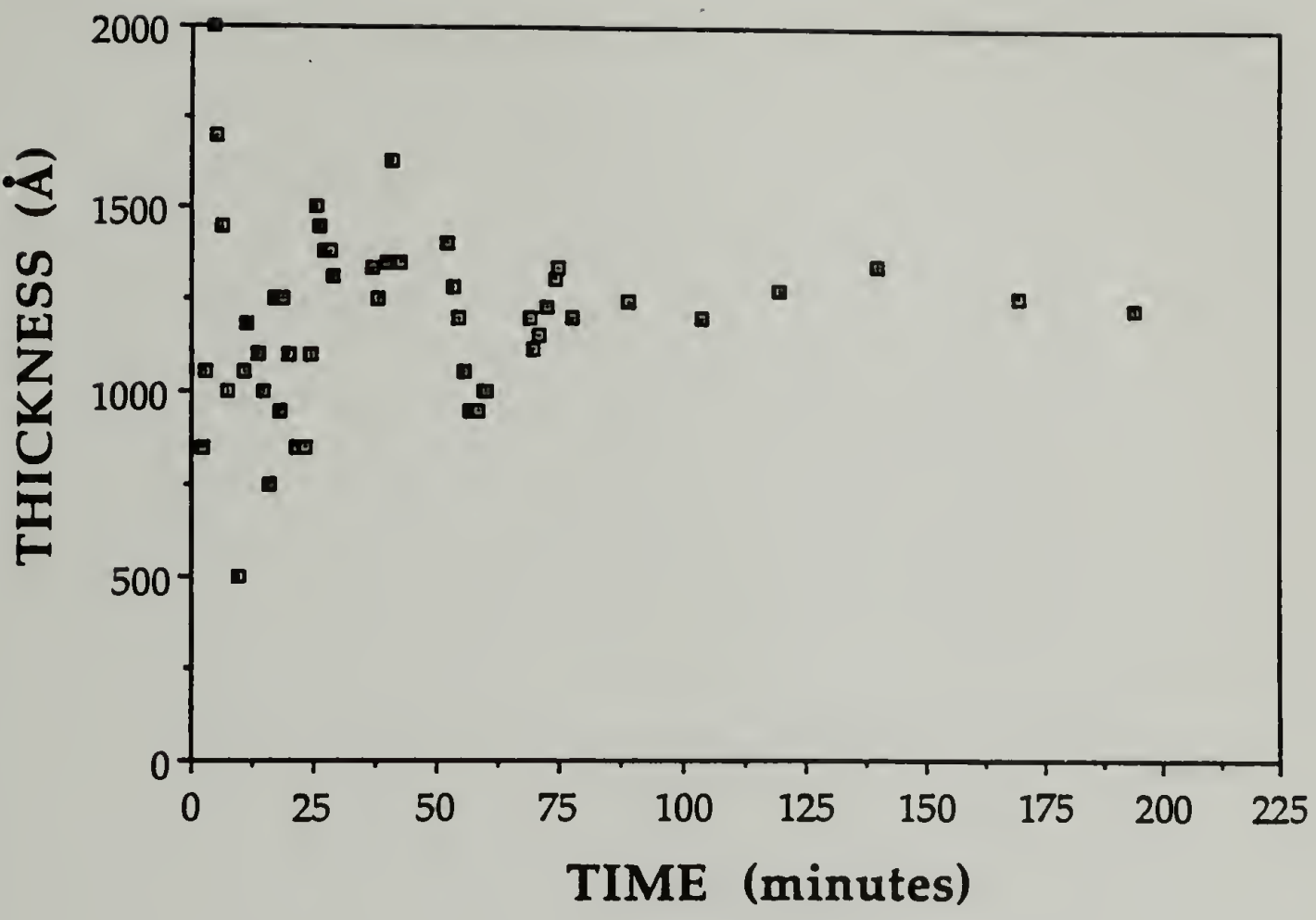

Figure 2.8. Thickness plotted as a function of time for an adsorbed PS (Mw = 8.5×10^6) layer on chrome with cyclohexane present at 35° C. A polymer concentration of 600 ppm was used.

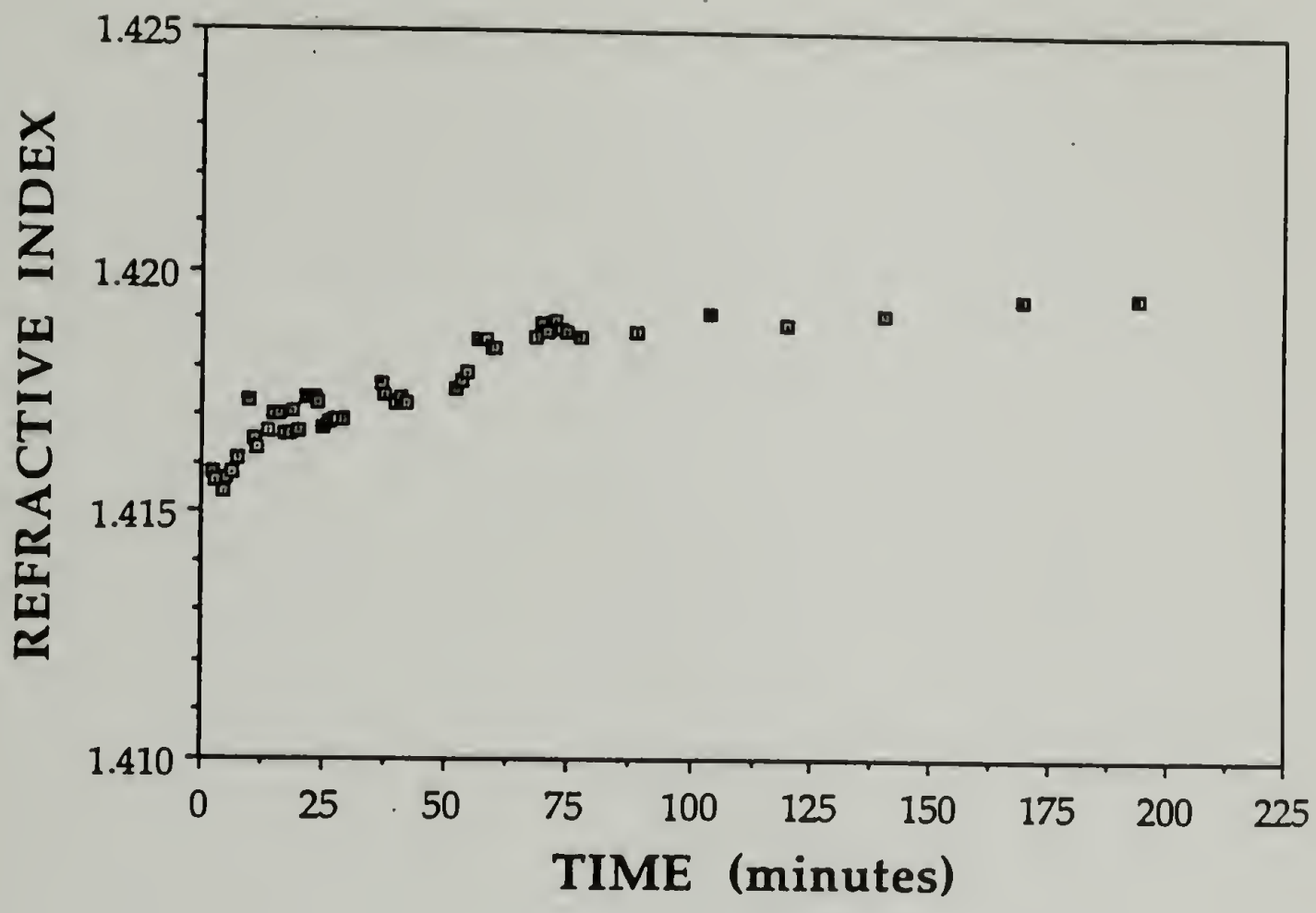

Figure 2.9 Refractive index of an adsorbed PS (Mw = 8.5×10^6) layer on chrome with cyclohexane present at 35° C as a function of time. A polymer concentration of 600 ppm was used.

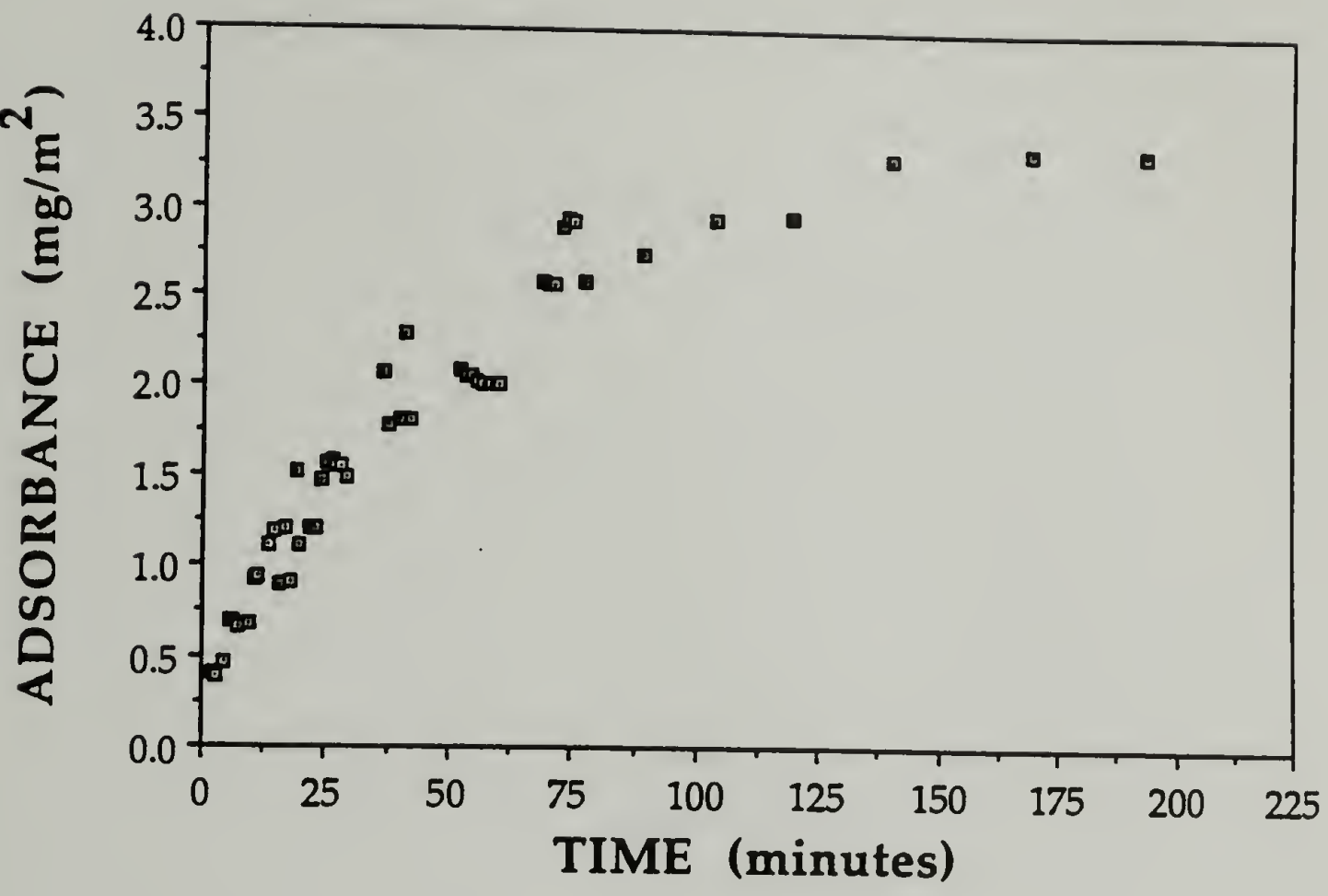

Figure 2.10. Adsorbance plotted as a function of time for PS (Mw = $8.5x10^6$) adsorbed onto chrome from cyclohexane at 35° C. A polymer concentration of 600 ppm was used.

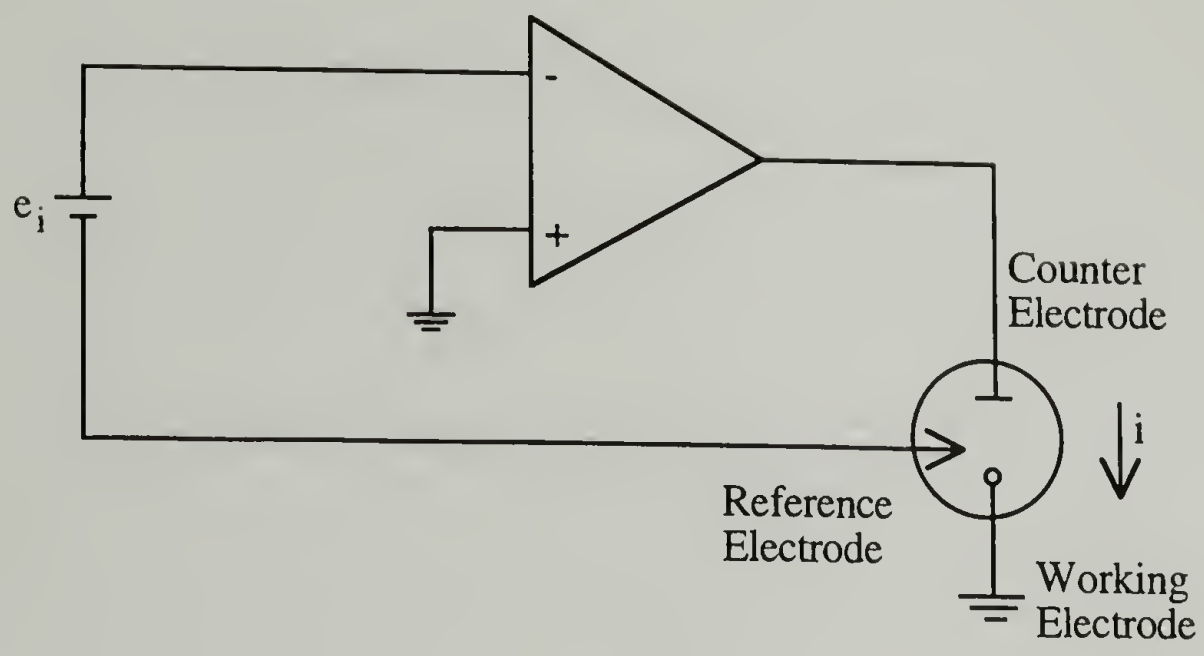

Figure 2.11. The simple electronic circuit upon which a potentiostat is based.

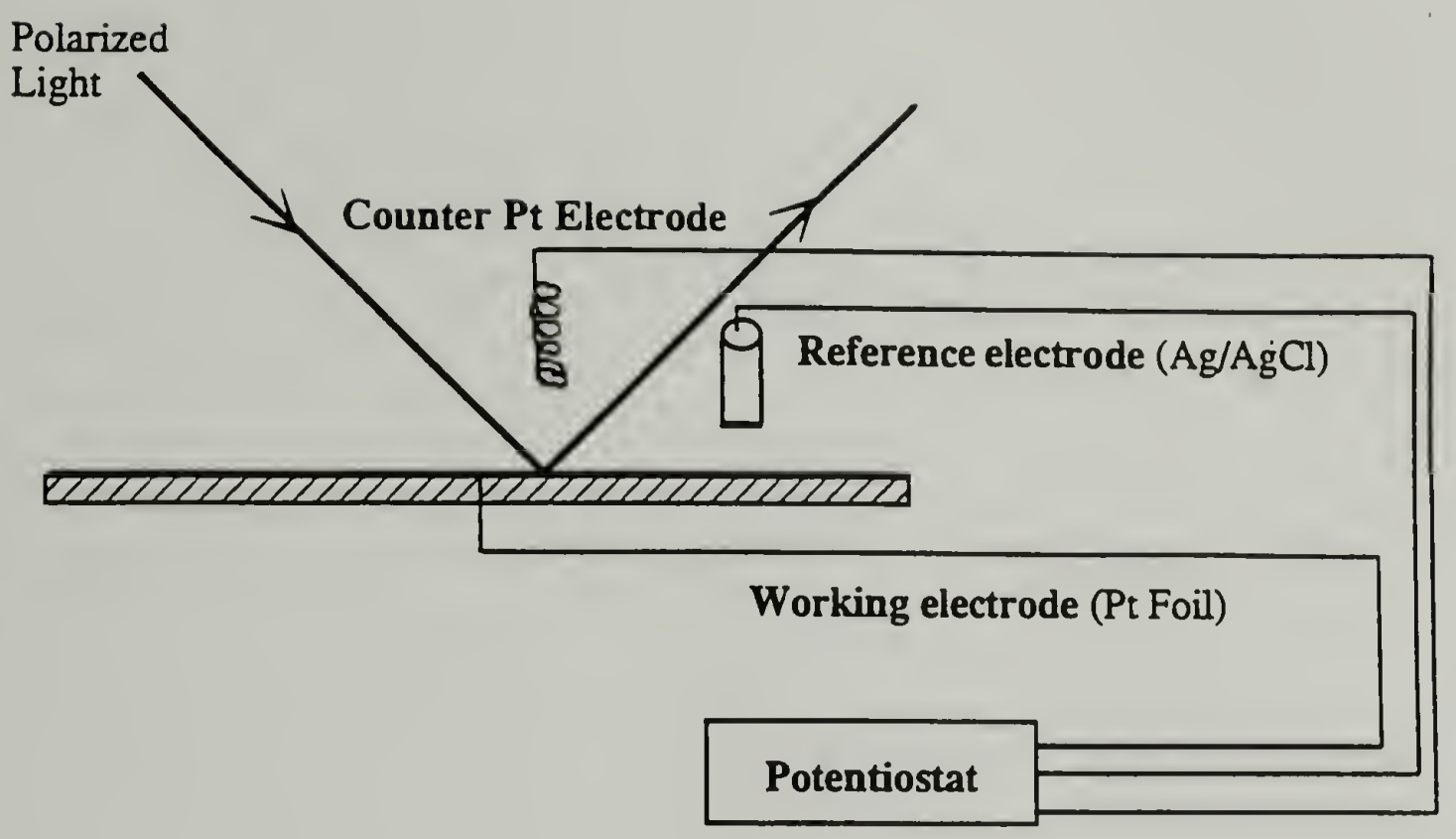

Figure 2.12. Application of a controlled potential at an adsorbing surface in the ellipsometer solution cell.

2.8 References

(1) McCrackin, F. L.; Passaglia, E.; Stromberg, R. R.; Steinberg, H. L. *Journal of Research of the National Bureau of Standards (Physics and Chemistry)* **1963**, *67A*, 363.

(2) Stromberg, R. R.; Passaglia, E.; Tutas, D. J. *Journal of Research of the National Bureau of Standards (Physics and Chemistry)* **1963**, *67A*, 431.

(3) Stromberg, R. R.; Passaglia, E.; Tutas, D. J. In *Ellipsometry in the Measurement of Surfaces and Thin Films*; NBS Misc. Publication #256: Washington, D.C., 1964; 281.

(4) McCrackin, F. L. *National Bureau of Standards Technical Note #479* **1969**.

(5) McCrackin, F. L.; Colson, J. P. In *Ellipsometry in the Measurement of Surfaces and Thin Films*; NBS Misc. Publication #256: Washington, D.C., 1964; 61.

(6) Stedman, M. *Chemical Physics Letters* **1968**, *2*, 457.

(7) Alexandrowicz, Z.; Katchalsky, A. *Journal of Polymer Science, Part A* **1963**, *1*, 3231.

(8) Atkins, P. W. In *Physical Chemistry*; Second Edition; W.H. Freeman and Company: San Francisco, 1982; 343.

(9) Miller, I. R.; Frommer, M. A. *Journal of Physical Chemistry* **1968**, *72*, 1834.

(10) Lee, J.-J.; Fuller, G. G. *Journal of Colloid and Interface Science* **1985**, *103*, 569.

(11) Lee, J.-J.; Fuller, G. G. *Macromolecules* **1984**, *17*, 375.

(12) Takahashi, A.; Kawaguchi, M.; Hirota, H.; Kato, T. *Macromolecules* **1980**, *13*, 884.

(13) Krigbaum, W. R.; Carpenter, D. K. *Journal of Physical Chemistry* **1955**, *59*, 1166.

(14) Outer, P.; Carr, C. I.; Zimm, B. H. *Journal of Chemical Physics* **1950**, *18*, 830.

CHAPTER 3

AN ELLIPSOMETRIC INVESTIGATION OF γ-GLOBULIN AT A PLATINUM ELECTRODE

3.1 Introduction

The role that electrostatic interactions play in polyelectrolyte adsorption is extremely complex, and therefore, a complete understanding remains elusive. These comparatively long-ranged interactions are thought to control the structure of a flexible polyelectrolyte layer at the solution/solid interface. However, few techniques provide insight into this adsorbed layer structure, and current knowledge is based on relatively few experiments. In our study, the effect of an applied surface potential on the thickness of an adsorbed polyelectrolyte layer is examined by combining *in situ* ellipsometry with voltammetry. Method development is crucial for obtaining accurate results. A first step is identification of a polyelectrolyte which could act as a control. This charged polymer should exhibit an extremely rigid conformation, preventing changes in adsorbed layer thickness with surface potential variations. A search of the literature pinpointed γ-globulin, a protein that possesses a rigid tertiary structure known to adsorb onto inert metal surfaces [1-4].

γ-Globulin, otherwise known as immunoglobulin G or IgG, is a Y-shaped molecule made up of 4 chains which are covalently linked together by 16 disulfide bonds (Figure 3.1). The 4 chains include 2 identical high molecular weight, or heavy, chains and 2 identical low molecular weight, or light, chains. The heavy chains originate at the Fc terminus (base of the Y), fold into the light chains located in the Fab portion of the molecule (arms of the Y), and extend to the Fab termini (tips of the Y).

Positioned at the Fab termini are chemically and structurally variable domains needed to form antigen-binding sites of great diversity. Constant domains are also present as they preserve the biological properties of each immunoglobulin class. The Fc regions and the Fab portion of the molecule are linked together by a flexible hinge allowing the Y-shaped γ-globulin molecule to become T-shaped under the influence of external factors. Compared to other proteins, γ-globulin has an extremely stable conformation, provided by the 16 disulfide bond linkages. Dimensions of this protein, given in Figure 3.1, were determined by Silverton *et al.* using X-ray crystallography [5]. Scanning tunneling microscopy gives comparable results [6,7]. Bovine γ-globulin has a reported molecular weight of 160,000 [8] and an isoelectric point of 6.8 [9]. The amphoteric nature of this biopolymer allows the charge on the molecule to be controlled by adjusting the pH of the solution. In addition to these hydrophilic groups, γ-globulin also contains hydrophobic regions which might provide an additional driving force for adsorption.

Blood proteins such as γ-globulin are known to adsorb onto artificial implants positioned in the cardiovascular system, causing thrombosis to occur [10]. The possible link between the surface charge of an implanted device and protein adsorption has long been examined [11-15]. The immobilization of proteins at electrically charged interfaces is also vital for technologies such as biosensors and immunoassays, which utilize electrochemical processes as a method of quantification [16-18]. Morrissey *et al.* [2] claimed a dependence of both protein conformation and adsorbance on an applied surface potential. However, other scientists were unable to relate protein adsorption to surface charge [12,13,19,20].

Because γ-globulin possesses a rigid tertiary structure, changes in protein conformation accompanying variation in applied surface potential appear improbable. Therefore, γ-globulin provides a control for our experiments, allowing a verification of the method by which ellipsometry can be combined with voltammetry to determine *in*

situ adsorbed layer thicknesses, refractive indexes, and adsorbances, none of which seem likely to vary with surface potential. Contrary to this expectation, Morrissey's ellipsometric results [2] suggest a change in adsorbed γ-globulin layer thickness and adsorbance with variation in applied surface potential.

3.2 Experimental

3.2.1 Materials

Bovine γ-globulin was purchased from Sigma Chemical Company (electrophoretic purity ~ 99%) and used without further purification. This protein is described in Table 3.1. Solutions were prepared by dissolving the protein in a phosphate buffer with a pH = 8.5 and an ionic strength I = 0.15 M. The buffer was made by dissolving reagent grade Na_2HPO_4 and $NaH_2PO_4 \cdot H_2O$ (Fisher) in ultra-pure, deionized water (Millipore Q, UF-OR). Buffered solutions were used because γ-globulin dissolved in 0.15 M, pH = 7.4 $NaClO_4$ gave irreproducible ellipsometric results, an effect likely due to small variations in the pH caused by the formation of hydrogen ions. Platinum foil (25 X 25 X 0.5 mm, 99.9985 % purity, Johnson Matthey) was used as the adsorbing surface. It was polished to a mirror finish with successively finer alumina grits (Buehler), ending with a particle size of 0.05 μm.

3.2.2 Instrumentation

A Rudolph Auto EL II nulling ellipsometer was used to monitor the adsorption of γ-globulin on the foil. A helium neon laser (wavelength = 632.8 nm) emitted an incident beam with the angle of beam incidence equal to 70°. *In situ* adsorption studies were carried out using the ellipsometer solution cell described in Section 2.4.

A three electrode potentiostat was used to apply the electric potential to the adsorbing surface. Details of this instrumentation are included in Section 2.6. Voltages

are reported with respect to a miniature Ag/AgCl electrode (Cypress Systems, Inc.) placed near the platinum surface. The counter electrode was a coiled 6 inch platinum wire (0.51 mm diameter, 99.95% purity, Fisher), also placed near this surface. The platinum foil itself was used as the working electrode.

3.2.3 Cleaning Procedure for the Platinum Foil

Before each experiment, the platinum surface was immersed in a 1:1 mixture of boiling sulfuric and nitric acid for 10 minutes to remove residual organic material. The surface was then rinsed with copious amounts of distilled water before mounting it in the ellipsometer solution cell. The cell was subsequently sealed and purged with N_2 to prevent interference from atmospheric CO_2. Following alignment of the cell in the ellipsometer, filtered (0.45 μm filter, Millipore Millex-HV) phosphate buffer was purged with N_2 and cannulated into the cell. Solution was allowed to reach an equilibrium temperature of 25° C (~ 8 hours). The surface was then cleaned electrochemically by cycling between -1.18 V and +1.32 V, potential extremes at which hydrogen ions are reduced and water is oxidized, respectively, in this buffer solution. Three ellipsometric measurements were taken at each extreme. Cycling continued until reproducible values for Δ and Ψ were determined at both potentials.

3.3 Effect of Initial Adsorbing Potential on γ-Globulin Adsorption

3.3.1 Experimental Procedure

After cleaning, the potential was lowered to -1.18 V and slowly raised to the selected potential at which γ-globulin adsorption was to be examined. Four initial adsorbing potentials were considered, -0.5, -0.4 V, 0.0 V, and +0.4 V. Ellipsometric measurements of the bare surface with only buffer present were first taken at the chosen

initial adsorbing potential to determine the complex refractive index of the bare platinum surface.

Using a syringe, 10 ml of the buffer solution was then removed from the cell and replaced by 10 ml of a concentrated bovine γ-globulin solution previously filtered through a 0.45 μm Millipore Millex-HV filter. The resulting protein concentration was 11.4 mg/ml, a concentration chosen to duplicate the conditions under which Morrissey *et al.* [2] detected adsorption. An ellipsometric measurement was taken immediately and then every 5 minutes thereafter until the variation in Δ and Ψ values became minimal (~4 hours). Constancy of Δ and Ψ suggested that an equilibrium temperature of 25° C was reached and a plateau in adsorbance attained.

3.3.2 Results

The complex refractive index N = n - ik of the bare platinum surface in the presence of phosphate buffer is first calculated from Δ and Ψ using McCrackin's NBS FORTRAN program (Section 2.3). This value of N is needed as a reference in determining the thickness and refractive index of the adsorbed γ-globulin layer. Figures 3.2 and 3.3 exemplify the time dependence of Δ and Ψ after γ-globulin is introduced to the platinum foil at 0.0 V. Similar curves are obtained when adsorbing γ-globulin at initial adsorbing potentials of -0.5, -0.4 V, and +0.4 V. Thicknesses and refractive indexes calculated from these Δ and Ψ values are shown in Figures 3.4 and 3.5. Next, the amount adsorbed is determined using Equation 2.6, which is repeated below:

$$A = (n_2 - n_1)\, t / (dn/dc)$$

where n_2 is refractive index of the adsorbed layer, n_1 is the refractive index of the buffered γ-globulin solution, t is the thickness of the adsorbed film, and dn/dc is the

refractive index increment of the γ-globulin solution. A value of 0.178 ml/g is used for the refractive index increment, as determined by differential refractometry (Otsuka Electronics, RM-102) at constant added salt dilution. The error in adsorbance calculated using dn/dc determined at constant added salt, as opposed to that determined at constant chemical potential, is less than 5% because the two dn/dc values differ by less than 0.01 ml/g [21]. Figure 3.6 shows the change in adsorbance with time.

The applied surface potential appears insignificant as far as the structure of the adsorbed layer is concerned. This finding is exemplified in Figures 3.7 and 3.8, where little difference can be detected in layer thickness and plateau adsorbance with variation in the initial potential at which the protein is adsorbed.

3.4 Effect of an Applied Surface Potential on an Adsorbed γ-Globulin Layer Ignoring Surface Oxidation/Reduction

3.4.1 Experimental Procedure

Following the experimental procedure described in 3.3.1, γ-globulin was adsorbed at a potential of 0.0 V. Once a plateau in adsorbance was attained, the buffered protein solution was siphoned out of the ellipsometer cell, which was rinsed with the phosphate buffer and filled with clean buffer solution containing no protein. Ellipsometric readings were again taken every 5 minutes until the variation in Δ and Ψ became minimal, a condition suggesting that an equilibrium temperature had again been reached. To determine the effect of an applied surface potential on the structure of the adsorbed protein layer, the potential was then decreased to -0.6 V. Ellipsometric measurements were taken at 5 minute intervals for a period of 30 minutes. The potential was then increased by 100 mV increments every 30 minutes up to a potential of +0.6 V and then decreased by 100 mV increments at 30 minute intervals back down to a

potential of -0.6 V. Ellipsometric measurements were constantly taken at 5 minute intervals.

3.4.2 Results

Values of Δ and Ψ of the clean platinum foil immersed in buffer at 0.0 V are used to determine the complex refractive index N of the surface. An adsorbed γ-globulin layer thickness of ~300 Å is calculated from the steady state values of Δ and Ψ for the protein-covered surface at the starting potential of 0.0 V. For the same layer, a plateau adsorbance of ~6.5 mg/m^2 is calculated using Equation 2.6. Upon replacement of the protein solution in the cell with clean phosphate buffer, the thickness of the adsorbed γ-globulin layer and the calculated amount of protein adsorbed do not change.

As the applied surface potential is cycled, Δ and Ψ change (Figures 3.9 and 3.10). Average values of Δ and Ψ are reported at each potential because measurements taken over the 30 minute time interval at any specific potential are not statistically different from one another. Assuming no surface oxidation/reduction, apparent adsorbed layer thicknesses and refractive indexes at potentials other than 0.0 V are calculated using N of the bare platinum foil at 0.0 V. As shown in Figure 3.11, the apparent thickness of the adsorbed protein layer appears to decrease from ~525 Å to ~25 Å when the potential is increased from -0.6 V to +0.6 V and to rise from ~25 Å to ~700 Å when the potential is lowered from +0.6 V to -0.6 V. The decrease in apparent adsorbed layer thickness associated with an increasing applied surface potential appears similar to that reported by Morrissey *et al.* [2]. As shown in Figure 3.12, the apparent refractive index of the adsorbed γ-globulin layer remains constant while the potential is increased from -0.6 V to +0.4 V. At potentials greater than or equal to +0.5 V, an abrupt increase in refractive index of the adsorbed layer is observed. The calculated values become unrealistically large, casting doubt on the ellipsometric analysis. When

the potential is subsequently lowered from +0.6 V to -0.6 V, the apparent refractive index of the layer decreases, attaining values similar to those previously found when the potential was raised.

Adsorbance appears to drop from ~6.5 mg/m^2 to ~ 5.0 mg/m^2 when the potential is first lowered from 0.0 V to -0.6 V (Figure 3.13). With a subsequent increase in potential from -0.6 V to +0.6 V, the apparent adsorbance remains constant until a high positive potential is reached, where an abrupt increase from ~ 5.0 mg/m^2 to ~7.0 mg/m^2 is observed. These results are similar to those reported by Morrissey *et al.* [2]. As the potential is lowered from +0.6 V to -0.1 V, the apparent adsorbance first increases slightly to ~8.0 mg/m^2 and then decreases to ~ 5.0 mg/m^2. The apparent adsorbance remains constant at ~5.0 mg/m^2 as potential is lowered further to -0.6 V. The adsorbance results become questionable when one recognizes that the amount of protein adsorbed at high positive potentials is greater than that amount adsorbed under the initial adsorbing conditions, even though no protein was present in the solution above the platinum surface.

3.5 Effect of an Applied Surface Potential on an Adsorbed γ-Globulin Layer Accounting for Surface Oxidation/Reduction

3.5.1 Experimental Procedure

Once the surface was electrochemically cleaned, the potential was lowered to -1.2 V and then increased by 100 mV steps to a potential of +1.3 V. At this stage, the potential was decreased by 100 mV increments, returning to the starting potential of -1.2 V. Three ellipsometric measurements were taken at each 100 mV step, with the average Δ and Ψ values reported. The voltage was again increased by 100 mV increments to a potential of -0.5 V. Using a syringe, 10 ml of the buffer solution was removed from the cell and 10 ml of a concentrated bovine γ-globulin solution added, producing a 11.4

mg/ml solution. After 4 hours, ellipsometric readings had stabilized. To determine the effect of surface potential, the applied potential was then increased by 100 mV increments every 30 minutes to a potential of +0.7 V, with ellipsometric measurements taken at 5 minute intervals.

3.5.2 Ellipsometric Results for a Clean Platinum Surface with Variation in Applied Surface Potential

The ellipsometric parameters of clean platinum immersed in the buffer alone are plotted as a function of applied surface potential in Figures 3.14 and 3.15. Reported Δ and Ψ values are an average of three complete potential cycles with measurements taken at each 100 mV step. Error bars reflect repeated cycling of potential. The observed changes in Δ and Ψ are indicative of the electrochemical processes that take place at the surface of the platinum electrode. These processes were deduced by Benziger *et al.* using infrared spectroscopy [22]. Appendix B contains cyclic voltammograms of the platinum surface under various conditions (Figures B.1 - B.3). At an applied surface potential of -1.2 V, the platinum surface is reduced, and the ellipsometric parameters Δ and Ψ both attain their maximum values. These values remain constant up to a potential of -0.2 V, suggesting that no electrochemistry occurs between -1.2 V and -0.2 V. However, when the surface potential is increased further, Δ and Ψ decrease due to the adsorption of OH (or O) on the surface. At a surface potential of ~+0.9 V, the electrolysis of water begins, causing O_2 to be produced [23,24]. The surface becomes fully oxidized, and Δ and Ψ reach their minimum values at a potential of +1.3 V. When the potential is once again decreased, OH (or O) begins to desorb from the platinum surface at a potential of -0.2 V, causing Δ and Ψ to increase. At potentials more negative than -0.4 V, the values of Δ and Ψ become constant and very close to those previously attained. The surface is once again reduced.

The potentials at which oxidation or reduction of the platinum surface occur in an aqueous environment are not universal, but specific to the pH at which the experiment is conducted. In this study, a pH of 8.5 was used. A more acidic solution would push the oxidation/reduction curves to more positive potentials, while a more basic solution would push these curves to increasingly negative potentials [22]. Figures B.4 - B.9 in Appendix B demonstrate the effect of pH on plots of Δ/Ψ as a function of applied surface potential. Between the two potential extremes, the values of Δ differ by ~1.8° , while the values of Ψ differ by ~0.16°. These changes in Δ and Ψ are similar to those reported in the literature [25-29] and greatly exceed the corresponding standard deviations of ±0.038° and ±0.013°, respectively, determined by averaging the standard deviations of the three ellipsometric readings taken at each applied potential.

The complex refractive index N of the platinum surface at each potential is calculated from the Δ and Ψ values plotted in Figures 3.16 and 3.17 using the McCrackin's NBS FORTRAN program. These Δ and Ψ (averages of three consecutive measurements taken at each 100 mV step) represent the final cycle of potential and are believed to better represent the state of the surface just before polymer adsorption than the averages obtained upon repeated cycling (Figures 3.14 and 3.15). These values are later used in determining adsorbed γ-globulin layer thicknesses and refractive indexes.

3.5.3 Ellipsometric Results for the Effects of Applied Potential on an Adsorbed γ-Globulin Layer

Ellipsometric parameters for the γ-globulin-covered platinum foil in the presence of the buffered protein solution are plotted as a function of applied surface potential in Figures 3.18 and 3.19. A comparison of Δ and Ψ obtained for the protein-covered platinum foil and those obtained for the bare platinum surface in the presence of buffer is shown in Figures 3.20 and 3.21. These ellipsometric parameters are further

compared in Appendix B (Figures B.10 - B.13). Because Δ and Ψ for the protein-covered surface during the 30 minute measurement period at each potential are not statistically different from one another, average Δ and Ψ values are used in determining the thickness and refractive index of the adsorbed γ-globulin layer at each potential. McCrackin's NBS program is employed to calculate the adsorbed γ-globulin layer thickness and refractive index at each applied potential using a single layer model and the Δ and Ψ values for the bare surface at the same potential. Results are shown in Figures 3.22 and 3.23. Error bars are also determined via McCrackin's program by inputting the standard deviations for Δ and Ψ (±0.038° and ±0.013°, respectively) as the experimental error. The true thickness and refractive index values lie within these calculated limits with a 95% probability. An average adsorbed γ-globulin layer thickness of ~ 250 Å is measured. No effect of applied surface potential on the thickness of an adsorbed protein layer is observed within the error of this experiment. These inferences directly contradict those previously reported by Morrissey *et al.* [2].

The amount of γ-globulin adsorbed onto the platinum surface from the buffered protein solution is calculated at ~7 mg/m^2 using Equation 2.6. Once a plateau in adsorbance is reached at the initial adsorbing potential, variation in applied surface potential does not change the amount adsorbed (Figure 3.24). The abrupt increase in adsorbance at high positive potentials, which Morrissey *et al.* [2] reported, is not observed in these experiments.

3.6 Discussion

3.6.1 Evidence for the Oxidation/Reduction of the Platinum Surface After Polymer Adsorption

The thickness, refractive index, and adsorbance returned by ellipsometry for an adsorbed layer are strongly affected by the optical properties assumed for the bare

surface. Previous researchers calculating thicknesses and adsorbances [2,25,30-32] ignored changes in the near-surface refractive index of a metal substrate as surface potential is varied. The claim has been put forward that changes in the optical properties of a platinum foil are insignificant after a protein layer is attached, even when the potential is varied within ranges where the bare surface is known to be oxidized and reduced. Under this claim, the adsorbed polymer is thought to completely passivate the metal surface, thereby preventing oxidation/reduction.

To convince the reader of this argument's faultiness, several lines of evidence will be presented. First, observation of γ-globulin adsorption at a series of discrete applied surface potentials finds no accompanying variations in layer structure. Thus, there is no obvious driving force for changes in layer thickness or adsorbance as potential is continuously varied for a single layer. Due to the rigid tertiary structure of γ-globulin, thickness invariance is expected. As discussed in 3.3.2 and illustrated in Figure 3.7, a layer thickness of ~ 275 Å is observed for γ-globulin adsorbed at steady potentials between -0.5 V and +0.4 V; this adsorption protocol imposes a steady surface chemistry before, during, and after polymer adsorption. In contrast, other experiments are conducted with surface potential varied after the polymer is introduced and adsorbed to steady state (3.5.2). Close agreement between the two experiments is only attained when surface oxidation/reduction is taken into account. For example, an adsorbed layer thickness of ~ 250 Å is determined for γ-globulin adsorbed at -0.5 V; the thickness of this layer remains unchanged as potential is increased by 100 mV increments to +0.7 V, a trend shown in Figure 3.22. If surface oxidation/reduction is ignored (3.4.2), as alternatively supposed in Figure 3.11, layer thickness decreases with increasing potential, an improbable result given the trends reported in 3.3.2. Similarly, adsorbances for the two protocols can be compared. When γ-globulin is initially adsorbed at potentials between -0.5 V and +0.4 V, an average adsorbance of ~ 6.8

mg/m^2 is determined, as depicted in Figure 3.8. Taking into account oxidation/reduction, a comparable adsorbance of ~7.0 mg/m^2 is measured irrespective of surface potential for a layer adsorbed at -0.5.V and subjected to potential variations between -0.5 V and +0.7 V. This result is shown in Figure 3.24. The near exact overlap of adsorbances between Figures 3.8 and 3.24 strongly suggests that surface chemistry continues after polymer adsorption has reached steady state.

A second evidence against surface passivation is the striking resemblance between the shape of the Δ versus applied potential curve for the bare platinum surface (Figure 3.14) and that for the protein-covered platinum surface (Figures 3.9 and 3.18). This similarity is also observed in the Ψ versus applied potential curve for the bare platinum surface (Figure 3.15) and that of the protein-covered platinum surface (Figures 3.10 and 3.19). Changes in Δ and Ψ for the bare surface can only be attributed to the electrochemical processes that take place at the surface. Logic would suggest that similar trends observed in Δ and Ψ for the protein-covered surface would arise from the same processes.

Still another evidence is the calculated refractive index of adsorbed γ-globulin layers, which becomes unrealistically high at large positive potentials when surface oxidation/reduction is ignored. Such unphysical refractive indices are found in Figure 3.12 at potentials more positive than +0.1 V. Figure 3.13 unveils a last evidence, unrealistically large adsorbances in the same positive potential range. If oxidation/reduction is ignored, calculated adsorbance may even exceed the adsorbance measured after the overlying solution is replaced by solvent. With no protein source, these high adsorbances are certainly incorrect.

Although these four pieces of evidence do not separately suffice to disprove the theory of surface passivation, together they provide an overwhelming unfavorable case. In contrast, the assumption of no passivation, which has been asserted in drawing

Figures 3.22-3.24, can simply and consistently explain all data. Unless water mobility is extraordinarily attenuated by adsorbed protein, there appears no obvious physical reason why surface oxidation and reduction should not proceed beneath a protein layer at a rate comparable to a bare surface. The question should not be whether passivation occurs or not but rather the extent to which the adsorbed protein can modify the ultimate level of oxidation/reduction. The present data suggest that no modification is a better first approximation than complete passivation.

3.6.2 Role of Electrostatic Interactions

The role that electrostatic interactions play in the alteration of an adsorbed γ-globulin layer appears to be minimal, as adsorbed layer thicknesses and adsorbances remain constant even when the protein is adsorbed at different initial surface potentials (Figures 3.7 and 3.8). In addition, no change in adsorbed layer thickness or adsorbance is observed with variation in applied surface potential once γ-globulin is adsorbed (Figures 3.22 and 3.24). Therefore, measurement of the potential at which the surface has zero charge (PZC) was not essential. Literature values for the PZC for platinum in basic solutions are found to range between -0.2 and -0.5 V [33-36]. However, this potential is highly dependent on the medium in which the metal surface is immersed as well as the crystal face which dominates [24]. At a pH of 8.5, γ-globulin is known to carry a net negative charge due to the dissociation of the carboxyl groups above its isoelectric point. Locally, however, the protein carries both positive and negative charges which may interact with the surface. Although variations in applied surface potential should alter the electrostatic interactions between the platinum surface and the charged protein molecules, these changes did not manifest themselves in measurable structural alterations of the adsorbed protein layer. This result can most likely be attributed to the rigid conformation of γ-globulin.

3.6.3 Structure of the Adsorbed γ-Globulin Layer

The effect of adsorption on the conformation of a γ-globulin molecule can be inferred if the molecular dimensions of this protein in solution are known. In our experiments, an ellipsometric thickness of ~250 Å is determined for the adsorbed γ-globulin layer on platinum. This thickness suggests that γ-globulin retains its native conformation upon adsorption, since a hydrodynamic radius of 120 Å is measured using dynamic light scattering (DLS) (ALV/DLS-5000) (See Appendix B, Figure B.14). Variation in applied surface potential most likely does not result in conformational change of the adsorbed protein molecule.

In an effort to further elucidate the structure of the adsorbed γ-globulin layer, a comparison is made between the experimentally determined amount of protein adsorbed and that calculated using the molecular dimensions of 235 x 44 x 44 Å and the known molecular weight [37-39]. If a compact, uniform adsorbed monolayer is assumed, an adsorbance of 2.7 mg/m^2 can be estimated for γ-globulin molecules adsorbed in a side-on arrangement. In contrast, if the molecules are adsorbed in an end-on arrangement, the amount of protein adsorbed is 13.7 mg/m^2. In our experiments, the amount of γ-globulin adsorbed is ~7 mg/m^2. This value lies somewhere between the two calculated extremes, suggesting that adsorbed γ-globulin molecules are positioned in a tilted arrangement or with a statistical variation of tilt angle. Surface potential variations do not change the amount of γ-globulin adsorbed, and therefore, one can speculate that the protein molecules do not reposition themselves upon variation of the applied electric field.

3.7 Conclusions

When analyzing ellipsometric data to determine adsorbed layer thickness and refractive index, as well as the amount of polymer adsorbed, it is crucial to take into

account the oxidation/reduction of the surface at the relevant applied surface potentials. In following this procedure with platinum, no change in the thickness of an adsorbed γ-globulin layer with variation in surface potential is observed. In addition, once a plateau in adsorbance of γ-globulin at a specified potential is reached, varying the potential does not change the amount of protein adsorbed. From these results, the structure of the adsorbed γ-globulin layer can be inferred. γ-Globulin appears to adsorb onto the platinum surface in its native conformation. Upon variation of the applied surface potential, no alteration in the structure of the adsorbed layer is observed. This result can be attributed to the extremely stable conformation of γ-globulin, resulting from 16 disulfide bond linkages.

Table 3.1. Description of γ-Globulin.

General Properties	
Molecular weight[a]	160,000
Isoelectric point[b]	pH 6.8
Composition (Amino Acid Groups)[c]	
Nonionic groups (serine, threonine, alanine, proline, valine, etc.)	74 %
Anionic groups (aspartic acid, glutamic acid)	17 %
Cationic groups (lysine, arginine, histidine)	9 %

[a]Andrade *et al.* [8]. [b]At the isoelectric point, the net charge of γ-globulin is zero. Johnson *et al.* [9]. [c]The structure is as follows:

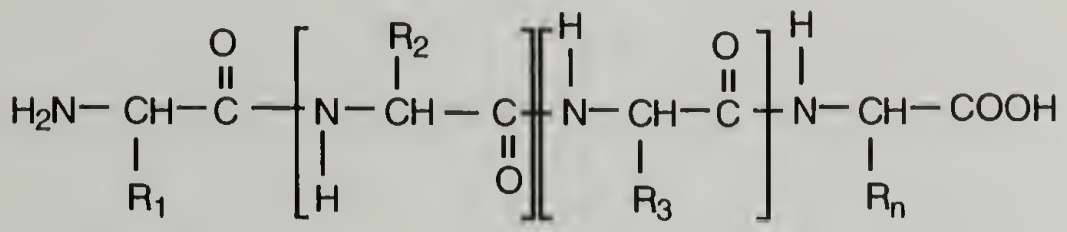

where R_n = amino acid group

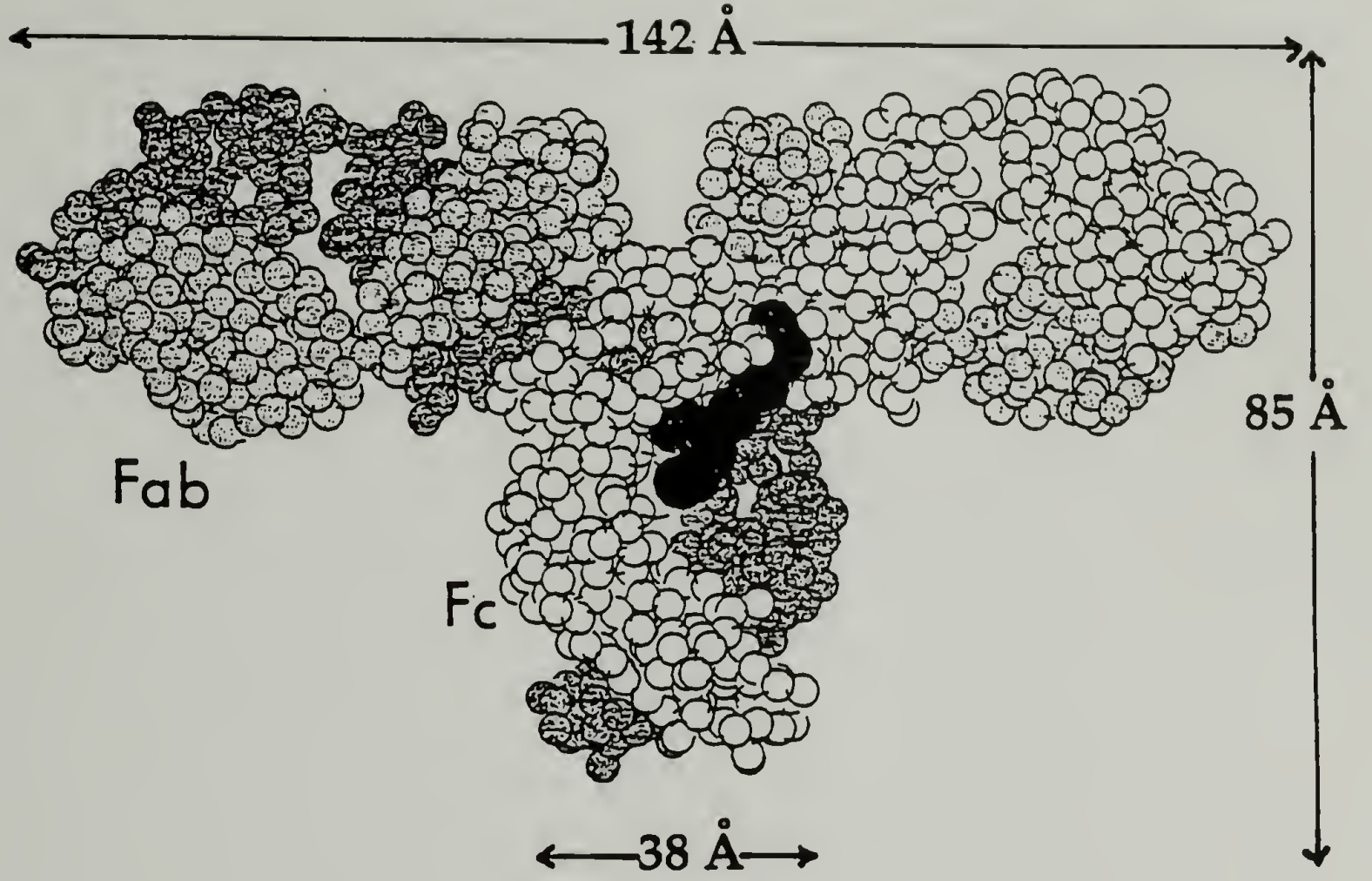

Figure 3.1. The structure of γ-globulin as suggested by Silverton *et al.* [5]. The two heavy chains are shown in white and dark gray. The two light chains are lightly shaded. The black spheres represent the individual hexose units of the complex carbohydrate. The dimensions given were determined by Silverton *et al.* [5] using X-ray crystallography.

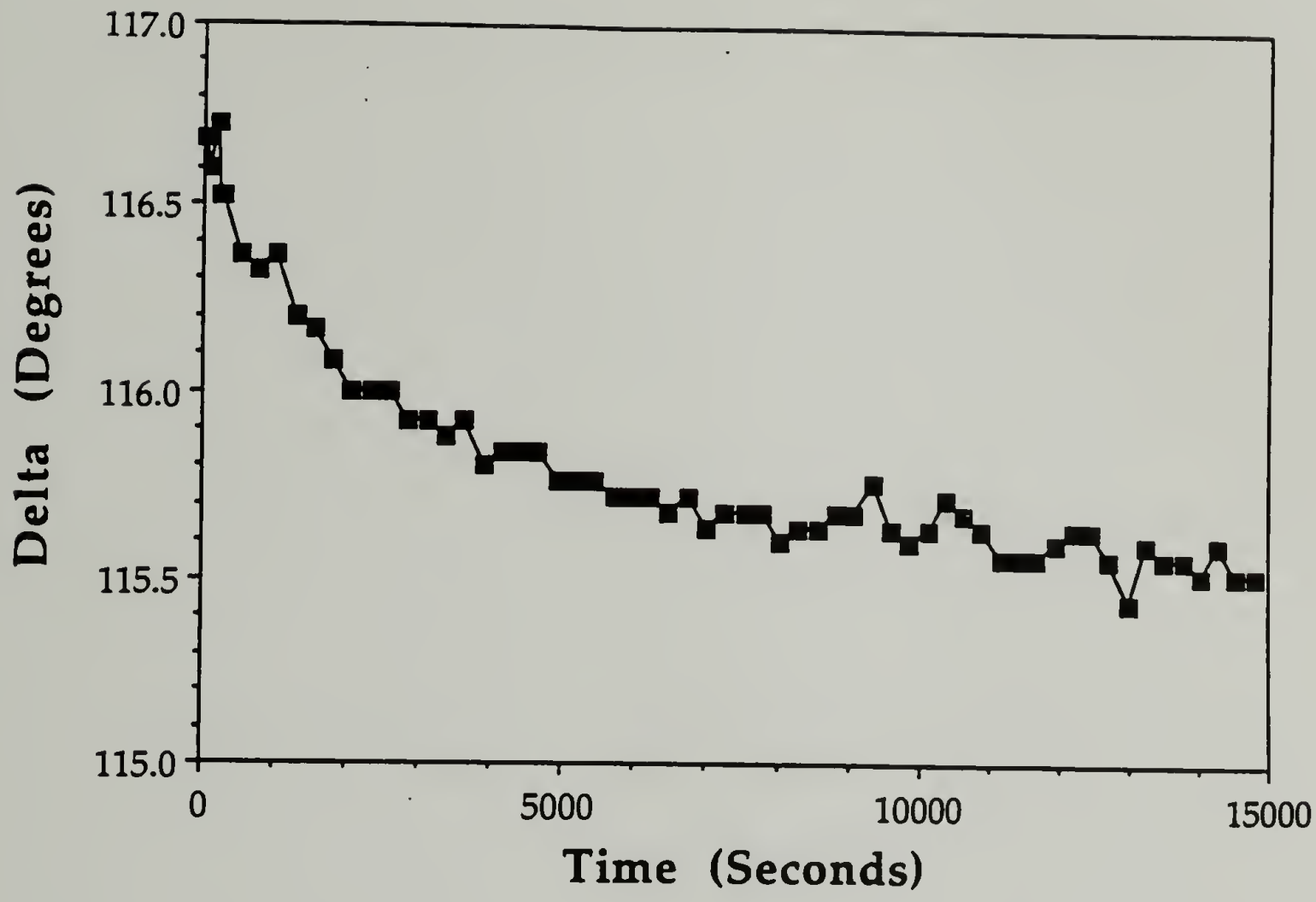

Figure 3.2. Delta plotted as a function of time for the adsorption of γ-globulin on platinum from a sodium phosphate buffer solution (pH = 8.5, I = 0.15 M) at 25° C and 0.0 V.

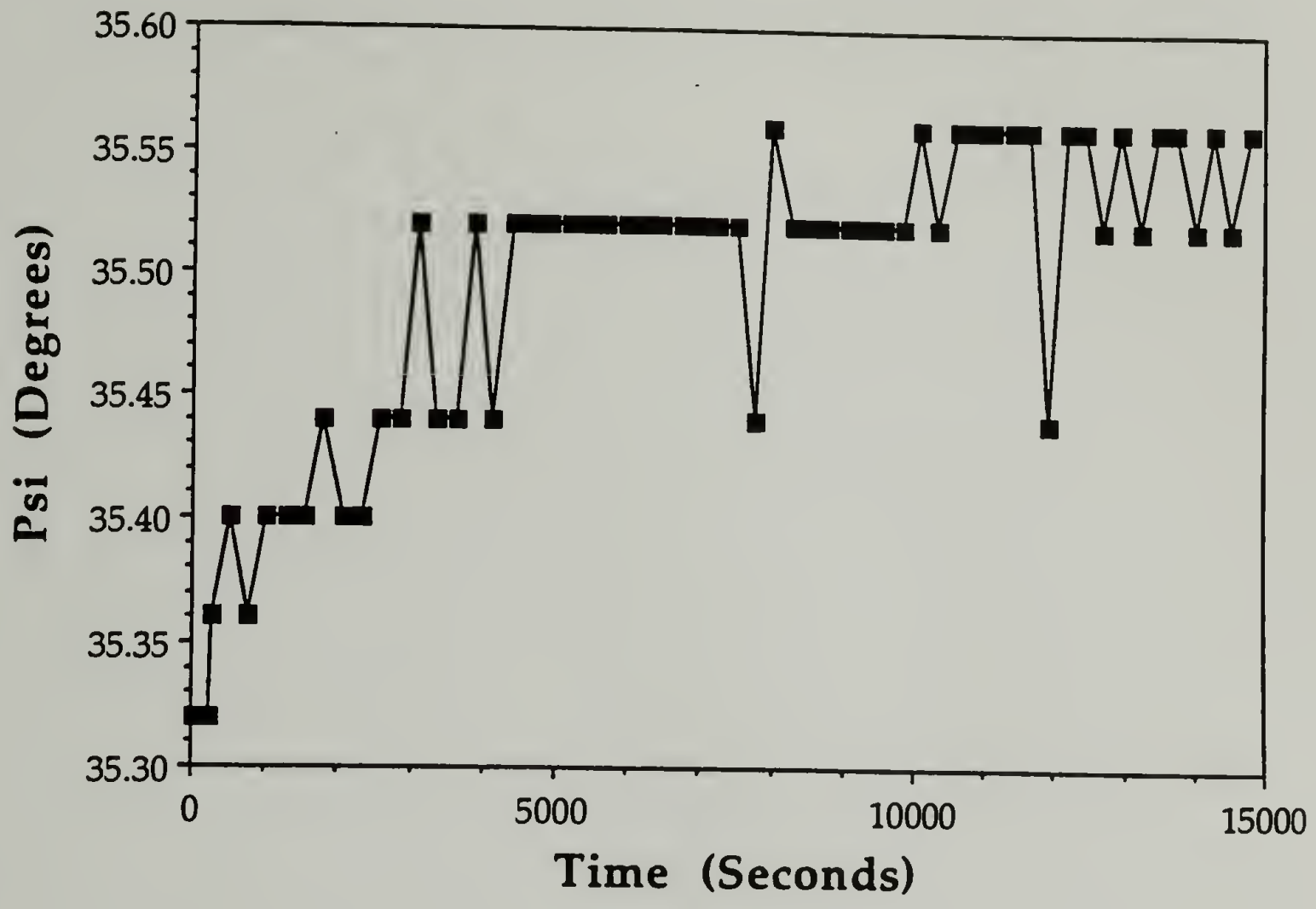

Figure 3.3. Psi plotted as a function of time for the adsorption of γ-globulin on platinum from a sodium phosphate buffer solution (pH = 8.5, I = 0.15 M) at 25° C and 0.0 V.

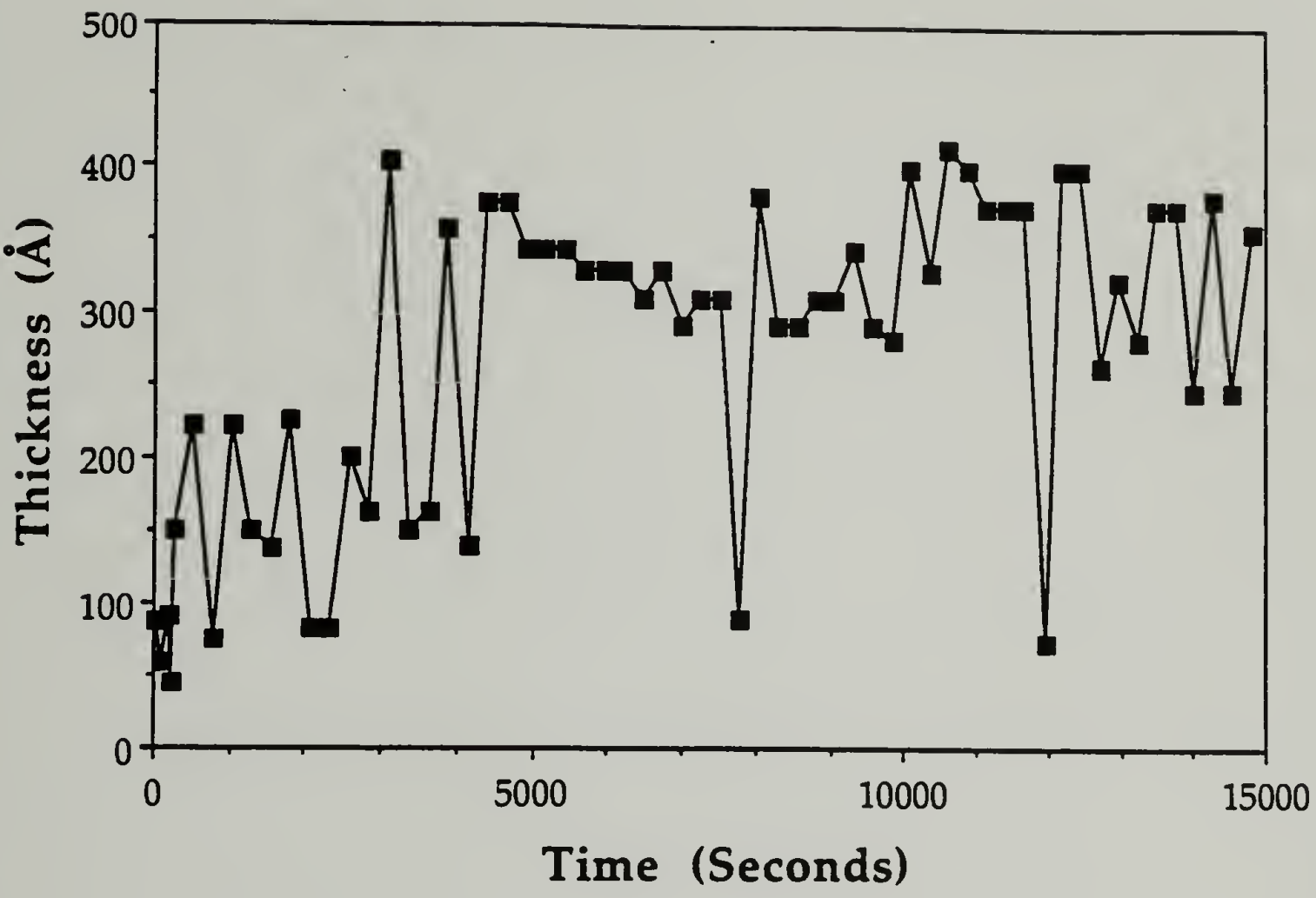

Figure 3.4. Thickness plotted as a function of time for the adsorption of γ-globulin on platinum in the presence of a sodium phosphate buffer solution (pH = 8.5, I = 0.15 M) at 25° C and 0.0 V.

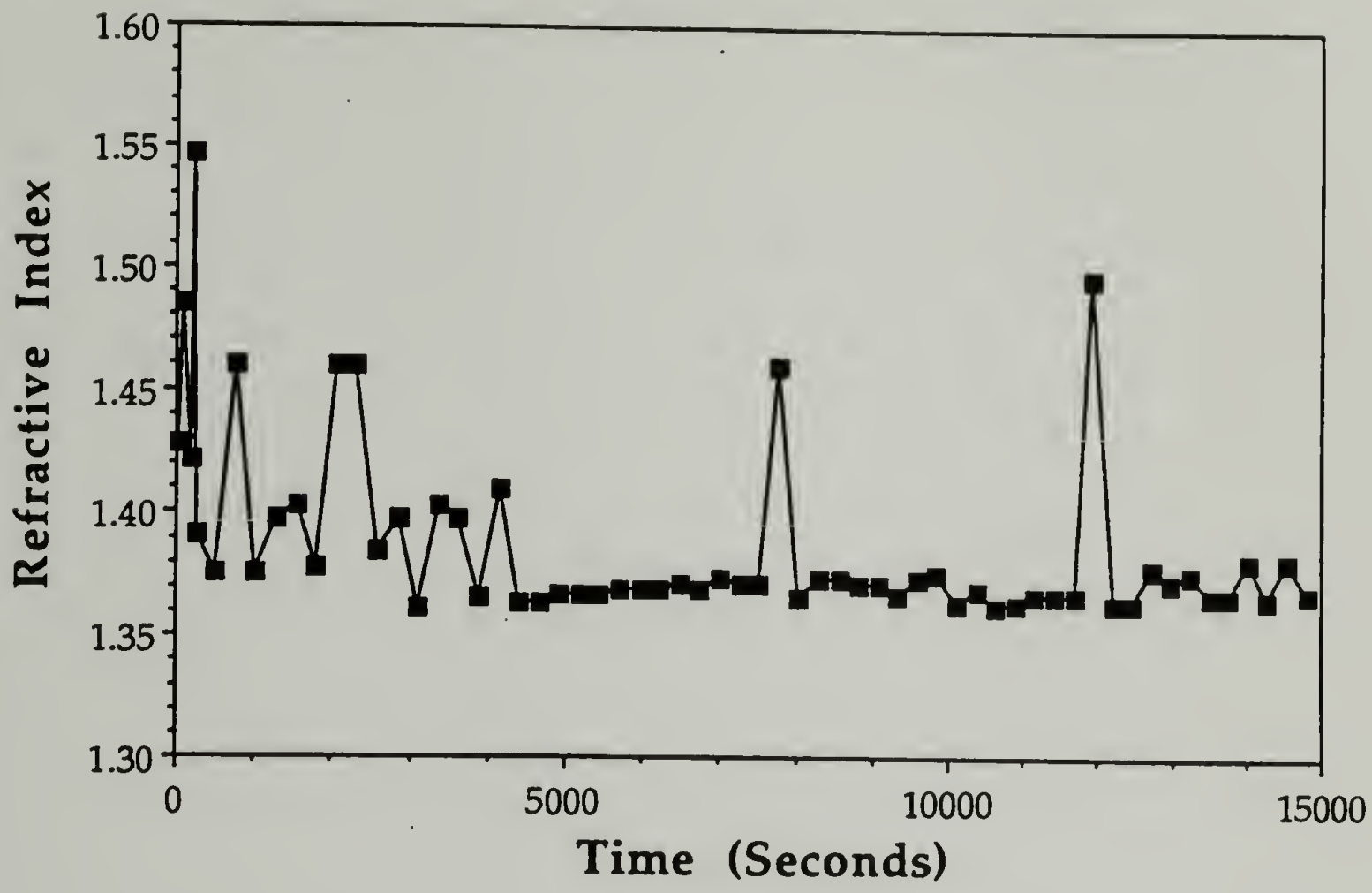

Figure 3.5 Refractive index of an adsorbed γ-globulin layer on platinum in the presence of a sodium phosphate buffer solution (pH = 8.5, I = 0.15 M) plotted as a function of time at 25° C and 0.0 V.

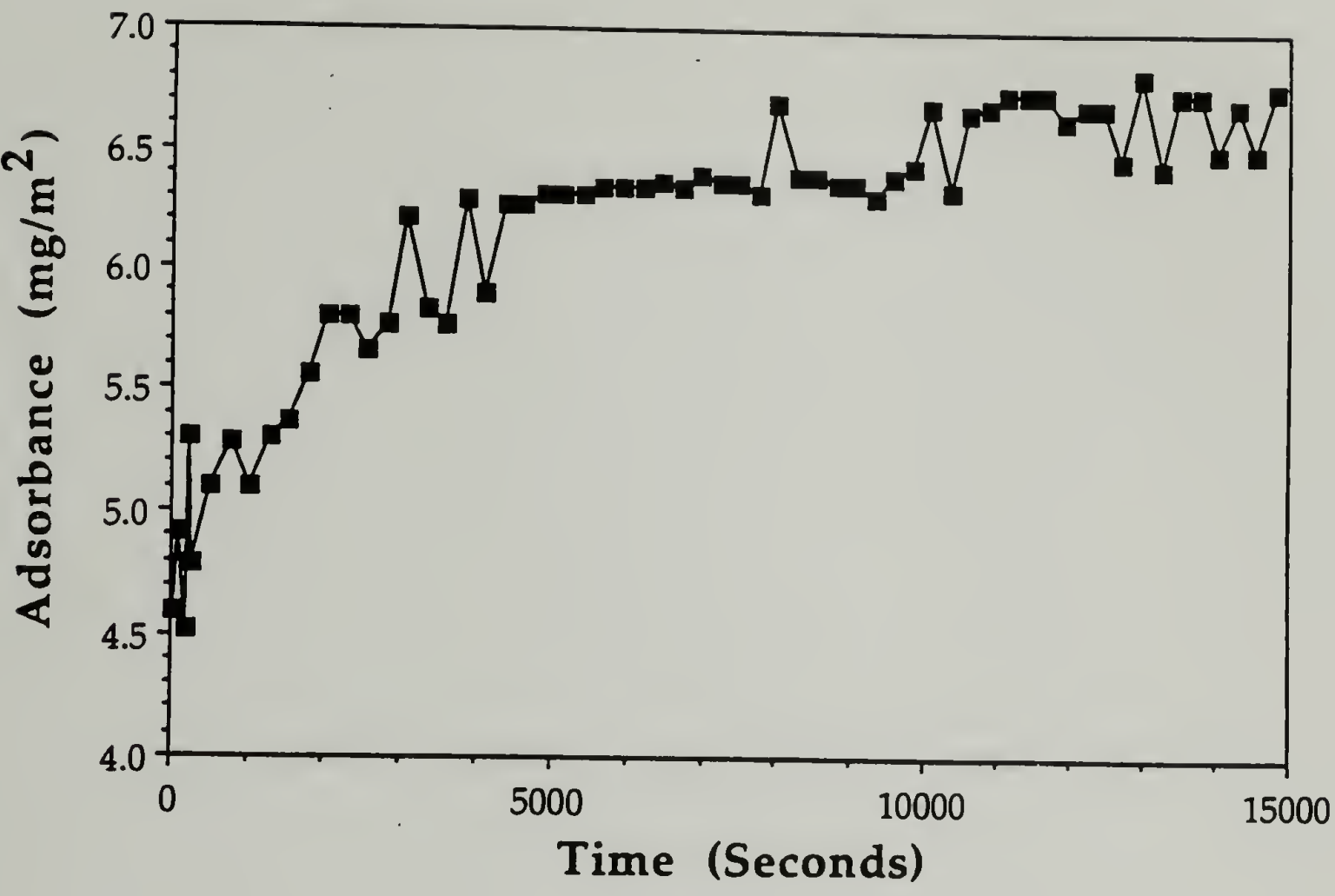

Figure 3.6. Adsorbance plotted as a function of time for γ-globulin on platinum in the presence of a sodium phosphate buffer solution (pH = 8.5, I = 0.15 M) at 25° C and 0.0 V.

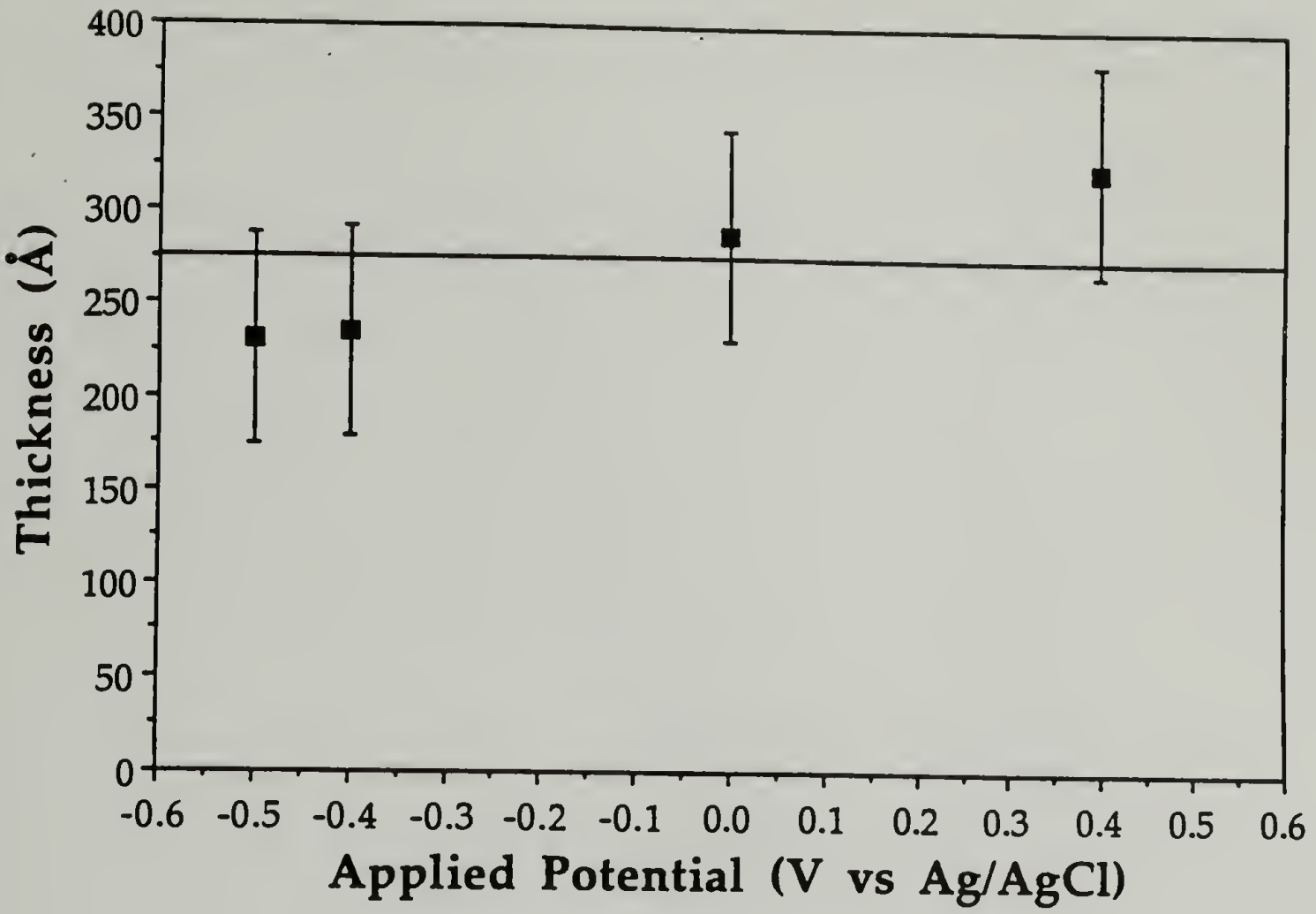

Figure 3.7. Adsorbed γ-globulin layer thickness on platinum in the presence of a sodium phosphate buffer solution (pH = 8.5, I = 0.15 M) at 25° C plotted as a function of initial adsorbing potential.

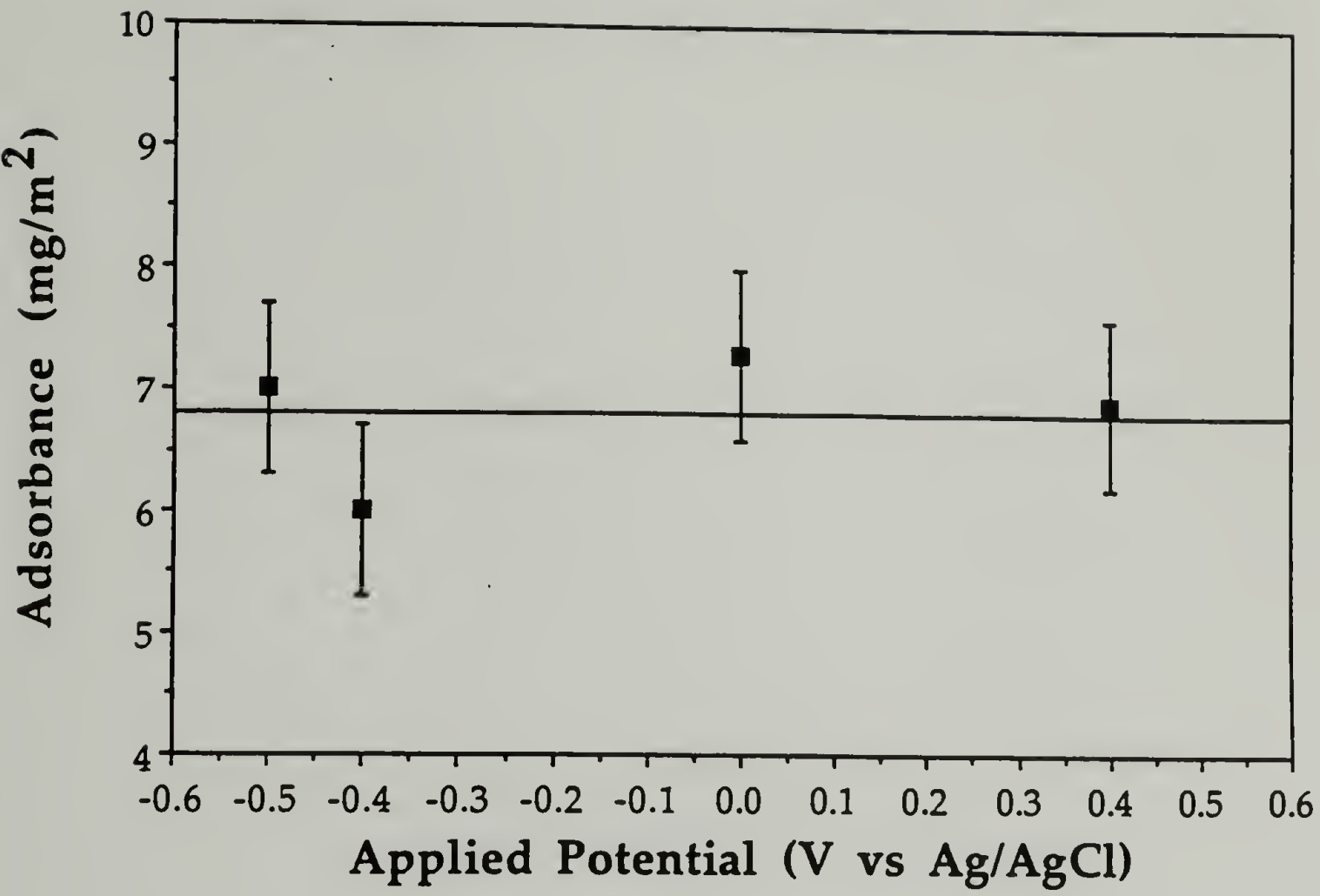

Figure 3.8. The amount of γ-globulin adsorbed on platinum in the presence of a sodium phosphate buffer solution (pH = 8.5, I = 0.15 M) at 25° C plotted as a function of initial adsorbing potential.

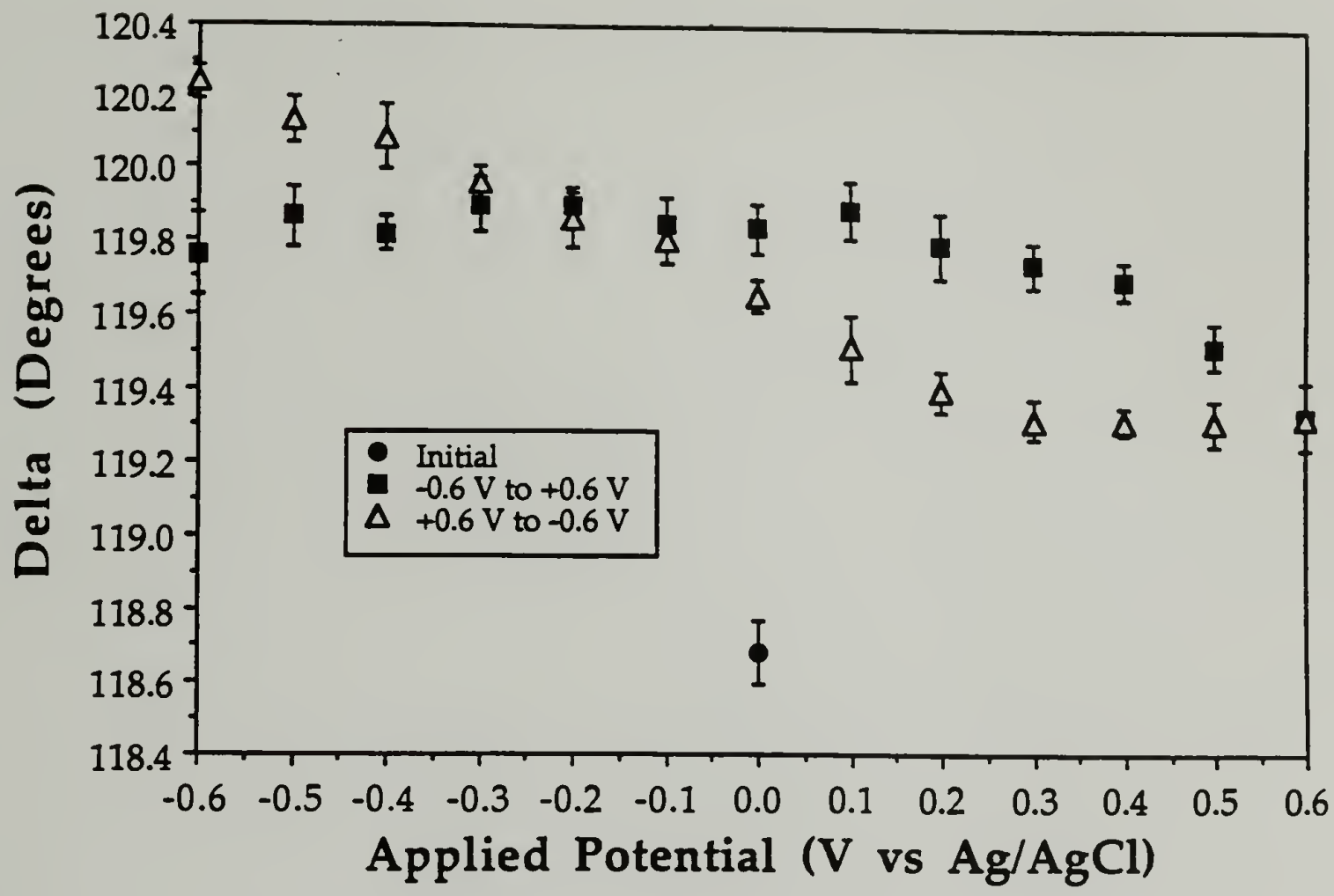

Figure 3.9. Delta plotted as a function of applied surface potential for the γ-globulin covered platinum foil in the presence of a sodium phosphate buffer (pH = 8.5, I = 0.15 M) at 25° C.

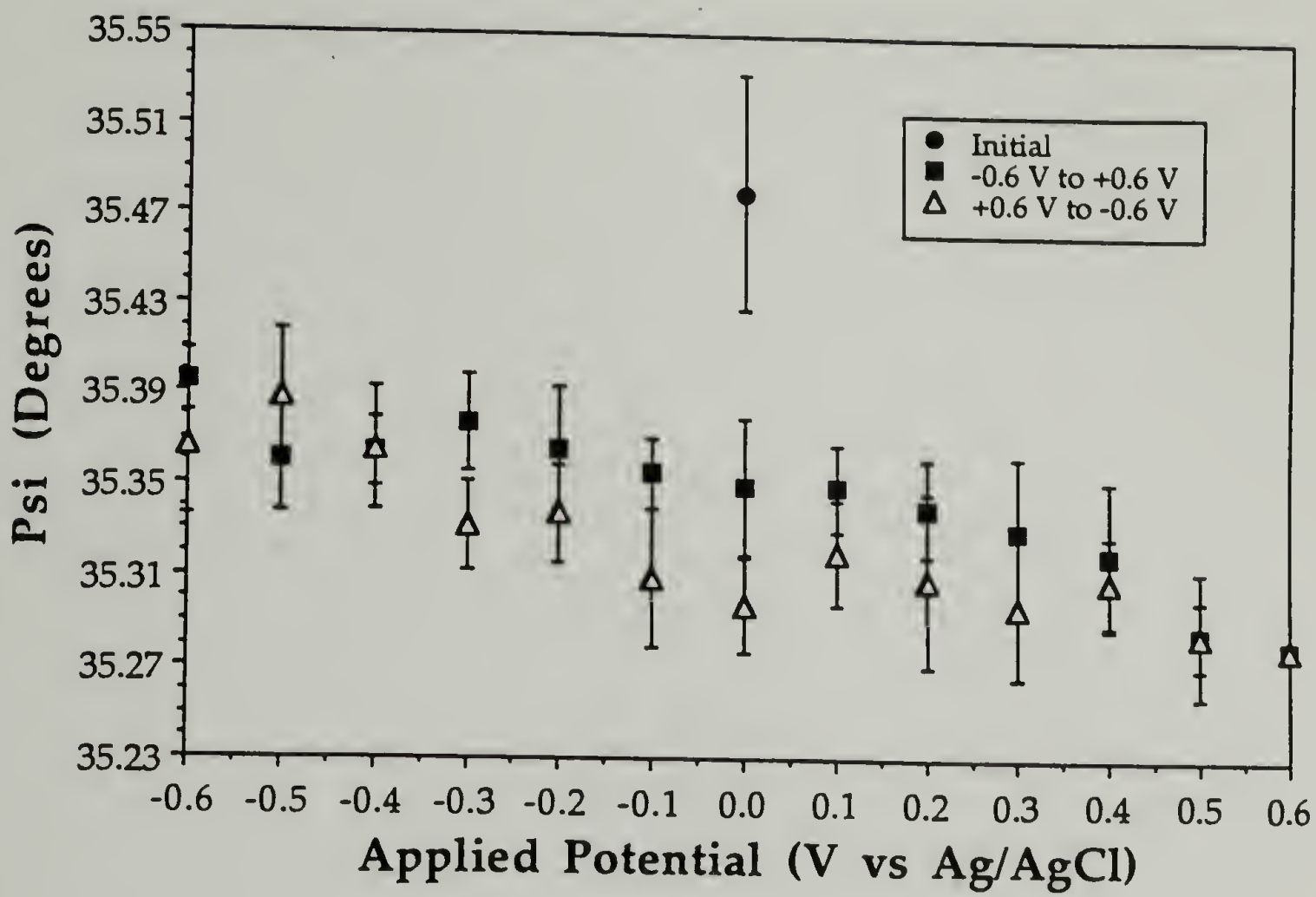

Figure 3.10. Psi plotted as a function of applied surface potential for the γ-globulin covered platinum foil in the presence of a sodium phosphate buffer (pH = 8.5, I = 0.15 M) at 25° C.

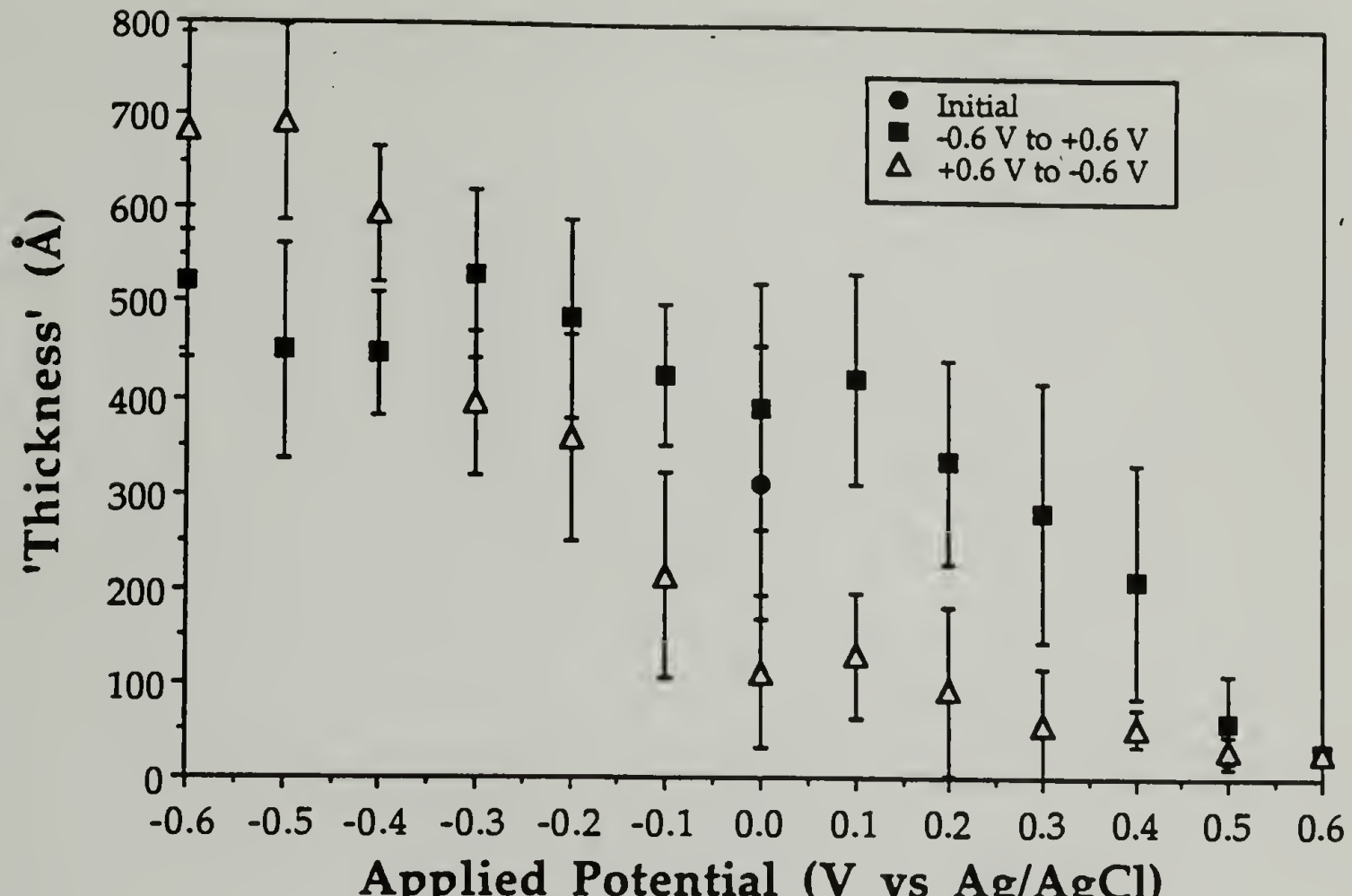

Figure 3.11. Plot of adsorbed γ-globulin layer thickness on a platinum foil in the presence of a phosphate buffer (pH = 8.5, I = 0.15 M) as a function of applied surface potential. Thicknesses were calculated from ellipsometric parameters ignoring effects of surface oxidation/reduction.

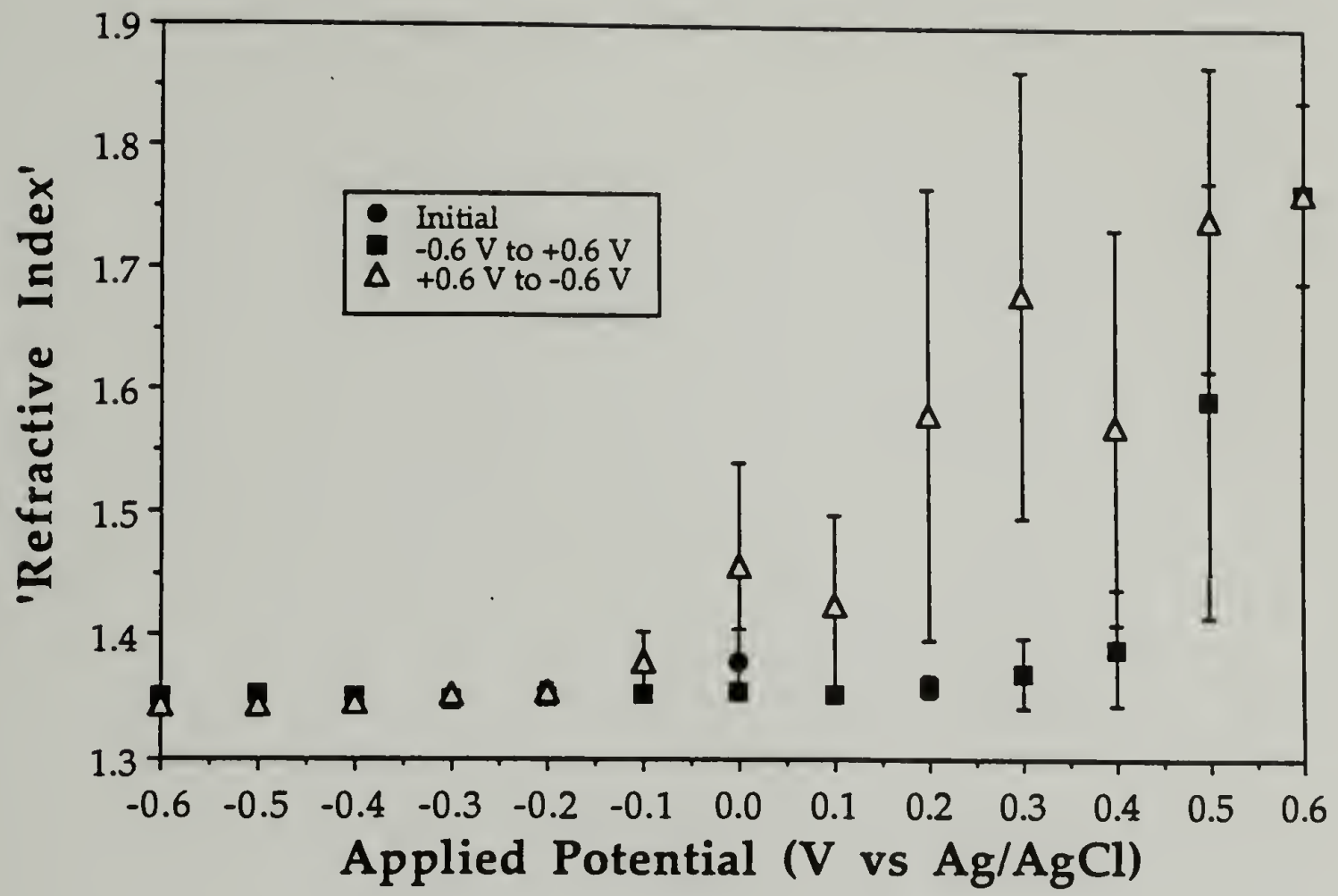

Figure 3.12. Plot of the refractive index of the adsorbed γ-globulin layer on a platinum foil in the presence of a phosphate buffer (pH = 8.5, I = 0.15 M) as a function of applied surface potential. Refractive indexes were calculated from ellipsometric parameters ignoring effects of surface oxidation/reduction.

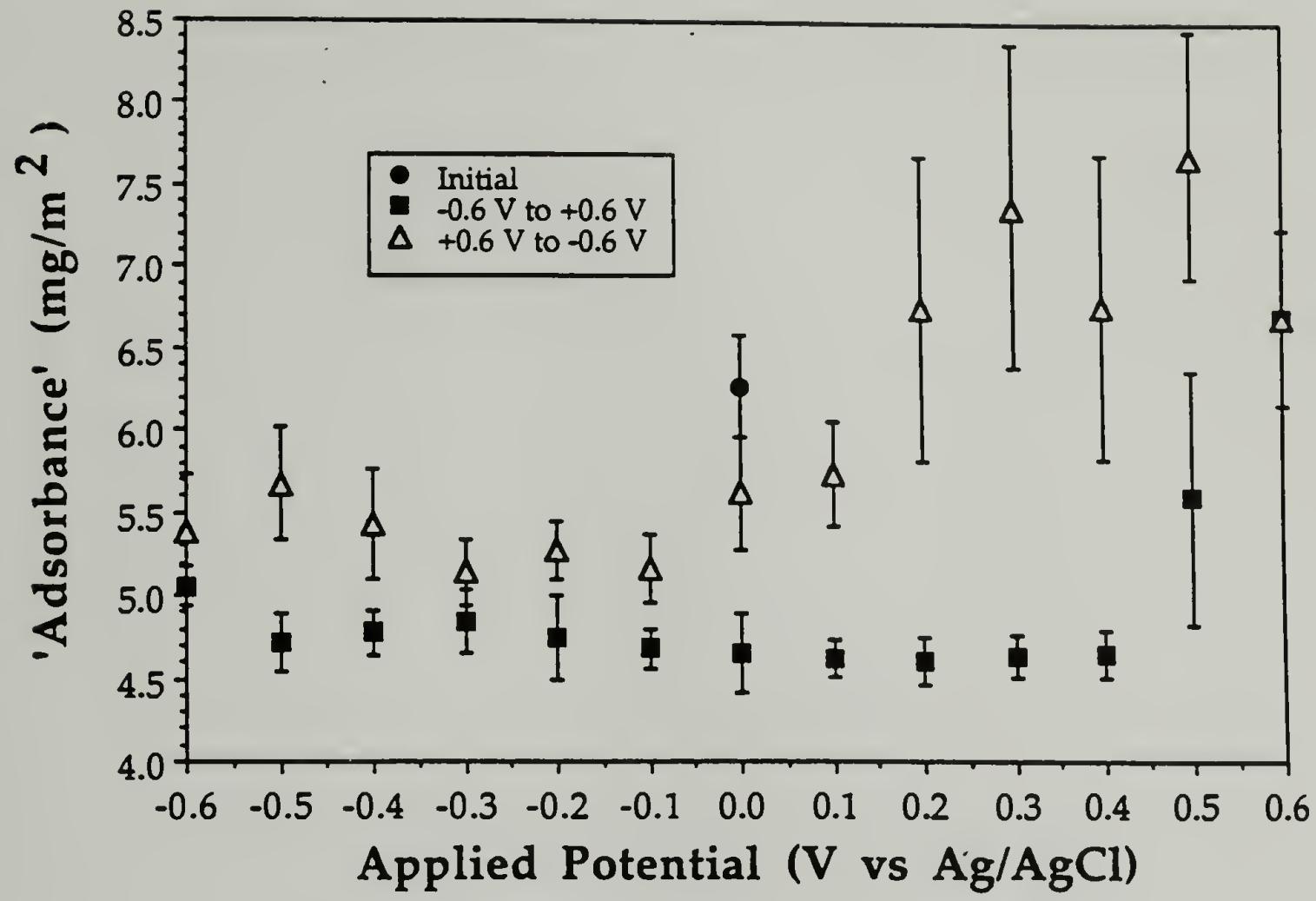

Figure 3.13. Plot the amount of γ-globulin adsorbed on a platinum foil in the presence of a phosphate buffer (pH = 8.5, I = 0.15 M) as a function of applied surface potential. Adsorbances were calculated from ellipsometrically measured thicknesses and refractive indexes assuming that no oxidation/reduction of the platinum surface occurred once the protein was adsorbed.

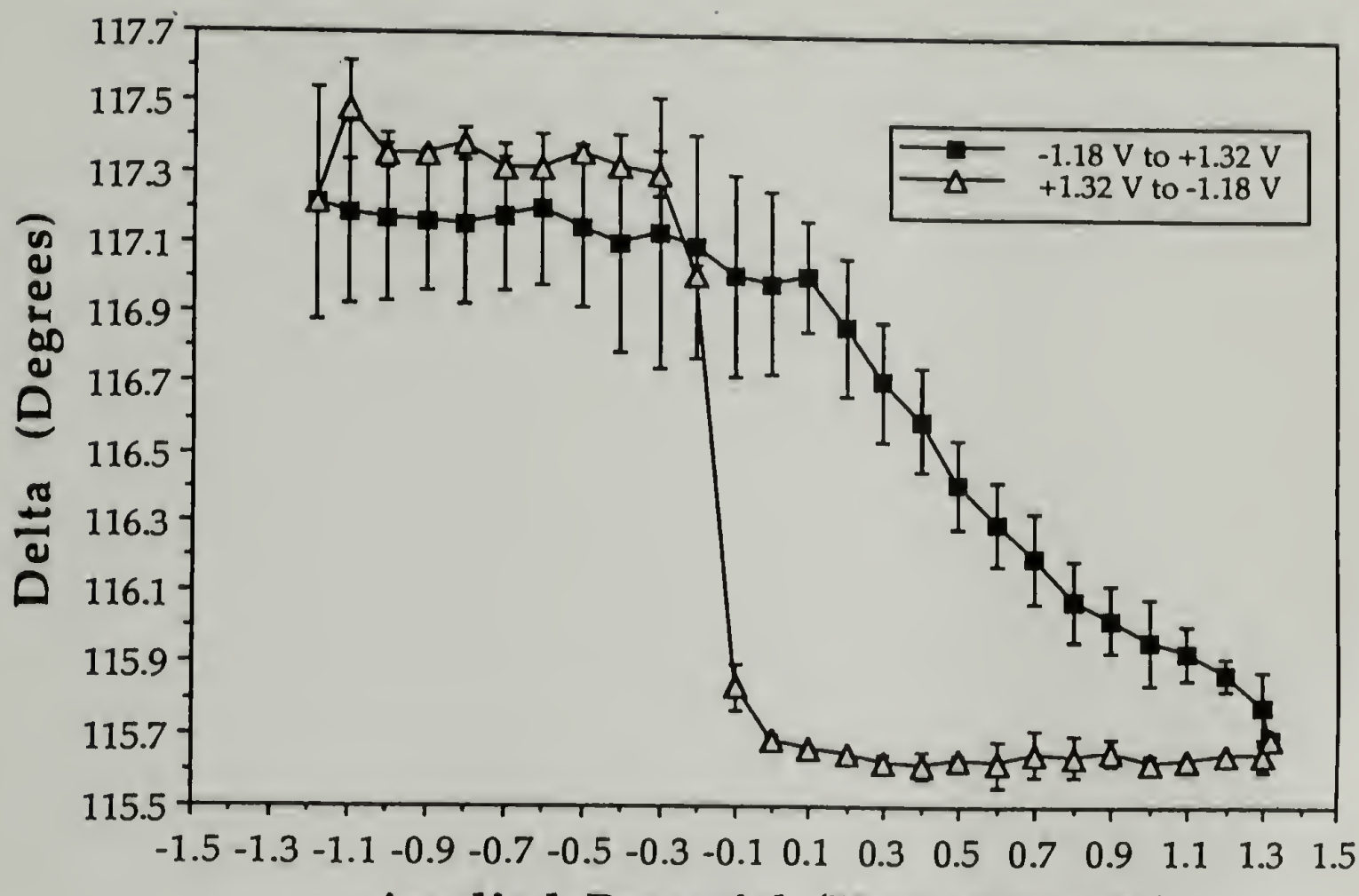

Figure 3.14. Delta plotted as a function of applied surface potential for a bare platinum surface in a sodium phosphate buffer (pH = 8.5, I = 0.15 M) at 25° C. The size of the error incurred for Delta with repeatedly cycling of potential is shown.

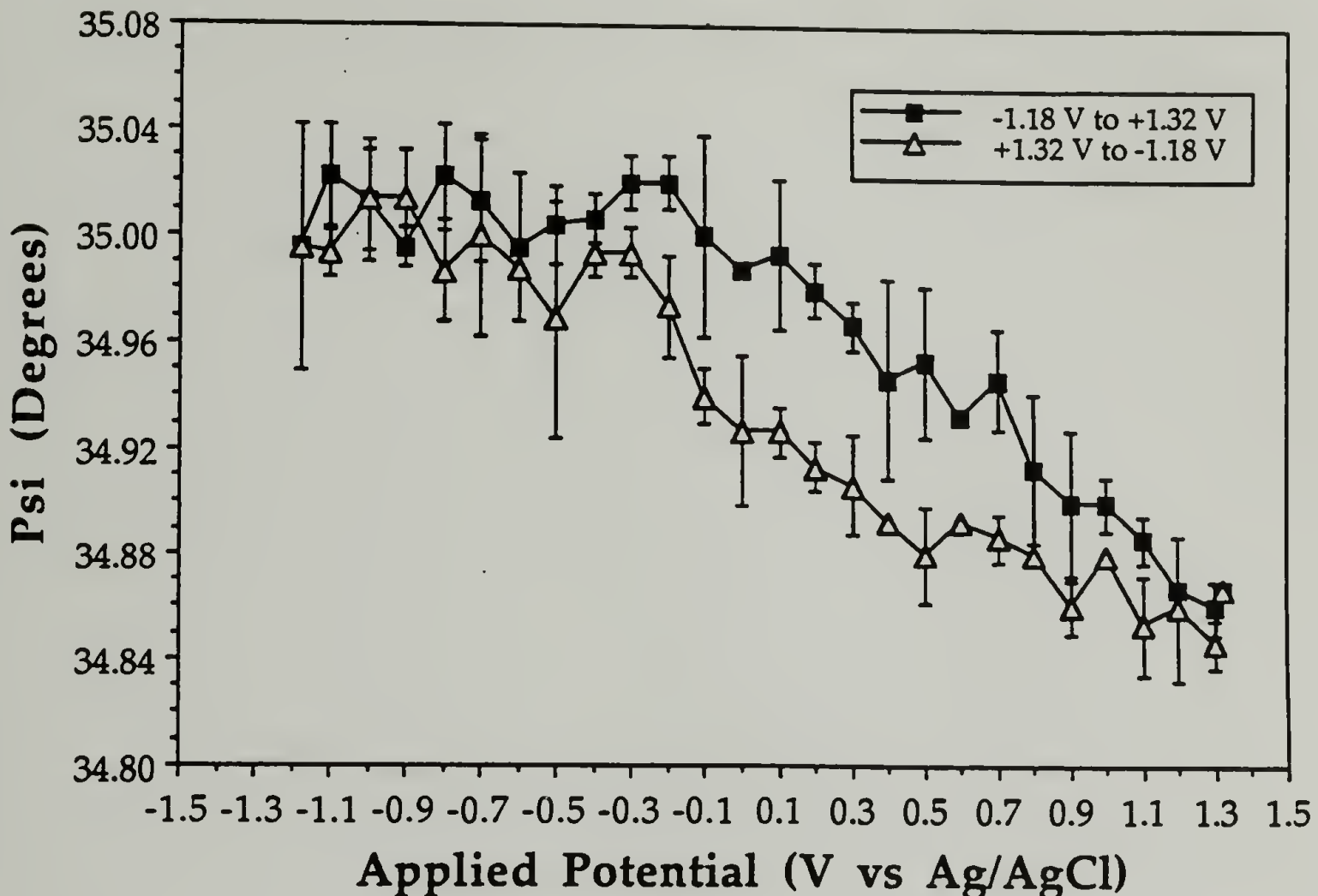

Figure 3.15. Psi plotted for a bare platinum surface in a sodium phosphate buffer (pH = 8.5, I = 0.15 M) at 25° C as a function of applied surface potential. The size of the error incurred for Psi with repeatedly cycling of potential is shown.

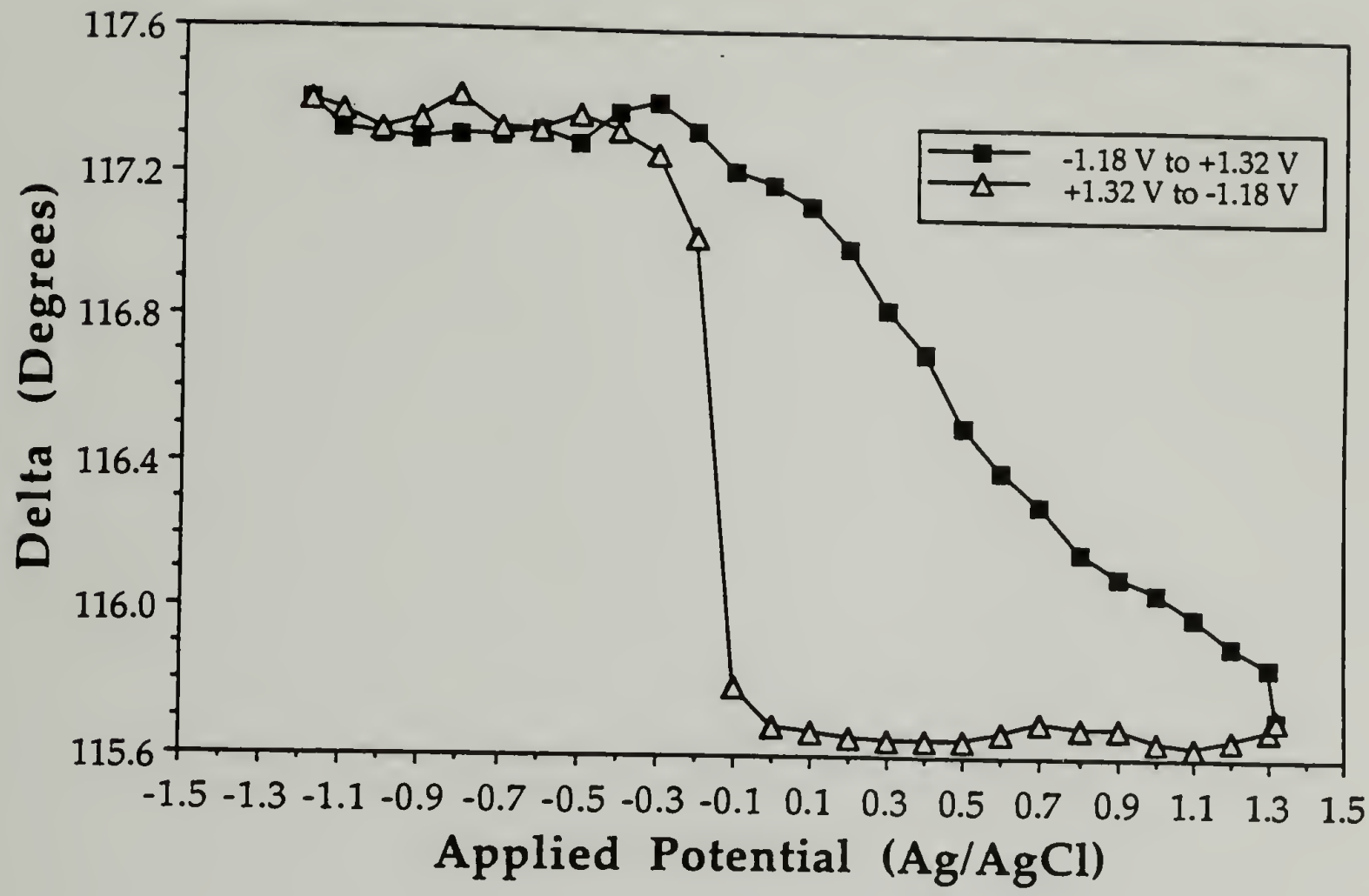

Figure 3.16. Delta plotted as a function of applied surface potential for a bare platinum surface in a sodium phosphate buffer (pH = 8.5, I = 0.15 M) at 25° C. The average of three ellipsometric measurements taken at each potential are shown.

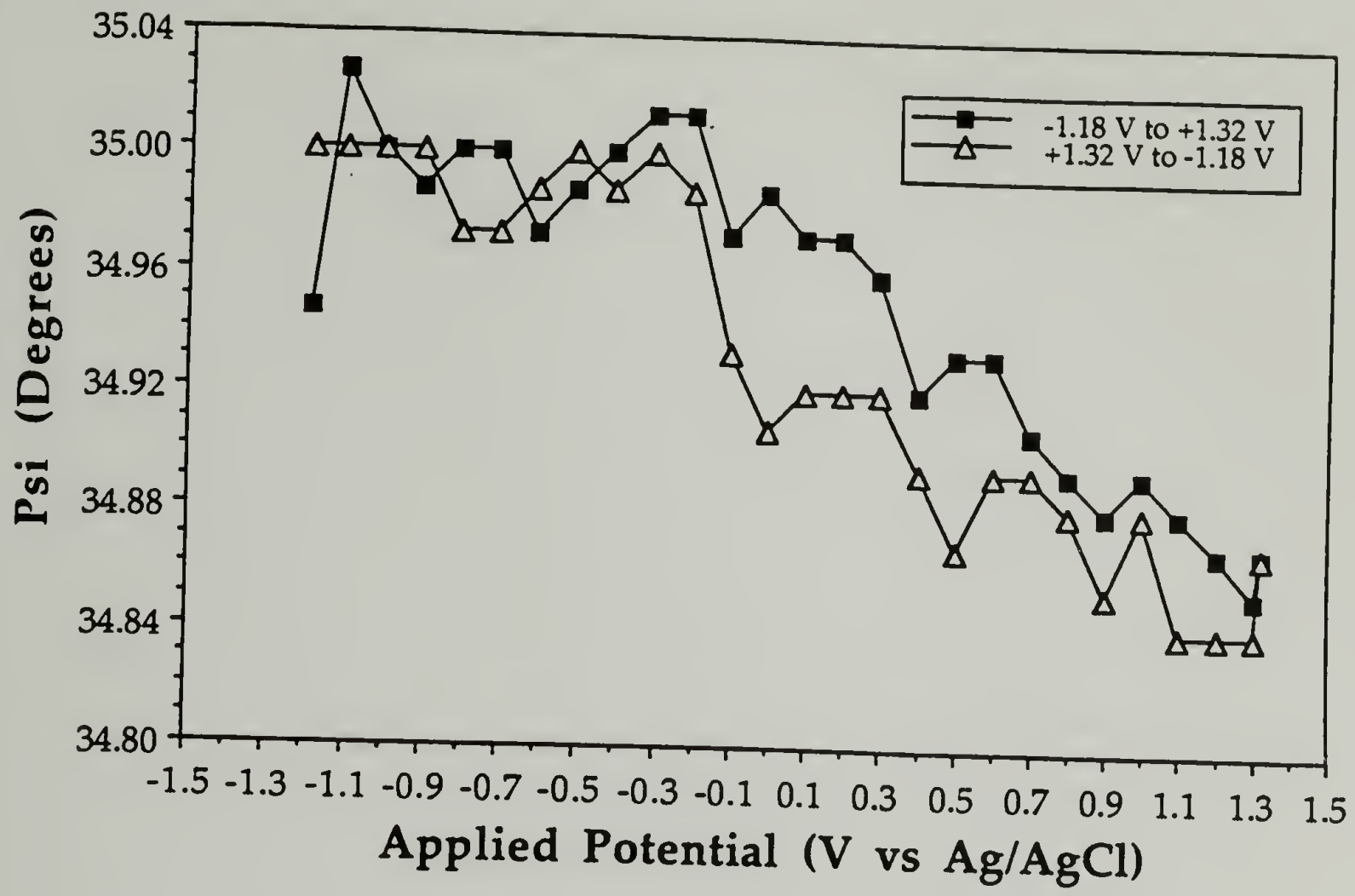

Figure 3.17. Psi plotted as a function of applied surface potential for a bare platinum surface in a sodium phosphate buffer (pH = 8.5, I = 0.15 M) at 25° C. The average of three ellipsometric measurements taken at each potential are shown.

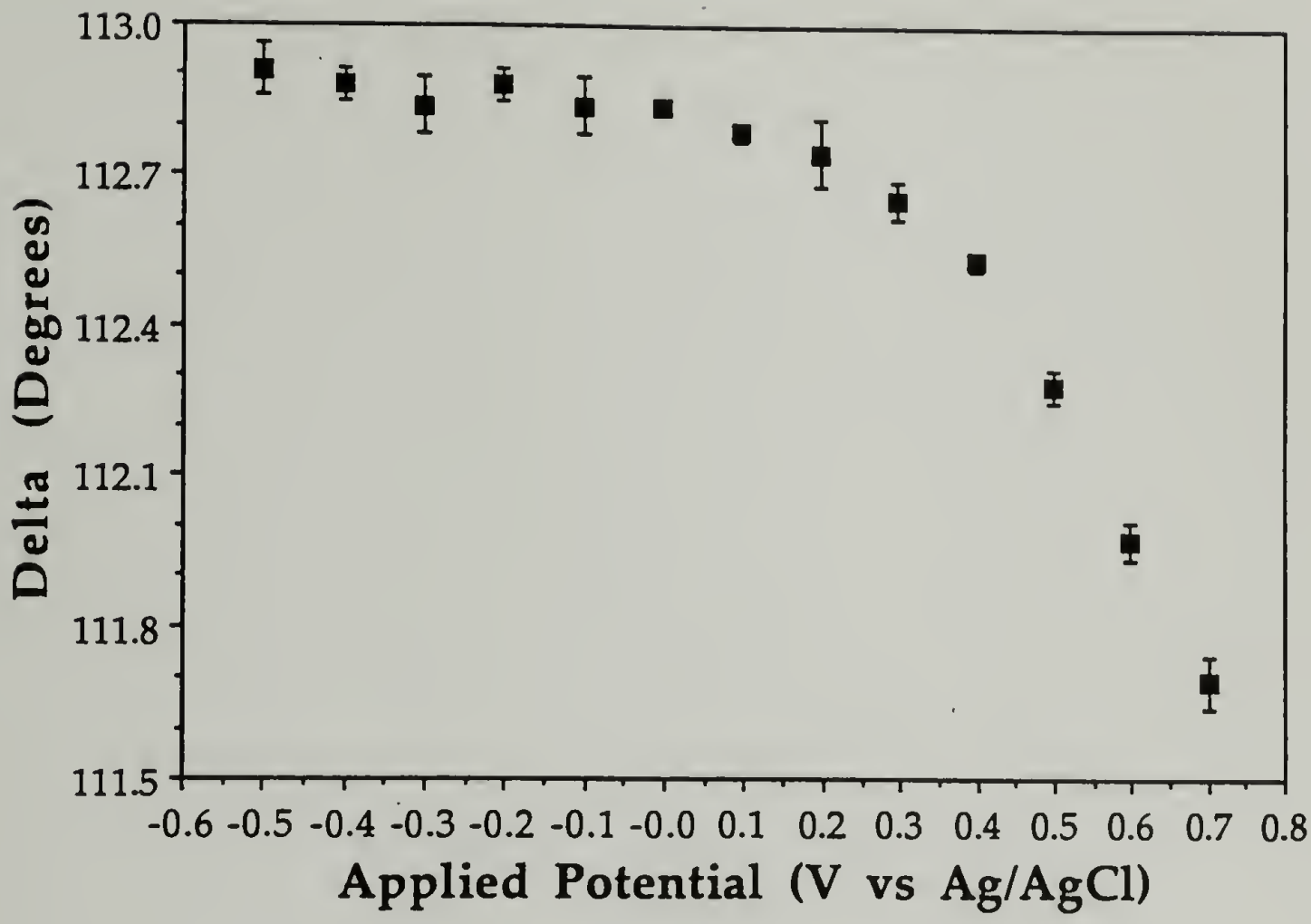

Figure 3.18. Delta plotted as a function of applied surface potential for the γ-globulin covered platinum foil in the presence of the buffered protein solution (pH = 8.5, I = 0.15 M) at 25° C.

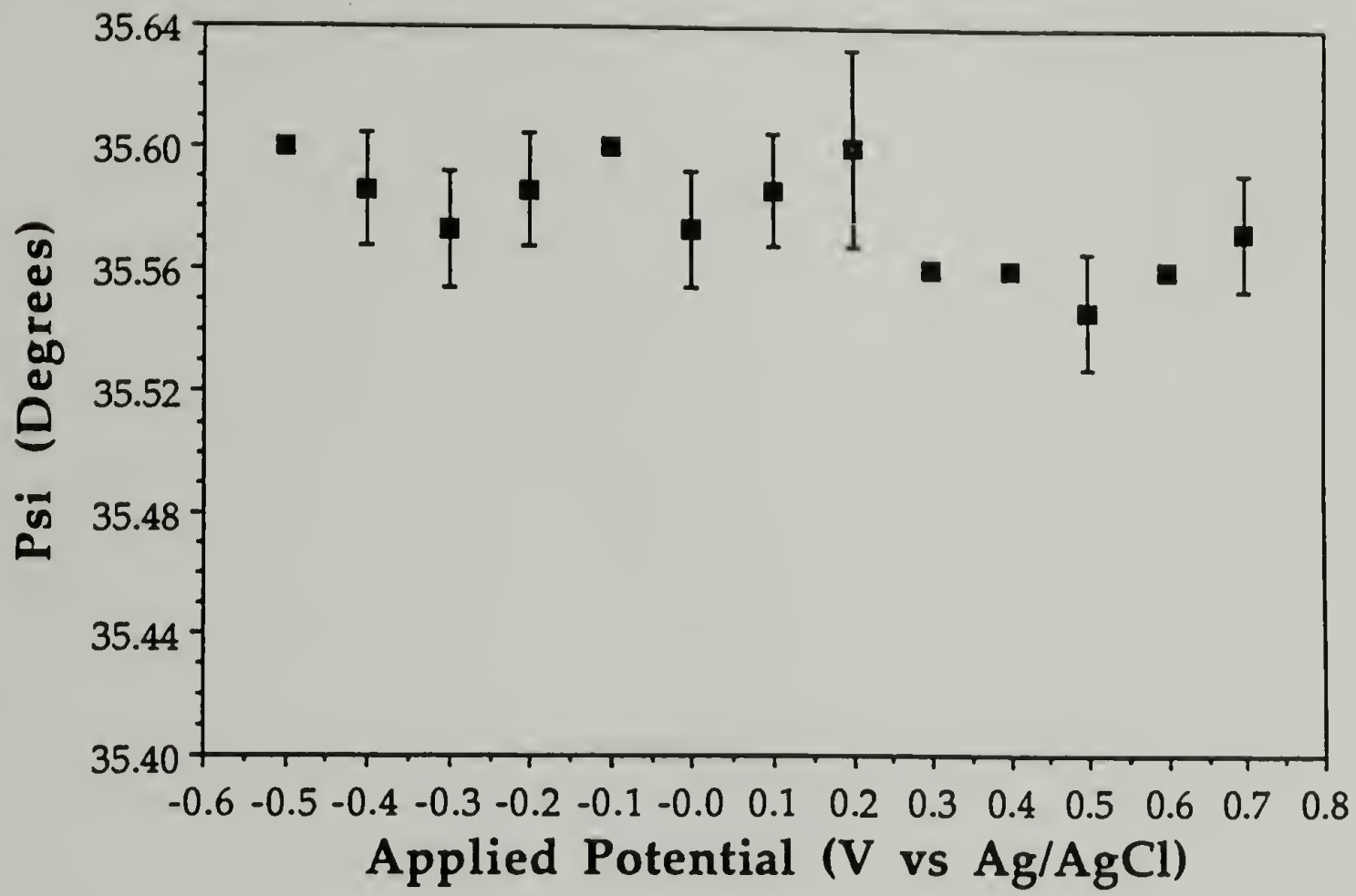

Figure 3.19. Psi plotted as a function of applied surface potential for the γ-globulin covered platinum foil in the presence of the buffered protein solution (pH = 8.5, I = 0.15 M) at 25° C.

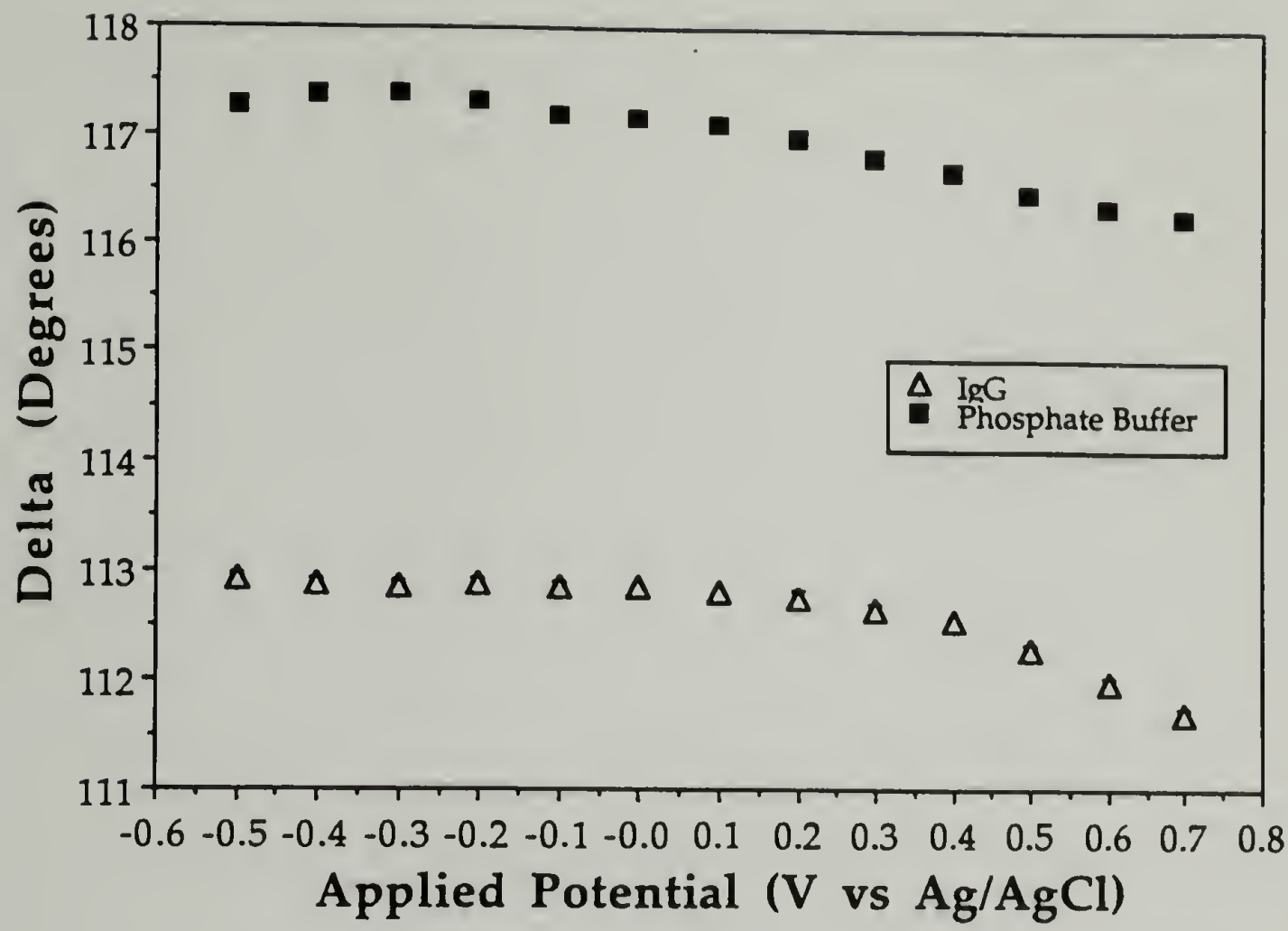

Figure 3.20. Comparison of the change in Delta with variation in applied surface potential for the bare platinum surface immersed in the phosphate buffer solution (pH = 8.5, I = 0.15 M) to that for the γ-globulin-covered platinum surface in the presence of the buffered protein solution (pH = 8.5, I = 0.15 M) at 25° C.

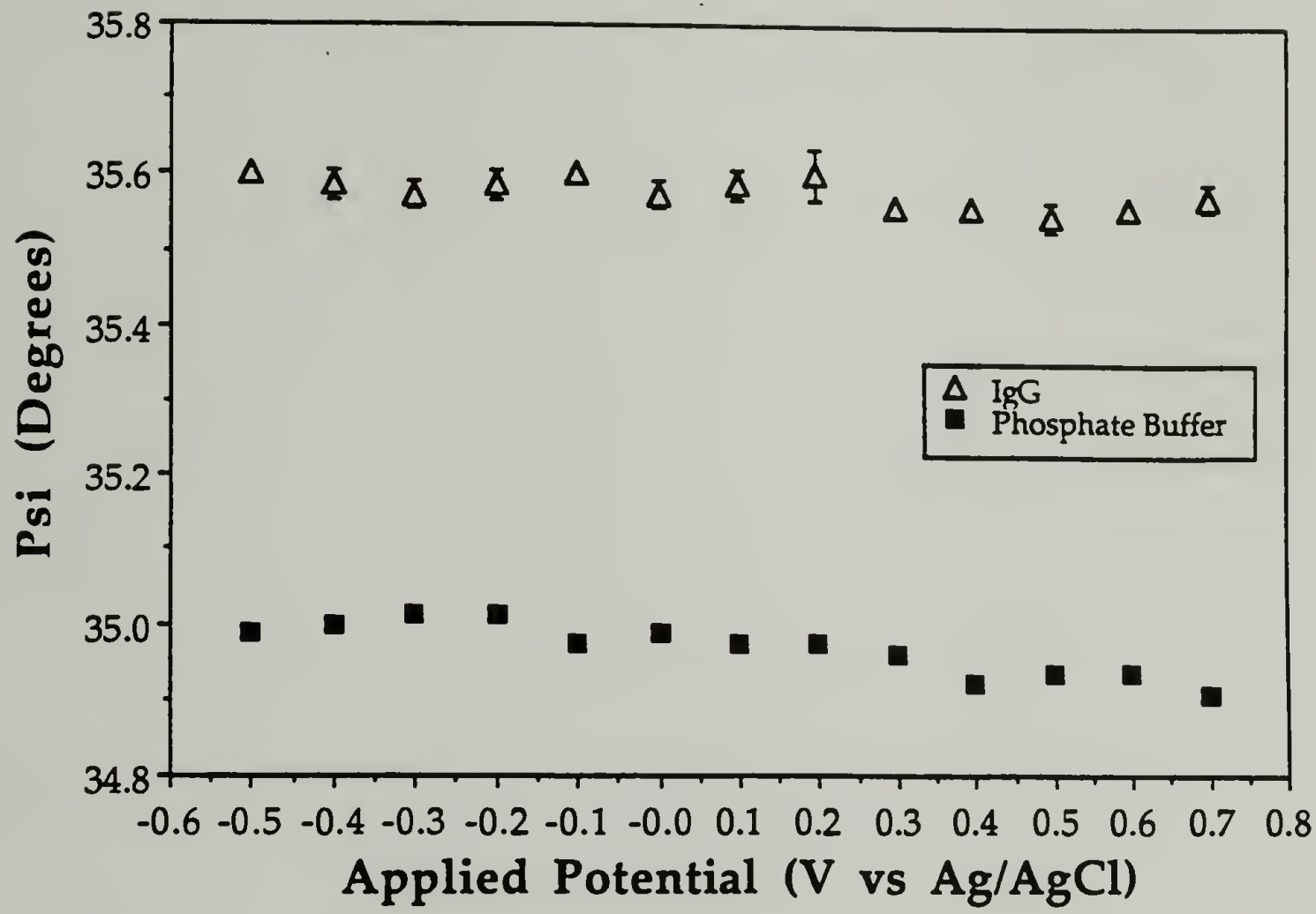

Figure 3.21. Comparison of the change in Psi with variation in applied surface potential for the bare platinum surface immersed in the phosphate buffer solution (pH = 8.5, I = 0.15 M) to that for the γ-globulin-covered platinum surface in the presence of the buffered protein solution (pH = 8.5, I = 0.15 M) at 25° C.

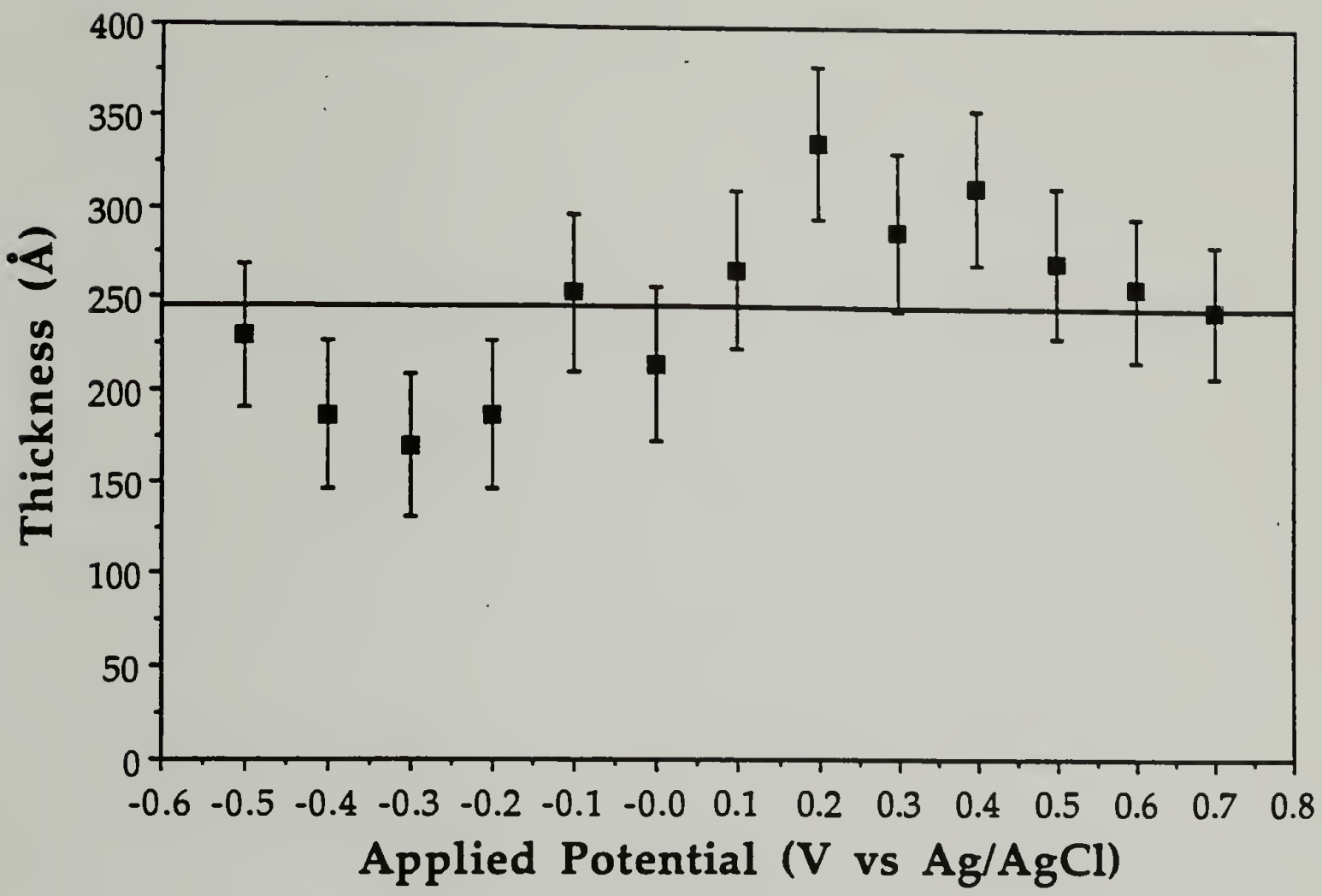

Figure 3.22. Plot of adsorbed γ-globulin layer thickness on a platinum foil in the presence of a buffered γ-globulin solution (pH = 8.5, I = 0.15 M) as a function of applied surface potential.

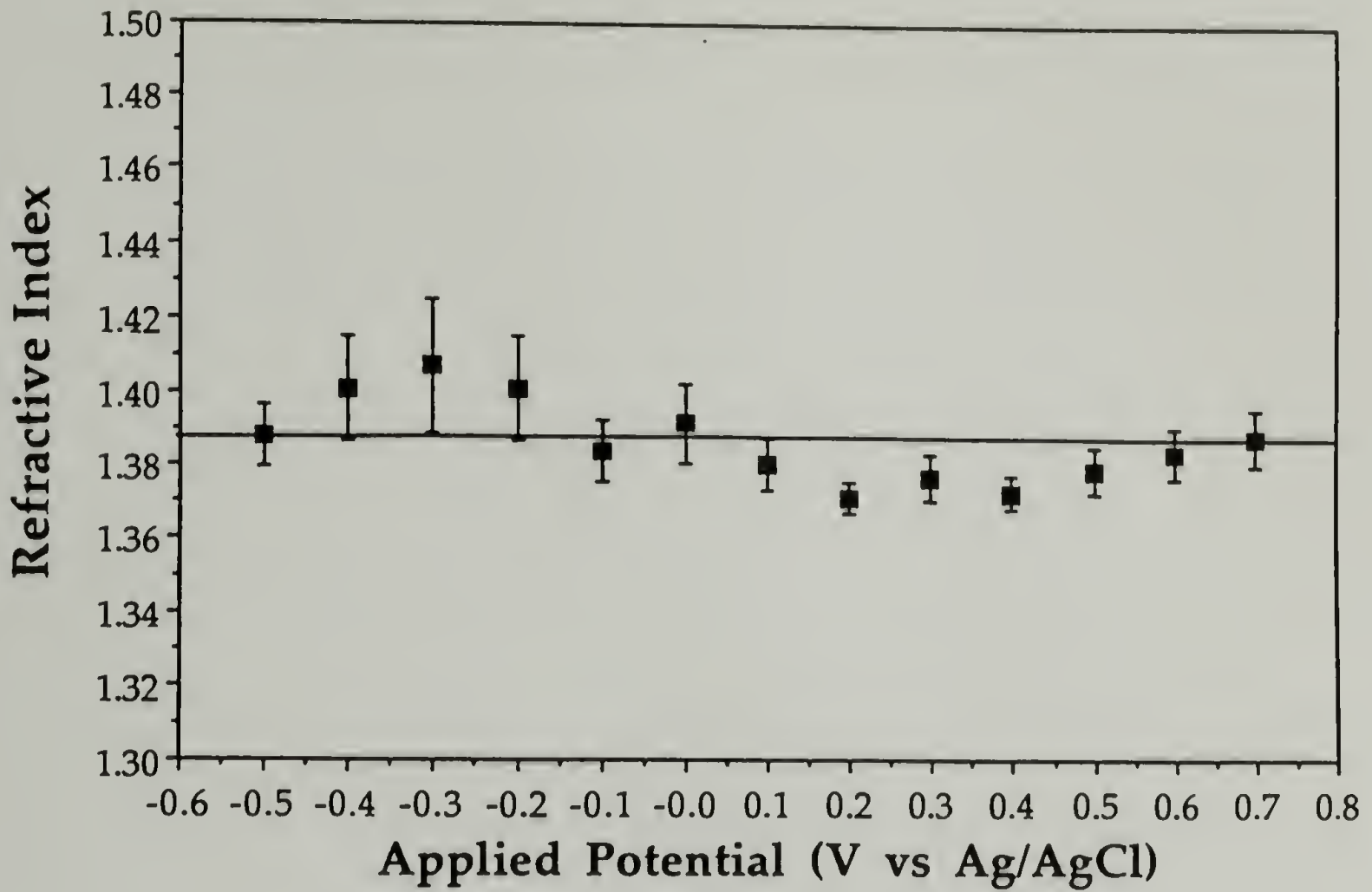

Figure 3.23. Plot of refractive index of the adsorbed γ-globulin layer on a platinum foil in the presence of a buffered γ-globulin solution (pH = 8.5, I = 0.15 M) as a function of applied surface potential.

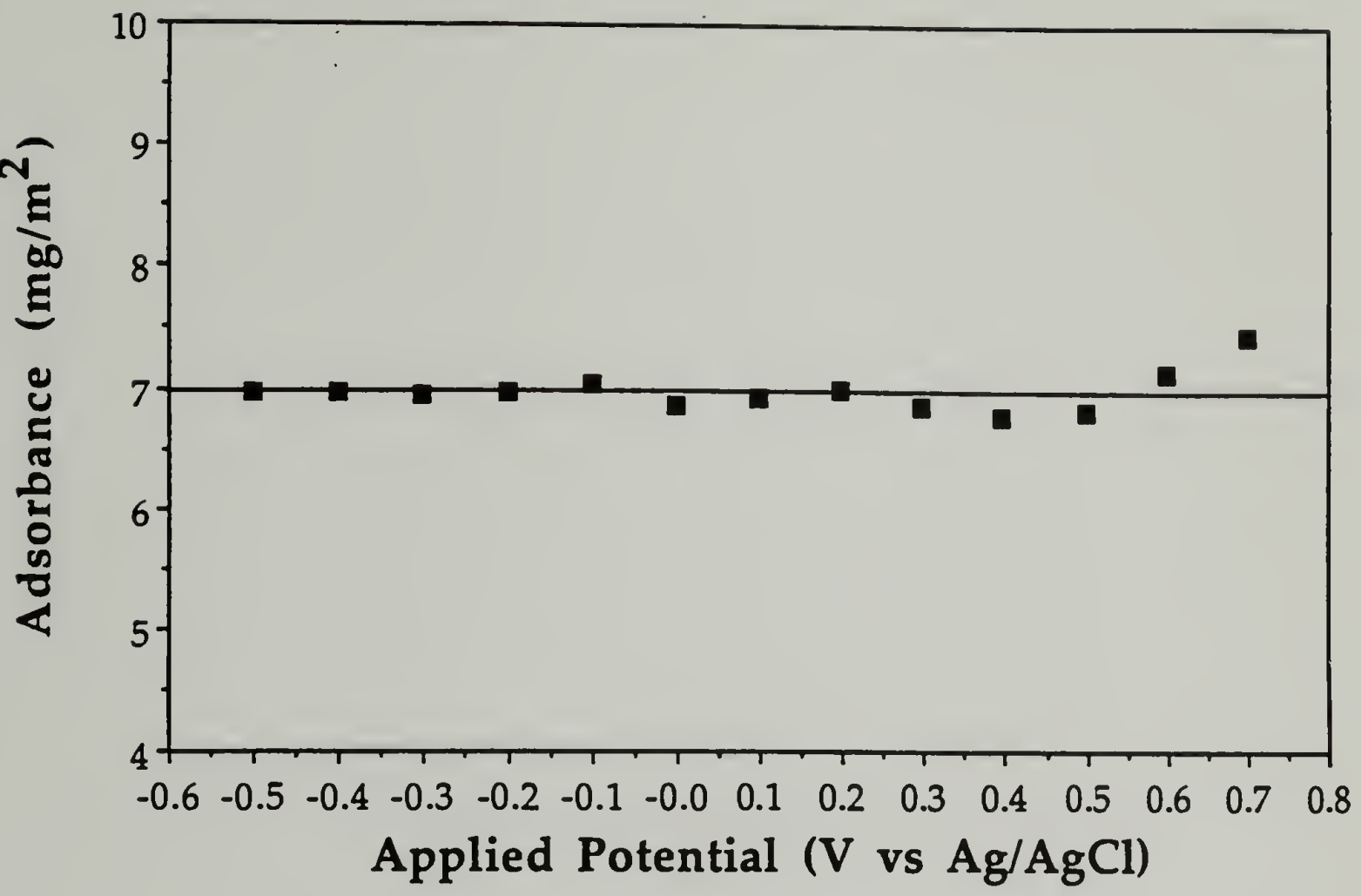

Figure 3.24. Plot of the amount of γ-globulin adsorbed on the platinum surface from a buffered γ-globulin solution (pH = 8.5, I = 0.15 M) as a function of applied surface potential.

3.8 References

(1) Emons, H.; Werner, G.; Heineman, W. R. *Analyst* **1990**, *115*, 405.

(2) Morrissey, B. W.; Smith, L. E.; Stromberg, R. R.; Fenstermaker, C. A. *Journal of Colloid and Interface Science* **1976**, *56*, 557.

(3) Morrissey, B. W. *Annals New York Academy of Sciences* **1977**, *283*, 50.

(4) Fontaine, M.; Rivat, C.; Ropartz, C.; Caullet, C. *Bulletin de la Societe Chimique de France* **1973**, *6*, 1873.

(5) Silverton, E. W.; Navia, M. A.; Davies, D. R. *Proceedings National Academy of Sciences, USA* **1977**, *74*, 5140.

(6) Leatherbarrow, R. J.; Stedman, M.; Wells, T. N. C. *Journal of Molecular Biology* **1991**, *221*, 361.

(7) Olk, C. H.; Heremans, J. *Journal of Vacuum Science and Technology* **1991**, *B 9*, 1268.

(8) Andrade, J.; Mankarious, S. In *5th International Symposium on HPLC of Proteins, Peptides and Polynucleotides*; Toronto, 1985; Paper No. 1027.

(9) Johnson, J. E.; Matijevic, E. *Journal of Colloid and Interface Science* **1990**, *138*, 255.

(10) Kim, S. W.; Lee, R. G.; Oster, H.; Coleman, D.; Andrade, J. D.; Lentz, D. J.; Olsen, D. *Transactions. American Society for Artifical Internal Organs* **1974**, *2*, 449.

(11) Chopra, P. S.; Srinivasan, S.; Lucas, T.; Sawyer, P. N. *Nature (London)* **1967**, *215*, 1494.

(12) Leininger, R. I.; Mirkovitch, V.; Beck, R. E.; Andrus, P. G.; Kolff, W. J. *Transactions. American Society for Artifical Internal Organs* **1964**, *10*, 137.

(13) Milligan, H. L.; Davis, J.; Edmark, K. W. *Journal of Biomedical Materials Research* **1968**, *2*, 51.

(14) Sawyer, P. N.; Srinivasan, S. *American Journal of Surgery and Gynecology* **1967**, *114*, 42.

(15) Srinivasan, S.; Sawyer, P. N. *Journal of Colloid and Interface Science* **1970**, *32*, 456.

(16) Minunni, M.; Skládal, P.; Mascini, M. *Analytical Letters* **1994**, *27*, 1475.

(17) Gyss, C.; Bourdillon, C. *Analytical Chemistry* **1987**, *59*, 2350.

(18) *Biosensors. Fundamentals and Applications*; Turner, A. P. F.; Karube, I.; Wilson, G. S., Ed.; Oxford University Press: Oxford, 1987.

(19) Arai, T.; Norde, W. *Colloids and Surfaces* **1990**, *51*, 1.

(20) Norde, W.; Arai, T.; Shirahama, H. *Biofouling* **1991**, *4*, 37.

(21) Perlmann, G. E.; Longsworth, L. G. *Journal of the American Chemical Society* **1948**, *70*, 2719.

(22) Benziger, J. B.; Pascal, F. A.; Bernasek, S. L.; Soriaga, M. P.; Hubbard, A. T. *Journal of Electroanalytical Chemistry* **1986**, *198*, 65.

(23) Adams, R. N. *Electrochemistry at Solid Electrodes*; Marcel Dekker, Inc.: New York, 1969.

(24) Gileadi, E. In *Electrode Kinetics for Chemists, Chemical Engineers, and Materials Scientists*VCH Publishers, Inc.: New York, 1993.

(25) Besio, G. J. Ph.D. Thesis, Princeton University, 1986.

(26) Parsons, R.; Visscher, W. H. M. *Journal of Electroanalytical Chemistry* **1972**, *36*, 329.

(27) Reddy, A. K. N.; Genshaw, M. A.; Bockris, J. O. *Journal of Chemical Physics* **1968**, *48*, 671.

(28) Vinnikov, Y. Y.; Shepelin, V. A.; Veselovskii, V. I. *Élektrokhimiya* **1973**, *9*, 534.

(29) Vinnikov, Y. Y.; Shepelin, V. A.; Veselovskii, V. I. *Élektrokhimiya* **1973**, *9*, 624.

(30) Ivarsson, B. A.; Hegg, P.-O.; Lundström, K. I.; Jönsson, U. *Colloids and Surfaces* **1985**, *13*, 169.

(31) Kawaguchi, M.; Hayashi, K.; Takahashi, A. *Colloids and Surfaces* **1988**, *31*, 73.

(32) Kawaguchi, M.; Hayashi, K.; Takahashi, A. *Macromolecules* **1988**, *21*, 1016.

(33) Andersen, T. N.; Anderson, J. L.; Eyring, H. *Journal of Physical Chemistry* **1969**, *73*, 3562.

(34) Campanella, L. *Journal of Electroanalytical Chemistry* **1970**, *28*, 228.

(35) Damaskin, B. B.; Petrii, O. A.; Batrakov, V. V. *Adsorption of Organic Compounds on Electrodes*; Plenum Press: New York-London, 1971.

(36) Kallay, N.; Torbic, Z.; Golic, M.; Matijevic, E. *Journal of Physical Chemistry* **1991**, *95*, 7028.

(37) Duschl, C.; Hall, E. A. H. *Journal of Colloid and Interface Science* **1991**, *144*, 368.

(38) Gölander, C.-G.; Kiss, E. *Journal of Colloid and Interface Science* **1988**, *121*, 240.

(39) Waldmann-Meyer, H.; Knippel, E. *Journal of Colloid and Interface Science* **1992**, *148*, 508.

CHAPTER 4

EFFECTS OF AN APPLIED SURFACE POTENTIAL AND IONIC STRENGTH ON THE STRUCTURE OF AN ADSORBED GELATIN LAYER

4.1 Introduction

The structure of a flexible polyelectrolyte layer at the solution/solid interface can be expected to reflect the electrostatic interactions between the charged polymer chains and the charged surface. A flattened conformation seems likely for flexible polyelectrolyte chains adsorbed onto oppositely charged surfaces while an extended conformation can be envisaged for charged polymers adsorbed onto similarly charged surfaces. Present knowledge of the adsorbed layer structure is derived from a relatively small number of experiments. To better understand the complex role played by electrostatic interactions in polyelectrolyte adsorption, *in situ* ellipsometry is used in this study to examine the effect of an applied surface potential on the thickness of a flexible polyelectrolyte layer at the solution/metal interface. Appendix A outlines many attempts to adsorb model, synthetic polyelectrolytes onto inert metal surfaces, none of which were successful. The adsorption of γ-globulin to platinum, discussed in Chapter 3, suggests that a flexible polyelectrolyte of similar composition might adsorb. Such an alternative was sought because a flexible chain conformation was deemed necessary to observe effects of potential on layer structure. Following this logic, gelatin was identified as a likely candidate due to its flexible amphoteric nature.

Gelatin is derived from collagen, the primary component of animal hides, bones, cartilage, and tendons. Native collagen, which exhibits a rigid-rod conformation, consists of three helical peptides chains (α chains, each with a molecular weight of ~

95,000) held in close parallel association. With an acid or base pretreatment and thermal denaturation (temperatures $\geq 39^{\circ}$ C), insoluble collagen can be transformed into water-soluble gelatin molecules, which exhibit a random coil conformation. Aqueous gelatin solutions contain a mixture of single (α), double (β), and triple (γ) stranded gelatin molecules, with the α and β forms dominating as depicted in Figure 4.1. Intermolecular crosslinks near the ends of the α chains, unaffected by mild chemical and thermal treatment, prevent complete dissociation of the chains in the original triple helix. A small number of the peptide backbone linkages are cleaved by the chemical pretreatment, and as a result, gelatin exhibits a typical polydispersity index in the range of 2 to 4.

The dominant amino acid sequence is the repeating triplet, -(glycine - X - Y)-, where X and Y are other amino acids. Proline almost always occupies the X position, while hydroxyproline is restricted to the Y position. Together, these three amino acids make up more than 50% of the molecule. The remaining portions of this protein are comprised of other nonpolar (alanyl, seryl, leucyl, valyl, threonyl, methionyl, and tyrosyl) as well as polar (glutamyl, aspartyl, lysyl, arginyl, and hystidyl) residues. Localized acidic or basic regions are not found, as polar side chains are randomly placed along the chain backbone. Because gelatin is a polyampholyte, gelatin chains exhibit a net anionic, neutral, or cationic charge depending on whether the solution pH is above, at, or below the isoelectric point (IEP). Locally, however, both positive and negative charges exist simultaneously on the gelatin chain at any moderate pH.

Using scattering methods, Pezron *et al.* [1] found the persistence length of gelatin to be on the order of 20 Å, which corresponds to six polypeptide units along the chain (two glycine-proline-Y sequences). Gelatin is therefore not as flexible as polystyrene, which has a persistence length of about 10 Å, but is more flexible than many other

biopolymers. Double-stranded DNA, for example, possesses a persistence length of 500-600 Å.

The literature reveals numerous studies of the adsorption of gelatin on silver halide crystals, reflecting the importance of gelatin as a colloidal protective agent in photographic emulsions. One of the first studies, by Curme and Natale [2] in the 1960s, concluded that gelatin adsorbed on AgBr sol in a conformation quite similar to that exhibited in aqueous solution, with maximum adsorption at the IEP. Kragh and Peacock [3] studied adsorption and desorption isotherms of gelatin on AgBr above and below the IEP, finding greater adsorption above the IEP. In addition, desorption of loosely bound gelatin was possible above the IEP. Measuring heats of adsorption, Berendsen and Borginon [4] found that the amount of gelatin adsorbed on AgBr was strongly pH-dependent, with the binding energy increasing at pH values below the IEP and remaining roughly constant above the IEP. Maternaghan *et al.* [5,6] were the first to use ellipsometry to examine adsorbed gelatin layer thicknesses and adsorbed amounts. Effects of pH, pAg, ionic strength, lattice face of AgBr, degree of phthalation, and molecular weight distribution were investigated. Their results indicated that gelatin molecules were adsorbed as 'monolayers' of random coils. The coils were laterally compressed but otherwise only moderately deformed when compared with coils in the solution state.

Studies of the adsorption of gelatin on surfaces other than silver halides are also found in the literature. Kudish and Eirich [7] adsorbed gelatin on Pyrex glass and stainless steel surfaces, measuring a maximum in the amount adsorbed at the IEP. When the surface and gelatin were oppositely charged, adsorbance remained substantial. When similarly charged, adsorption was still detected, suggesting that non-electrostatic attractions play a role in the adsorption process. Kawanishi *et al.* [8] measured the forces between gelatin layers adsorbed onto mica surfaces from KCl solutions. Their results

suggest that gelatin adsorbs in a flat configuration at pH values below the IEP, a regime where electrostatic forces between gelatin and mica are attractive. Above the IEP, a more extended gelatin conformation was observed, presumably due to repulsive interactions. At the IEP, a minimum in adsorption was detected, contrary to the previous literature. Kamiyama and Israelachvili [9] systematically investigated the adsorption of gelatin on mica as a function of pH and ionic strength using a surface force apparatus. Changes in chain conformation, exemplified by measured brush-layer thicknesses, appeared to be highly dependent on pH, with salt concentration having less of an effect. Results of their study are summarized in Table 4.1 and described pictorially in Figure 4.2. Contrary to intuitive expectations, significant adsorption was detected above the IEP, a pH range where both protein and surface displayed the same net negative charge. Adsorption was attributed to the formation of discrete ionic bonds between the negative surface groups on mica and positive basic groups on gelatin, bonds that exist even when the net charge is negative.

All of these studies strongly suggest the importance of electrostatic interactions on the adsorption of gelatin chains to charged interfaces. Therefore, it seems probable that the structure of an adsorbed gelatin layer can be controlled by the application of a potential to the adsorbing surface. In the following chapter, effects of an applied surface potential on the adsorbed gelatin layer thickness and the amount of protein adsorbed are examined using ellipsometry. Ionic strength is also a parameter in these studies.

4.2 Experimental

4.2.1 Materials

The gelatin selected for these experiments (Eastman Kodak Company) was an alkali-pretreated bone gelatin, deionized with a mixed-bed, ion-exchange resin. A

description of the protein is given in Table 4.2. Solutions were prepared by soaking the freeze-dried protein in phosphate buffer solutions at room temperature overnight and then heating the solutions to 40° C to allow for complete dissolution. Phosphate buffers, pH = 7.0 and ionic strengths I of 0.01 M and 1.0 M, were prepared by dissolving reagent grade Na_2HPO_4 and $NaH_2PO_4 \cdot H_2O$ (Fisher) in ultra-pure, deionized water (Millipore Q, UF-OR). Dynamic light scattering (DLS) (ALV/DLS-5000) was used to determine the hydrodynamic radius of gelatin as a function of ionic strength (Figure 4.3). Our results are comparable to those reported by Boedtker and Doty [10] and Pezron *et al.* [1]. (Appendix C, Figures C.1, C.4, and C.5, show the effect of pH on the hydrodynamic radius of gelatin as well as on the structure of the adsorbed layer.) A platinum foil (25 X 25 X 0.5 mm, 99.9985 % purity, Johnson Matthey) was used as the adsorbing surface. It was polished to a mirror finish with successively finer alumina grits (Buehler), ending with a particle size of 0.05 μm.

4.2.2 Instrumentation

A Rudolph Auto EL II nulling ellipsometer was used to monitor the adsorption of gelatin onto the foil. The incident light of wavelength 632.8 nm and incidence angle 70° was emitted from a helium neon laser. *In situ* adsorption studies were carried out using the newly constructed ellipsometer solution cell discussed in Section 2.4.

A potentiostat was used to apply an electric potential to the adsorbing surface. Details of this instrumentation are included in Section 2.6. Three electrodes were connected to the potentiostat and also inserted into the solution cell. The reference electrode was a miniature Ag/AgCl electrode (Cypress Systems, Inc.) in 3 M KCl saturated with AgCl. All voltages reported in this chapter are stated with respect to this reference electrode. The counter electrode was a coiled 6 inch platinum wire (0.51 mm

diameter, 99.95% purity, Fisher). The platinum foil described above was used as the working electrode.

4.2.3 Cleaning Procedure for the Platinum Foil

The platinum surface was cleaned by first immersing it in a 1:1 dilution of boiling sulfuric and nitric acid for 10 minutes to remove any residual adsorbed organic material. The surface was then rinsed with copious amounts of distilled water and immediately mounted in the ellipsometer solution cell. The cell was sealed shut and purged with N_2 to remove atmospheric CO_2. Following careful alignment of the cell in the ellipsometer, phosphate buffer, which had been passed through a 0.45 μm filter (Millipore Millex-HV) and purged with N_2, was cannulated into the cell. This solution was allowed to reach the measurement temperature of 40° C over a 12 hour period. The surface was then cleaned *in situ* by repeated electrochemical reduction at -1.3 V and oxidation at +1.4 V, potential extremes at which hydrogen ions are reduced and water is oxidized, respectively, in this buffer. Three ellipsometric measurements were taken at each extreme. This procedure was continued until reproducible values of Δ and Ψ were obtained at each extreme. Once electrochemically cleaned, adsorption experiments could be carried out.

4.3 Effects of the Initial Adsorbing Potential and Ionic Strength on Gelatin Adsorption

4.3.1 Experimental Procedure

After electrochemical cleaning, the applied potential was lowered to -1.3 V and then increased to the potential selected for gelatin adsorption. Ellipsometric measurements of the bare platinum surface with buffer present were taken at this potential to determine the complex refractive index $N = n - ik$ of the surface.

Using a syringe, 20 ml of the buffer solution was then removed from the cell. This volume was replaced by filtering (0.45 μm Millipore Millex-HV filter) 20 ml of a concentrated gelatin solution near 40° C into the cell . The resulting protein concentration was 10 mg/ml. This concentration was chosen to be similar to the γ-globulin concentration used in the preceding experiments (Chapter 3). Ellipsometric measurements were taken immediately and every 5 minutes thereafter until the variation in Δ and Ψ values became minimal (~3 hours). This steadiness suggested that not only was the equilibrium temperature of 40° C reached, but that a plateau in adsorbance was also attained.

4.3.2 Results

The complex refractive index of the bare platinum surface in the presence of buffer is calculated from the values of Δ and Ψ obtained at the initial adsorbing potential using McCrackin's NBS FORTRAN program (Section 2.3). The value of N is subsequently used as a reference in determining the thickness and refractive index of the adsorbed gelatin layer. Figures 4.4 and 4.5 exemplify the time-dependent changes in Δ and Ψ as gelatin is adsorbed onto the platinum foil at the specified potential. McCrackin's NBS single-layer program is used to calculate the adsorbed gelatin layer thicknesses and refractive indexes from these Δ and Ψ values (Figures 4.6 and 4.7).

The amount of gelatin adsorbed onto the platinum surface from the buffered protein solution is calculated using Equation 2.6, which is reiterated below:

$$A = (n_2 - n_1)\, t \,/\, (dn/dc)$$

where n_2 is refractive index of the adsorbed gelatin layer, n_1 is the refractive index of the buffered gelatin solution in which the platinum foil is immersed, t is the thickness of

the adsorbed film, and dn/dc is the refractive index increment of the gelatin solution. A value of 0.18 ml/g is used for the refractive index increment of the gelatin solution as determined by differential refractometry (Otsuka Electronics, RM-102) at constant added salt dilution. Figure 4.8 shows the change in adsorbance with time.

Variation in the initial adsorbing potential has little effect on the adsorbed gelatin layer thickness (Figures 4.9 and 4.11) or the amount of gelatin adsorbed (Figures 4.10 and 4.12), suggesting that the structure of the layer is independent of applied surface potential. Comparison of Figures 4.9 and 4.11 show a small effect of ionic strength on the thickness of the adsorbed gelatin layer. However, the amount of gelatin adsorbed varies little with ionic strength, a point best seen by Figures 4.10 and 4.12.

4.4 Effect of an Applied Surface Potential on an Adsorbed Gelatin Layer Correcting for Surface Oxidation/Reduction

4.4.1 Experimental Procedure

Once the surface was cleaned, the potential was lowered to -1.3 V and subsequently increased by 100 mV steps to +1.4 V. The same pattern was then reversed, as the potential was dropped in 100 mV increments, returning to the starting potential of -1.3 V. Three ellipsometric measurements were taken at each 100 mV step with the average Δ and Ψ values reported. A first set of ellipsometric parameters was collected for the bare surface, before exposure to gelatin.

From -1.3 V, the voltage was again increased in 100 mV increments to a potential of 0.0 V, where adsorption of gelatin was to take place. This potential was chosen for two reasons: first, ellipsometric results for the adsorption of gelatin at 0.0 V were always easily converted into thickness and refractive index values, a statement untrue for adsorption of gelatin at potentials $\leq$ -0.4 V; secondly, between the potentials of -0.6 and +0.1 V, no electrochemistry occurred on the platinum surface, allowing the

voltage to be returned to -0.6 V without changing the surface characteristics. Sample was introduced and measured by the methods described in 4.3.1. In order to determine the effect of surface potential, the voltage applied to the layer was initially lowered to -0.6 V and subsequently increased by 100 mV increments every 30 minutes to a potential of +0.3 V, with ellipsometric measurements taken at 5 minute intervals.

4.4.2 Ellipsometric Results for a Clean Platinum Surface with Variation in Applied Surface Potential

The ellipsometric parameters Δ and Ψ of a clean platinum foil immersed in a sodium phosphate buffer (pH = 7.0, I = 0.10 M) are plotted as a function of surface potential in Figures 4.13 and 4.14. The reported Δ and Ψ are an average of three measurements taken at each 100 mV step and represent one complete cycle of potential. As stated in Chapter 3, over a bare surface, changes in Δ and Ψ with potential are indicative of the electrochemical processes taking place at the platinum electrode. These processes were deduced by Benziger *et al.* using infrared spectroscopy [11]. At a surface potential of -1.3 V, the platinum surface is reduced, and Δ and Ψ reach their maximum values. These values remain constant up to a potential of +0.1 V, suggesting that no electrochemistry occurs between -1.3 V and +0.1 V. However, when the surface potential is increased further, Δ and Ψ drop due to the adsorption of OH (or O) on the surface. At a surface potential of ~+1.1 V, the electrolysis of water begins, causing O_2 to be produced [12,13]. As the surface becomes oxidized, Δ and Ψ reach their minimum values at a potential of +1.4 V. Lowering the potential to +0.1 V, OH (or O) begins to desorb from the platinum surface, causing Δ and Ψ to increase. At potentials more negative than +0.1 V, Δ and Ψ become constant and very close to those previously attained at these potentials. The surface is once again reduced.

Between the two potential extremes, the values of Δ differ by ~1.8° , while the values of Ψ differ by ~0.16°. These changes are similar to those reported in the literature [14-18] and greatly exceed the corresponding standard deviations of ±0.033° and ±0.017°, respectively, determined by averaging the standard deviations of the three ellipsometric readings taken at each applied potential. The complex refractive index for the bare platinum is found to vary with applied surface potential due to changes in the chemical nature of the platinum surface.

4.4.3 Ellipsometric Results for the Effects of Applied Potential on an Adsorbed Gelatin Layer

The parameters Δ and Ψ obtained for the gelatin-covered platinum foil in the presence of the buffered protein solution are plotted as a function of applied surface potential in Figures 4.15 and 4.16. A comparison of Δ and Ψ obtained for the protein-covered platinum foil and those obtained for the bare platinum surface in the presence of the phosphate buffer is shown in Figures 4.17 and 4.18. These ellipsometric parameters are further compared in Appendix C (Figures C.2 - C.3).

Because Δ and Ψ for the protein-covered surface during the 30 minute measurement period at each potential are not statistically different, averages are used in determining the thickness and refractive index of the adsorbed gelatin layer at each potential. The complex refractive index of the bare platinum foil at the same potential is employed as the reference value from which changes upon adsorption are measured. McCrackin's NBS program is used to calculate the adsorbed gelatin layer thickness and refractive index at each applied potential. The results are shown in Figures 4.19 and 4.20. Error bars are determined through McCrackin's program by inputting the standard deviations for Δ and Ψ ($\pm$ 0.033° and $\pm$ 0.017°, respectively) as the experimental error for the measurement. The true thickness and refractive index values

lie within these calculated limits with a 95% probability. An average adsorbed gelatin layer thickness of ~ 370 Å is determined. No effect of applied surface potential on the thickness of an adsorbed protein layer is observed within experimental error.

The amount of gelatin adsorbed onto the platinum surface from the buffered protein solution is calculated to be ~ 3.1 mg/m^2 using Equation 2.6. Once a plateau in adsorbance is reached at the initial adsorbing potential, variation in applied surface potential does not change the amount adsorbed (Figure 4.21).

4.5 Discussion

4.5.1 Effect of an Applied Surface Potential on the Structure of the Adsorbed Gelatin Layer

Because gelatin is a flexible polyampholyte, variation in the electrostatic interactions between the protein and the platinum surface was expected to alter the structure of an adsorbed gelatin layer. Surprisingly, the results of our study prove otherwise. Adsorbed gelatin layer thicknesses and plateau adsorbances are shown to be independent of the surface potential at which gelatin is initially adsorbed onto the platinum foil (Figures 4.9 - 4.12). This result suggests that there is no driving force for structural changes in the adsorbed gelatin layer with variation in potential. When adsorbing gelatin at a potential 0.0 V and subsequently varying the surface potential between -0.6 and +0.3 V, no change is observed in adsorbed layer thickness or amount adsorbed (Figures 4.19 and 4.21, respectively) within the error of the experiment.

A probable explanation for these results is as follows. Gelatin adsorbs onto platinum as a fairly dense layer, demonstrated by a measured adsorbance of ~ 2 to ~ 3 mg/m^2 and an adsorbed layer thickness of ~ 350 to ~ 500 Å. At a pH of 7.0, the net charge on gelatin is negative. Locally, however, this protein carries both positive and negative charges along its backbone. Because the chains in the adsorbed layer are so

closely associated with one another, the electrostatic interactions between segments of the chains are high. Consequently, the adsorbed gelatin layer is overwhelmed by these segment-segment interactions and oblivious to variations in applied surface potential (Figure 4.22).

Because of the minimal role that surface-segment electrostatic interactions play in the alteration of an adsorbed gelatin layer, the potential of zero surface charge (PZC) was not measured. Literature values for the PZC for platinum in neutral salt solutions are found to range between -0.2 and +0.2 V [19-22], with values highly dependent on the medium in which the metal surface is immersed, as well as the crystal face which dominates [13].

As evidenced in Chapter 3, oxidation/reduction of the platinum surface does occur with variation in applied surface potential even after the protein has been adsorbed onto the surface. Therefore, the ellipsometric data for the gelatin-covered surface are corrected for surface oxidation/reduction when determining adsorbed layer thicknesses, refractive indexes, and adsorbances. The correction procedure utilizes the difference in the Δ value obtained for the bare platinum surface and that measured for the gelatin-covered platinum surface at the same surface potential ($\delta\Delta$) (Figures 4.17 and C.2). The same is done for Ψ ($\delta\Psi$) (Figures 4.18 and C.3). Because small differences in $\delta\Delta$ or $\delta\Psi$ result in large changes in layer thicknesses and adsorbances, experimental error can be magnified when calculating adsorbed layer properties. Thickness and adsorbance results least subject to distortion are those obtained at surface potentials where no electrochemistry occurs on the bare metal surface. In the experiments described above, this window of potential is between -1.3 V and +0.1 V. To extend these potential limits further, care must be taken to accurately account for surface oxidation. Because the amount of gelatin adsorbed on platinum is approximately half that of γ-globulin (i.e., $\delta\Delta$ and $\delta\Psi$ measured for gelatin adsorption are half those

obtained of γ-globulin adsorption), there is less tolerance for experimental errors in δΔ and δΨ. As might be expected, the greatest chance for error in δΔ and δΨ arises when ellipsometric parameters change rapidly with potential (potentials greater than +0.1 V in this experiment). Therefore, adsorbed gelatin layer thicknesses, refractive indexes, and adsorbances are only determined to a potential of +0.3 V. At potentials greater than this threshold, errors in δΔ and δΨ result in unrealistic values for adsorbed layer properties.

4.5.2 Effect of Ionic Strength on the Structure of the Adsorbed Gelatin Layer

Ionic strength I appears to have only a very slight effect on the structure of an adsorbed gelatin layer at a pH of 7.0. At I = 0.01 M, the average adsorbed layer thickness in phosphate buffer is determined to be ~ 490 Å ± 100 Å. Increasing I to 0.1 M, thereby screening charge to a greater extent, causes a small decrease to ~ 370 Å ± 100 Å. These results are similar to those reported by Kamiyama and Israelachvili [9] at the same pH (Table 4.1, Figure 4.2). Attempts to determine gelatin layer thicknesses at higher ionic strengths met with little success, as the measured Δ and Ψ could not be matched with corresponding thickness and refractive index values. The failure suggests that the increased salt concentration interferes in some way with the ellipsometric measurement.

Dynamic light scattering is used to determine the hydrodynamic radius R_h of gelatin as a function of I. Knowing the protein's molecular dimensions in solution, the effect of adsorption on the conformation of gelatin can be inferred. An average hydrodynamic radius of 152 Å is measure for gelatin in phosphate buffer at pH = 7.0 and I = 0.01 M or 0.1 M. Virtually no effect of salt concentration on the size of this molecule is observed (Figure 4.3). The ellipsometric thickness for an adsorbed flexible polymer layer has been shown to be 1.7 times greater than the root-mean square

thickness t_{rms} [23], the latter being somewhat larger than the radius of gyration R_g but smaller than the root-mean square end-to-end distance. Herning *et al.* [24] determined R_g/R_h for their gelatin system (pH = 7.0, 0.1 M NaCl) to be 1.5, but cautioned that the ratio should depend on the chain configuration (linear or branched), the molecular weight, the solvent quality, and the polydispersity index. Theoretical models [25,26] predict this ratio to lie between 1.72 and 1.86, but experimental values [27,28] are generally lower. Assuming $R_g/R_h = 1.5$, the gelatin used in our experiments possesses a R_g of 228 Å at pH = 7.0 and 0.01 M < I < 0.1 M. From the length of a peptide bond (3-3.5 Å) and the number of amino acid residues in the chain (~ 1000), the root-mean square end-to-end distance of gelatin is 3000-3500 Å. The R_g and root-mean square end-to-end distance of gelatin are compared with the t_{rms} values obtained for adsorbed gelatin layers. Dividing measured ellipsometric thicknesses by 1.7, t_{rms} = 289 Å (I = 0.01 M) and 215 Å (I = 0.1 M), suggesting that gelatin adsorbs on platinum in a random coil conformation which is not significantly distorted with applied surface potential.

Complementing the thickness result, little effect of ionic strength on the amount of gelatin adsorbed is observed. Adsorbances of 2.4 ± 1.0 mg/m^2 and 2.0 ± 1.0 mg/m^2 are calculated for gelatin adsorbed onto platinum from the phosphate buffer at I = 0.01 M and 0.1 M, respectively. Assuming a molecular weight of 100,000, the area occupied by one adsorbed gelatin molecule is therefore ~70 - 81 nm^2.

4.6 Conclusions

Although gelatin is a flexible polyampholyte, no change in adsorbed layer thickness or amount of protein adsorbed is measured during variation of surface potential, after correction of the ellipsometric data for oxidation/reduction of the platinum surface. Relating solution conformation of gelatin determined by dynamic

light scattering to adsorbed layer dimensions, gelatin is found to adsorb onto platinum in a random coil conformation at all potentials examined. A probable explanation for these results is that lateral segment-segment interactions within a flexible polyelectrolyte layer are more important to layer structure than the long range segment-surface interactions. Ionic strength is confirmed to have little, if any, effect on the structure of the adsorbed layer at a pH of 7.0, a trend similar to the results reported by Kamiyama and Israelachvili [9].

Table 4.1. Results of Kamiyama and Israelachvili's study [9] for the adsorption of gelatin on mica as a function of pH and ionic strength (I). A surface force apparatus was used to measure brush-layer thickness (L).

	pH = 3.5	**IEP = 5.0**	**pH = 7.5**
I = 0.0001	L = 150 Å	L = 300 Å	L = 650 Å
I = 0.001	L = 150 Å	L = 620 Å	L = 500 Å
I = 0.01	L = 100 Å	L = 250 Å	L = 470 Å

Table 4.2. Description of Gelatin.

General Properties	
Molecular weight of single α chain	95,000
Polydispersity[a]	~ 2.0
Isoelectric point[b]	pH 4.9
Composition (Amino Acid Groups)[c]	
Nonionic groups (glycine, alanine, proline, hydroxyproline, etc.)	80 %
Anionic groups (glutamic acid, aspartic acid, etc.)	12 %
Cationic groups (lysine, arginine, histidine, hydroxylysine, etc.)	8 %

[a]Determined by Rose [29]. [b]Determined by measuring pH after mixed-bed ion-exchange resin treatment [30]. At the IEP, the net charge of gelatin is zero. [c]The structure is as follows:

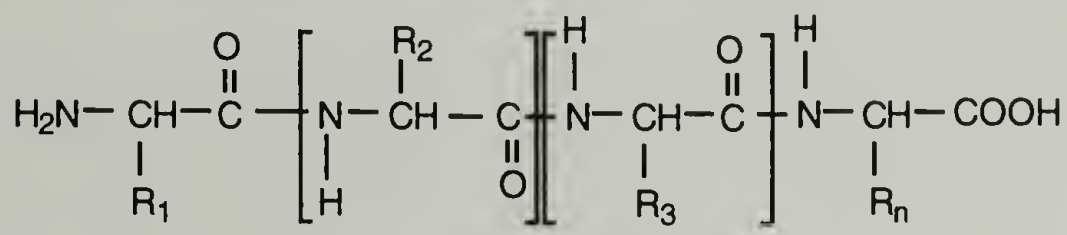

where R_n = amino acid group (n ~ 1000)

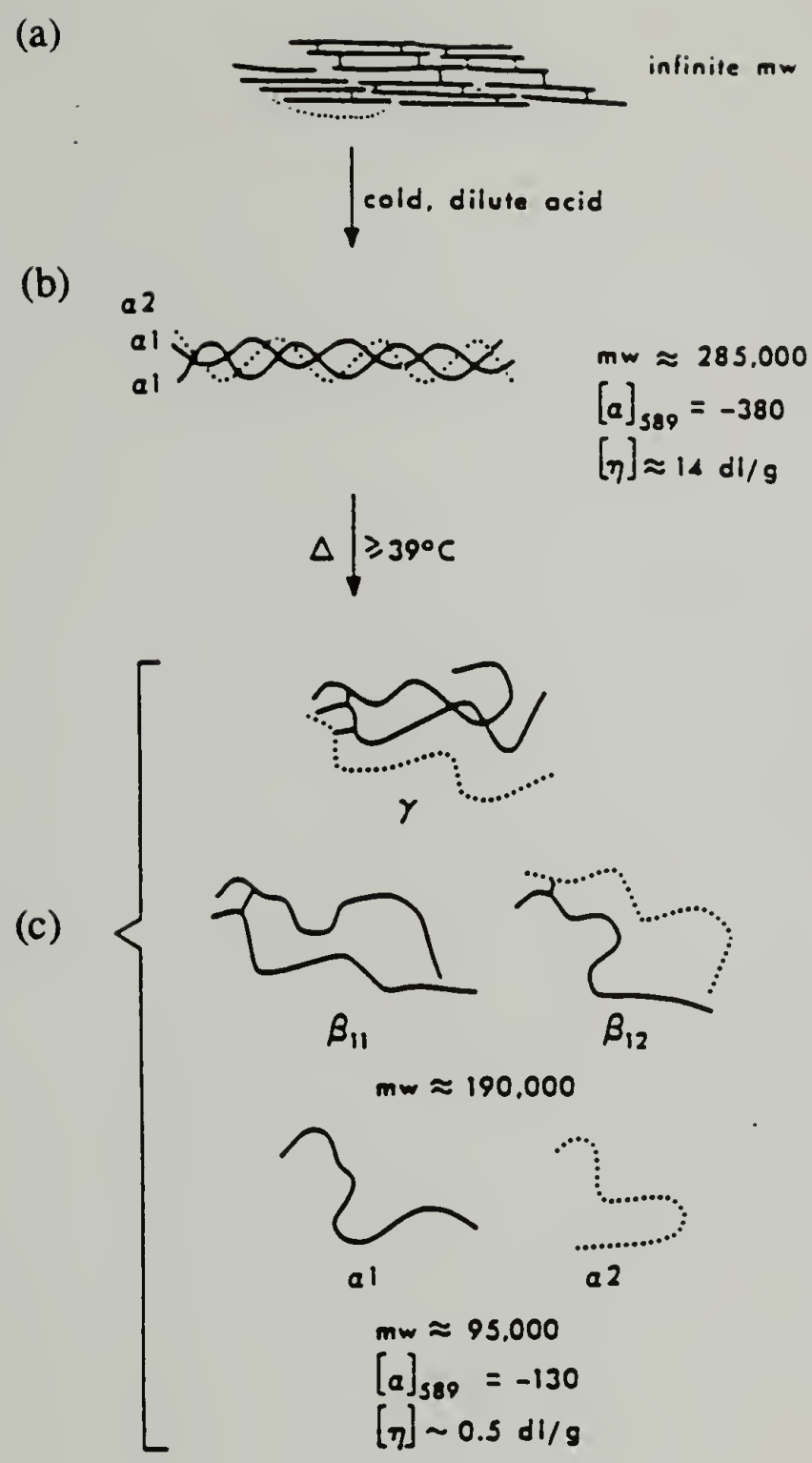

Figure 4.1. Various levels of collagen protein organization as depicted by Rose [29]: (a) Highly crosslinked array of collagen molecules in fibrous tissue. (b) A single collagen molecule composed of three α chains. (c) The three kinds of random-coil gelatin molecules that can result from thermally denaturing the native molecule.

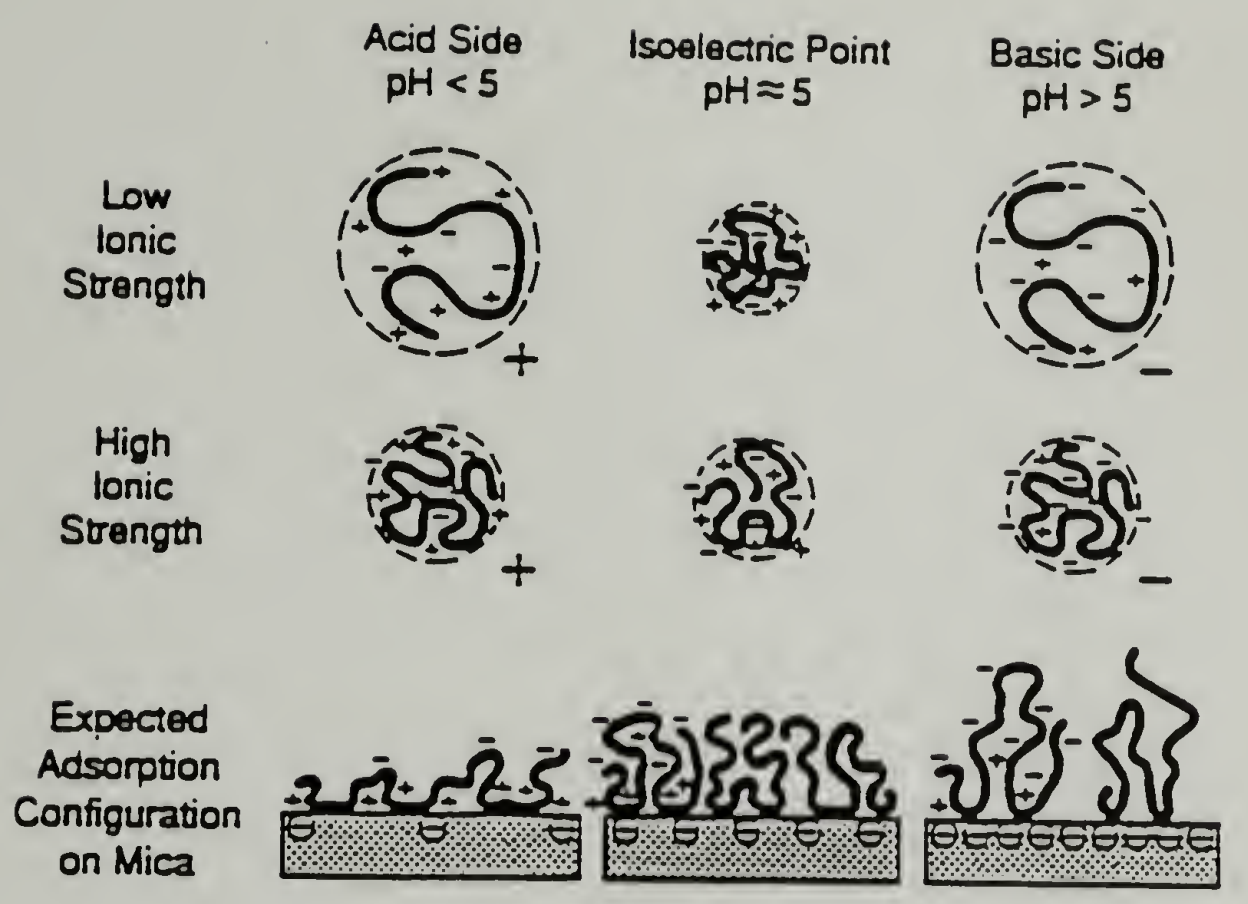

Figure 4.2. Likely coil configurations of gelatin in solution and when adsorbed onto a negatively charge mica surface as a function of pH and ionic strength as suggested by Kamiyama and Israelachvili [9].

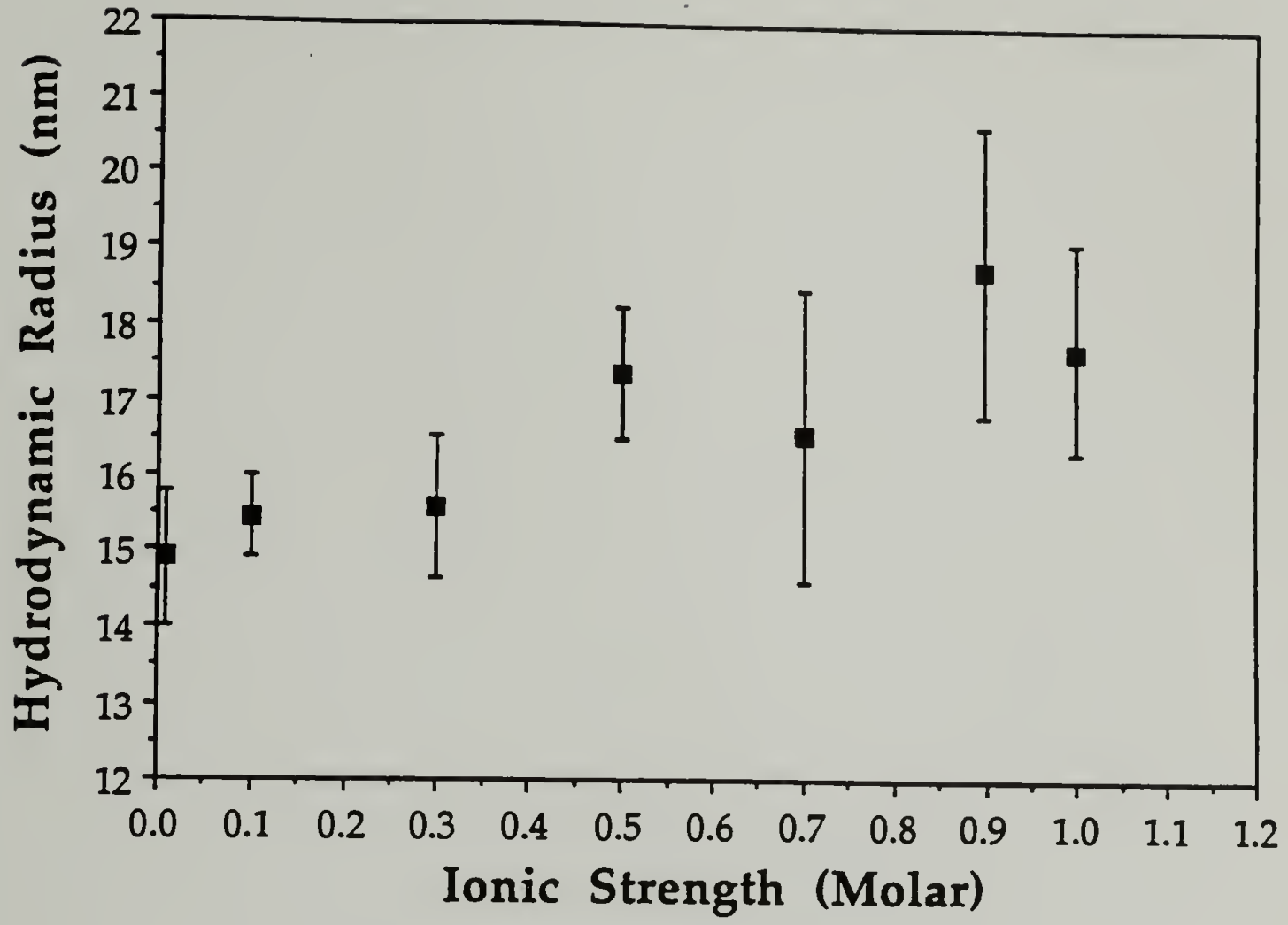

Figure 4.3. Hydrodynamic radius of gelatin in sodium phosphate buffer at a pH = 7.0 as a function of ionic strength determined by dynamic light scattering.

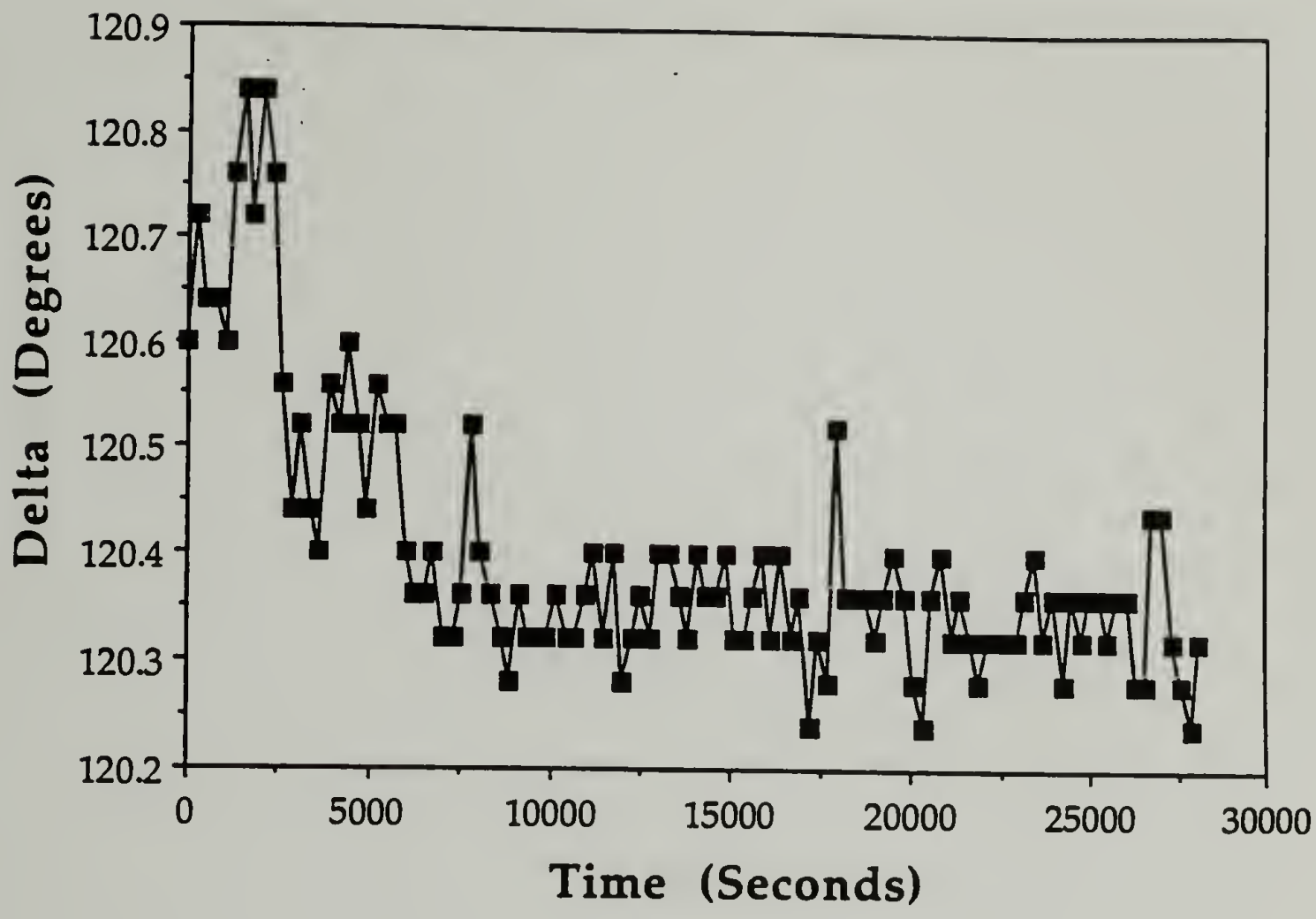

Figure 4.4. Delta as a function of time for the adsorption of gelatin on platinum from a sodium phosphate buffer solution (pH = 7.0, I = 0.10 M) at 40° C and 0.0 V.

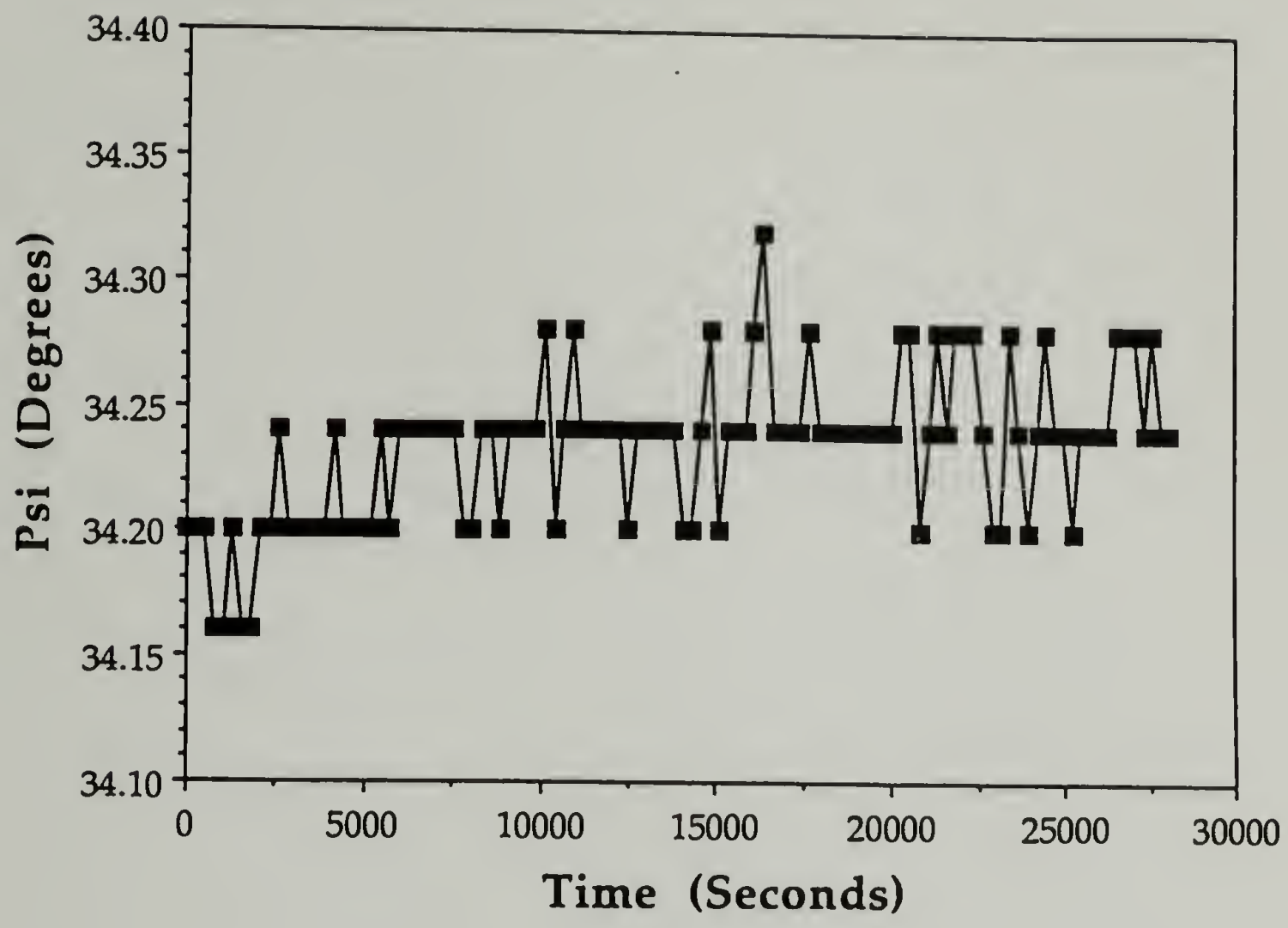

Figure 4.5. Psi as a function of time for the adsorption of gelatin on platinum from a sodium phosphate buffer solution (pH = 7.0, I = 0.10 M) at 40° C and 0.0 V.

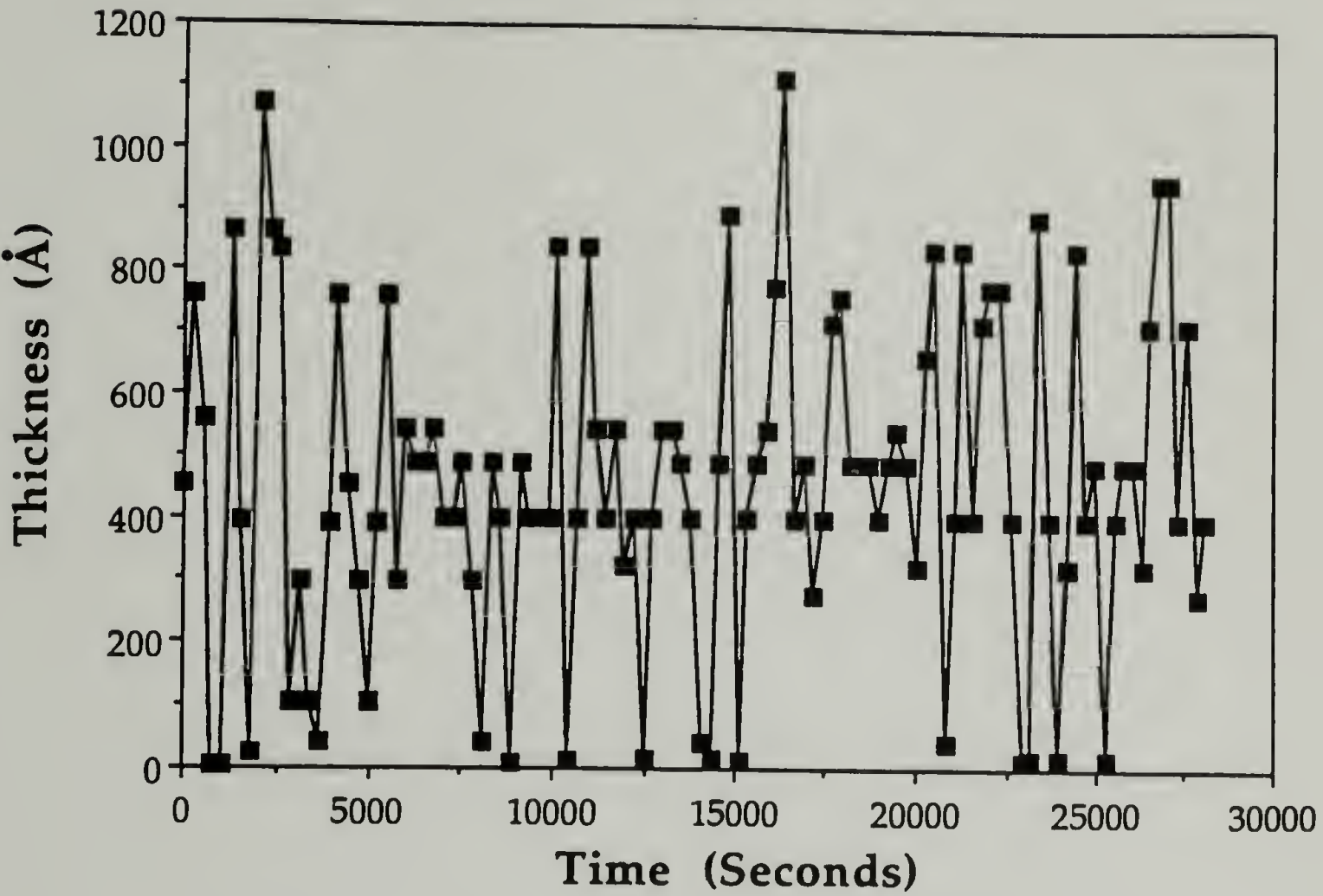

Figure 4.6. Thickness plotted as a function of time for the adsorption of gelatin on platinum in the presence of a sodium phosphate buffer solution (pH = 7.0, I = 0.10 M) at 40° C and 0.0 V.

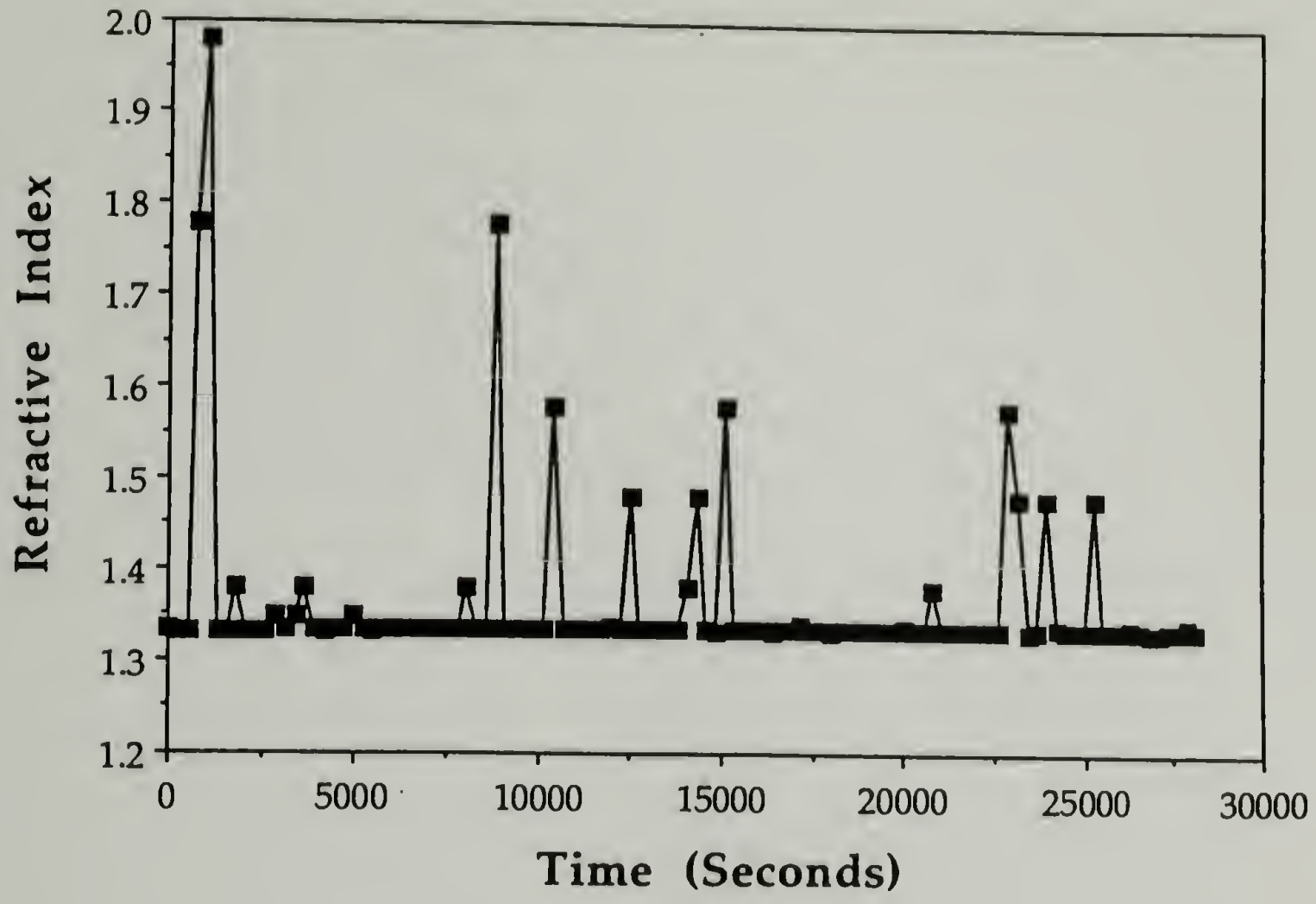

Figure 4.7 Refractive index of an adsorbed gelatin layer on platinum in the presence of a sodium phosphate buffer solution (pH = 7.0, I = 0.10 M) plotted as a function of time at 40° C and 0.0 V.

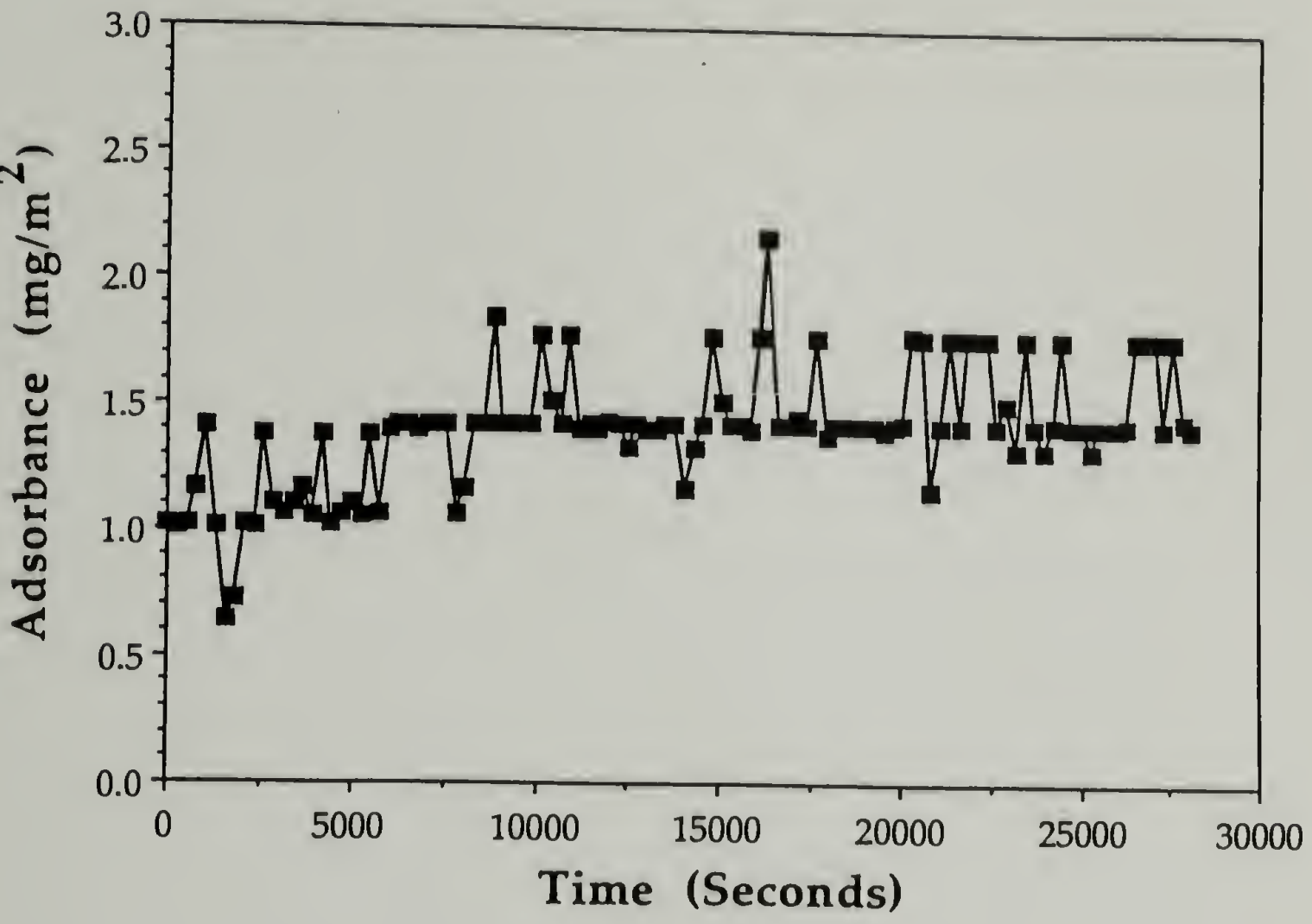

Figure 4.8. Adsorbance plotted as a function of time for gelatin on platinum in the presence of a sodium phosphate buffer solution (pH = 7.0, I = 0.10 M) at 40° C and 0.0 V.

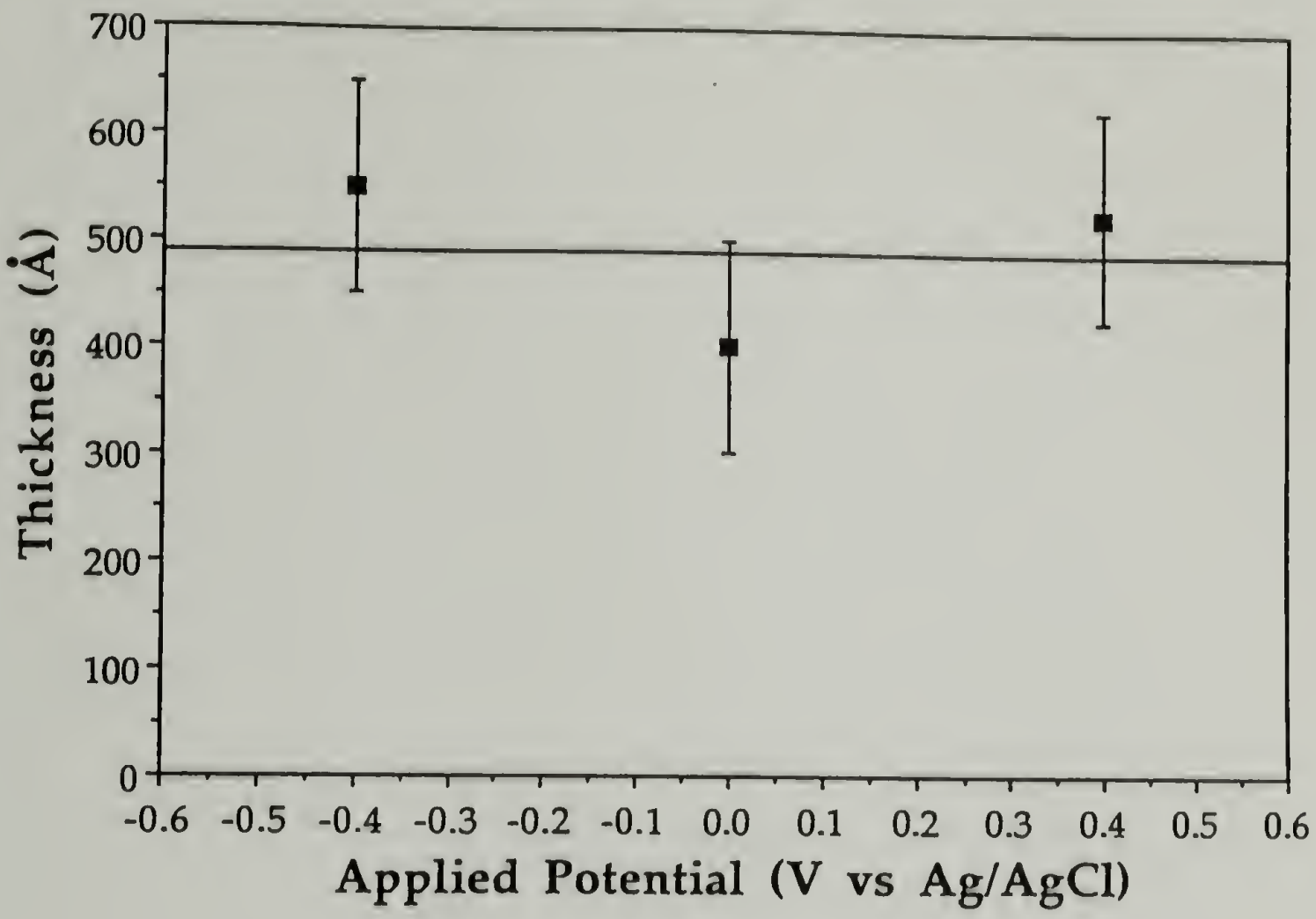

Figure 4.9. Adsorbed gelatin layer thickness on platinum in the presence of a sodium phosphate buffer solution (pH = 7.0, I = 0.10 M) at 40° C as a function of initial adsorbing potential.

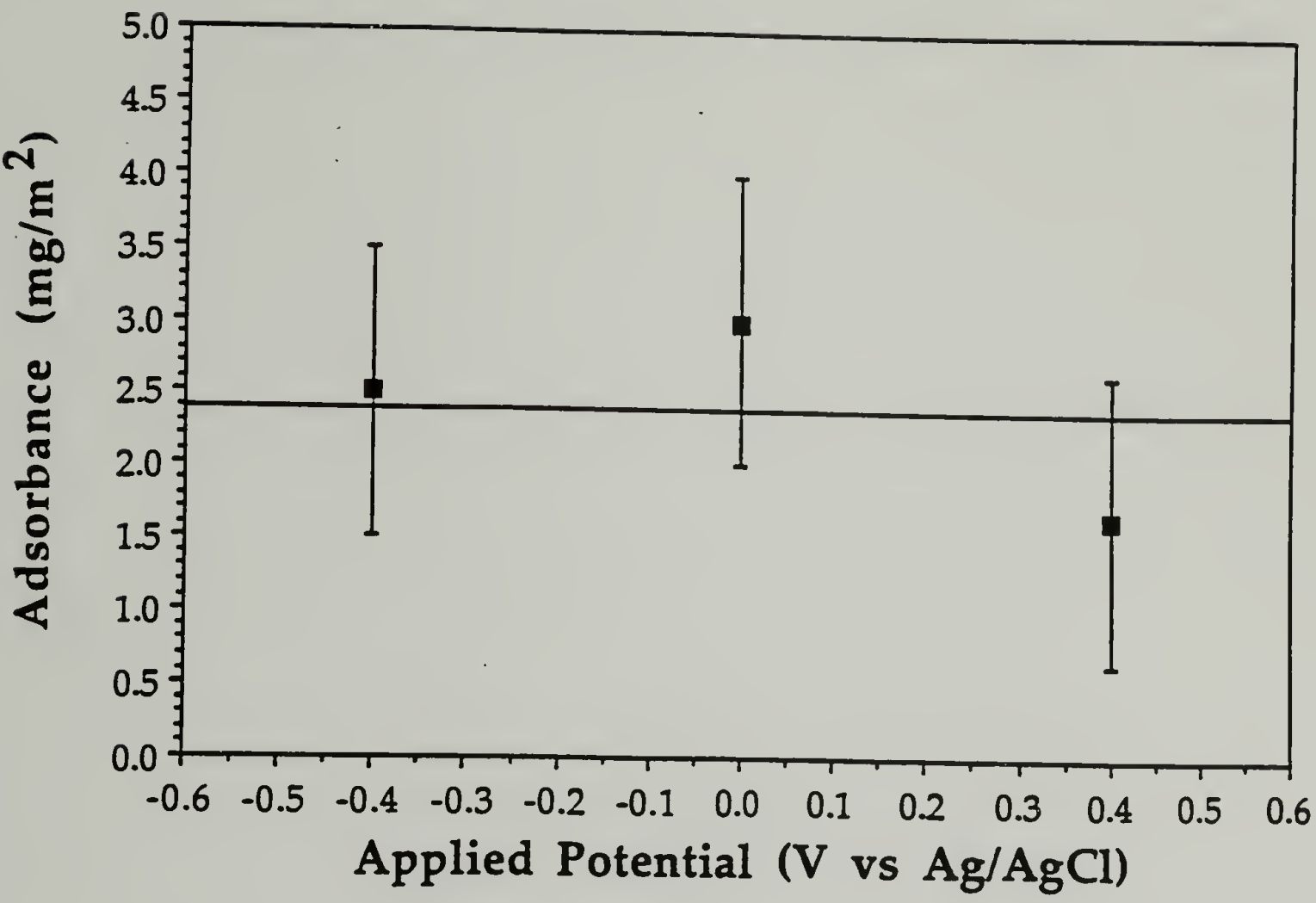

Figure 4.10. The amount of gelatin adsorbed on platinum in the presence of a sodium phosphate buffer solution (pH = 7.0, I = 0.10 M) at 40° C as a function of initial adsorbing potential.

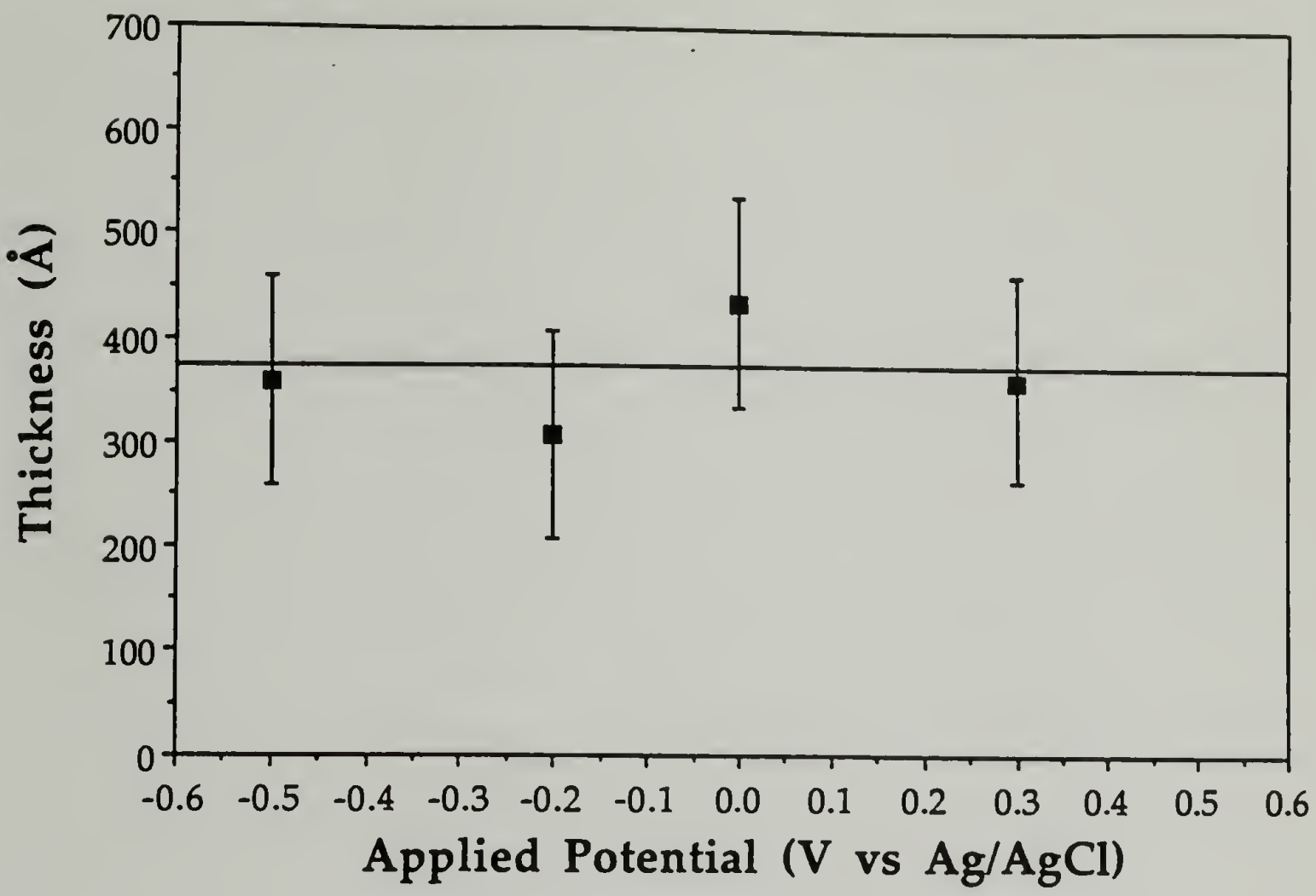

Figure 4.11. Adsorbed gelatin layer thickness on platinum in the presence of a sodium phosphate buffer solution (pH = 7.0, I = 0.01 M) at 40° C as a function of initial adsorbing potential.

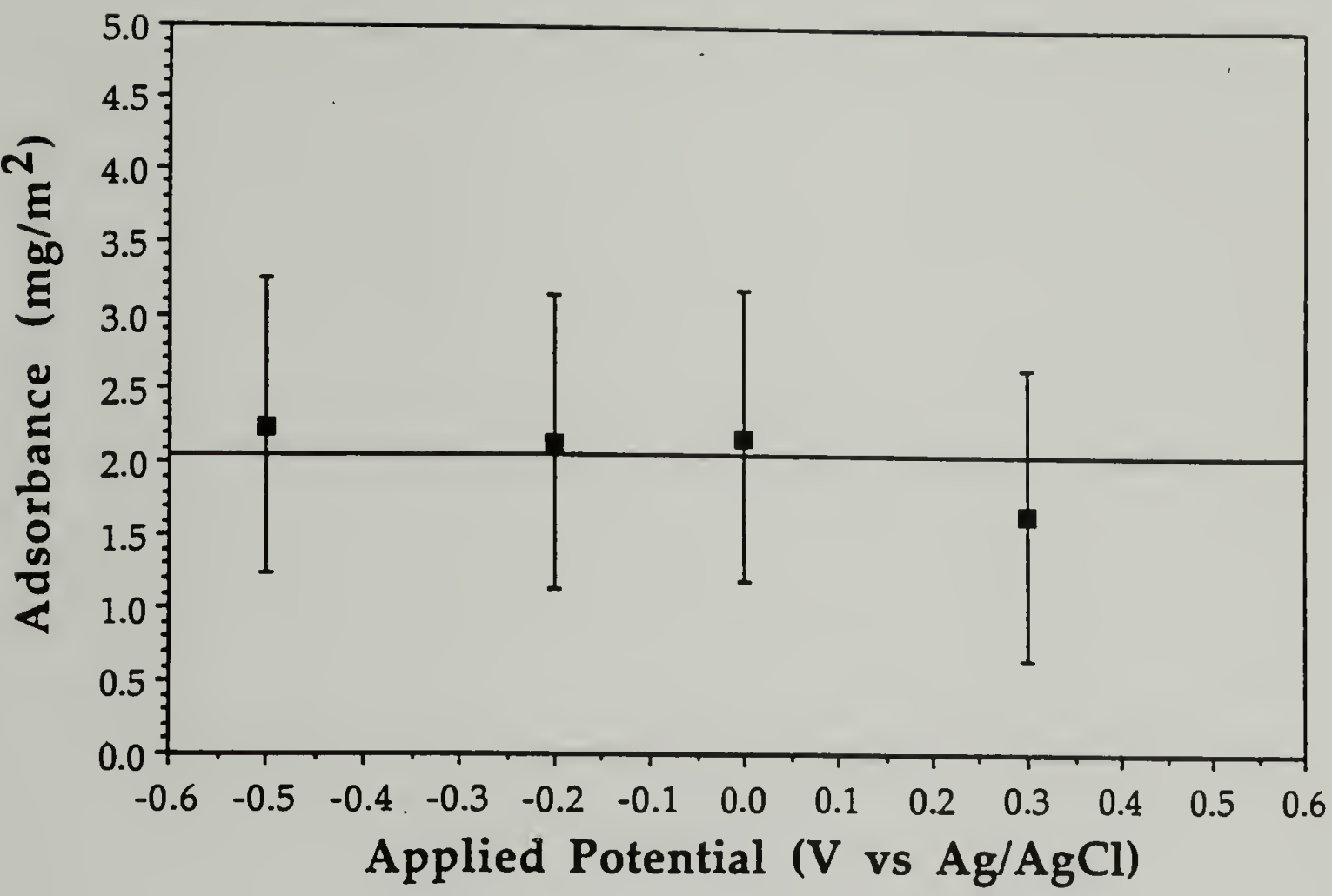

Figure 4.12. The amount of gelatin adsorbed on platinum in the presence of a sodium phosphate buffer solution (pH = 7.0, I = 0.01 M) at 40° C as a function of initial adsorbing potential.

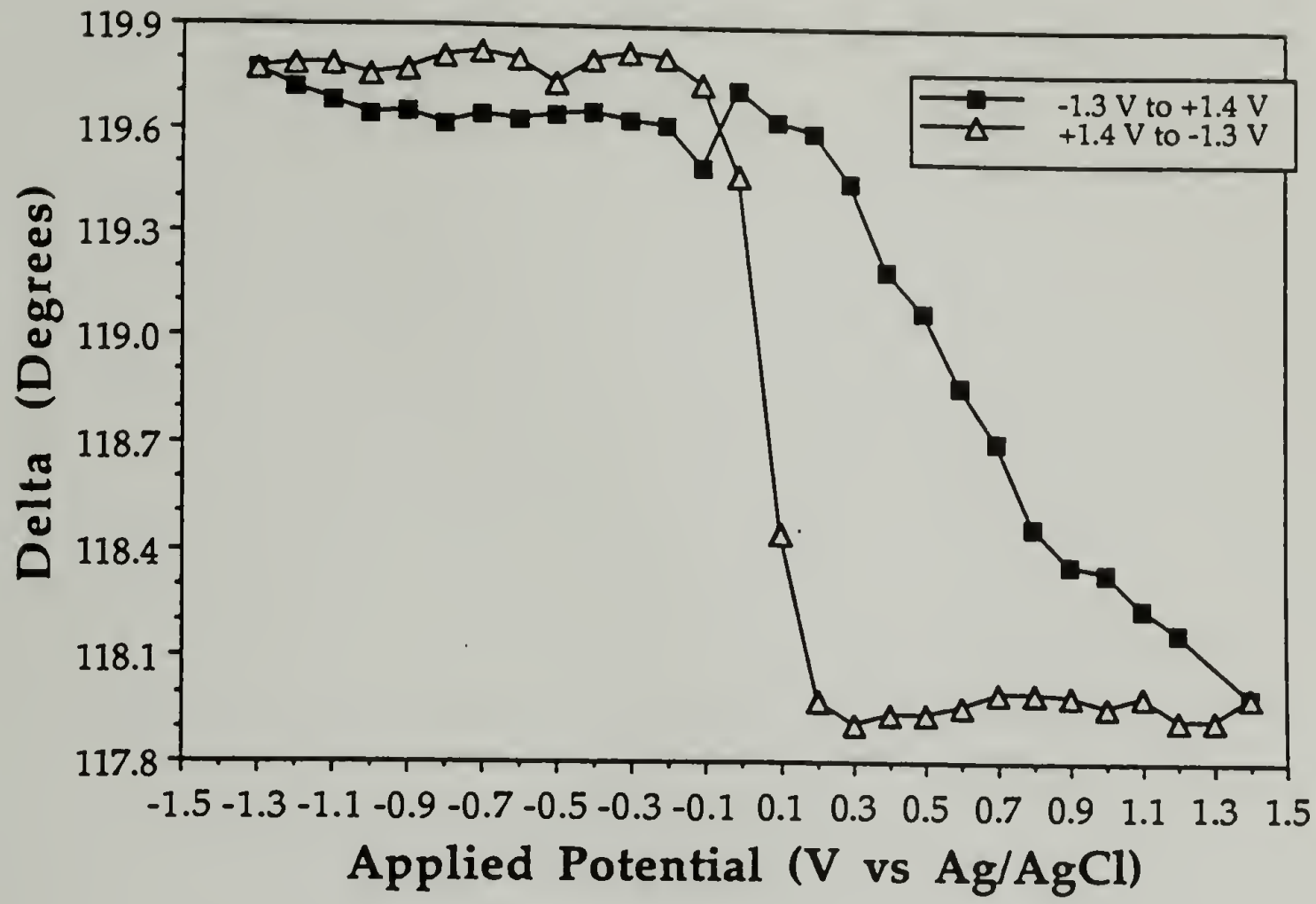

Figure 4.13. Delta plotted as a function of applied surface potential for a bare platinum surface immersed in a sodium phosphate buffer (pH = 7.0, I = 0.10 M) at 40° C. The average of three ellipsometric measurements taken at each potential are shown.

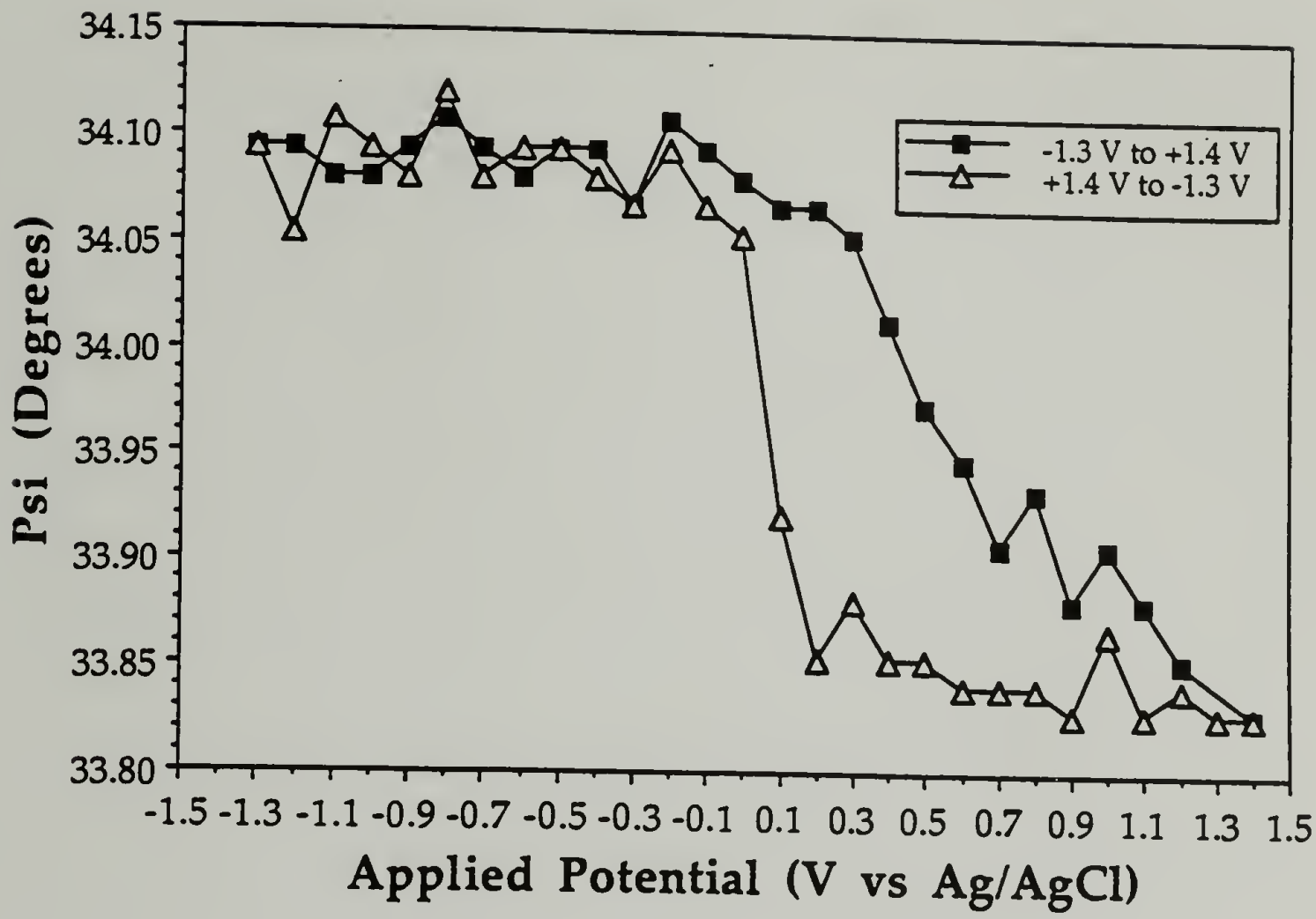

Figure 4.14. Psi plotted as a function of applied surface potential for a bare platinum surface immersed in a sodium phosphate buffer (pH = 7.0, I = 0.10 M) at 40° C. The average of three ellipsometric measurements taken at each potential are shown.

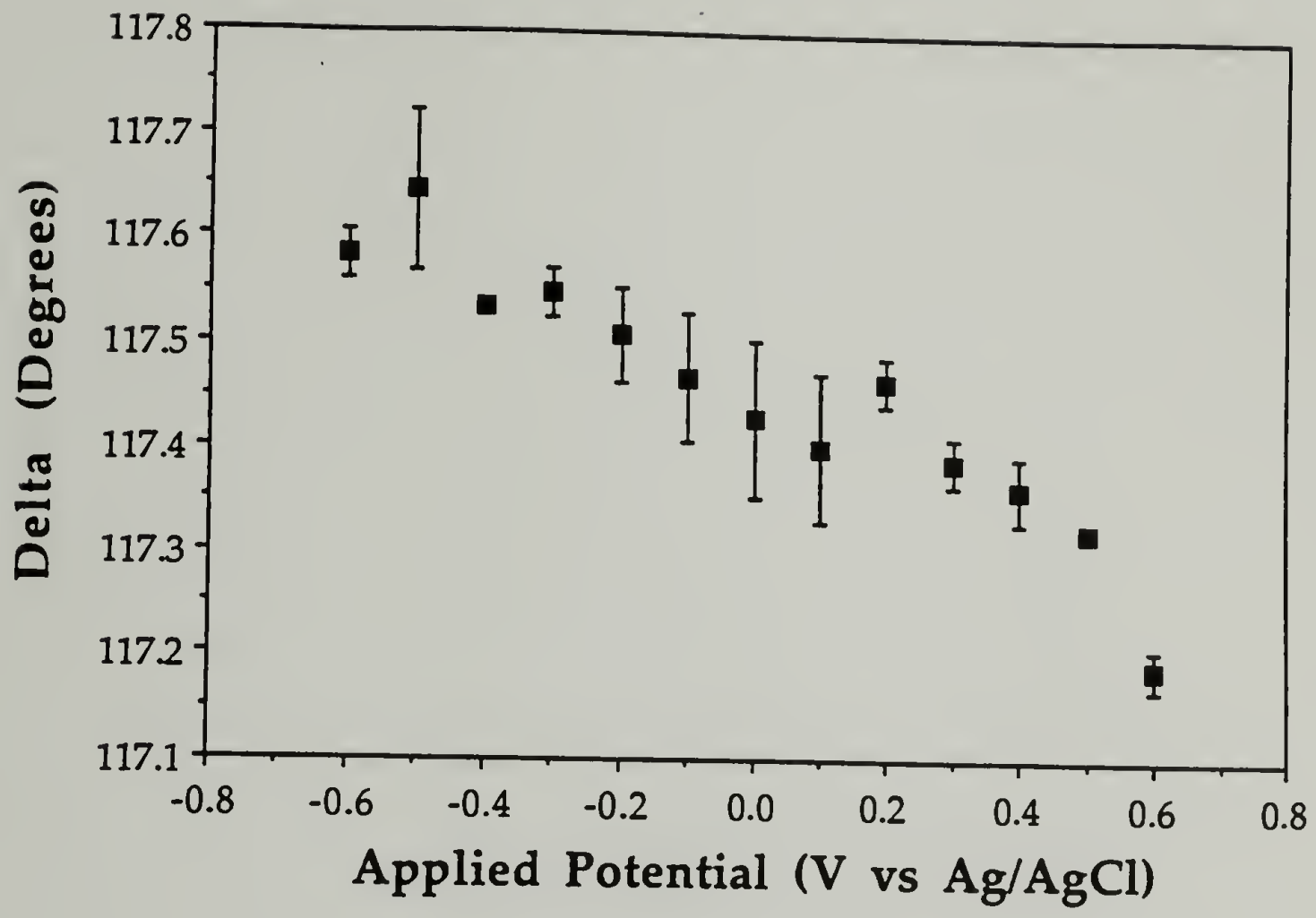

Figure 4.15. Delta plotted as a function of applied surface potential for the gelatin-covered platinum foil in the presence of the buffered protein solution (pH = 7.0, I = 0.10 M) at 40° C.

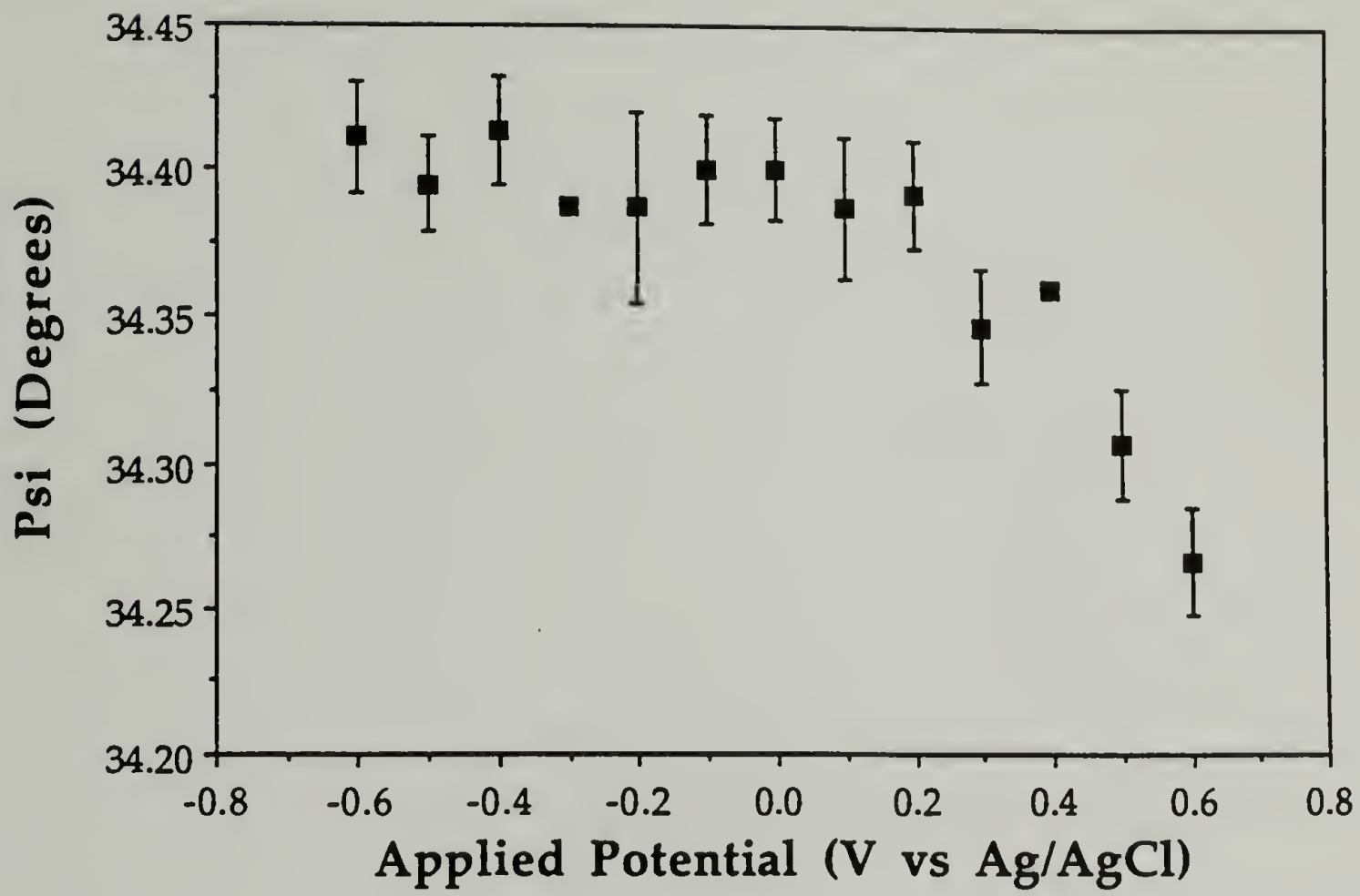

Figure 4.16. Psi plotted as a function of applied surface potential for the gelatin-covered platinum foil in the presence of the buffered protein solution (pH = 7.0, I = 0.10 M) at 40° C.

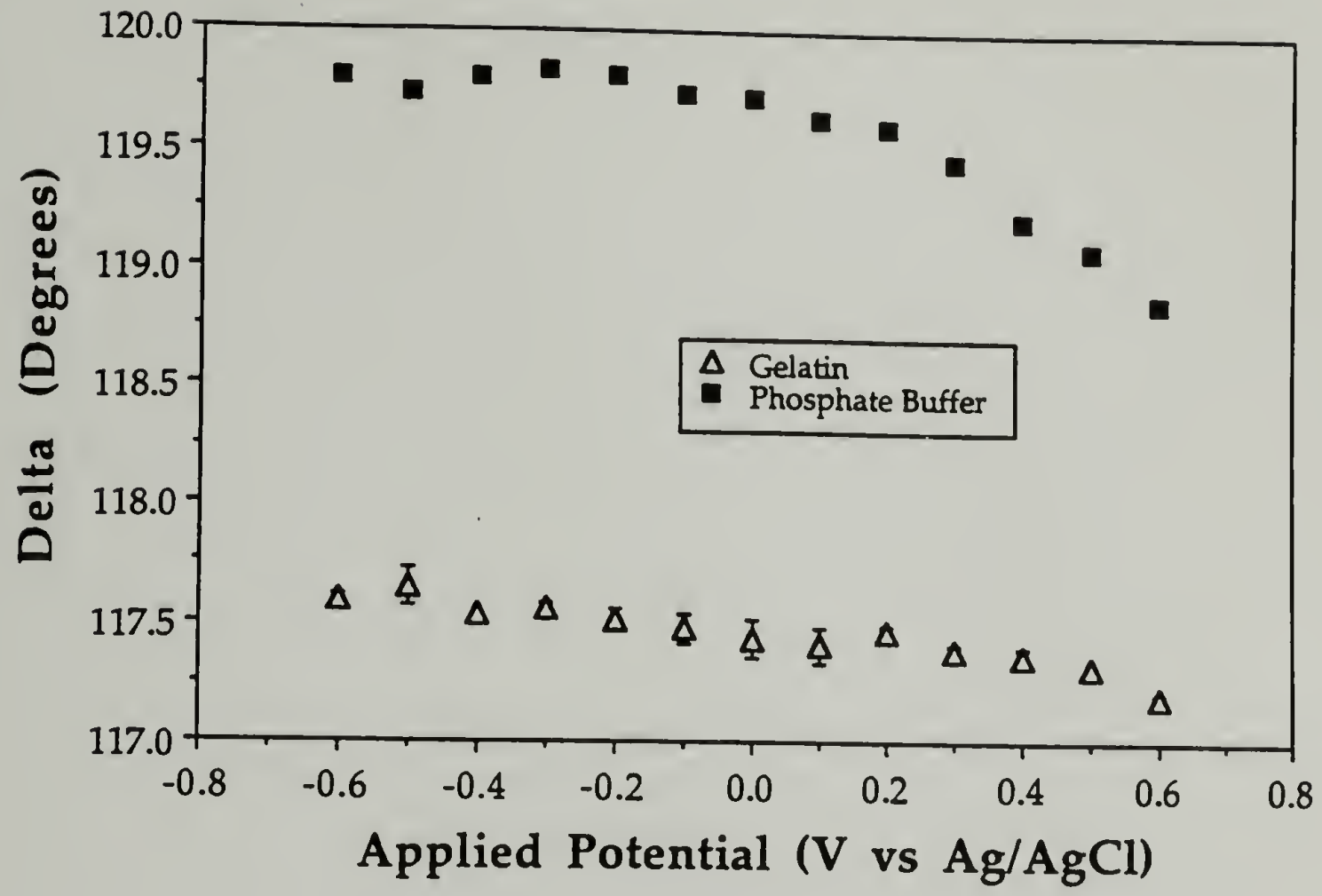

Figure 4.17. Comparison of the change in Delta with variation in applied surface potential for the bare platinum surface immersed in the phosphate buffer solution (pH = 7.0, I = 0.10 M) to that for the gelatin-covered platinum surface in the presence of the buffered protein solution (pH = 7.0, I = 0.10 M) at 40° C.

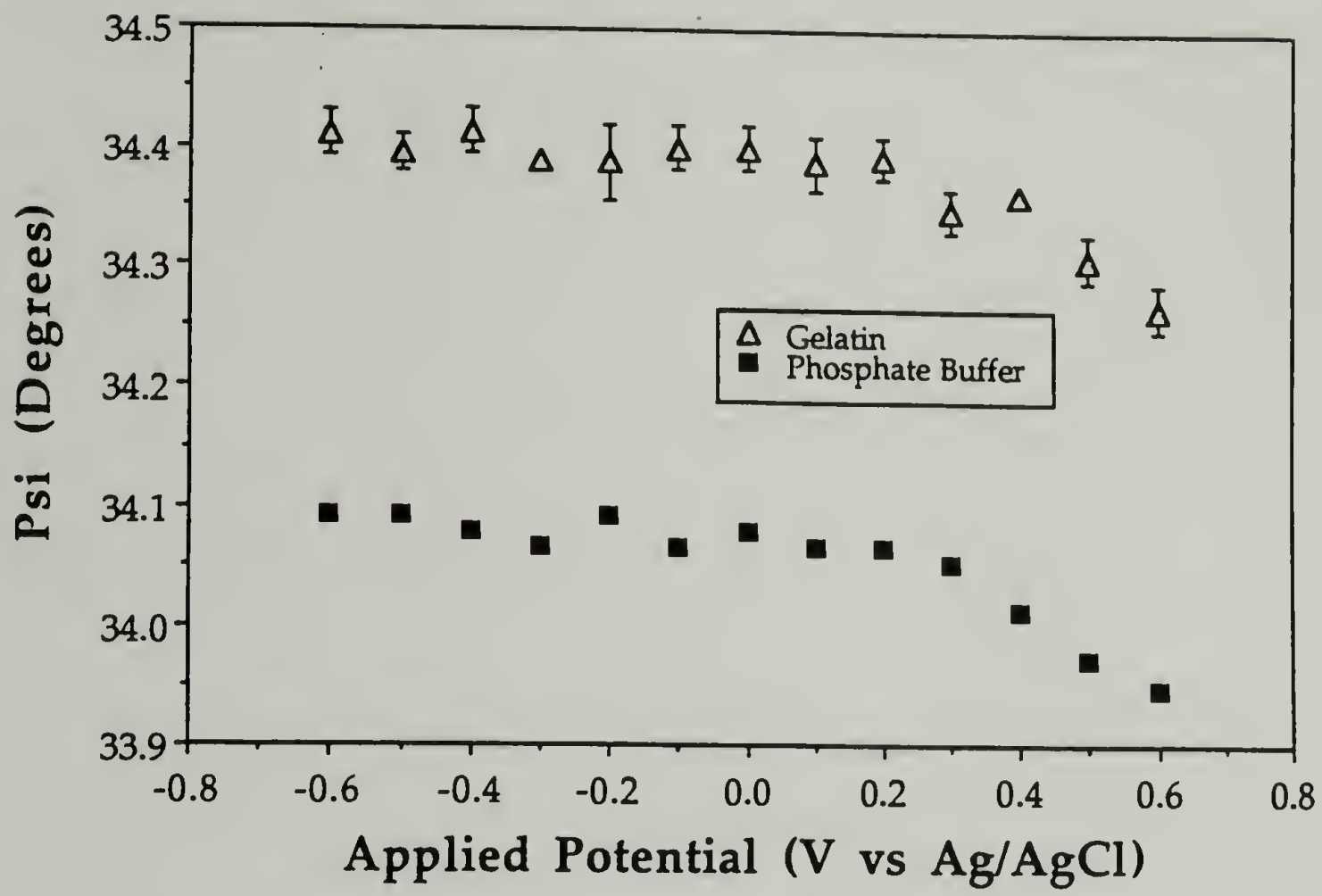

Figure 4.18. Comparison of the change in Psi with variation in applied surface potential for the bare platinum surface immersed in the phosphate buffer solution (pH = 7.0, I = 0.10 M) to that for the gelatin-covered platinum surface in the presence of the buffered protein solution (pH = 7.0, I = 0.10 M) at 40° C.

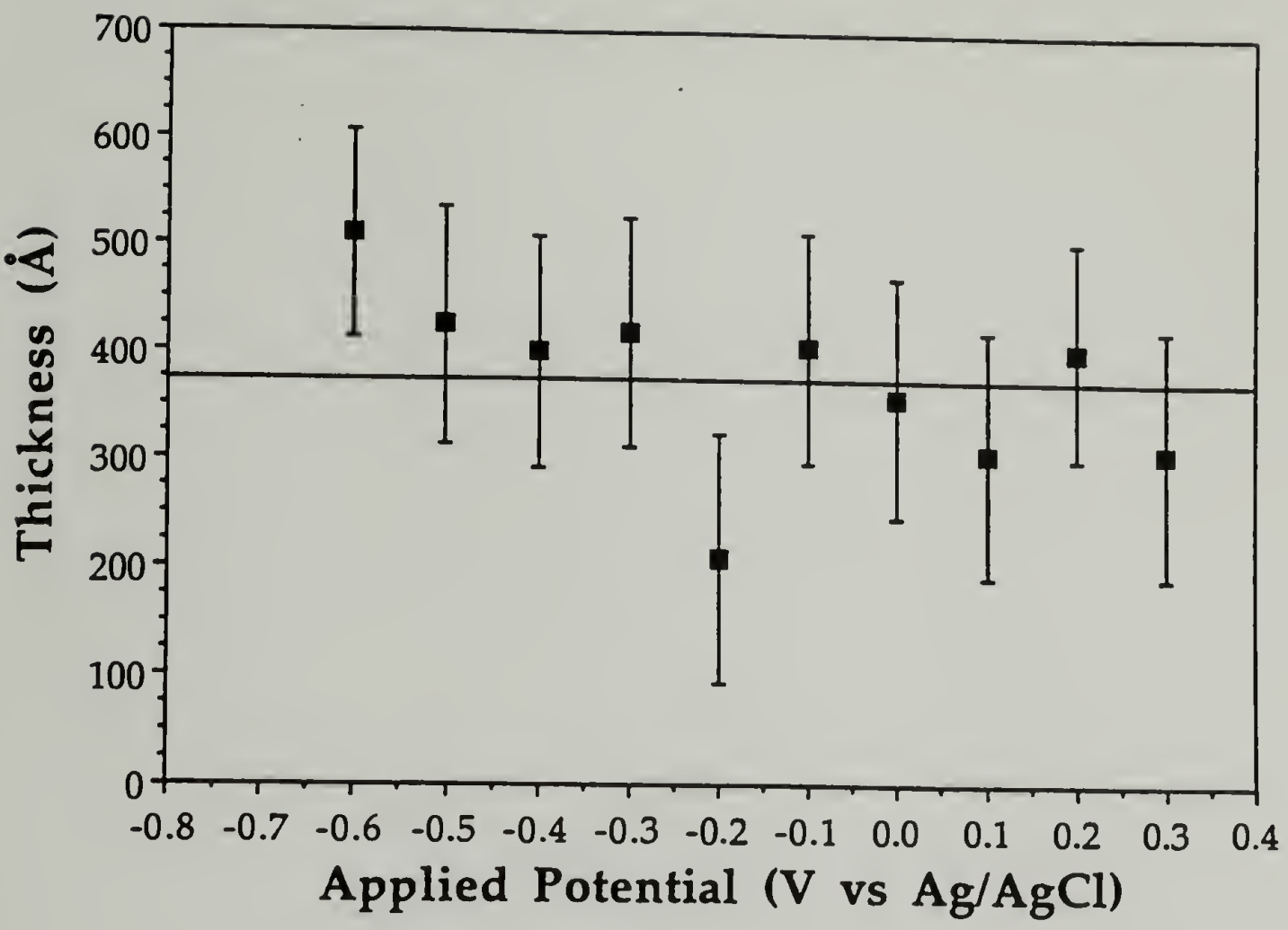

Figure 4.19. Plot of adsorbed gelatin layer thickness on a platinum foil in the presence of a buffered protein solution (pH = 7.0, I = 0.10 M) at 40° C as a function of applied surface potential.

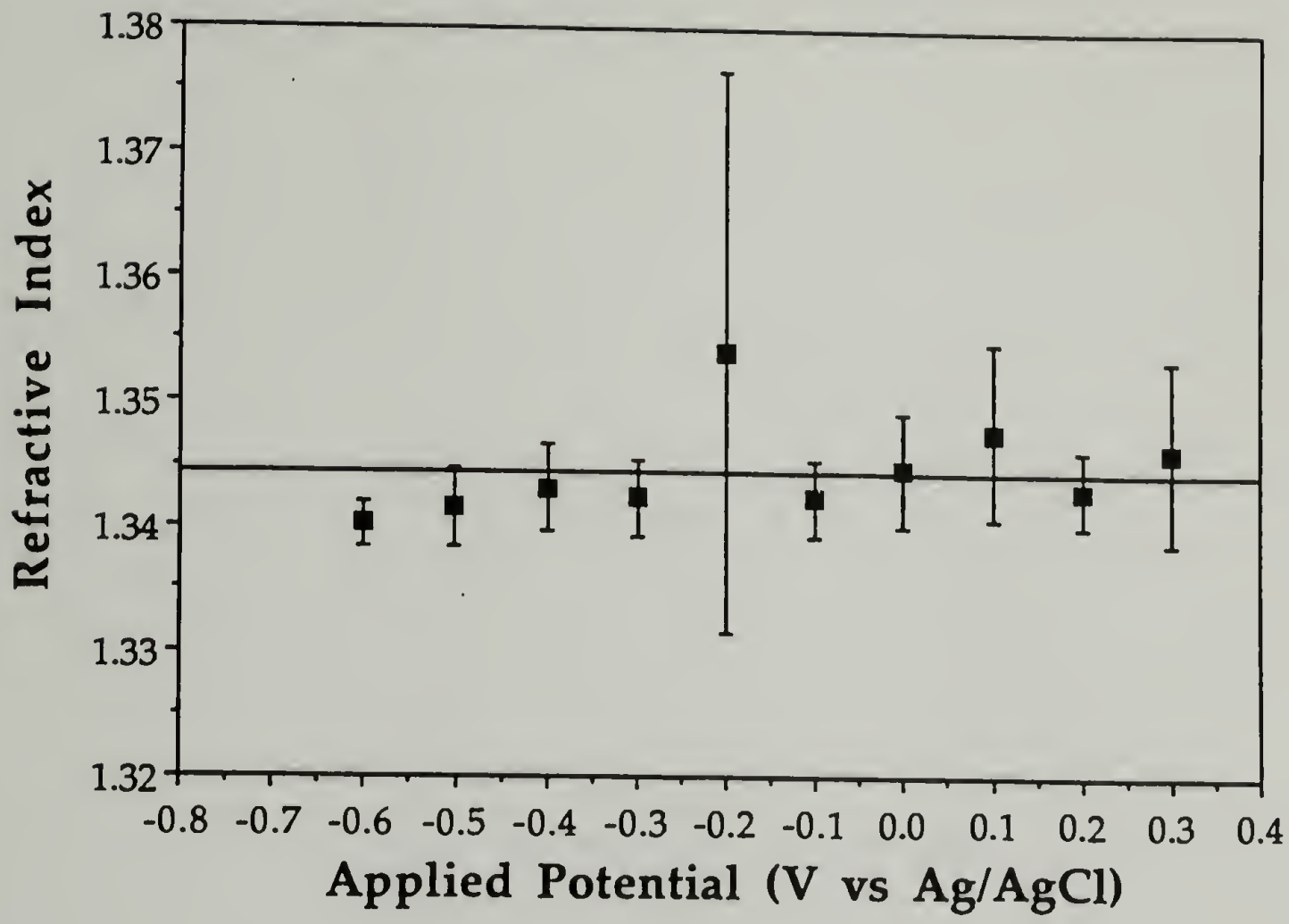

Figure 4.20. Plot of refractive index of the adsorbed gelatin layer on a platinum foil in the presence of a buffered protein solution (pH = 7.0, I = 0.10 M) at 40° C as a function of applied surface potential.

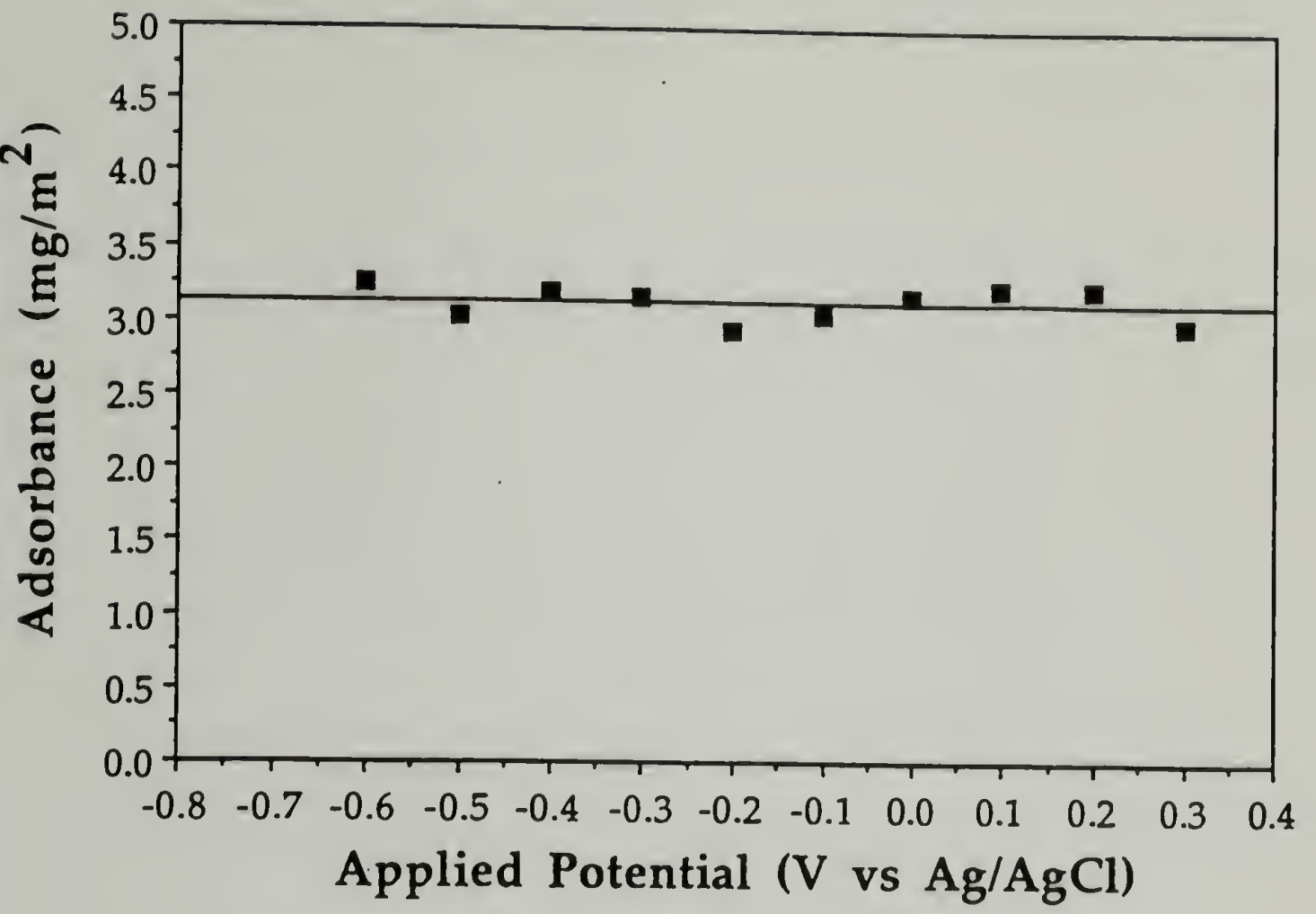

Figure 4.21. Plot of the amount of gelatin adsorbed on the platinum surface from a buffered gelatin solution (pH = 7.0, I = 0.10 M) at 40° C as a function of applied surface potential.

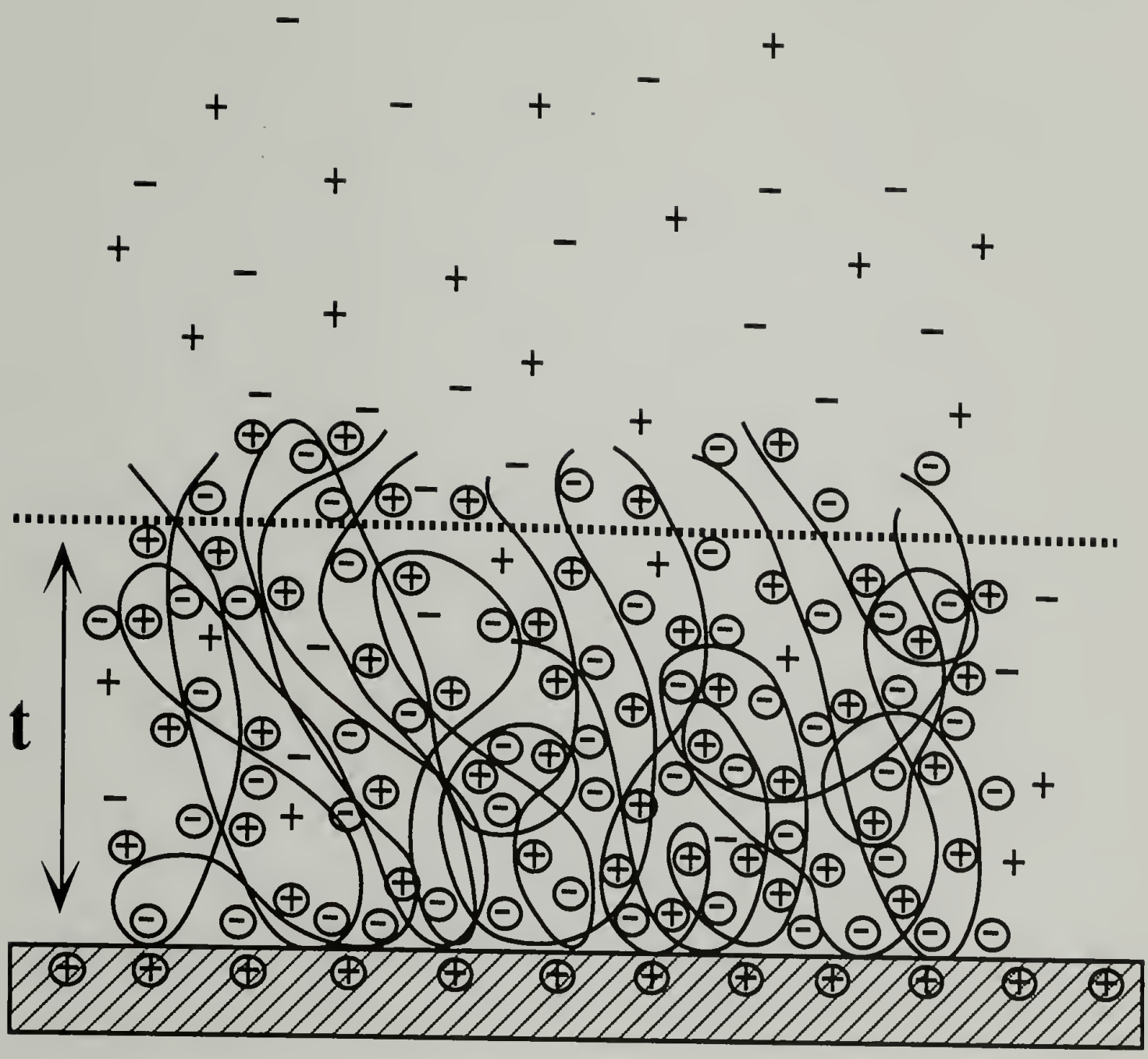

Figure 4.22. Cartoon of gelatin adsorption on a charged platinum surface. Lateral segment-segment interactions appear to be more important to layer thickness than segment-surface interactions.

4.7 References

(1) Pezron, I.; Djabourov, M.; Leblond, J. *Polymer* **1991**, *32*, 3201.

(2) Curme, H. G.; Natale, C. C. *Journal of Physical Chemistry* **1964**, *68*, 3009.

(3) Kragh, A. M.; Peacock, R. *Journal of Photographic Science* **1967**, *15*, 220.

(4) Berendsen, R.; Borginon, H. *Journal of Photographic Science* **1968**, *16*, 194.

(5) Maternaghan, T. J.; Ottewill, R. H. *Journal of Photographic Science* **1974**, *22*, 279.

(6) Maternaghan, T. J.; Bangham, O. B.; Ottewill, R. H. *Journal of Photographic Science* **1980**, *28*, 1.

(7) Kudish, A. T.; Eirich, F. R. *Proteins at Interfaces*; American Chemical Society: Anaheim, CA, 1987; Vol. 343.

(8) Kawanishi, N.; Christenson, H. K.; Ninham, B. W. *Journal of Physical Chemistry* **1990**, *94*, 4611.

(9) Kamiyama, Y.; Israelachvili, J. *Macromolecules* **1992**, *25*, 5081.

(10) Boedtker, H.; Doty, P. *Journal of Physical Chemistry* **1954**, *58*, 968.

(11) Benziger, J. B.; Pascal, F. A.; Bernasek, S. L.; Soriaga, M. P.; Hubbard, A. T. *Journal of Electroanalytical Chemistry* **1986**, *198*, 65.

(12) Adams, R. N. *Electrochemistry at Solid Electrodes*; Marcel Dekker, Inc.: New York, 1969.

(13) Gileadi, E. In *Electrode Kinetics for Chemists, Chemical Engineers, and Materials Scientists*VCH Publishers, Inc.: New York, 1993.

(14) Besio, G. J. Ph.D. Thesis, Princeton University, 1986.

(15) Parsons, R.; Visscher, W. H. M. *Journal of Electroanalytical Chemistry* **1972**, *36*, 329.

(16) Reddy, A. K. N.; Genshaw, M. A.; Bockris, J. O. *Journal of Chemical Physics* **1968**, *48*, 671.

(17) Vinnikov, Y. Y.; Shepelin, V. A.; Veselovskii, V. I. *Élektrokhimiya* **1973**, *9*, 534.

(18) Vinnikov, Y. Y.; Shepelin, V. A.; Veselovskii, V. I. *Élektrokhimiya* **1973**, *9*, 624.

(19) Andersen, T. N.; Anderson, J. L.; Eyring, H. *Journal of Physical Chemistry* **1969**, *73*, 3562.

(20) Campanella, L. *Journal of Electroanalytical Chemistry* **1970**, *28*, 228.

(21) Damaskin, B. B.; Petrii, O. A.; Batrakov, V. V. *Adsorption of Organic Compounds on Electrodes*; Plenum Press: New York-London, 1971.

(22) Kallay, N.; Torbic, Z.; Golic, M.; Matijevic, E. *Journal of Physical Chemistry* **1991**, *95*, 7028.

(23) McCrackin, F. L.; Colson, J. P. In *Ellipsometry in the Measurement of Surfaces and Thin Films*; NBS Misc. Publication #256: Washington, D.C., 1964; 61.

(24) Herning, T.; Djabourov, M.; Leblond, J. *Polymer* **1991**, *32*, 3211.

(25) Weill, G.; des Cloiseaux, J. *Journal de Physique II* **1979**, *40*, 99.

(26) Burchard, W. *Advances in Polymer Science* **1980**, *48*, 1.

(27) Akcasu, A. Z.; Han, C. *Macromolecules* **1979**, *12*, 276.

(28) Adam, M.; Delsanti, M. *Journal de Physique II* **1976**, *37*, 1045.

(29) Rose, P. I. In *The Theory of the Photographic Process*; Fourth Edition; T. H. James, Ed.; Macmillan Publishing Co., Inc.: New York, 1977; 51.

(30) Janus, J.; Kenchington, A. W.; Ward, A. G. *Research (London)* **1951**, *4*, 247.

CHAPTER 5

CONCLUSIONS AND FUTURE WORK

5.1 Conclusions

This thesis examines the effect of an applied surface potential on the structure of an adsorbed polyelectrolyte layer at the solution/metal interface. Attempts to adsorb model, synthetic polyelectrolytes, such as poly(styrene sulfonate), poly(acrylic acid), poly(vinylpyridine), poly-(L-lysine), and poly-(L-glutamic acid) onto inert metal surfaces met with little success. No adsorption was detected using ellipsometry. This surprising null result suggests that attractive electrostatic forces between the polymer and surface cause these highly charged polyelectrolyte chains to adsorb in extremely flattened conformations with adsorbances smaller than the detection limits of the instrument. In the absence of nonelectrostatic forces to anchor the chains, repulsive electrostatic forces oppose adsorption. These forces provide an impetus for chain extension from the surface in the case where nonelectrostatic forces are of sufficient strength to pin down the chains. Faced with these dual problems, an alternative candidate needed to be identified for this project. A search of the literature revealed the adsorption of biological macromolecules onto inert metal surfaces [1-12]. Many biopolymers contain both acidic and basic groups which allow the charge on the polymer to be controlled by adjusting the pH. In addition to these hydrophilic groups, hydrophobic regions are also present which may provide an additional driving force for adsorption or increase the dimensions of the adsorbed layer, facilitating detection by ellipsometry.

One such biopolymer, γ-globulin, was identified as an ideal candidate for the development of a method by which *in situ* ellipsometry could be combined with voltammetry to correctly determined adsorbed layer thicknesses and adsorbances. Because of this protein's extremely rigid conformation, resulting from 16 disulfide bond linkages, no effect of an applied surface potential on the structure of this adsorbed layer was expected. Previous investigators reported changes in adsorbed layer thickness with surface potential as segments are attracted and repelled from the surface [2,6,13-15]. However, surface oxidation/reduction effects were neglected by these investigators when analyzing ellipsometric results, based on a belief that protein adsorption passivates the surface. This thinking, however, is absurd; otherwise, physisorption would be widely used as a means to protect surfaces of such structures as buildings, bridges, or even architectural ruins. Our investigation of the adsorption of γ-globulin on platinum provides evidence for surface oxidation/reduction with variation in surface potential despite polymer adsorption. When all effects are properly considered, an adsorbed γ-globulin layer thickness of ~250 Å and an adsorbance of ~ 7.0 mg/m^2 are determined at a pH of 8.5, where the polymer carries a net negative charge. Subsequent variation in surface potential has no effect on layer thickness or adsorbed amount. These results suggest that γ-globulin adsorbs in its native conformation and that the surface potential does not affect the structure of this rigid layer.

In contrast, adsorbed layer alterations with surface potential are anticipated for flexible polyelectrolyte chains. Because of the unsuccessful attempts to adsorb model, synthetic polyelectrolytes onto inert metals, a flexible polyelectrolyte, similar in composition to γ-globulin, was desired. A search of possible candidates identified gelatin. Upon adsorption of this protein from a phosphate buffer at a pH of 7.0 and a temperature of 40° C, a layer thickness between 370 and 490 Å is determined, with adsorbances varying between 2.0 to 2.4 mg/m^2 irrespective of ionic strength. These

values suggest that gelatin adsorbs onto platinum in a random coil conformation. Variation in surface potential again does not change the adsorbed layer thickness or amount adsorbed, once ellipsometric results are corrected for surface oxidation/reduction, a result which was unexpected for a flexible polyelectrolyte system. Therefore, lateral segment-segment interactions within this flexible polyelectrolyte layer appear to be more important to layer structure than long range segment-surface interactions.

5.2 Future Work

Our investigation has brought us a step closer to understanding the complex role of electrostatic interactions in the adsorption of polyelectrolytes at solution/solid interfaces. However, further work is necessary to elucidate the conditions under which the structure of an adsorbed charged polymer layer can be controlled by surface potential. The results of our study suggest that surface potential effects can be best observed when lateral segment-segment interactions are minimized, thereby maximizing segment-surface interactions. To accomplish this feat, polyelectrolyte chains could be end-grafted at a controlled density to an inert metal surface. The known specific binding of organosulfur compounds on gold might be exploited [16-20].

Optimal grafting density for the exploitation of surface potential will depend on such factors as type and number of charges along the backbone of the polymer chain, surface charge density, and ionic strength. Polyampholytes which simultaneously possess positive and negative charges exhibit both attractive and repulsive segment-segment and segment-surface interactions, making their adsorption behavior very complex. The chances of observing structural rearrangements of such polymers with surface potential variations are greatest at low grafting densities where the chains are invisible to one another. However, minimal surface coverage eliminates the use of

ellipsometry for detection purposes. Instead, atomic force microscopy or scanning tunneling microscopy might be employed to observe changes in chain conformation as a function of surface potential.

In contrast, highly charged homopolymers exhibit only repulsive segment-segment interactions, with segment-surface interactions being either entirely repulsive or entirely attractive. At high grafting densities, repulsive segment-segment interactions are believed to cause the polymer chains to become fully extended from the surface, thereby preventing a repulsive surface potential from stretching the chains further. Ionic strength effects should also be examined, as increasing salt concentration screens electrostatic repulsions and might cause collapse of extended charged brushes by decreasing repulsive segment-segment interactions. Ellipsometry can be used in this case to determine changes in layer thickness and adsorbance, provided grafting densities are high enough for detection purposes. Neutron reflectivity directly measures the density profile of the grafted chains, yielding more in-depth information about the structure of the polymer layer.

A study of the effect of an applied surface potential on the structure of an adsorbed charged-neutral diblock copolymer would help elucidate the role of electrostatic interactions in polyelectrolyte adsorption. Design of a suitable synthetic copolymer that would allow preferential adsorption of one block (neutral block) to the surface and the extension of the other block (charged block) into solution, forming a brush, is needed. The water-soluble diblock copolymer, poly(tert-butylstyrene) - sodium poly(styrene sulfonate) is such an example. Adsorbed layer thicknesses and adsorbances could again be monitored using *in situ* ellipsometry as a function of surface potential, charge on the polymer, and ionic strength.

Although metals such as platinum and gold are relatively inert, the present study has shown that surface oxidation/reduction with potential variation occurs even with

polymer adsorption. To eliminate this surface electrochemistry, which can dramatically add to experimental error in ellipsometric measurements, mercury is suggested as a better surface. A liquid mercury electrode is advantageous because no charge transfer occurs across the metal-solution interface over a potential range of ~1.5 V. Although the reduction of water at this surface is thermodynamically possible, reduction occurs at a very slow rate in the applicable potential range, preventing surface oxidation/reduction. In addition, the liquid nature of mercury allows its surface to be easily renewed or cleaned, thus providing highly reproducible surface behavior.

5.3 References

(1) Emons, H.; Werner, G.; Heineman, W. R. *Analyst* **1990**, *115*, 405.

(2) Ivarsson, B. A.; Hegg, P.-O.; Lundström, K. I.; Jönsson, U. *Colloids and Surfaces* **1985**, *13*, 169.

(3) Liedberg, B.; Ivarsson, B.; Lundström, I.; Salaneck, W. R. *Progress in Colloid and Polymer Science* **1985**, *70*, 67.

(4) Liedberg, B.; Ivarsson, B.; Hegg, P.-O.; Lundström, I. *Journal of Colloid and Interface Science* **1986**, *114*, 386.

(5) Miller, I. R. *Journal of Molecular Biology* **1961**, *3*, 229.

(6) Morrissey, B. W.; Smith, L. E.; Stromberg, R. R.; Fenstermaker, C. A. *Journal of Colloid and Interface Science* **1976**, *56*, 557.

(7) Morrissey, B. W. *Annals New York Academy of Sciences* **1977**, *283*, 50.

(8) Raspor, B. *Journal of Electroanalytical Chemistry* **1991**, *316*, 223.

(9) Razumas, V.; Nylander, T.; Arnebrant, T. *Journal of Colloid and Interface Science* **1994**, *164*, 181.

(10) Roscoe, S. G.; Fuller, K. L. *Journal of Colloid and Interface Science* **1992**, *152*, 429.

(11) Roscoe, S. G.; Fuller, K. L.; Robitaille, G. *Journal of Colloid and Interface Science* **1993**, *160*, 243.

(12) Tengvall, P.; Lestelius, M.; Liedberg, B.; Lundström, I. *Langmuir* **1992**, *8*, 1236.

(13) Besio, G. J. Ph.D. Thesis, Princeton University, 1986.

(14) Kawaguchi, M.; Hayashi, K.; Takahashi, A. *Colloids and Surfaces* **1988**, *31*, 73.

(15) Kawaguchi, M.; Hayashi, K.; Takahashi, A. *Macromolecules* **1988**, *21*, 1016.

(16) Nuzzo, R. G.; Allara, D. L. *Journal of the American Chemical Society* **1983**, *105*, 4481.

(17) Nuzzo, R. G.; Fusco, F. A.; Allara, D. L. *Journal of the American Chemical Society* **1987**, *109*, 2358.

(18) Bain, C. D.; Whitesides, G. M. *Journal of the American Chemical Society* **1988**, *110*, 5897.

(19) Bain, C. D.; Troughton, E. B.; Tao, Y.-T.; Evall, J.; Whitesides, G. M.; Nuzzo, R. G. *Journal of the American Chemical Society* **1989**, *111*, 321.

(20) Bain, C. D.; Biebuyck, H. A.; Whitesides, G. M. *Langmuir* **1989**, *5*, 723.

APPENDIX A

OTHER POLYELECTROLYTE SYSTEMS EXAMINED FOR WHICH LITTLE OR NO ADSORPTION WAS DETECTED USING ELLIPSOMETRY

The following appendix describes polyelectrolyte systems which were examined as possible candidates for studying the effects of an applied surface potential on the structure of an adsorbed charged polymer layer. Few of these candidates, however, proved to be viable candidates for this study, and therefore, are only reported in this appendix so that other researchers might benefit from these failed attempts.

This appendix is divided into three sections. The first section describes the screening method used to determine which polyelectrolyte systems would adsorb onto inert metal surfaces in the absence of an applied electric field. The second section gives a complete list of those polyelectrolyte systems tested in the ellipsometer solution cell with the presence of an applied electric field. In the final section of this appendix, a simple experiment is presented which demonstrates the importance of electrostatic interactions in the adsorption of polyelectrolytes at charged interfaces.

First, the experimental protocol used to screen possible polyelectrolyte candidates for their adsorption on inert metal surfaces is described. These initial experiments were performed outside of the ellipsometer solution cell, in the absence of an applied electric field, so that the amount of time required for screening might be reduced. Gold was chosen as the adsorbing surface because it was an inert metal, similar to platinum, and could be obtained for much less the cost.

A gold surface (Brysen Optical Corporation, glass microscope slide coated with a 5000 Å thick gold layer, 99.998% purity) was washed with absolute alcohol and dried

under nitrogen. Ellipsometry (AutoEL II nulling ellipsometer, Rudolph Research) was used to measure Δ and Ψ of this bare surface from which the complex refractive index could be determined. To avoid the unwanted adsorption of contaminates from the air, the gold surface was immediately inserted into a glass vial containing a previously prepared polyelectrolyte solution. After a 24 hour time period, the surface was removed from the glass vial, washed with approximately 50 ml of water, and dried under nitrogen. Ellipsometry was once again used to measure the Δ and Ψ values of the surface onto which the polymer had now been adsorbed. The differences in Δ and Ψ ($\delta\Delta$ and $\delta\Psi$) before and after adsorption are reported in Table A.1 for each polymer system tested. Those systems exhibiting $\delta\Delta$ and $\delta\Psi$ values similar to values obtained for γ-globulin were further tested in the ellipsometer solution cell. γ-Globulin was used as the standard for comparison in these screening experiments as its adsorption on platinum was easily detected using *in situ* ellipsometry (Chapter 3).

Table A.2 lists the polyelectrolyte systems which were tested in the ellipsometer solution cell for their adsorption onto platinum. The general protocol for these experiments was as follows. The platinum surface was first cleaned by immersing it in a 1:1 dilution of boiling sulfuric and nitric acid for 10 minutes to remove any residual adsorbed organic material. The surface was then rinsed with copious amounts of distilled water and immediately mounted in the ellipsometer solution cell. Following alignment of the cell in the ellipsometer, solvent was pipetted into the cell. When the desired equilibrium temperature had been reached, the surface was then cleaned electrochemically by repeatedly cycling between oxidative and reductive potentials. Cycling was continued until reproducible values for the ellipsometric parameters Δ and Ψ were determined at both extremes. Once the surface had been electrochemically cleaned, the potential was adjusted to that stated in Table A.2. The ellipsometric parameters of the bare platinum surface were then measured and the complex refractive

index determined. The polymer solution was subsequently introduced into the cell. Ellipsometric measurements were taken immediately and every 5 minutes thereafter for a period of approximately 8 hours. The adsorbed layer thicknesses, refractive indexes, and adsorbances could be determined from the changes in Δ and Ψ before and after adsorption. Unfortunately, however, little if any change in the ellipsometric parameters could be detected for most of these polyelectrolyte systems, suggesting the no adsorption had occurred. An exception to this generalization was poly-(L-lysine). This polyamino acid appears to adsorb onto platinum at an applied surface potential of 0.0 V with an average adsorbed layer thickness of 400 Å and an adsorbance of 1 mg/m^2. Due to the noise present in the ellipsometric data for this system, poly-(L-lysine) was not studied further.

Because of the difficulty encountered in attempting to adsorb polyelectrolytes on inert metal surfaces with or without an applied electric field, a simple experiment was done to renew our faith in the importance of electrostatic interactions when adsorbing polyelectrolytes on charged substrates. Two charged polymer systems were adsorbed onto silicon wafers which possessed a positive, negative, or no surface charge (Table A.3).

The experimental protocol was as follows. Three silicon wafers, a positively charged wafer (p-doped, resistivity = 65-80 Ω/cm), a negatively charged wafer (n-doped, resistivity = 0.001-0.005 Ω/cm), and a wafer with essentially no surface charge (n-doped, resistivity = 100-150 Ω/cm), were washed with absolute alcohol and dried under nitrogen. Ellipsometry was used to measure the parameters, Δ and Ψ, for each of these bare substrates in order to determine the complex refractive index of each surface. The silicon wafers were then inserted into glass vials containing either a NaPSS solution or a PVP solution. After a 24 hour time period at the temperature specified in Table A.3, each wafer was removed from its glass vial, washed with approximately 50 ml of

water, and dried under nitrogen. Ellipsometry was once again used to measure the Δ and Ψ values of each surface. The largest change found in these values before and after adsorption ($\delta\Delta$ and $\delta\Psi$) suggests that NaPSS, a negatively charged polymer, adsorbs most strongly on the positively charged silicon wafer, while PVP, a positively charged polymer, is most strongly attracted to the negatively charged wafer.

Table A.1. Adsorption of polyelectrolyte systems on gold. Changes in the ellipsometric parameters Δ and Ψ, determined before and after adsorption, are reported. Ellipsometric measurements were made on dried polymer films.

POLYMER	Mw	CONC. (mg/ml)	SOLVENT	TEMP.	$-\delta\Delta$	$+\delta\Psi$
γ-Globulin	160,000	11.4	Sodium Phosphate Buffer (pH=8.5, μ=0.15)	RT	7.88	0.00
NaPSS	690,000	10.0	1.0 M NaCl	RT	1.00	0.00
NaPSS	690,000	10.0	0.1M $CaCl_2$	RT	1.36	0.00
NaPSS	690,000	10.0	25% H_2O/ 75% MeOH	RT	0.20	0.00
2-PVP	1,000,000	10.0	0.09 M NaCl 0.01 M HCl	RT	1.54	0.04
2-PVP	1,000,000	4.5	0.09 M NaCl 0.01 M HCl	RT	2.28	0.00
4-PVP	200,000	10.0	0.09 M NaCl 0.01 M HCl	RT	1.40	0.00
4-PVP	200,000	2.5	0.09 M NaCl 0.01 M HCl	RT	1.92	0.00
PAA	1,000,000	3.0	50% H_2O/ 50% MeOH	RT	1.28	0.00

Continued, next page.

Table A.1. continued

NaPMAA	685,000	0.1	0.50 M NaCl	43 C	2.00	0.00
PLL, HBr	100,500	5.0	Sodium Bicarbonate Buffer (pH = 11)	RT	1.63	0.00
PLL	100,500	5.0	Sodium Phosphate Buffer (pH = 7)	RT	4.36	0.00

Note: NaPSS is poly(styrene sulfonate), sodium salt; 2-PVP is poly(2-vinylpyridine); 4-PVP is poly(4-vinylpyridine); PAA is poly(acrylic acid); NaPMAA is poly(methacrylic acid), sodium salt; PLL, HBr is poly-(L-lysine), hydrobromide, and RT stands for room temperature.

Table A.2. Adsorption of polyelectrolyte systems on platinum. Experiments were done in the ellipsometer solution cell.

POLYMER	Mw	CONC. (mg/ml)	SOLVENT	TEMP. (°C)	APPLIED SURFACE POTENTIAL (V vs Ag/AgCl)
NaPSS	1,060,000	0.4	0.1 M NaCl	RT	No Potential
NaPSS	1,060,000	0.4	0.5 M NaCl	RT	No Potential
NaPSS	1,060,000	0.4	0.5 M NaCl	RT	+0.2
NaPSS	690,000	0.4	H_2O Acidified with $HClO_4$ to a pH = 2.5	RT	+0.1
2-PVP	300,000-400,000	0.1	H_2O Acidified with $HClO_4$ to a pH = 2.5	RT	- 0.4
4-PVP	200,000	2.0	0.09 M NaCl 0.01 M HCl	25	0.0
PAA	1,000,000	1.0	50% H_2O/ 50% MeOH 0.06 M NaCl	25	0.0
PAA	1,000,000	0.5	50% Acetate Buffer (pH=3.7, μ = 0.01)/ 50% MeOH	25	0.0

Continued, next page.

Table A.2. continued

PAA	1,000,000	0.5	75% Acetate Buffer (pH=3.7, μ = 0.01)/ 25% MeOH	25	0.0
PAA	1,000,000	0.5	75% Acetate Buffer (pH=7.4, μ = 0.1)/ 25% MeOH	25	0.0
PLL, HBr	223,400	2.5	0.13 M $NaClO_4$ (pH = 7.0)	25	0.0
PGA, Na	120,500	8.3	Sodium Phosphate Buffer (pH=7.0, μ=0.1)	25	0.0
PGA-PGA(OEt) (1:1)	70,000-150,000	4.2	Sodium Phosphate Buffer (pH=8.5, μ=0.15)	25	0.0

Note: NaPSS is poly(styrene sulfonate), sodium salt; 2-PVP is poly(2-vinylpyridine); 4-PVP is poly(4-vinylpyridine); PAA is poly(acrylic acid); PLL, HBr is poly-(L-lysine), hydrobromide; PGA, Na is poly-(L-glutamic acid), sodium salt; PGA-PGA(OEt) is a random copolymer of L-glutamic acid and L-glutamic acid with an ethoxy group. RT stands for room temperature.

Table A.3. Adsorption of two polyelectrolyte systems on silicon wafers. The wafer had been doped to give them a specific surface charge.

Silicon Wafer Type	Surface Charge	Adsorption of NaPSS	Adsorption of 2-PVP
N-Doped (100-150Ω/cm)	Neutral	$\delta\Delta = 8.19$, $\delta\Psi = 0.06$	$\delta\Delta = 3.38$, $\delta\Psi = 0.00$
N-Doped (0.001-0.005 Ω/cm)	Negative	$\delta\Delta = 3.03$, $\delta\Psi = 0.04$	$\delta\Delta = 12.19$, $\delta\Psi = 0.26$
P-Doped (65-80 Ω/cm)	Positive	$\delta\Delta = 13.56$, $\delta\Psi = 0.39$	$\delta\Delta = 2.99$, $\delta\Psi = 0.05$

Note adsorption conditions:

Sodium Poly(styrene sulfonate):
400 ppm NaPSS (Mw = 1.2 million) in distilled water
0.5 M NaCl
23° C

Poly(2-vinylpyridine):
100 ppm 2-PVP (Mw = 300,000-400,000) in distilled water
0.9 N HCl
30° C

APPENDIX B

SUPPLEMENTAL DATA FOR CHAPTER 3

Cyclic voltammograms of the platinum electrode under various conditions are presented in Figures B.1 through B.3.

Figures B.4 through B.9 demonstrate the effect of pH on the ellipsometric parameters Δ and Ψ of a bare platinum surface as a function of applied surface potential. Three pH's are examined, 5.7, 7.0, and 8.5. Hysteresis loops are pushed to more positive potentials at lower pH values.

Superimposition of the plots of the ellipsometric parameters Δ and Ψ versus applied surface potential for the γ-globulin covered platinum surface and the bare platinum surface are shown in Figures B.10 through B.13.

Dynamic light scattering (ALV/DLS-5000) is used to determine the hydrodynamic radius of γ-globulin as a function of ionic strength in a sodium phosphate buffer at a pH = 7.5 (Figure B.14). Measurements are made at a concentration of 1 mg/ml and 25° C. The slight increase in radius with ionic strength that is observed is most probably due to an increase in viscosity of the buffer with increasing salt concentration which is not accounted for in this data.

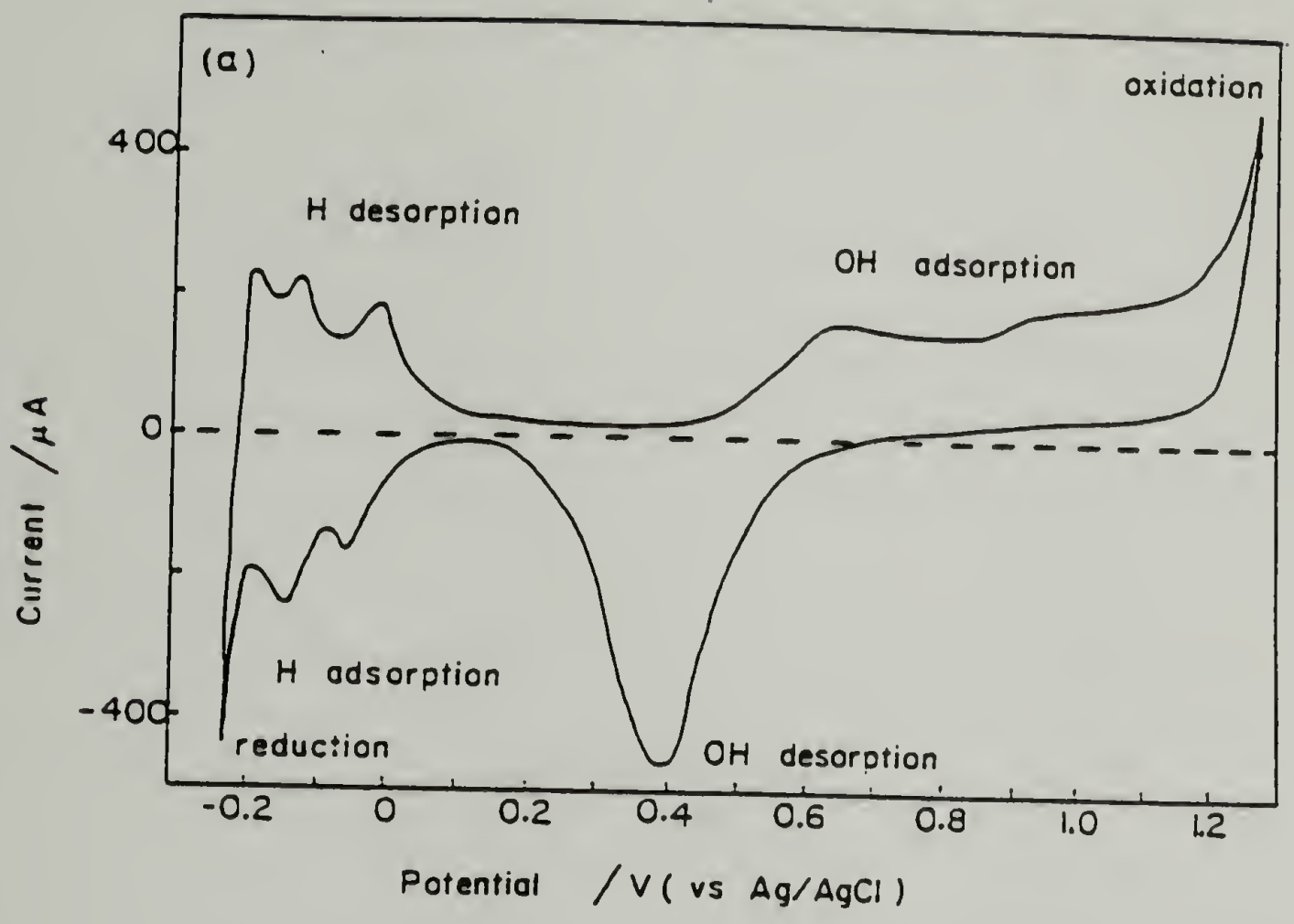

Figure B.1. Cyclic voltammogram of platinum electrode in 1M $HClO_4$ as determined by Benziger *et al.* referenced in Chapter 2. (Electrode area 1.44 cm^2; potential sweep rate 4 mV/s; 1 M Ag/AgCl reference electrode.)

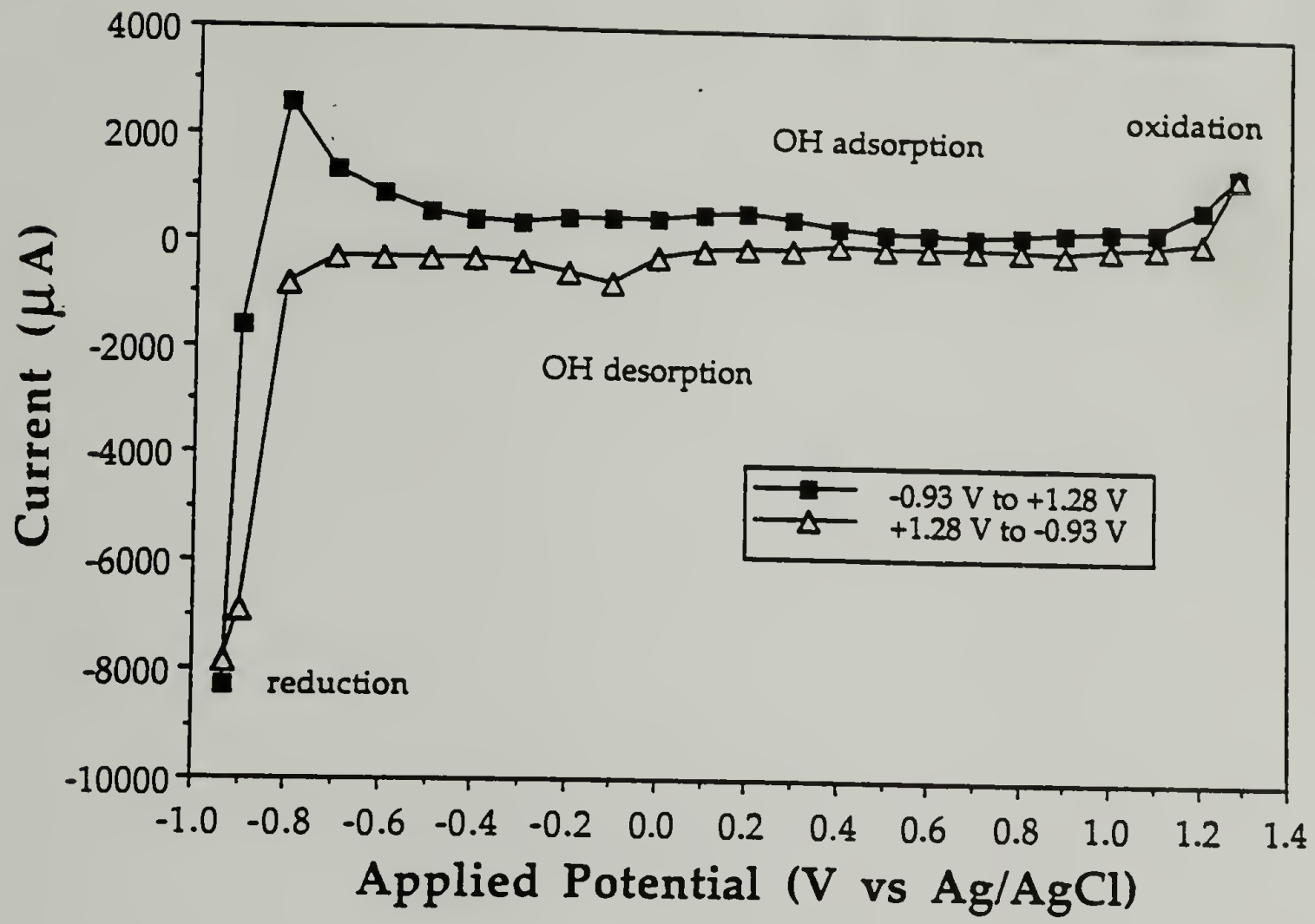

Figure B.2. Cyclic voltammogram of platinum electrode in distilled water. (Electrode area 6.25 cm^2; potential sweep was done by hand at a rate ~0.1 mV/s; 3 M Ag/AgCl reference electrode.)

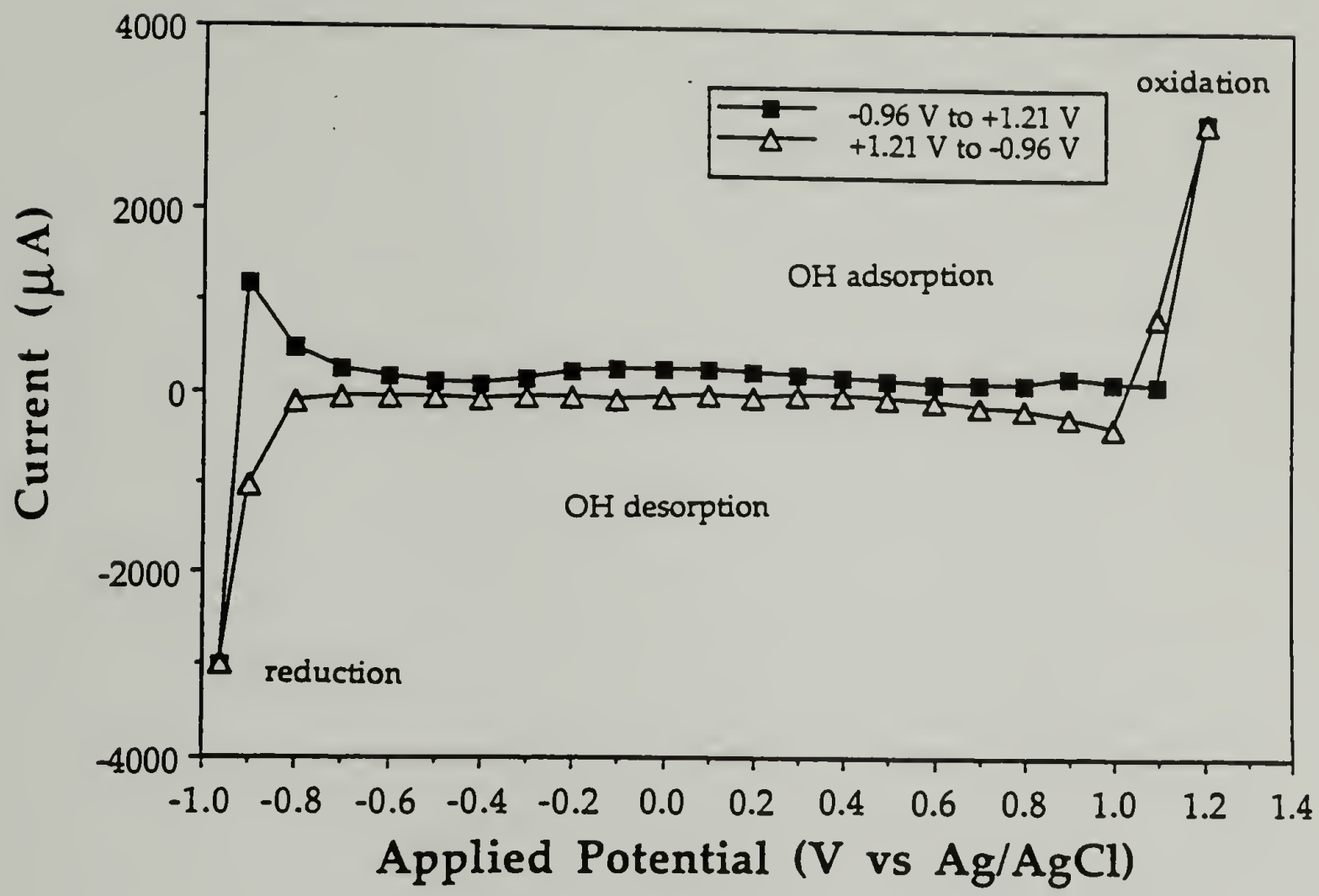

Figure B.3. Cyclic voltammogram of platinum electrode in 0.1 M NaCl. (Electrode area 6.25 cm^2; potential sweep was done by hand at a rate ~0.1 mV/s; 3 M Ag/AgCl reference electrode.)

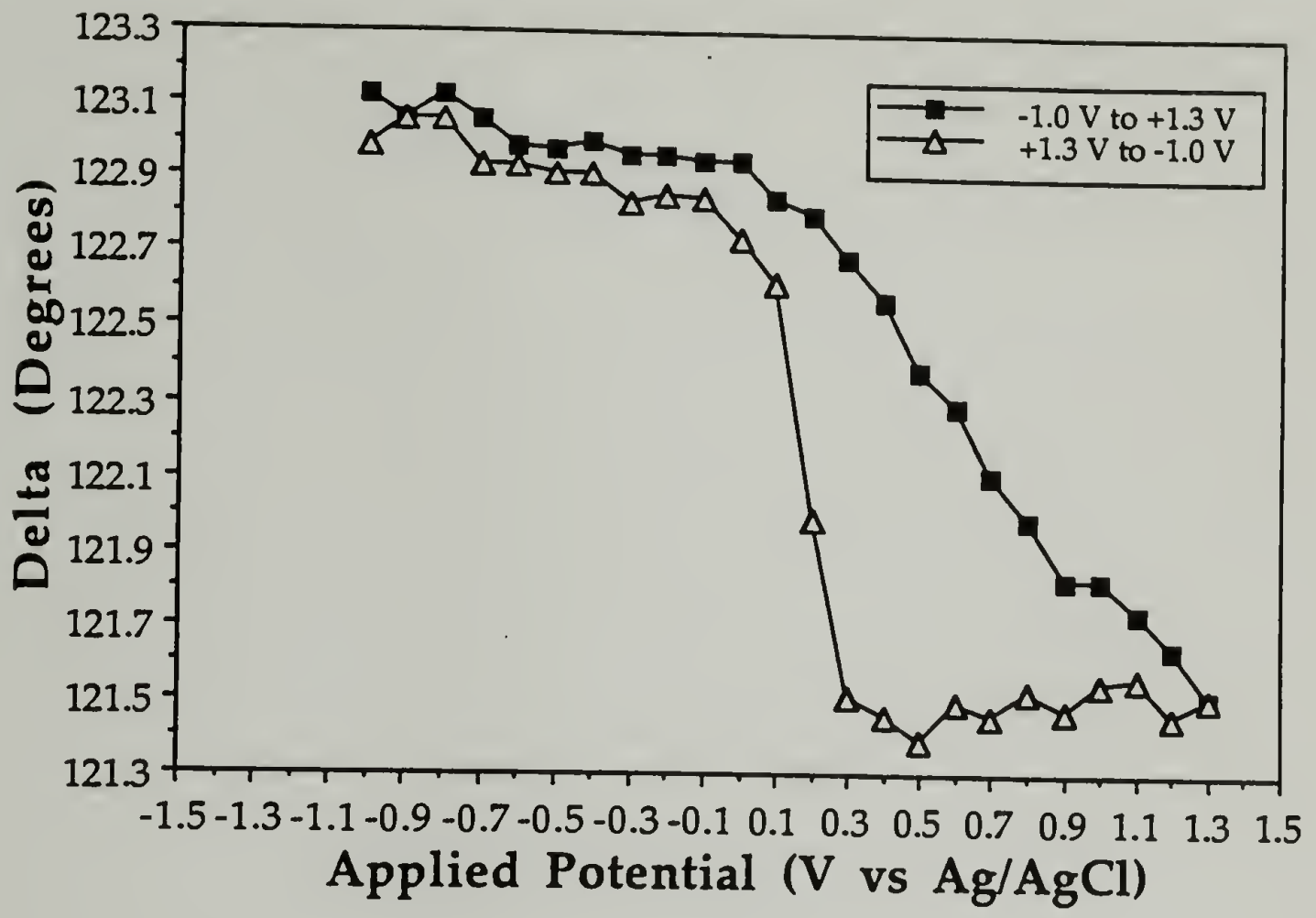

Figure B.4. Delta plotted as a function of applied surface potential for a bare platinum surface in a sodium phosphate buffer (pH = 5.7, I = 0.15 M) at 25° C. The average of three measurements taken at each potential are shown.

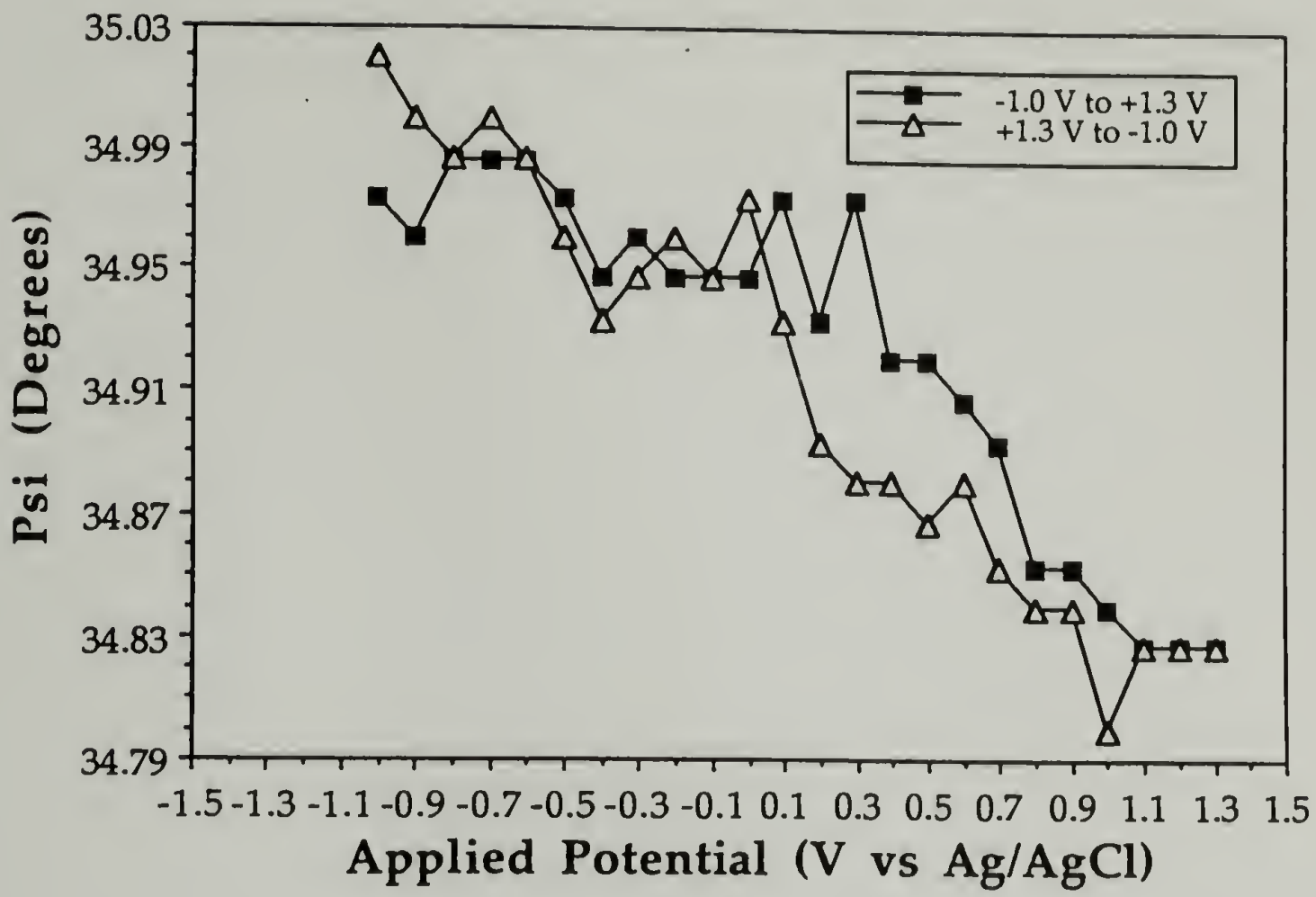

Figure B.5. Psi plotted as a function of applied surface potential for a bare platinum surface in a sodium phosphate buffer (pH = 5.7, I = 0.15 M) at 25° C. The average of three measurements taken at each potential are shown.

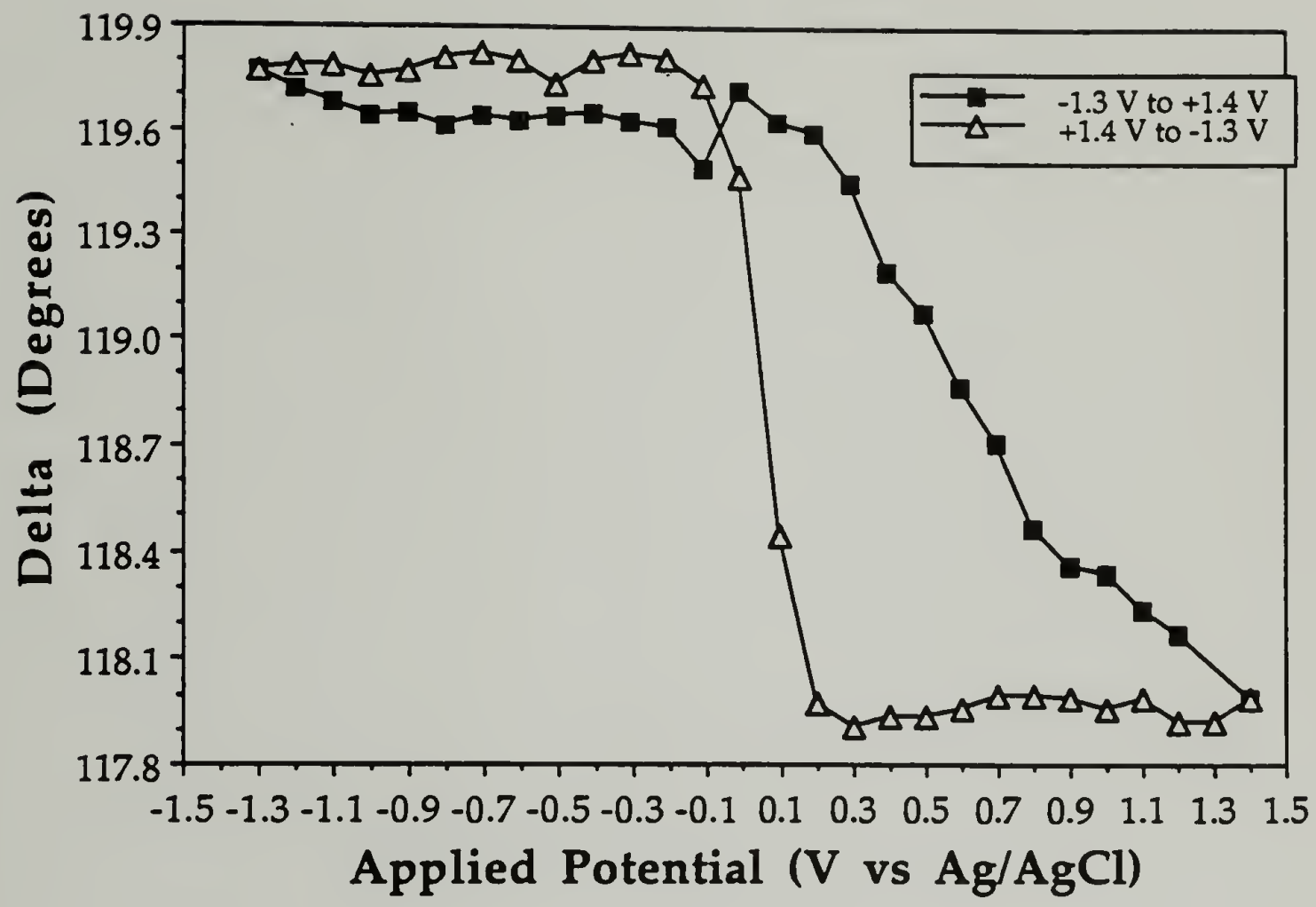

Figure B.6. Delta plotted as a function of applied surface potential for a bare platinum surface in a sodium phosphate buffer (pH = 7.0, I = 0.10 M) at 40° C. The average of three measurements taken at each potential are shown.

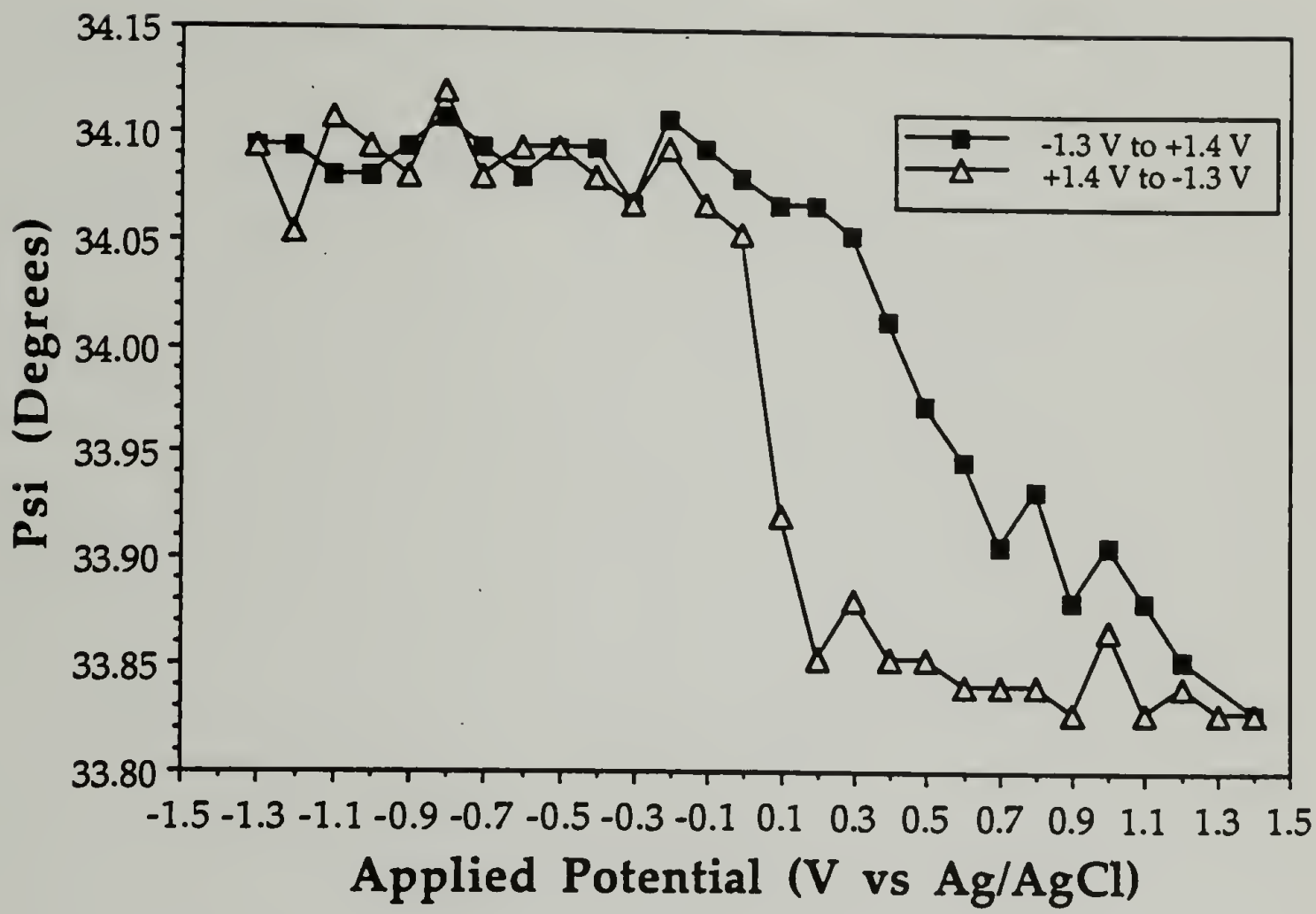

Figure B.7. Psi plotted as a function of applied surface potential for a bare platinum surface in a sodium phosphate buffer (pH = 7.0, I = 0.10 M) at 40° C. The average of three measurements taken at each potential are shown.

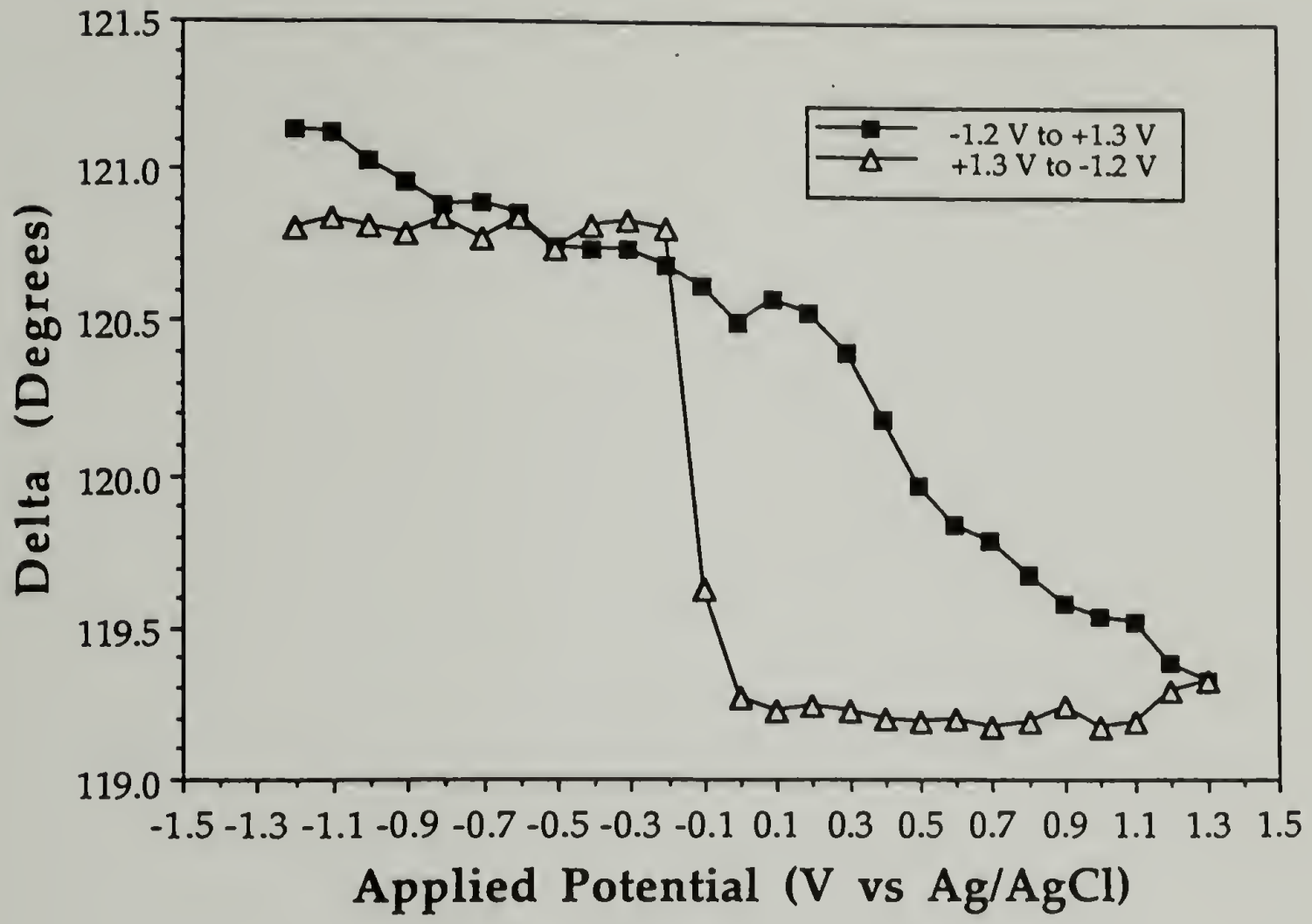

Figure B.8. Delta plotted as a function of applied surface potential for a bare platinum surface in a sodium phosphate buffer (pH = 8.5, I = 0.15 M) at 25° C. The average of three measurements taken at each potential are shown.

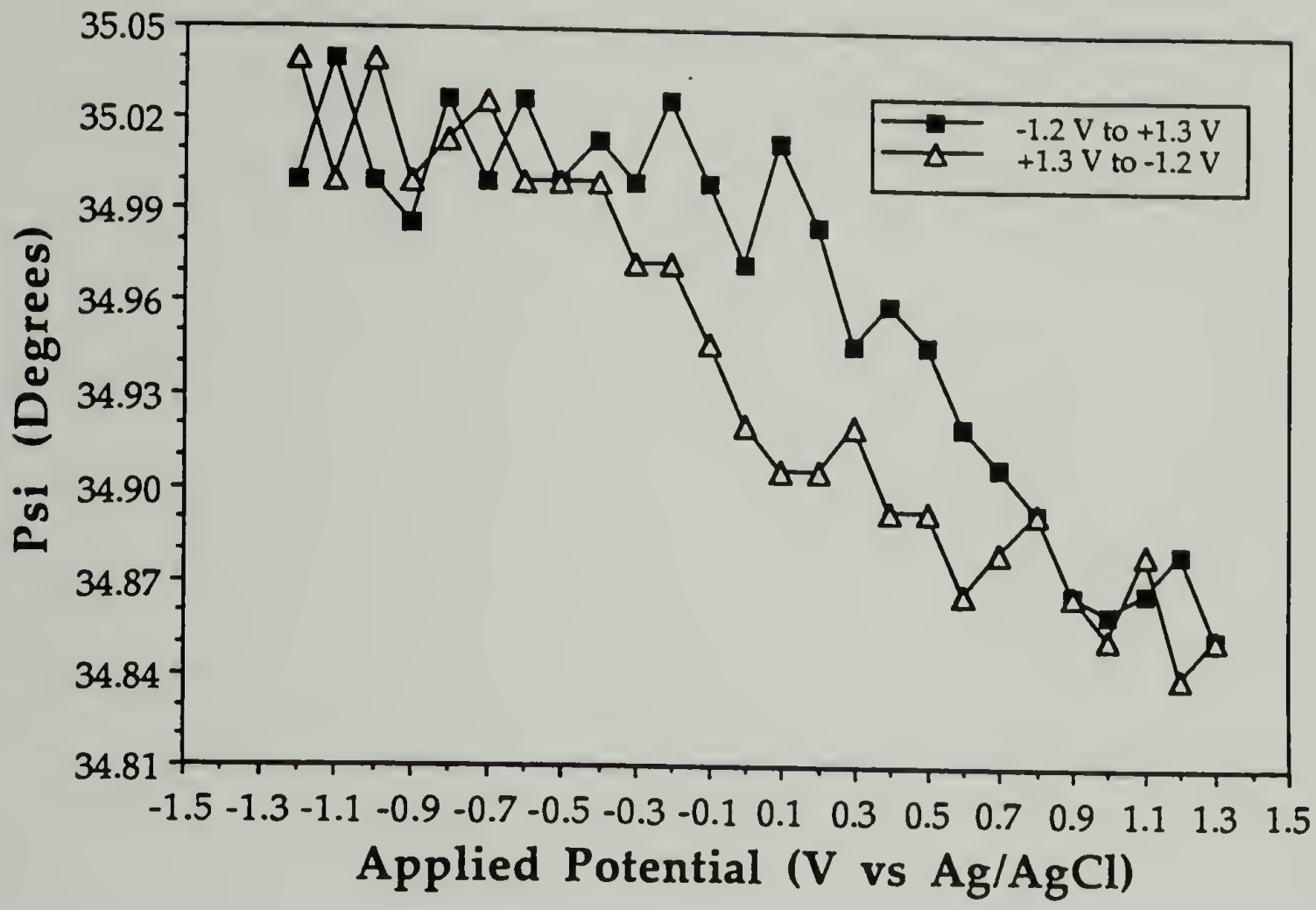

Figure B.9. Psi plotted as a function of applied surface potential for a bare platinum surface in a sodium phosphate buffer (pH = 8.5, I = 0.15 M) at 25° C. The average of three measurements taken at each potential are shown.

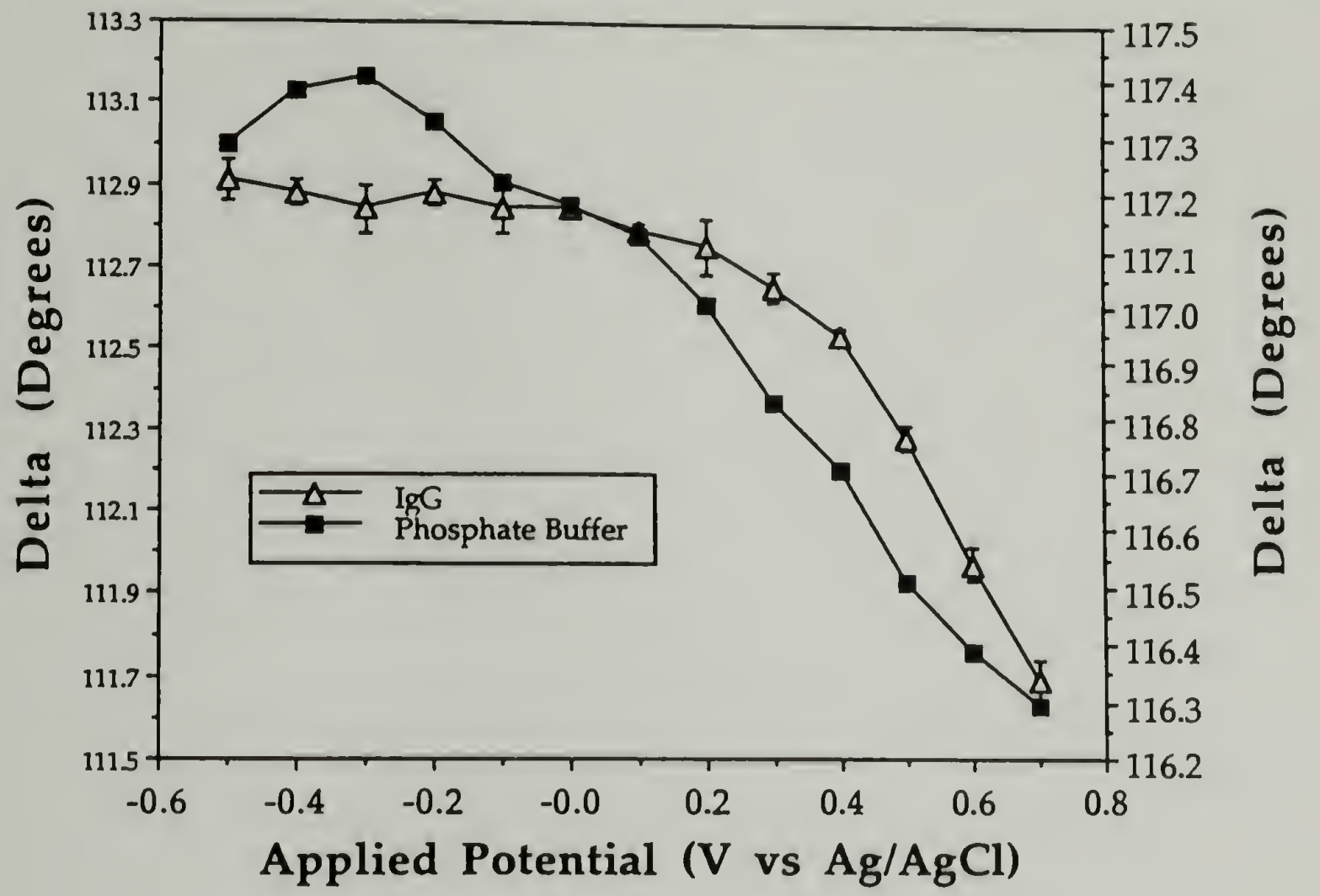

Figure B.10. Superimposition of the plots of Delta vs. applied potential for the γ-globulin covered platinum foil in the presence of the buffered protein solution (pH = 8.5, I = 0.15 M) at 25° C and for the bare platinum surface in the presence of the phosphate buffer (pH = 8.5, I = 0.15 M) at 25° C. Adsorbed layer thicknesses, refractive indexes, and adsorbances shown in Figure 3.22 - 3.24 were directly determined from this comparison.

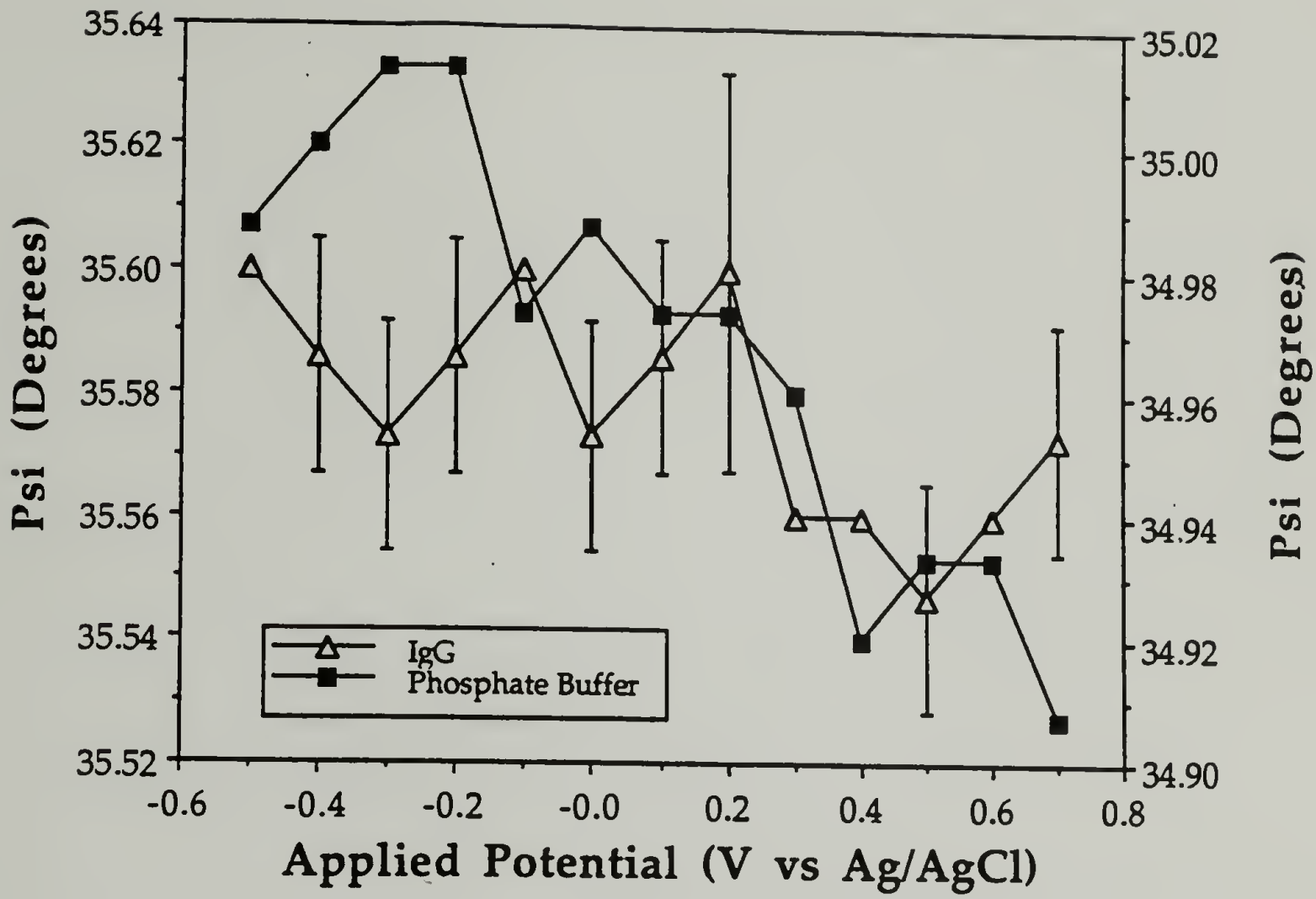

Figure B.11. Superimposition of the plots of Psi vs. applied potential for the γ-globulin covered platinum foil in the presence of the buffered protein solution (pH = 8.5, I = 0.15 M) at 25° C and for the bare platinum surface in the presence of the phosphate buffer (pH = 8.5, I = 0.15 M) at 25° C. Adsorbed layer thicknesses, refractive indexes, and adsorbances shown in Figure 3.22 - 3.24 were directly determined from this comparison.

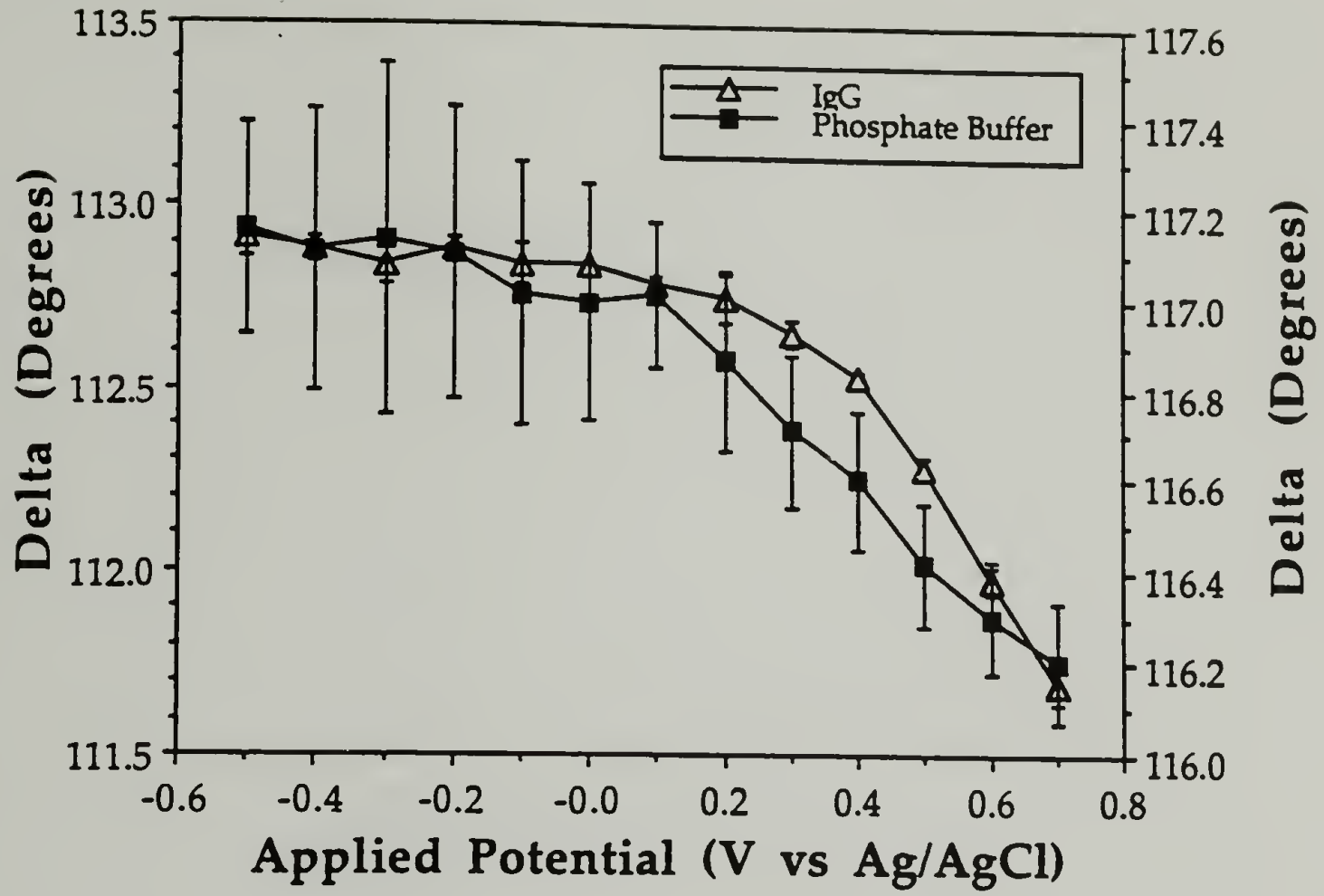

Figure B.12. Superimposition of the plots of Delta vs. applied potential for the γ-globulin covered platinum foil in the presence of the buffered protein solution (pH = 8.5, I = 0.15 M) at 25° C and for the bare platinum surface in the presence of the phosphate buffer (pH = 8.5, I = 0.15 M) at 25° C determined upon repeated cycling of potential.

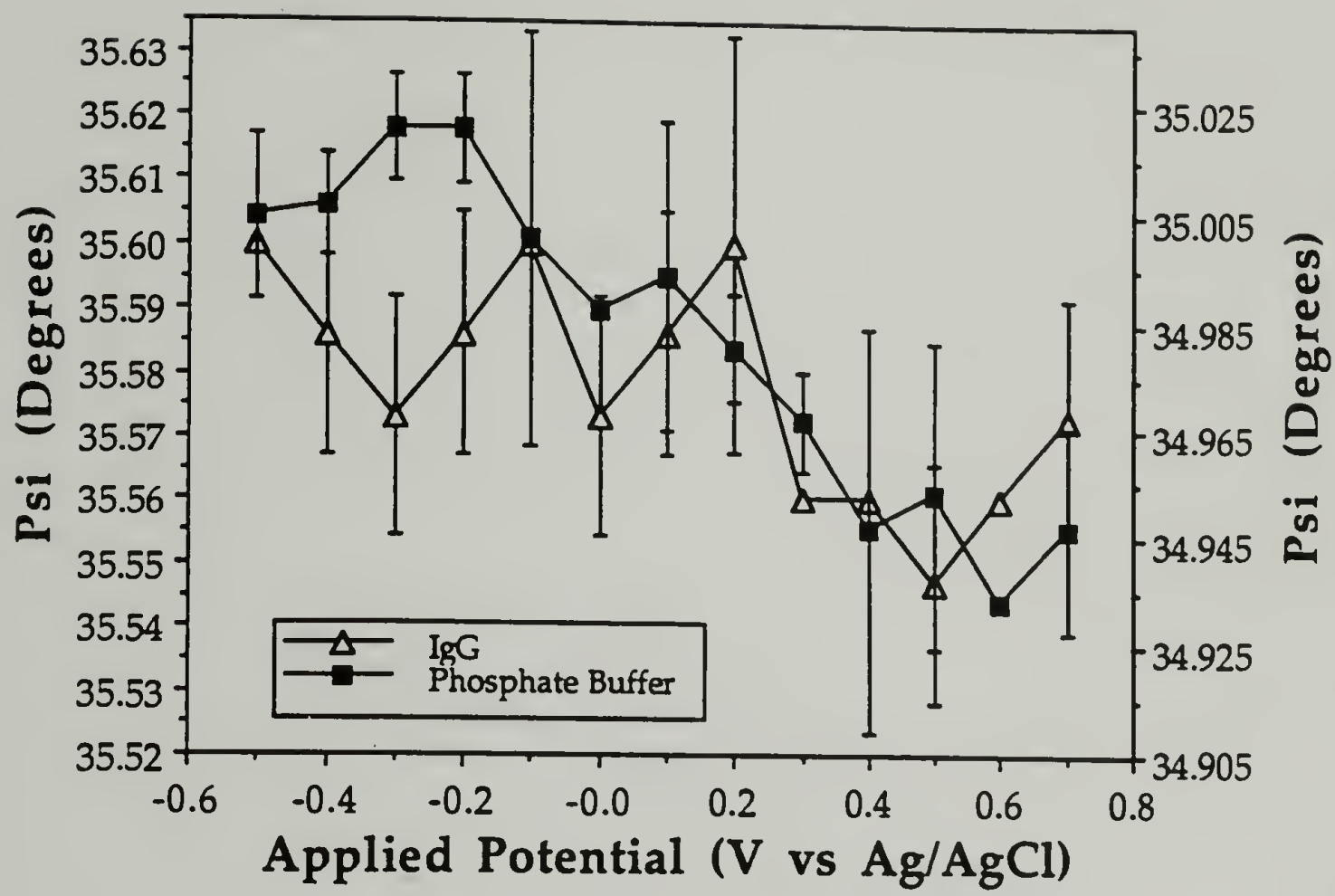

Figure B.13. Superimposition of the plots of Psi vs. applied potential for the γ-globulin covered platinum foil in the presence of the buffered protein solution (pH = 8.5, I = 0.15 M) at 25° C and for the bare platinum surface in the presence of the phosphate buffer (pH = 8.5, I = 0.15 M) at 25° C determined upon repeated cycling of potential.

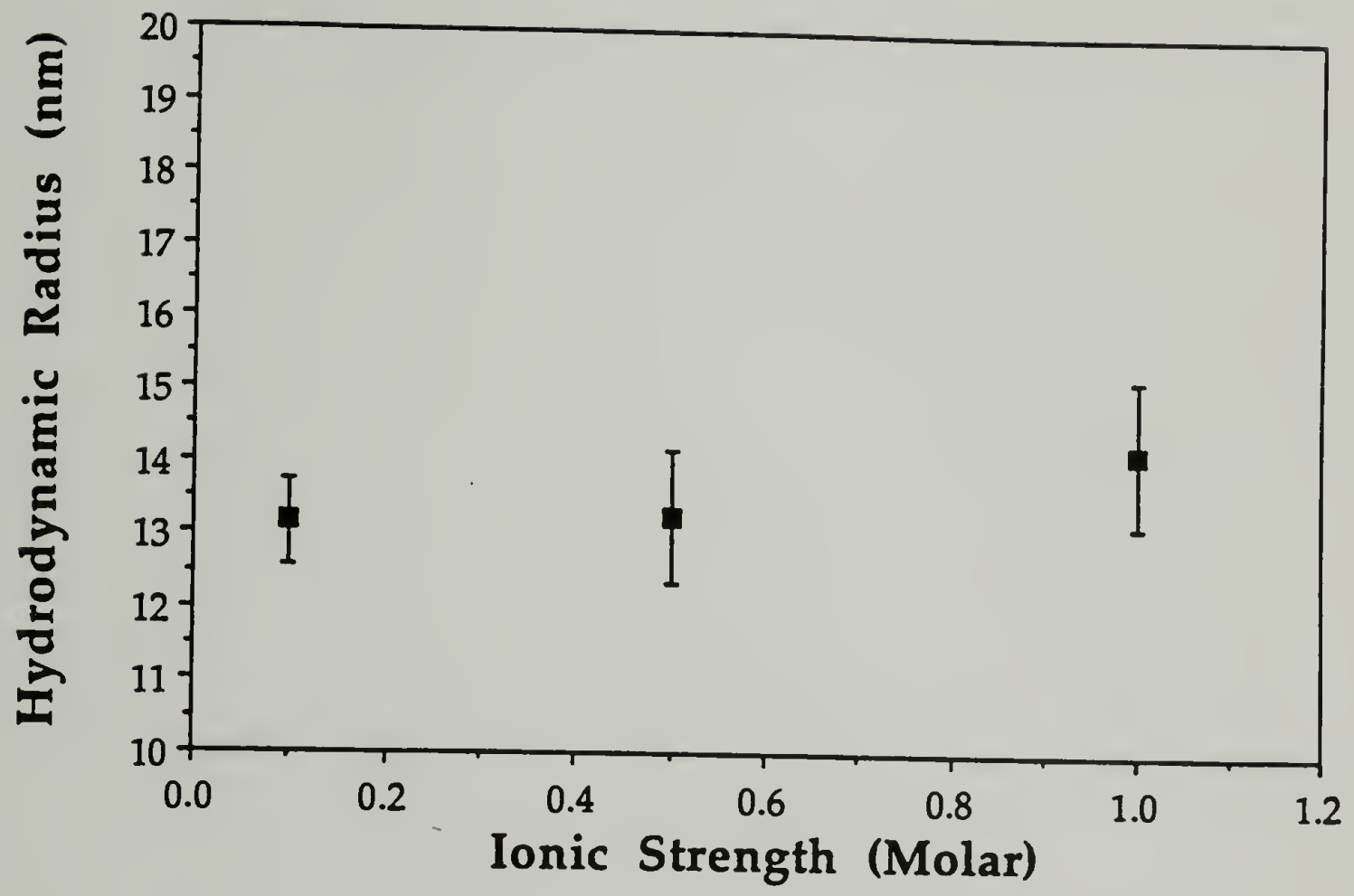

Figure B.14. Hydrodynamic radius of γ-globulin in sodium phosphate buffer at a pH = 7.5 as a function of ionic strength determined by dynamic light scattering.

APPENDIX C

SUPPLEMENTAL DATA FOR CHAPTER 4

Dynamic light scattering (DLS) (ALV/DLS-5000) was employed to determine the hydrodynamic radius of gelatin as a function of pH (Figure C.1). A sodium phosphate buffer (I = 0.01 M) was used to attain a pH of 7.0. Acetate buffers (I = 0.01 M), which had been prepared by dissolving reagent grade sodium acetate (Fisher) in ultra-pure, deionized water (Millipore Q, UF-OR) and adding glacial acetic acid (Fisher) to adjust the pH, were used to attain pH values of 3.5 and 5.0. Gelatin was dissolved in these buffers at a concentration of 1 mg/ml and DLS measurements were made at 40° C to determine the hydrodynamic radius. Our results compare favorably with dimensions previously determined by Boedtker and Doty (Reference 9 in Chapter 4).

Superimposition of the plots of the ellipsometric parameters Δ and Ψ vs. applied surface potential for the gelatin-covered platinum surface immersed in the protein-containing buffered solution (pH = 7.0, I = 0.10 M) at 40° C and the bare platinum surface immersed in the phosphate buffer (pH = 7.0, I = 0.10 M) at 40° C are shown in Figures C.2 and C.3, respectively. From these plots, a striking resemblance can be observed between the shape of the curves obtained for the gelatin-covered platinum surface and for those obtained for the bare platinum surface.

Figures C.4 and C.5 show an adsorbed layer thickness of ~70 Å and an adsorbance of ~3.7 mg/m^2 for gelatin adsorbed from a phosphate buffer (I = 0.1 M) at a pH of 3.5, where the gelatin possesses a net positive charge. No effect of initial adsorbing potential on the structure of the adsorbed layer is observed. Direct comparison can be made between these thickness and adsorbance values and those

measured at a pH of 7.0 (~490 Å and ~2.4 mg/m^2, Figures 4.9 and 4.10). Gelatin appears to adsorb in a dense, compact layer (refractive index ~ 1.50) at a pH of 3.5 in contrast to the more extended conformation (refractive index ~1.34) observed at a pH of 7.0. These changes in adsorbed layer structure at different pH values do not correlate with the dimensions observed for the polymer chain in solution (Figure C.1).

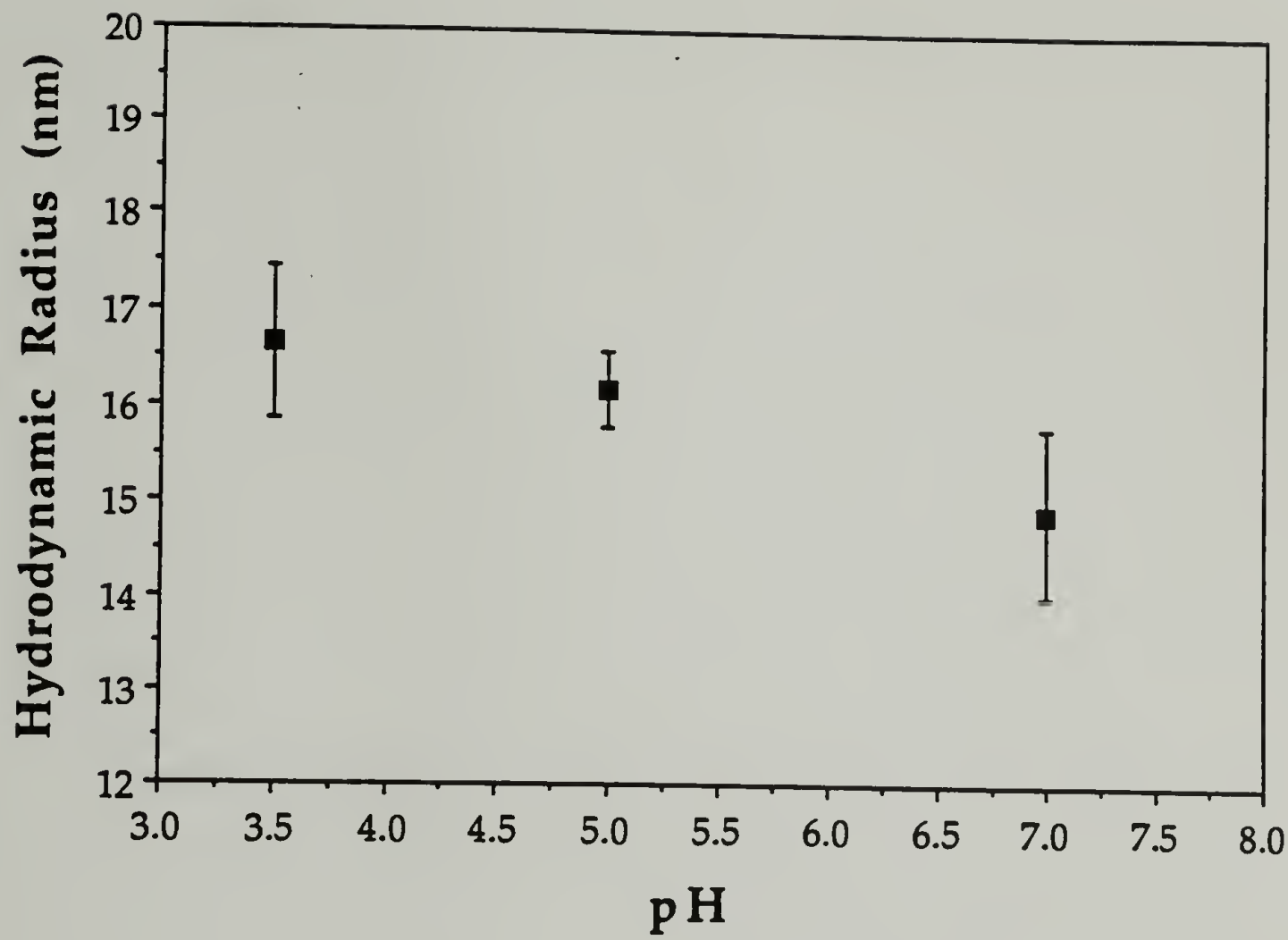

Figure C.1. Hydrodynamic radius of gelatin as a function of pH as determined by dynamic light scattering.

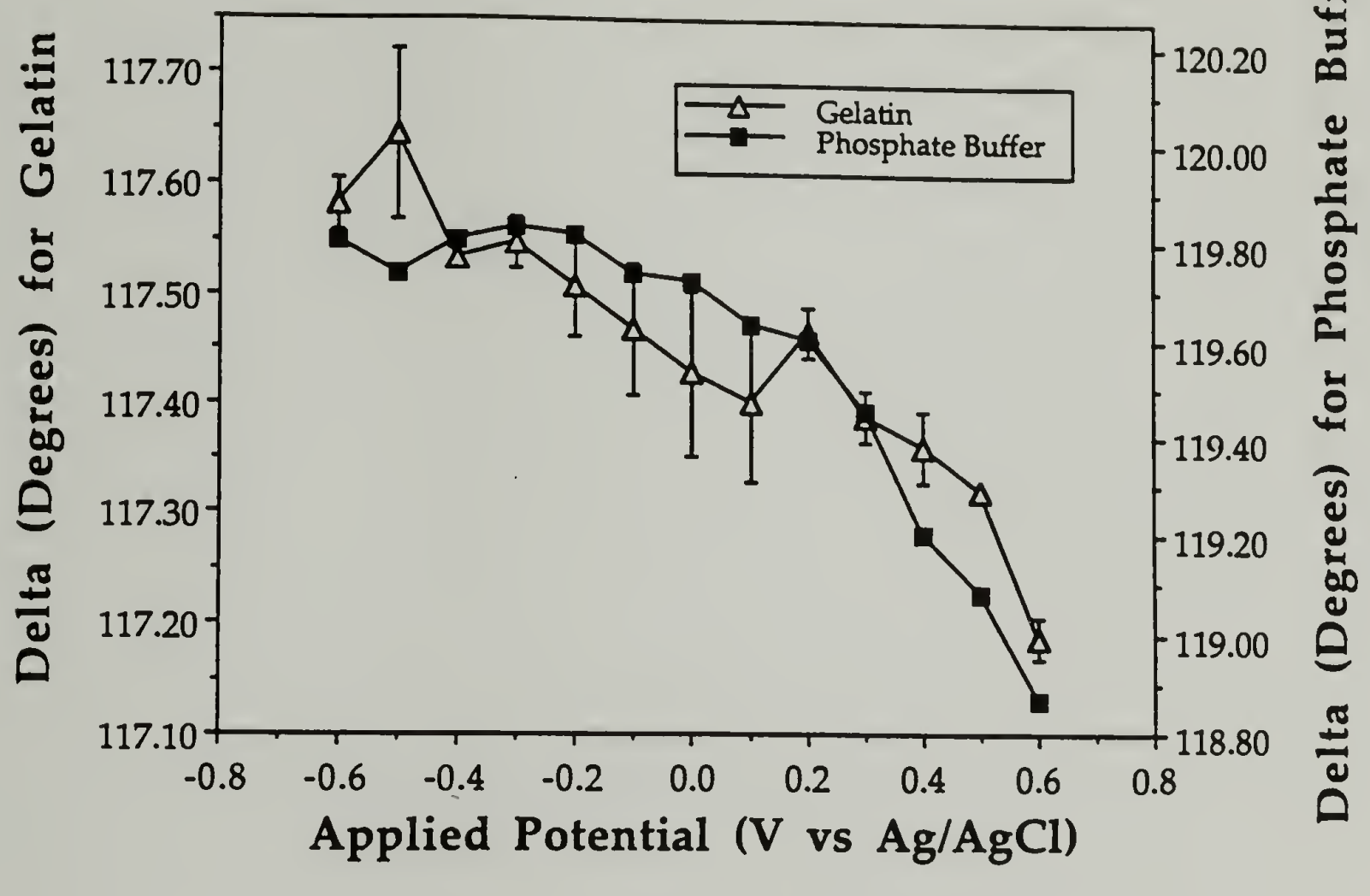

Figure C.2. Superimposition of the plots of Delta vs. applied potential for the gelatin-covered platinum foil in the presence of the buffered protein solution (pH = 7.0, I = 0.1 M) at 40° C and for the bare platinum surface in the presence of the phosphate buffer (pH = 7.0, I = 0.10 M) at 40° C.

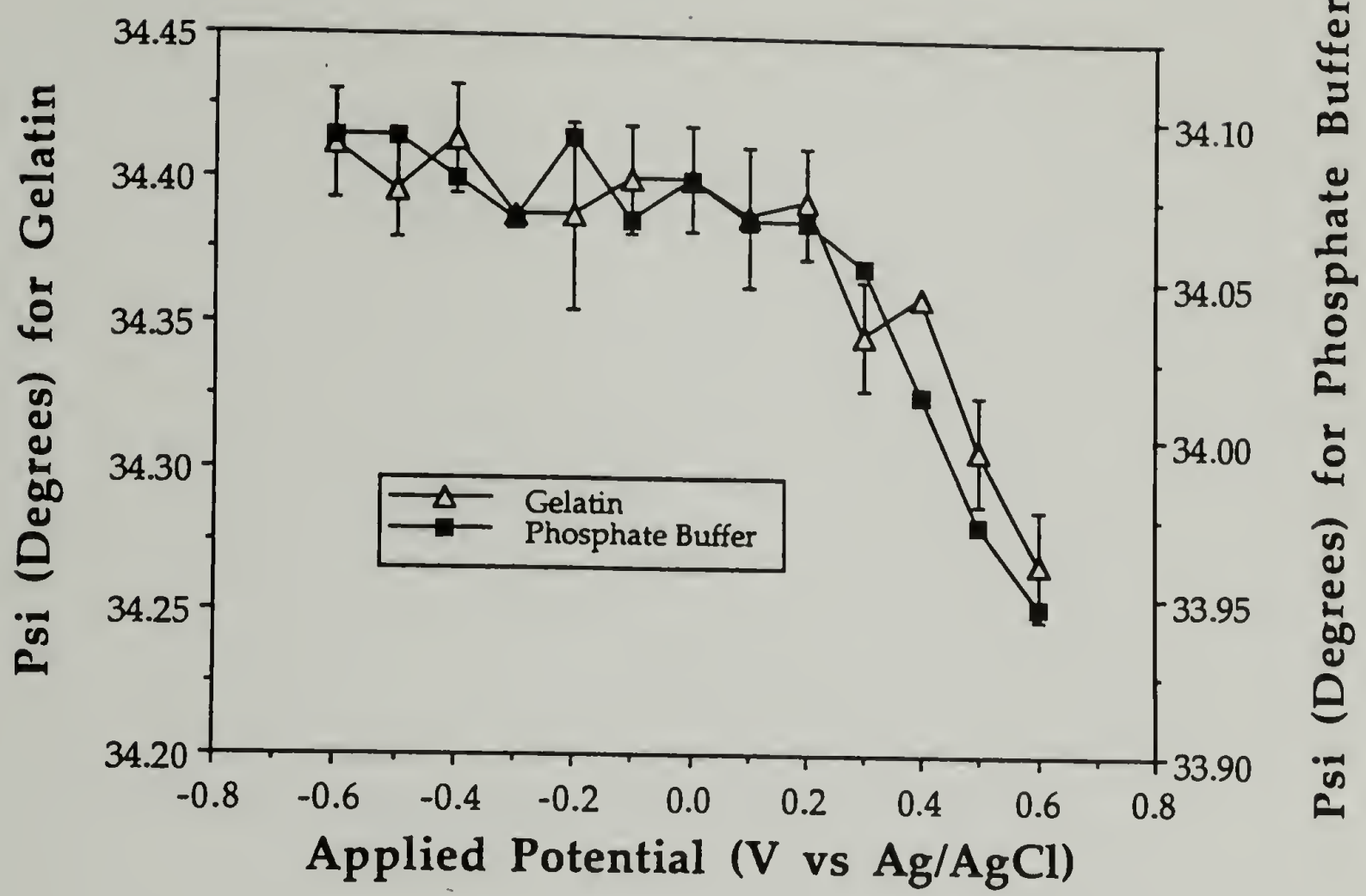

Figure C.3. Superimposition of the plots of Psi vs. applied potential for the gelatin-covered platinum foil in the presence of the buffered protein solution (pH = 7.0, I = 0.10 M) at 40° C and for the bare platinum surface in the presence of the phosphate buffer (pH = 7.0, I = 0.10 M) at 40° C.

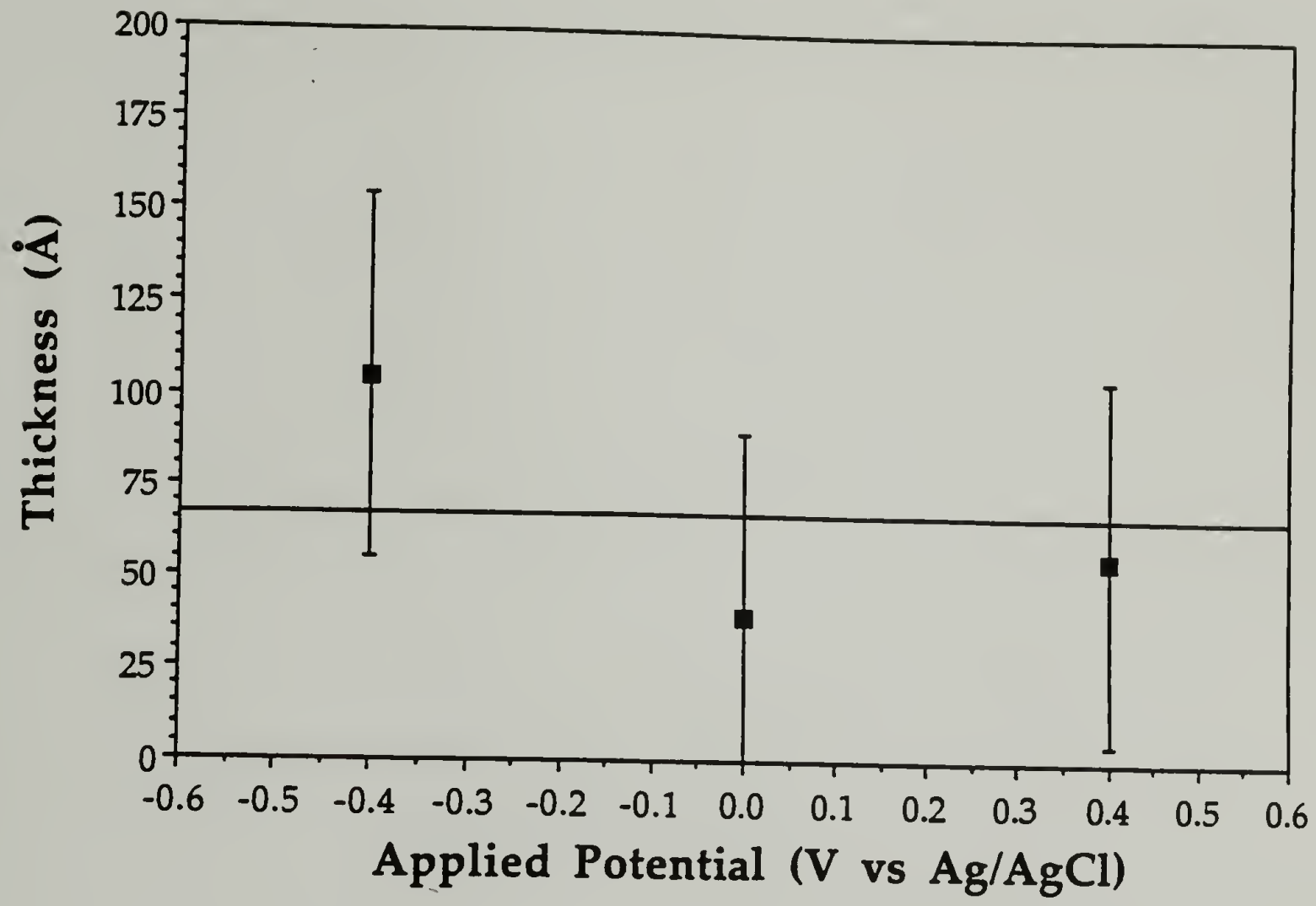

Figure C.4. Adsorbed gelatin layer thickness on platinum in the presence of an acetate buffer solution (pH = 3.5, I = 0.10 M) at 40° C as a function of initial adsorbing potential.

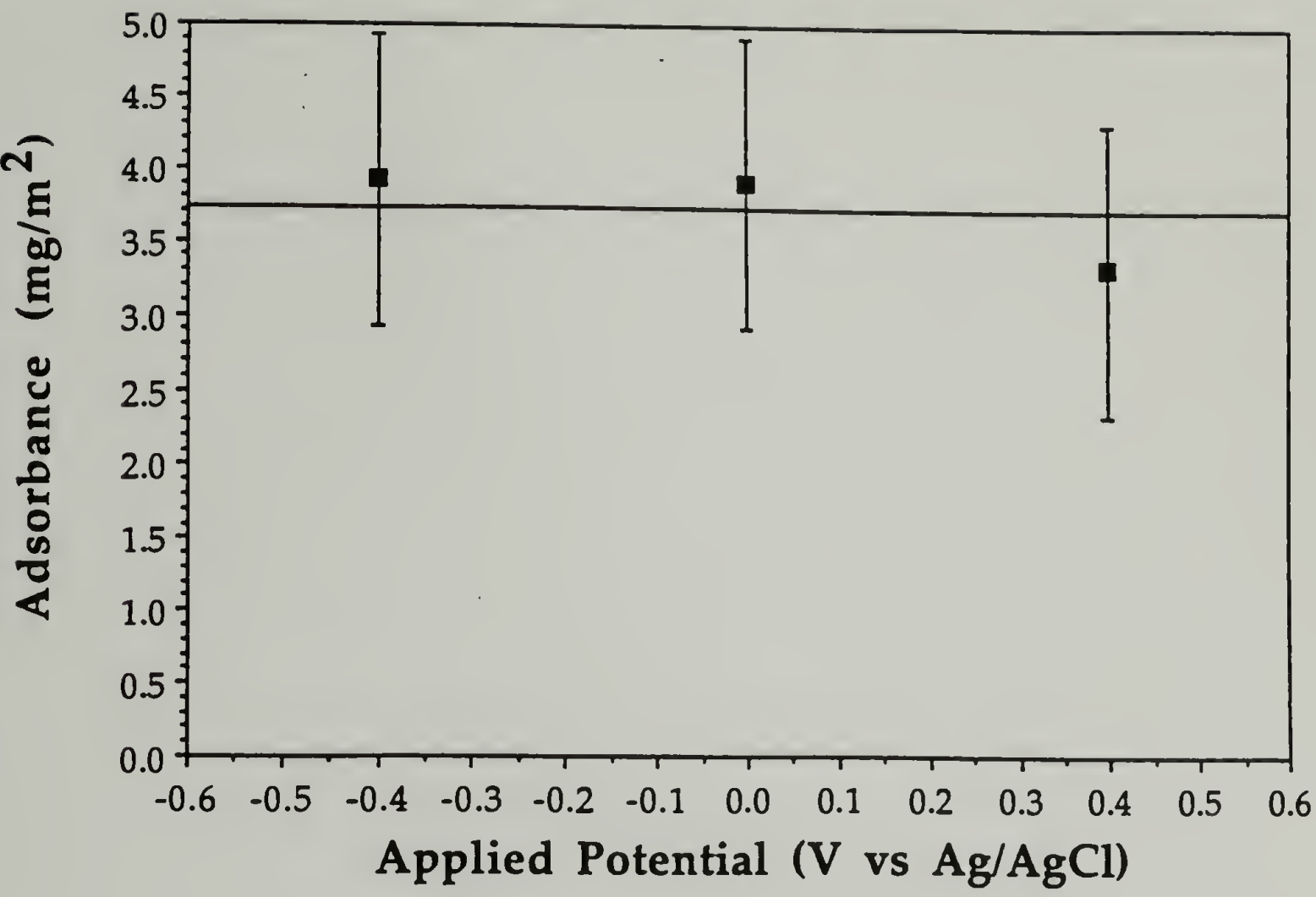

Figure C.5. The amount of gelatin adsorbed on platinum in the presence of an acetate buffer solution (pH = 3.5, I = 0.10 M) at 40° C as a function of initial adsorbing potential.

BIBLIOGRAPHY

(1) Adam, M.; Delsanti, M. *Journal de Physique II* **1976**, *37*, 1045.

(2) Adams, R. N. *Electrochemistry at Solid Electrodes*; Marcel Dekker, Inc.: New York, 1969.

(3) Akcasu, A. Z.; Han, C. *Macromolecules* **1979**, *12*, 276.

(4) Alexander, S. *Journal de Physique II* **1977**, *38*, 977.

(5) Alexandrowicz, Z.; Katchalsky, A. *Journal of Polymer Science, Part A* **1963**, *1*, 3231.

(6) Andersen, T. N.; Anderson, J. L.; Eyring, H. *Journal of Physical Chemistry* **1969**, *73*, 3562.

(7) Andrade, J.; Mankarious, S. In *5th International Symposium on HPLC of Proteins, Peptides and Polynucleotides*; Toronto, 1985; Paper No. 1027.

(8) Arai, T.; Norde, W. *Colloids and Surfaces* **1990**, *51*, 1.

(9) Argillier, J.-F.; Tirrell, M. *Theoretica Chimica Acta* **1992**, *82*, 343.

(10) Atkins, P. W. In *Physical Chemistry*; Second Edition; W.H. Freeman and Company: San Francisco, 1982; 343.

(11) Bagchi, P.; Birnbaum, S. M. *Journal of Colloid and Interface Science* **1981**, *83*, 460.

(12) Bain, C. D.; Whitesides, G. M. *Journal of the American Chemical Society* **1988**, *110*, 5897.

(13) Bain, C. D.; Troughton, E. B.; Tao, Y.-T.; Evall, J.; Whitesides, G. M.; Nuzzo, R. G. *Journal of the American Chemical Society* **1989**, *111*, 321.

(14) Bain, C. D.; Biebuyck, H. A.; Whitesides, G. M. *Langmuir* **1989**, *5*, 723.

(15) Barford, W.; Ball, R. C.; Nex, C. M. M. *Journal. Chemical Society (London). Faraday Transactions. I* **1986**, *82*, 3233.

(16) Benziger, J. B.; Pascal, F. A.; Bernasek, S. L.; Soriaga, M. P.; Hubbard, A. T. *Journal of Electroanalytical Chemistry* **1986**, *198*, 65.

(17) Berendsen, R.; Borginon, H. *Journal of Photographic Science* **1968**, *16*, 194.

(18) Besio, G. J. Ph.D. Thesis, Princeton University, 1986.

(19) Blaakmeer, J.; Böhmer, M. R.; Cohen Stuart, M. A.; Fleer, G. J. *Macromolecules* **1990**, *23*, 2301.

(20) Blaakmeer, J.; Cohen Stuart, M. A.; Fleer, G. J. *Journal of Colloid and Interface Science* **1990**, *140*, 314.

(21) Boedtker, H.; Doty, P. *Journal of Physical Chemistry* **1954**, *58*, 968.

(22) Böhmer, M. R.; Evers, O. A.; Scheutjens, J. M. H. M. *Macromolecules* **1990**, *23*, 2288.

(23) Bonekamp, B. C. Ph.D. Thesis, Wageningen University, The Netherlands, 1984.

(24) Bonekamp, B. C.; Lyklema, J. *Journal of Colloid and Interface Science* **1986**, *113*, 67.

(25) Bonekamp, B. C. *Colloids and Surfaces* **1989**, *41*, 267.

(26) Burchard, W. *Advances in Polymer Science* **1980**, *48*, 1.

(27) Campanella, L. *Journal of Electroanalytical Chemistry* **1970**, *28*, 228.

(28) Chopra, P. S.; Srinivasan, S.; Lucas, T.; Sawyer, P. N. *Nature (London)* **1967**, *215*, 1494.

(29) Cohen Stuart, M. A.; Cosgrove, T.; Vincent, B. *Advances in Colloid and Interface Science* **1986**, *24*, 143.

(30) Cohen Stuart, M. A. *Journal de Physique II* **1988**, *49*, 1001.

(31) Cohen Stuart, M. A.; Fleer, G. J.; Lyklema, J.; Norde, W.; Scheutjens, J. M. H. M. *Advances in Colloid and Interface Science* **1991**, *34*, 477.

(32) Cosgrove, T.; Obey, T. M.; Vincent, B. *Journal of Colloid and Interface Science* **1986**, *111*, 409.

(33) Curme, H. G.; Natale, C. C. *Journal of Physical Chemistry* **1964**, *68*, 3009.

(34) Damaskin, B. B.; Petrii, O. A.; Batrakov, V. V. *Adsorption of Organic Compounds on Electrodes*; Plenum Press: New York-London, 1971.

(35) Dan, N.; Tirrell, M. *Macromolecules* **1993**, *26*, 4310.

(36) de Gennes, P. G. *Macromolecules* **1980**, *13*, 1069.

(37) Dickinson, E.; Lal, M. *Advances in Molecular Relaxation and Interaction Processes* **1980**, *17*, 1.

(38) Durand, G.; Lafuma, F.; Audebert, R. *Progress in Colloid and Polymer Science* **1988**, *266*, 278.

(39) Duschl, C.; Hall, E. A. H. *Journal of Colloid and Interface Science* **1991**, *144*, 368.

(40) Edwards, S. F. *Proceedings Physics Society* **1965**, *85*, 613.

(41) Eisenberg, A.; King, M. *Ion Containing Polymers*; Adademic Press: New York, 1977.

(42) Elaissari, A.; Haouam, A.; Huguenard, C.; Pefferkorn, E. *Journal of Colloid and Interface Science* **1992**, *149*, 68.

(43) Emons, H.; Werner, G.; Heineman, W. R. *Analyst* **1990**, *115*, 405.

(44) Evers, O. A.; Fleer, G. J.; Scheutjens, J. M. H. M.; Lyklema, J. *Journal of Colloid and Interface Science* **1986**, *111*, 446.

(45) Fernandez, V. L.; Reimer, J. A.; Denn, M. M. *Journal of the American Chemical Society* **1992**, *114*, 9634.

(46) Fleer, G. J.; Lyklema, J. In *Adsorption from Solution at the Solid/Liquid Interface*; G. D. Parfitt and C. H. Rochester, Ed.; Academic Press: London, 1983; 153.

(47) Fleer, G. J.; Cohen Stuart, M. A.; Scheutjens, J. M. H. M.; Cosgrove, T.; Vincent, B. *Polymers at Interfaces*; Chapman & Hall: London, 1993.

(48) Foissy, A.; Attar, A. E.; Lamarche, J. M. *Journal of Colloid and Interface Science* **1983**, *96*, 275.

(49) Fontaine, M.; Rivat, C.; Ropartz, C.; Caullet, C. *Bulletin de la Societe Chimique de France* **1973**, *6*, 1873.

(50) Furusawa, K.; Kanesaka, M.; Yamashita, S. *Journal of Colloid and Interface Science* **1984**, *99*, 341.

(51) Garrell, R. L.; Beer, K. D. *Langmuir* **1989**, *5*, 452.

(52) Gebhard, H.; Killmann, E. *Makromolekulare Chemie* **1976**, *53*, 171.

(53) Gebhardt, J. E.; Fuerstenau, D. W. *Colloids and Surfaces* **1983**, *7*, 221.

(54) Gileadi, E. In *Electrode Kinetics for Chemists, Chemical Engineers, and Materials Scientists*VCH Publishers, Inc.: New York, 1993.

(55) Gölander, C.-G.; Kiss, E. *Journal of Colloid and Interface Science* **1988**, *121*, 240.

(56) Granfeldt, M. K.; Miklavic, S. J.; Marcelja, S.; Woodward, C. E. *Macromolecules* **1990**, *23*, 4760.

(57) Gyss, C.; Bourdillon, C. *Analytical Chemistry* **1987**, *59*, 2350.

(58) Herning, T.; Djabourov, M.; Leblond, J. *Polymer* **1991**, *32*, 3211.

(59) Hesselink, F. T. *Journal of Electroanalytical Chemistry and Interfacial Electrochemistry* **1972**, *37*, 317.

(60) Hesselink, F. T. *Journal of Colloid and Interface Science* **1977**, *60*, 448.

(61) Hesselink, F. T. In *Adsorption from Solution at Solid/Liquid Interface*; C. H. Rochester and G. D. Parfitt, Ed.; Academic Press: London, 1983; 377.

(62) Hoeve, C. A. J. *Journal of Chemical Physics* **1966**, *44*, 1505.

(63) Hoeve, C. A. J. *Journal of Polymer Science* **1970**, *C30*, 361.

(64) Ivarsson, B. A.; Hegg, P.-O.; Lundström, K. I.; Jönsson, U. *Colloids and Surfaces* **1985**, *13*, 169.

(65) Janus, J.; Kenchington, A. W.; Ward, A. G. *Research (London)* **1951**, *4*, 247.

(66) Johnson, J. E.; Matijevic, E. *Journal of Colloid and Interface Science* **1990**, *138*, 255.

(67) Kallay, N.; Torbic, Z.; Golic, M.; Matijevic, E. *Journal of Physical Chemistry* **1991**, *95*, 7028.

(68) Kamiyama, Y.; Israelachvili, J. *Macromolecules* **1992**, *25*, 5081.

(69) Kawaguchi, M.; Takahashi, A. *Macromolecules* **1983**, *16*, 1465.

(70) Kawaguchi, M.; Hayashi, K.; Takahashi, A. *Macromolecules* **1984**, *17*, 2066.

(71) Kawaguchi, M.; Hayashi, K.; Takahashi, A. *Colloids and Surfaces* **1988**, *31*, 73.

(72) Kawaguchi, M.; Hayashi, K.; Takahashi, A. *Macromolecules* **1988**, *21*, 1016.

(73) Kawaguchi, M.; Takahashi, A. *Advances in Colloid and Interface Science* **1992**, *37*, 219.

(74) Kawanishi, N.; Christenson, H. K.; Ninham, B. W. *Journal of Physical Chemistry* **1990**, *94*, 4611.

(75) Kim, S. W.; Lee, R. G.; Oster, H.; Coleman, D.; Andrade, J. D.; Lentz, D. J.; Olsen, D. *Transactions. American Society for Artifical Internal Organs* **1974**, *2*, 449.

(76) Klein, J.; Luckham, P. F. *Macromolecules* **1986**, *19*, 2007.

(77) Koutsoukos, P. G.; Mumme-Young, C. A.; Norde, W.; Lyklema, J. *Colloids and Surfaces* **1982**, *5*, 93.

(78) Kragh, A. M.; Peacock, R. *Journal of Photographic Science* **1967**, *15*, 220.

(79) Krigbaum, W. R.; Carpenter, D. K. *Journal of Physical Chemistry* **1955**, *59*, 1166.

(80) Kudish, A. T.; Eirich, F. R. *Proteins at Interfaces*; American Chemical Society: Anaheim, CA, 1987; Vol. 343.

(81) Leatherbarrow, R. J.; Stedman, M.; Wells, T. N. C. *Journal of Molecular Biology* **1991**, *221*, 361.

(82) Lee, J.-J.; Fuller, G. G. *Macromolecules* **1984**, *17*, 375.

(83) Lee, J.-J.; Fuller, G. G. *Journal of Colloid and Interface Science* **1985**, *103*, 569.

(84) Leininger, R. I.; Mirkovitch, V.; Beck, R. E.; Andrus, P. G.; Kolff, W. J. *Transactions. American Society for Artifical Internal Organs* **1964**, *10*, 137.

(85) Liedberg, B.; Ivarsson, B.; Lundström, I.; Salaneck, W. R. *Progress in Colloid and Polymer Science* **1985**, *70*, 67.

(86) Liedberg, B.; Ivarsson, B.; Hegg, P.-O.; Lundström, I. *Journal of Colloid and Interface Science* **1986**, *114*, 386.

(87) Lipatov, Y. S.; Sergeeva, L. M. *Adsorption of Polymers*; Wiley: New York, 1974.

(88) Lippert, J. L.; Brandt, E. S. *Langmuir* **1988**, *4*, 127.

(89) Marques, C.; Joanny, J. F.; Leibler, L. *Macromolecules* **1988**, *21*, 1051.

(90) Marra, J.; van der Schee, H. A.; Fleer, G. J.; Lyklema, J. In *Adsorption from Solution*; R. H. Ottewill, C. H. Rochester and A. L. Smith, Ed.; Academic Press: 1983; 245.

(91) Marra, J.; Hair, M. L. *Journal of Physical Chemistry* **1988**, *92*, 6044.

(92) Maternaghan, T. J.; Ottewill, R. H. *Journal of Photographic Science* **1974**, *22*, 279.

(93) Maternaghan, T. J.; Bangham, O. B.; Ottewill, R. H. *Journal of Photographic Science* **1980**, *28*, 1.

(94) McCrackin, F. L.; Passaglia, E.; Stromberg, R. R.; Steinberg, H. L. *Journal of Research of the National Bureau of Standards (Physics and Chemistry)* **1963**, *67A*, 363.

(95) McCrackin, F. L.; Colson, J. P. In *Ellipsometry in the Measurement of Surfaces and Thin Films*; NBS Misc. Publication #256: Washington, D.C., 1964; 61.

(96) McCrackin, F. L. *National Bureau of Standards Technical Note #479* **1969**.

(97) McLaren, A. D. *Journal of Physical Chemistry* **1954**, *58*, 129.

(98) Miklavic, S. J.; Marcelja, S. *Journal of Physical Chemistry* **1988**, *92*, 6718.

(99) Miklavic, S. J.; Woodward, C. E.; Jönsson, B.; Åkesson, T. *Macromolecules* **1990**, *23*, 4149.

(100) Miller, I. R. *Journal of Molecular Biology* **1961**, *3*, 229.

(101) Miller, I. R.; Frommer, M. A. *Journal of Physical Chemistry* **1968**, *72*, 1834.

(102) Milligan, H. L.; Davis, J.; Edmark, K. W. *Journal of Biomedical Materials Research* **1968**, *2*, 51.

(103) Milner, S. T.; Witten, T. A.; Cates, M. E. *Europhysics Letters* **1988**, *5*, 413.

(104) Milner, S. T.; Witten, T. A.; Cates, M. E. *Macromolecules* **1988**, *21*, 2610.

(105) Minunni, M.; Skládal, P.; Mascini, M. *Analytical Letters* **1994**, *27*, 1475.

(106) Misra, S.; Varanasi, S. *Macromolecules* **1989**, *22*, 4173.

(107) Mizutani, T. *Journal of Colloid and Interface Science* **1981**, *82*, 162.

(108) Morrissey, B. W.; Stromberg, R. R. *Journal of Colloid and Interface Science* **1974**, *46*, 152.

(109) Morrissey, B. W.; Smith, L. E.; Stromberg, R. R.; Fenstermaker, C. A. *Journal of Colloid and Interface Science* **1976**, *56*, 557.

(110) Morrissey, B. W. *Annals New York Academy of Sciences* **1977**, *283*, 50.

(111) Muthukumar, M. *Journal of Chemical Physics* **1987**, *86*, 7230.

(112) Niwa, M.; Shimoguchi, M.; Higashi, N. *Journal of Colloid and Interface Science* **1992**, *148*, 592.

(113) Niwa, M.; Mori, T.; Higashi, N. *Macromolecules* **1993**, *26*, 1936.

(114) Norde, W.; Lyklema, J. *Journal of Colloid and Interface Science* **1978**, *66*, 257, 266, 277, 285, 295.

(115) Norde, W. *Colloids and Surfaces* **1984**, *10*, 21.

(116) Norde, W. *Advances in Colloid and Interface Science* **1986**, *25*, 267.

(117) Norde, W. In *Surfactants in Solution*; K. L. Mittal and P. Bothorel, Ed.; Plenum Press: New York, 1986; Vol. 5; 1027.

(118) Norde, W.; Lyklema, J. *Colloids and Surfaces* **1989**, *38*, 1.

(119) Norde, W.; Arai, T.; Shirahama, H. *Biofouling* **1991**, *4*, 37.

(120) Nuzzo, R. G.; Allara, D. L. *Journal of the American Chemical Society* **1983**, *105*, 4481.

(121) Nuzzo, R. G.; Fusco, F. A.; Allara, D. L. *Journal of the American Chemical Society* **1987**, *109*, 2358.

(122) Olk, C. H.; Heremans, J. *Journal of Vacuum Science and Technology* **1991**, *B 9*, 1268.

(123) Outer, P.; Carr, C. I.; Zimm, B. H. *Journal of Chemical Physics* **1950**, *18*, 830.

(124) Papenhuijzen, J.; van der Schee, H. A.; Fleer, G. J. *Journal of Colloid and Interface Science* **1985**, *104*, 540.

(125) Papenhuijzen, J.; Fleer, G. J.; Bijsterbosch, B. H. *Journal of Colloid and Interface Science* **1985**, *104*, 530.

(126) Parsons, R.; Visscher, W. H. M. *Journal of Electroanalytical Chemistry* **1972**, *36*, 329.

(127) Perlmann, G. E.; Longsworth, L. G. *Journal of the American Chemical Society* **1948**, *70*, 2719.

(128) Pezron, I.; Djabourov, M.; Leblond, J. *Polymer* **1991**, *32*, 3201.

(129) Pincus, P. *Macromolecules* **1991**, *24*, 2912.

(130) Ploehn, H. J.; Russel, W. B. *Advances in Chemical Engineering* **1990**, *15*, 137.

(131) Raspor, B. *Journal of Electroanalytical Chemistry* **1991**, *316*, 223.

(132) Razumas, V.; Nylander, T.; Arnebrant, T. *Journal of Colloid and Interface Science* **1994**, *164*, 181.

(133) Reddy, A. K. N.; Genshaw, M. A.; Bockris, J. O. *Journal of Chemical Physics* **1968**, *48*, 671.

(134) Robb, I. D. *Comprehensive Polymer Science* **1989**, *2*, 733.

(135) Roe, R. J. *Journal of Chemical Physics* **1974**, *60*, 4192.

(136) Roscoe, S. G.; Fuller, K. L. *Journal of Colloid and Interface Science* **1992**, *152*, 429.

(137) Roscoe, S. G.; Fuller, K. L.; Robitaille, G. *Journal of Colloid and Interface Science* **1993**, *160*, 243.

(138) Rose, P. I. In *The Theory of the Photographic Process*; Fourth Edition; T. H. James, Ed.; Macmillan Publishing Co., Inc.: New York, 1977; 51.

(139) Ross, R. S.; Pincus, P. *Macromolecules* **1992**, *25*, 2177.

(140) Sawyer, P. N.; Srinivasan, S. *American Journal of Surgery and Gynecology* **1967**, *114*, 42.

(141) Scheutjens, J. M. H. M.; Fleer, G. J. *Journal of Physical Chemistry* **1979**, *83*, 1619.

(142) Scheutjens, J. M. H. M.; Fleer, G. J. *Journal of Physical Chemistry* **1980**, *84*, 178.

(143) Schurr, J. M.; Smith, S. B. *Biopolymers* **1990**, *29*, 1161.

(144) Shirahama, H.; Takeda, K.; Suzawa, T. *Journal of Colloid and Interface Science* **1986**, *109*, 552.

(145) Shoichet, M. S.; McCarthy, T. J. *Macromolecules* **1991**, *23*, 1441.

(146) Silberberg, A. In *Encyclopedia of Polymer Science and Engineering*Wiley: New York, 1985; Vol. 1; 577.

(147) Silverton, E. W.; Navia, M. A.; Davies, D. R. *Proceedings National Academy of Sciences, USA* **1977**, *74*, 5140.

(148) Soderquist, M. E.; Walton, A. G. *Journal of Colloid and Interface Science* **1980**, *75*, 386.

(149) Srinivasan, S.; Sawyer, P. N. *Journal of Colloid and Interface Science* **1970**, *32*, 456.

(150) Stedman, M. *Chemical Physics Letters* **1968**, 2, 457.

(151) Stromberg, R. R.; Passaglia, E.; Tutas, D. J. *Journal of Research of the National Bureau of Standards (Physics and Chemistry)* **1963**, *67A*, 431.

(152) Stromberg, R. R.; Passaglia, E.; Tutas, D. J. In *Ellipsometry in the Measurement of Surfaces and Thin Films*; NBS Misc. Publication #256: Washington, D.C., 1964; 281.

(153) Stromberg, R. R.; Tutas, D. J.; Passaglia, E. *Journal of Physical Chemistry* **1965**, *69*, 3955.

(154) Takahashi, A.; Kawaguchi, M.; Hirota, H.; Kato, T. *Macromolecules* **1980**, *13*, 884.

(155) Takahashi, A.; Kawaguchi, M. *Advances in Polymer Science* **1982**, *46*, 1.

(156) Takahashi, A.; Kawaguchi, M.; Hayashi, K.; Kato, T. *Polymer Adsorption and Dispersion Stability*; American Chemical Society: Washington, 1984; Vol. 240.

(157) Tengvall, P.; Lestelius, M.; Liedberg, B.; Lundström, I. *Langmuir* **1992**, *8*, 1236.

(158) Turner, A. P. F.; Karube, I.; Wilson, G. S., Ed.; *Biosensors. Fundamentals and Applications*; Oxford University Press: Oxford, 1987.

(159) van de Steeg, H. G. M.; Cohen Stuart, M. A.; de Keizer, A.; Bijsterbosch, B. H. *Langmuir* **1992**, *8*, 2538.

(160) van der Schee, H. A. Ph.D. Thesis, Wageningen University, The Netherlands, 1984.

(161) van der Schee, H. A.; Lyklema, J. *Journal of Physical Chemistry* **1984**, *88*, 6661.

(162) van Dulm, P.; Norde, W.; Lyklema, J. *Journal of Colloid and Interface Science* **1981**, *82*, 77.

(163) Vinnikov, Y. Y.; Shepelin, V. A.; Veselovskii, V. I. *Élektrokhimiya* **1973**, *9*, 534.

(164) Vinnikov, Y. Y.; Shepelin, V. A.; Veselovskii, V. I. *Élektrokhimiya* **1973**, *9*, 624.

(165) Waldmann-Meyer, H.; Knippel, E. *Journal of Colloid and Interface Science* **1992**, *148*, 508.

(166) Wang, T. K.; Audebert, R. *Journal of Colloid and Interface Science* **1988**, *121*, 32.

(167) Weill, G.; des Cloiseaux, J. *Journal de Physique II* **1979**, *40*, 99.

(168) Wiegel, F. W. *Journal of Physics A* **1977**, *10*, 299.

(169) Wiegel, F. W. In *Phase Transitions and Critical Phenomena*; C. Domb and J. L. Lebowitz, Ed.; Academic: New York, 1983; Vol. 7.

(170) Wittmer, J.; Joanny, J. F. *Macromolecules* **1993**, *26*, 2691.

(171) Zhulina, E. B.; Priamitsyn, V. A.; Borisov, O. V. *Polymer Science USSR* **1989**, *31*, 205.

(172) Zhulina, E. B.; Borisov, O. V.; Priamitsyn, V. A. *Journal of Colloid and Interface Science* **1990**, *137*, 495.

(173) Zhulina, E. B.; Borisov, O. V.; Birshtein, T. M. *Journal de Physique II* **1992**, *2*, 63.